The copyright of this thesis vests in the author. No quotation from it or information derived from it is to be published without full acknowledgement of the source. The thesis is to be used for private study or non-commercial research purposes only.

Published by the University of Cape Town (UCT) in terms of the non-exclusive license granted to UCT by the author.

University of Cape Town

A Comparative Evaluation of Manufacturing Technologies and Their Effect on Morphology and Mechanical Properties of Poly-(Propylene-Ethylene) Copolymers

BY

Maitse P. Sello

University of Cape Town

A dissertation submitted to the Faculty of Engineering and Built Environment of the University of Cape Town in fulfillment of the requirements for the degree of Master of Science in Applied Science.

Centre for Materials Engineering

University of Cape Town

2002

University of Cape Town

ACKNOWLEDGEMENTS

I would like to express my sincere appreciation to the following people for their help with this project:

- Dr K. Marcus, my supervisor for his input and helping me through project discussion
- Dr B. Sole, my co-supervisor at Sasol Polymers, for his research input and materials supply
- UCT Electron Microscope Unit (EMU) staff for their patience in teaching me the operational procedures for electron microscopy research, with special thanks to: Mr M. Jaffer (TEM), Mrs M. Waldron (SEM) and Mr W. Williams (photography); their help is highly appreciated
- Centre For Materials Engineering (CME) technical staff for their assistance throughout the time I have spent on my research project, with special thanks to: Mrs M. Topic (technical assistance), Mr. G. Newins & Mr P. Jacobs (sample preparations), Mr J. Petersen (photography) and Mrs D. Young (for keeping the work place neat and tidy)
- Mr T. Ntsoane at iThemba Labs for the x-ray diffraction works
- Mr J. Vermeulen at the University of Stellenbosch, for the DMA analysis
- Dr J. Fourie at Cape Technikon, for the use of Ft-IR
- Ms J. Henry and Mrs N. Africa for their administrative support
- The staff and students at CME, both present or past, for their teaching, support and words of encouragement
- Sasol Polymers for sponsoring my research project
- Centre for Materials Engineering and NRF for their financial support during my studies

I would like to express my greatest gratitude to all members of my family, for their encouragement, support and guidance throughout the path my life.

"Learning is such a process that is not possible to tell exactly how one acquired a given body of knowledge. This thesis is dedicated to all those who taught me and helped me to acquire that knowledge over the years."

University of Cape Town

NOMENCLATURE

α, β, γ	Crystalline forms / molecular relaxations within the copolymer
λ	wavelength of incident x-ray beam
η_r	viscosity ratio
$\Delta H_{o/m}$	enthalpy of change for 100% pure or melted samples
D	crystal size
D_n	average number particle size
D_w	average weight particle size
D_w/D_n	particle size distribution
DBT	ductile– to - brittle transition
DMA	dynamic Mechanical Analysis
DSC	differential Scanning Calorimetry
E'	storage modulus
E"	loss modulus
EPR	ethylene-propylene rubber
FBR	fluidised bed reactor
Ft-IR	Fourier transform infrared
HSBR	horizontal stirred bed reactor
ID	interparticle distance
iPP	isotactic polypropylene
MFI	melt flow index
MW	molecular weight
MWD	molecular weight distribution
$NaIO_4$	sodium periodate
NaOCl	sodium hypochloride
OsO_4	osmium tetraoxide
PE	polyethylene
PP	polypropylene
$RuCl_3$	ruthenium trichloride
RuO_2	ruthenium dioxide
RuO_4	ruthenium tetraoxide
SEM	scanning electron microscopy
T_{db}	ductile-to-brittle transition temperature
T_g	glass transition temperature
T_m	melt temperature
tan δ	ratio of E'/ E"
TEM	transmission electron microscopy
VSBR	vertical stirred bed reactor
WAXS	wide-angle x-ray scattering
X_c	degree of crystallinity

University of Cape Town

ABSTRACT

This project is a technological benchmark exercise for Sasol Polymers where different poly (propylene-ethylene) copolymer grades from five foremost licensed manufacturing PP technologies are evaluated. These copolymer grades were manufactured using the following processes: Novolen PP technology (Sasol grades), Innovene PP technology (BP grades), Spheripol PP technology (Basell grades), Univation PP technology (DOW grades) and Borstar PP technology (Borealis grades). Form this investigation, thirty different grades where evaluated to determine their structural morphology in relation to their physical and mechanical properties. For the ease of analysis, the grades are grouped into three ethylene content ranges; low ethylene contents (below 8%), medium ethylene contents (between 8 – 10%) and high ethylene contents (above 10%). Within each of these ethylene content ranges, there is a melt flow index (MFI) range, which increases from low to high. The differences in the MFI added further complications, especially when trying to determine optimum mechanical properties of the copolymer grades.

The impact test results show that the toughness is at a maximum at low MFI, and then drops drastically as the MFI increases. Since an addition of ethylene improves the toughness of the copolymer, it was observed that by considering MFI's below 35 g/10 min, the toughness could be enhanced by increasing ethylene content. Grades with MFI's below 35 g/10 min show a drastic increase in impact strength at ethylene content around 8.5%. SEM results show that particle size and spacing are independent of ethylene contents for the grades examined. However, for the BP and DOW grades, the ratio between interparticle distance and particle size decrease steadily with increasing ethylene content. The Basell and BP grades showed a narrow rubber particle size distribution followed by Sasol grades. The DOW grades showed a broad particle size distribution. TEM results show that the internal morphology of the rubber particles differ from grade to grade, with the Sasol and BP grades showing several numbers PE inclusions within the rubber particles, whilst Basell grades having only few PE inclusions. It was observed that those grades with several PE inclusions have a better impact performance compared with those with fewer inclusions.

University of Cape Town

It was concluded that the Innovene PP technology overall produces the best grades as was observed with the BP grades, followed by the Novolen and Spheripol PP technology. The Univation PP technology produced the worst grades in terms of their particle morphology, and mechanical and physical properties. The Borstar PP technology could be ranked anywhere between the Novolen and Spheripol PP technologies. Since it has similar features to Spheripol PP technology, a big difference in the morphology of their grades could not be expected.

University of Cape Town

TABLE OF CONTENTS

ACKNOWLEDGEMENTS I

NOMENCLATURE II

ABSTRACT III

TABLE OF CONTENTS V

CHAPTER ONE 1

1 GENERAL INTRODUCTION 1

1.1 INTRODUCTION 1

1.2 RESEARCH MOTIVATION 4

1.3 RESEARCH OBJECTIVES 4

1.4 OUTLINE OF THESIS 5

CHAPTER TWO 6

2 LITERATURE REVIEW 6

2.1 MORPHOLOGICAL STRUCTURE OF POLYPROPYLENE 6
2.1.1 Introduction 6
2.1.2 Tacticity and Crystallinity 7
2.1.3 Polypropylene Copolymers 10
2.1.4 Molecular Weight and Molecular Weight Distribution 12

2.2 MANUFACTURING OF IMPACT COPOLYMERS 17
2.2.1 The Montell Spheripol PP Process 17
2.2.2 The Union Carbide UNIPOL Process 19
2.2.3 The BASF Novolen® PP Process 20
2.2.4 The AMOCO/Chisso Innovene Process 21
2.2.5 The Borstar Process 23

2.3 PHYSICAL PROPERTIES OF POLYPROPYLENE COPOLYMERS 25
2.3.1 Morphology of Injected Moulded Polypropylene 25
2.3.2 Effect of the Processing Conditions 26
2.3.3 Effect of the Modifying Phase 28
2.3.4 Toughening Mechanisms 29
2.3.5 Characterisation of Impact Copolymers 29
2.3.6 Characteristics of the Elastomer in Polymer Modification 36
2.3.7 Thermal Properties of Polymers 39

2.4 DUCTILE-BRITTLE TRANSITION 42
2.4.1 Effect of Morphological Parameters on the Ductile to Brittle Transition 43

2.5 END USE PROPERTIES OF THE IMPACT COPOLYMERS 46
2.5.1 Mechanical Properties 47

University of Cape Town

CHAPTER THREE 49

3 EXPERIMENTAL TECHNIQUES 49

3.1 MATERIALS USED 49
3.1.1 Sample Preparation 49

3.2 MORPHOLOGICAL CHARACTERISATION 51
3.2.1 Transmission Electron Microscopy (TEM) 51
3.2.1.1 Block Trimming 51
3.2.1.2 Staining 52
3.2.1.3 Ultra-thin Sectioning 53
3.2.2 Scanning Electron Microscopy (SEM) 54

3.3 THERMAL PROPERTIES 55
3.3.1 Dynamic Mechanical Thermal Analysis 55
3.3.2 Differential Scanning Calorimetry (DSC) 55
3.3.2.1 Calibration of the DSC 56
3.3.2.2 DSC Runs of the Copolymer Grades 56

3.4 PHYSICAL PROPERTIES OF THE COPOLYMER GRADES 57
3.4.1 Wide Angle X-Ray Scattering (WAXS) 57
3.4.2 Fourier Transform Infra-Red Spectroscopy (FTIR) 58

3.5 MECHANICAL TESTING 58
3.5.1 Impact Testing 58
3.5.1.1 Tensile Impact Testing 58
3.5.1.2 Drop Weight Impact Testing 60

CHAPTER FOUR 62

4 EXPERIMENTAL RESULTS 62

4.1 INTRODUCTION 62

4.2 THERMAL ANALYSIS 63
4.2.1 Differential Scanning Calorimetry (DSC) Results 63
4.2.2 Dynamic Mechanical Analysis (DMA) Results 66

4.3 PHYSICAL ANALYSIS 75
4.3.1 Fourier Transform Infrared (FT-IR) Results 75
4.3.2 Wide-Angle X-ray Scattering (WAXS) Results 79

4.4 MECHANICAL BEHAVIOUR 86
4.4.1 Effect of the Material Parameters on Mechanical Properties 86
4.4.2 Effect of the Melt Flow Index (MFI) on Mechanical Properties 87
4.4.3 Effect of Ethylene Content on Mechanical Properties 94
4.4.4 Effect of Percentage Crystallinity on Mechanical Properties 100

4.5 MORPHOLOGICAL CHARACTERISATION 104
4.5.1 Scanning Electron Microscopy (SEM) 104
4.5.2 Transmission Electron Microscopy (TEM) 115

CHAPTER FIVE 126

5 DISCUSSION 126

University of Cape Town

5.1 INTRODUCTION 126

5.2 MECHANICAL PROPERTIES 126
5.2.1 Effect of Matrix Parameters on Mechanical Properties 126
5.2.2 Effect of Ethylene Content on Mechanical Properties 129

5.3 PHYSICAL PROPERTIES 129
5.3.1 DSC, WAXS and FTIR 129

5.4 MICROSTRUCTURAL ANALYSIS 132
5.4.1 SEM and TEM 132

5.5 DYNAMIC MECHANICAL PROPERTIES 137

5.6 EFFECT OF MANUFACTURING TECHNIQUES 138

CHAPTER SIX 141

6 CONCLUSIONS 141

RECOMMENDATIONS FOR FUTURE WORK 143

CHAPTER SEVEN 144

7 REFERENCES 144

8 APPENDICES 150

University of Cape Town

CHAPTER ONE

GENERAL INTRODUCTION

1.1 INTRODUCTION

Polypropylene (PP) homopolymer and its copolymers are well established thermoplastic commodities in both the South African and international markets. These polymers have found a wide range of increasing applications in consumer products, packaging, film, textile and in the automotive industry. One of the advantages of iPP is that it can be fabricated easily using different processes such as injection moulding, blow moulding and extrusion. Furthermore, because of its attractive cost-to-performance ratio, this has led to substitution of many applications dominated by other thermoplastics. Also, when evaluating the cost-to-performance of the manufactured item, one should not only concentrate on the mechanical properties and cost of the material used, but also on the elements pertaining to processing and structural design of the moulded item.

PP is a highly versatile material for the following reasons: (1) it can be synthesised with different morphological structures, with the use of both high yield catalysts and new processes, (2) it can be blended with other polymeric materials (in particular rubbers) and can contain high amount of fillers and reinforcing agents, and (3) it can be modified by grafting functional groups to produce polymer blends that are bi-phasic[1]. This has led PP's rapid growth in the global demand for commodity thermoplastic and its emergence as a true engineering thermoplastic with a wide range of applications. Figure 1.1 below shows the Western European PP consumption for the year 1999, being similar to the South African PP market with regard to the packaging industry[2].

University of Cape Town

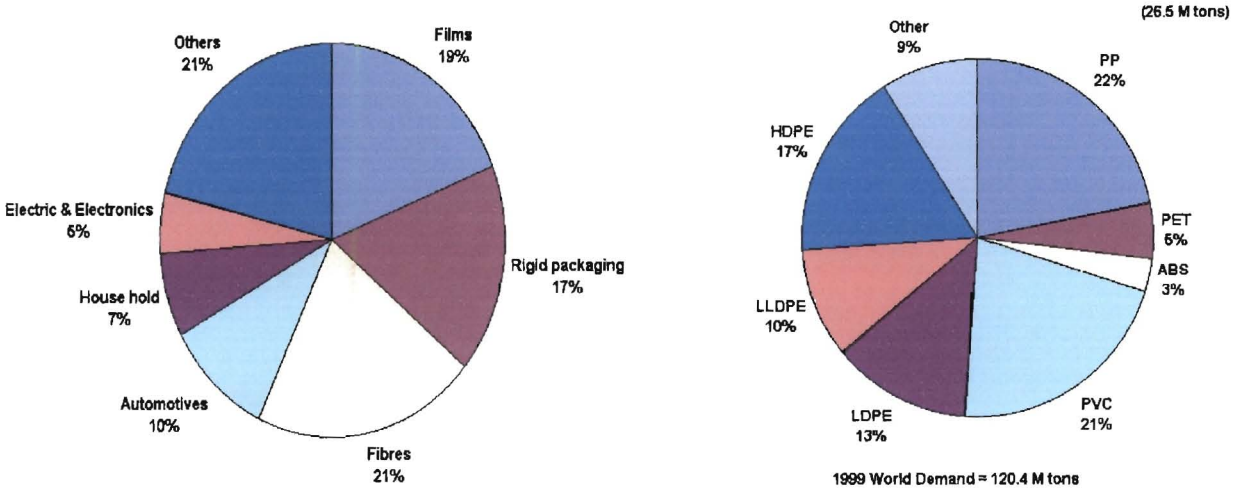

Figure 1.1 Polypropylene consumption details in the year 1999 [after ref. 2]

Isotactic polypropylene (iPP) homopolymer is a semi-crystalline polymer with very interesting mechanical - and thermal properties, though its strength particularly at low temperatures is not sufficient for applications as an engineering thermoplastic. The strength of iPP can be improved by blending it with ethylene-propylene rubber (EPR). The iPP/EPR blends are either produced by mechanical compounding in post-reactor synthesis or prepared by in-reactor blending techniques. In comparison to iPP/EPR blends formed by mechanical blending, blends prepared by in-reactor techniques have been proven to be better both in superior mechanical properties and in lower production costs. This is because the rubber particle phase can reach a high degree of dispersion and few manufacturing steps are involved. Typical reactor blends are prepared by the continuous sequential homo-polymerisation of propylene in the first reactor using a suitable advanced catalyst for the process, followed by ethylene and propylene copolymerisation in the second reactor. Each reactor may operate under different conditions of temperature, pressure and monomer compositions, thus producing a completely different polymer in each stage of the process. The final product from this process is strictly a bi-phasic copolymeric material, but it is commonly referred to as an impact block copolymer.

A variety of processes that are currently in use for the production of polypropylene and its copolymers include the loop, continuous-stirred tank, horizontal stirred bed and fluidised-bed technologies. Some of the major licensed technologies that are used

University of Cape Town

today in the manufacturing of the polypropylene homopolymer and their copolymers are listed in the Table 1.1 below.

Table 1.1 Processes, licensors and reactor conditions of polypropylene copolymerisation[3]

	BASF	Amoco/Chisso	Union Carbide	Montell
Process	Novolen	Innovene	UNIPOL	Spheripol
Medium	Gas	Gas	Gas	Slurry-liquid monomer
Reactor*	VSBR	HSBR	FBR	2 loop in series
Size (m^3)	25 – 50	n/a	n/a	$45m^3$ in each loop
Catalyst used	$TiCl_3$ & $TiCl_4/MgCl_3$	$TiCl_4/MgCl_3$	$TiCl_4/MgCl_3$	$TiCl_4/MgCl_3$
Temperature (°C)	50-100	57-93	n/a	70
Pressure (atm)	20-35	19-23	n/a	35-40
Reported yield (g/g cat)	100000-20000	Up to 30000	Up to 40000	Up to 50000

University of Cape Town

In each of these continuous processes, the reactor residence-time distribution is unique and it has a significant effect on the rubber content, ethylene content and the total resulting polymer properties. Therefore, it would be expected that the copolymer grades produced using the different manufacturing technologies to have different morphologies. The difference in morphologies is directly related to the type of catalytic system used and the processing conditions of the reactors. Hydrogen gas is fed into each stage of polymerization to control the molecular weight of the copolymers. The activity of the catalyst involves the sequential distribution of ethylene and propylene in the rubbery ethylene-propylene phase, which is dispersed in the iPP matrix. Since the rubber phase is added to increase the impact strength of the product at low temperature, its composition have a direct effect on impact strength of the copolymers.

1.2 Research Motivation

In many industries today there is major emphasis in weight savings of the part and lowering manufacturing cost, and improving productivity in an effort to stay globally competitive. Therefore, the new industrial strategy in the polymer field requires the transformation of the manufacturing industries from a "product-oriented" management into a "need-oriented" operative administration. This is in order to detect increasing and developing demands and quickly respond with products complying with needs as soon as they arise. From the product point of view, the most complete fulfilment of these requirements seems to come from the transformation of polymer mass "commodities" into specialties through simple and controlled production technologies. Therefore, to stay globally competitive, most industries undergo technological benchmark exercises. This statement brings us to the main objective of this research. Sasol Polymers is undergoing a technology benchmark exercise, by specifically evaluating polymers from five other leading licensed technologies, of which the impact copolymers formed part of this exercise.

University of Cape Town

1.3 Research Objectives

The specific objectives of this project was to:

- Characterise different grades of polypropylene impact copolymers produced using five different manufacturing technologies
- Determine the microstructural differences in the copolymers obtained from the different techniques
- Determine the physical and microstructural properties that give the most balanced or optimum mechanical properties
- Compare and rate the performance of the technology used to manufactured these grades

1.4 Outline of Thesis

In *Chapter two* a concise overview of polypropylene and its copolymers is given as well as a short description of PP manufacturing technologies. Literature on PP/EPR blends is also reviewed. *Chapter three* gives information on the experimental techniques used in this study. *Chapter four* deals with the experimental results, followed by *Chapter five* which discusses and interprets the observations from these results. *Chapter six* deals with the conclusions drawn from these observations followed by recommendations made to Sasol Polymers.

University of Cape Town

CHAPTER TWO

LITERATURE REVIEW

2.1 MORPHOLOGICAL STRUCTURE OF POLYPROPYLENE

2.1.1 INTRODUCTION

The morphology of a polymer describes the arrangement of the monomers within the chain on a crystallographic level through to the dispersion of rubbery particulates on a macroscopic level. In polypropylene, a variety of ordered features are found across the hierarchy of the morphological scale. Close packing and ordering of the macromolecules is broadly described by crystallinity and is a function of various molecular features within the chain. Features such as polymer branching, tacticity and copolymerisation directly influence the degree of ordering within the polymer. All of these factors affect both the mechanical and physical properties of a polymeric component.

Many different catalyst systems are currently being used for propylene polymerisation within the industry. These catalysts are design in such a way so as to be able to achieve five major objectives in polymerisation. These objectives are:

1. to have a high polymerisation activity such that removal of catalyst residues is not required while all the necessary and desired product qualities are maintained;

2. the ability to produce a polymer with the necessary and desired molecular weight distribution;

3. the ability to prepare polymers with a controlled degree of tacticity, without requiring costly operations to remove undesired polymer fractions;

4. the ability to obtain a granular polymer with a controlled morphology, particle size distribution and compactness, so as to achieve the maximum saving,

University of Cape Town

simplicity and versatility, both in terms of the production process and product properties;

5. the capability of producing hetero-phasic or better multi-phasic products by direct synthesis[4].

The most significant catalytic groups include supported and unsupported Ziegler-Natta- (i.e. $TiCl_4/MgCl_2$ and $TiCl_3$), chromium oxide- and recently, Metallocene-based systems. The kinetics that controls the polymerisation process is quite complex and may involve multiple sites on the catalyst surface, reactions with the co-catalyst and electron donors. In addition, the polymerisation may involve chain transfer agents such as hydrogen for molecular weight control and several monomers may be simultaneously polymerised.

University of Cape Town

2.1.2 Tacticity and Crystallinity

The tacticity or stereoregularity of the polymer molecule is of profound importance for the properties of the polymer. Tacticity affects the forces acting between adjacent molecules and hence the mechanical and physical properties of the polymer. It also affects the ordering or crystallinity of the polymer chains, which in turn affect mechanical properties. Tacticity arises in all chain polymers in which atoms of an all-carbon backbone carry two dissimilar atoms or groups. Depending on the spatial arrangement of the R-groups (in the case of polypropylene (PP) the R-group is the methyl (CH_3-) moiety). In Figure 2.1(a), three stereoisomers of polypropylene can be observed viz. isotactic-, syndiotactic- and atactic polypropylene. Isotactic chains result from the head-to-tail addition of propylene monomer units, where the methyl groups always have the same configuration with respect to the polymer backbone. Syndiotactic chains result from the same head-to-tail addition of propylene monomer units, with the methyl groups having an alternating configuration with respect to the polymer backbone. Atactic chains do not have any consistent placement of the methyl groups.

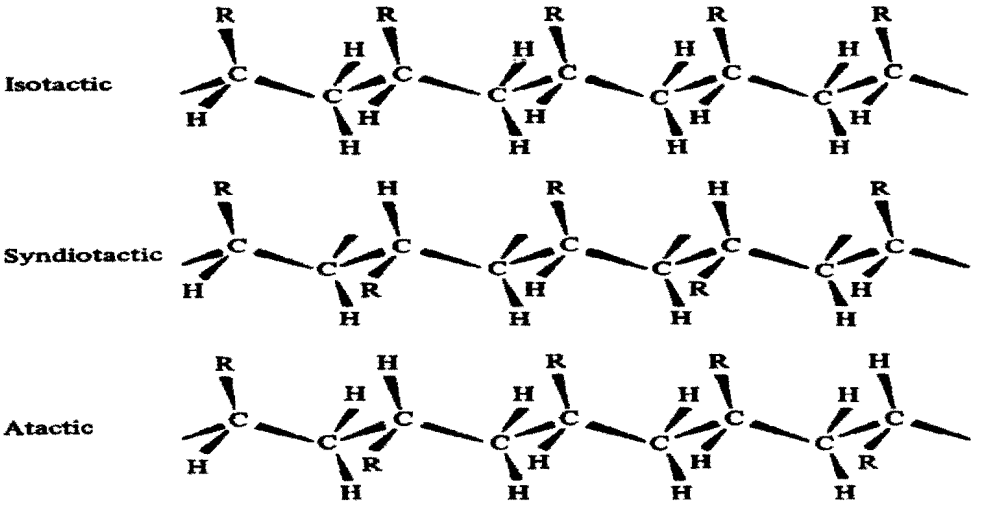

(a)

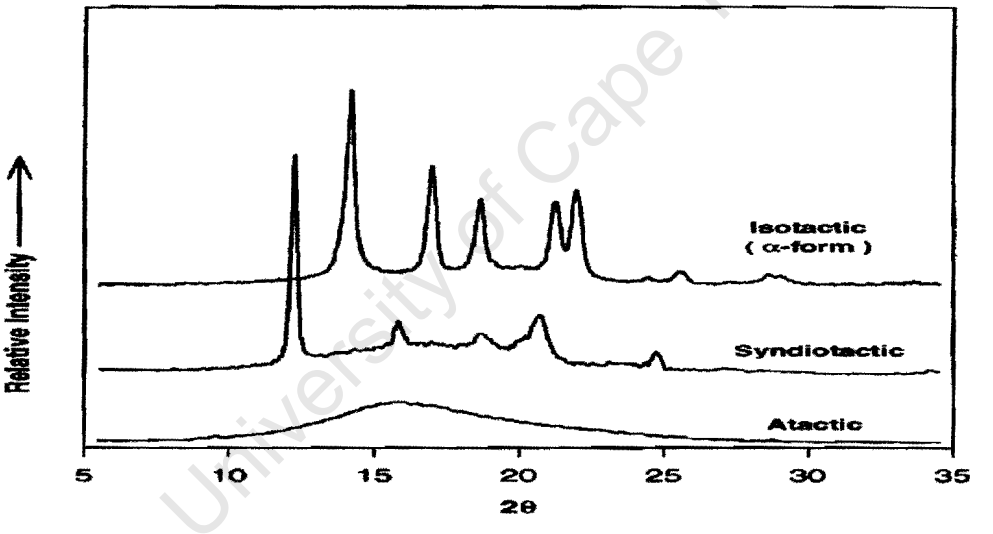

(b)

University of Cape Town

Figure 2.1 (a) Schematic illustration of the tacticity along the polymer chain backbone (note R=CH_3- groups) [after ref. 5], (b) wide-angle X-ray scattering patterns of isotactic, syndiotactic, and atactic PP [after ref. 6]

Figure 2.1(b) shows pronounce crystalline reflections obtained from wide-angle x-ray diffraction, when the polypropylene (PP) chains contain either regular isotactic or syndiotactic sequences. These patterns are related to the specific crystal unit cell symmetries for isotactic and syndiotactic PP. Atactic PP does not crystallise, and as a

result the wide-angle x-ray diffraction pattern shows no strong reflections, exhibiting only a very broad and diffuse scattering[6].

In polypropylene, the morphological feature that is associated with crystallinity is the structure, size and dispersion of spherulites. Spherulites have diameters usually in the range 0.5-100 μm and are characteristic of polymers that have crystallised from the melt in the absence of stress or flow[7]. Spherulites consist of fibrils that radiate from a centre of nucleation. These fibrils consist of crystallites or lamellae that trap amorphous material between them as they grow. When thin films of the polymer is viewed under polarised light, a characteristic Maltese cross pattern can be observed, as shown in Figure 2.2.

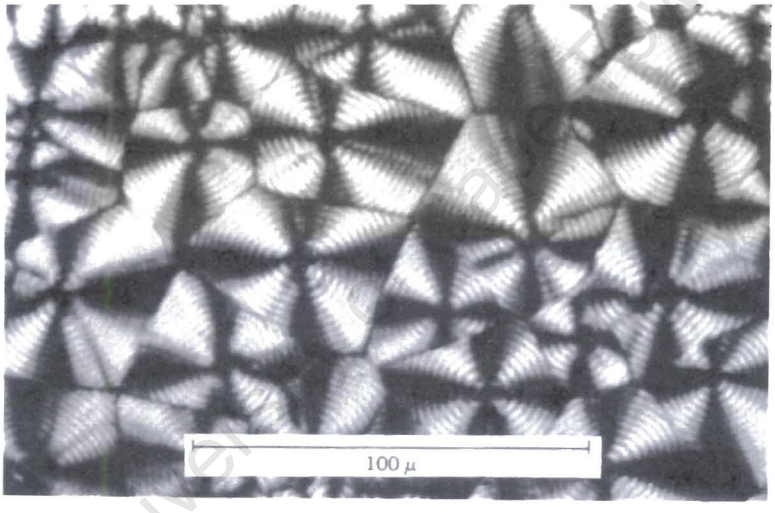

Figure 2.2 Morphology of the spherulites of PP viewed under polarised light [after ref. 7]

University of Bath Library

Nucleation, spherulite growth rate, the degree of supercooling and the rate of cooling control the crystallisation of homo- and copolymers. The crystallisation behaviour of blends is more complex due to the existence of the second crystallising or non-crystallising component[8].

The isothermal crystallisation kinetics can be analysed using the Avrami equation[9]:

$$X_c(t,T) = 1 - exp(-kt^n)$$

[Equation 2.1]

where X_c *(t,T)* is the volume fraction of crystalline material at time *t* at the isothermal crystallisation temperature *T*, *n* is the Avrami exponent which is related to crystal growth geometry, and the crystallisation rate coefficient *k*, is a parameter of the crystallisation growth rate. This coefficient is related to the nucleation type, crystal growth and crystallisation temperature. Volumes of literature have addressed this relationship, primarily using optical microscopy, differential scanning calorimetry (DSC) and dilatometry.

2.1.3 POLYPROPYLENE COPOLYMERS

Copolymers are another type of polymer structure that arises when two or more different kinds of monomers are combined in a single polymer chain. For example, polyethylene (PE) and PP may be copolymerised to give a copolymer, which has properties somewhat different from the parent homopolymers. To be able to describe the polymer structure fully, it is necessary to know how the two types of monomer are arranged within the chain. Three possible distinct polymer classes can be envisaged viz. alternating -, random - and block copolymers. In an alternating copolymer the two monomers are arranged in alternating positions along the backbone whereas in a random copolymer they are randomly arranged. In a block copolymer, the same monomers are clustered in blocks along the chain. The structures of these three basic copolymer classes together with the graft copolymer and the terpolymer are shown schematically in Figure 2.3.

University of Cape Town

The terminology used in the polymer industry for impact block copolymers, refer to a polymer composite consisting of a homopolymer polypropylene matrix and an elastomeric ethylene propylene rubber (EPR) phase dispersed in it. The impact block copolymers usually contain up to about 40% ethylene-propylene copolymer rubber (EPR), intimately dispersed within the matrix, usually isotactic PP homopolymer[6]. The EPR phase is added to increase the impact strength of the product, especially at low temperatures. In order to optimise impact strength, this usually implies negligible EPR crystallinity, which requires an EPR of approximately 50 mol.% ethylene content. By varying the amount of the EPR phase relative to the homopolymer phase, low-to-high impact strength products can be produced. A polyethylene phase can be added to the impact copolymer in a third stage of polymerisation, to produce a low blush-resistant

product that reduces stress whitening[3]. The compositions, molecular weights, amounts and morphologies of the dispersed EPR and continuous homopolymer phases are crucial parameters to have an effective impact copolymer.

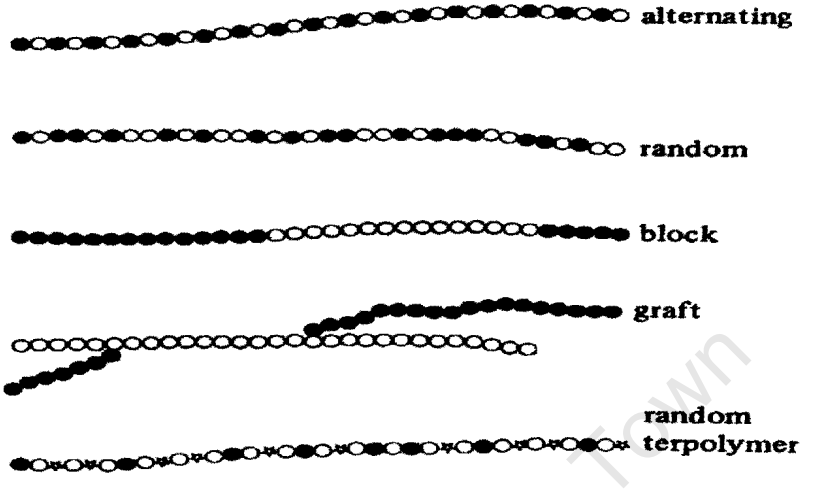

Figure 2.3 Simplified schematic of the classification of copolymers [after ref. 7]

Blends of iPP/EPR are usually prepared by in-situ reactor blending techniques, which has proved to produce polymers with superior mechanical properties at low production cost. This is because the rubber phase can reach a high degree of dispersion in the in-situ blends. A typical in-situ blend is prepared by sequential homopolymerisation of propylene in the first reactor, followed by ethylene-propylene copolymerisation in the second reactor. See section 2.2 for the manufacturing processes of the iPP/EPR[10].

One of the most significant challenges in the production of impact copolymers is to control the morphology of the growing catalyst/polymer particle, which can have a pronounced effect on the operation of the process. The incorporation and dispersion of the EPR phase in the growing polymer particle is controlled by the morphology of the previously produced catalyst/homopolymer particle. Two possible structures can arise form the addition of the EPR phase to homopolymer, as indicated in Figure 2.4.

All the EPR is usually formed at the active site of the catalyst, which is surrounded by a layer of polypropylene homopolymer from the first reactor. One possible scenario is for the EPR phase to remain contained within the micro-particles forming a "core-shell"

University of Cape Town

type micro-morphology. However, transmission electron microscopy (TEM) of the sectioned and stained impact copolymer shows that the majority of the amorphous EPR actually migrates into the interstices of the homopolymer particle. Very little EPR remains inside of the micro-particles[3]. For low-to-medium EPR levels, the EPR phase appears as a rubbery particle intimately dispersed within the pre-existing voids of the homopolymer matrix[4]. At very high EPR contents, the EPR phase becomes a continuous phase and the particles is acknowledged to be a free flowing elastomeric polymer (see Figure 2.22). This heterophasic structure is depicted in the "pore-filling" model in Figure 2.4. One major consequence of the "pore-filling" model of impact copolymers is the effect of the EPR phase on the porosity of the polymer granules. As the level of the EPR phase is increased, the porosity of the granules will steadily decrease.

University of Cape Town

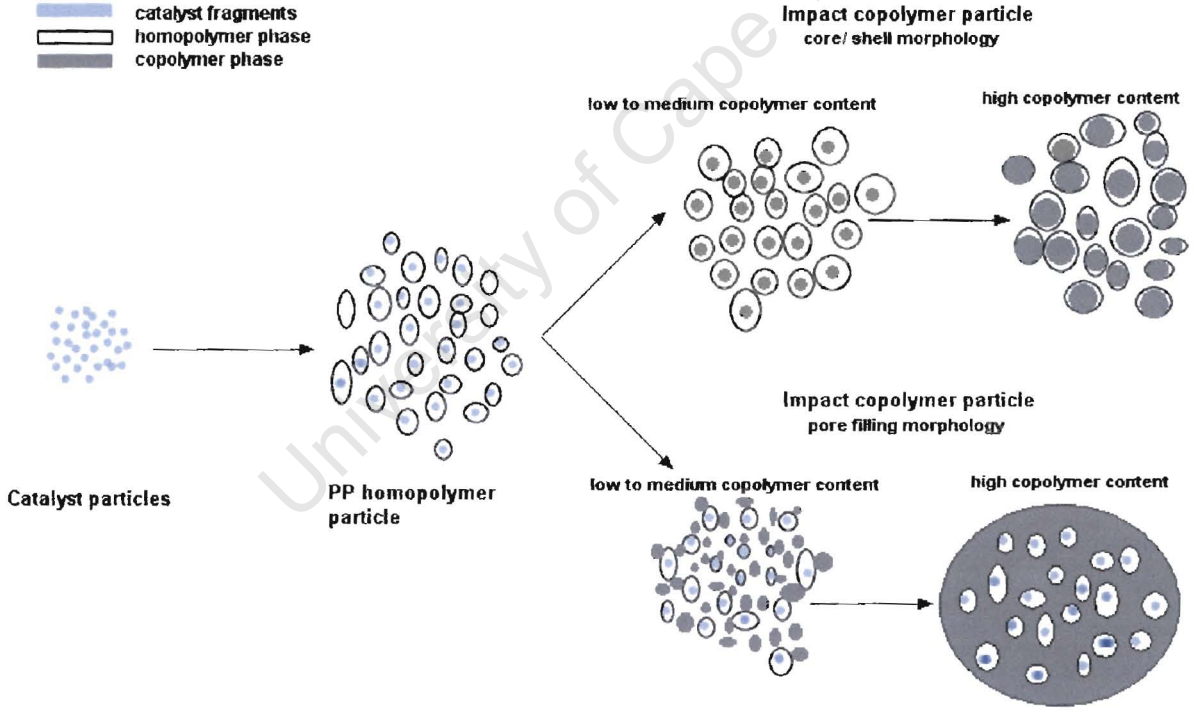

Figure 2.4 Morphology model of the impact propylene copolymers [after ref. 3]

2.1.4 Molecular Weight and Molecular Weight Distribution

The most important factors that characterise the properties of polymers such as polypropylene are density and molecular weight. The molecular weight of the polymer

is an average value since the individual polymer molecules possess different chain lengths i.e. a distribution of chain lengths occurs in bulk polymers. The molecular weight of the polymer is determined by the average molecular weight, which is defined by $\overline{M} = m/n$, where *m* is the weight of the sample and *n* the number of moles in the sample. Some properties of polymeric materials can be strongly linked to the molecular weight of the sample as shown in Figure 2.5. Some polymers with a high degree of polymerisation, may be stiff and brittle at room temperature whilst at a low degree of polymerisation, the same polymers are sticky and soft [11].

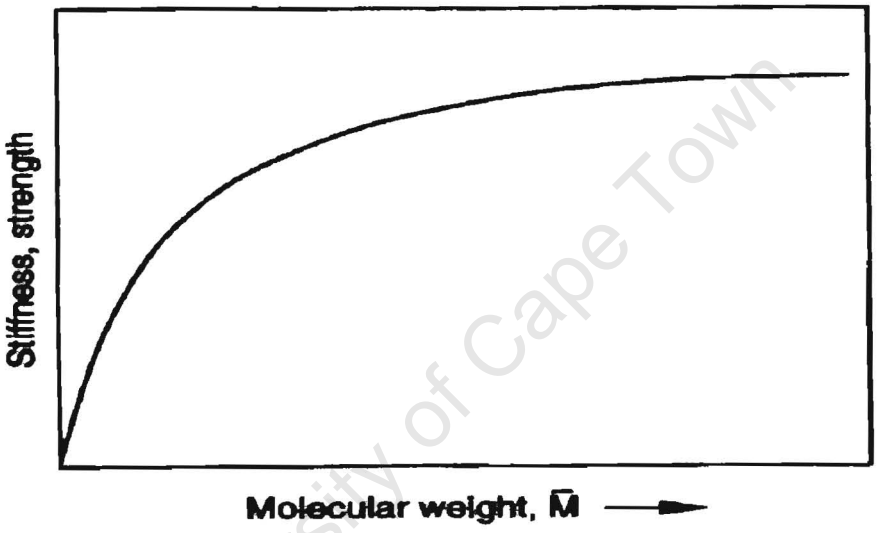

Figure 2.5 Influences of the molecular weight on the mechanical properties of the polymeric material [after ref. 11]

University of Cape Town

The relationship between the molecular weight, temperature and properties of a typical polymeric material is shown in Figure 2.6. Properties such as stiffness, strength and flow temperature increase with molecular weight and may reach an asymptotic maximum, whereas the degradation temperature steadily decreases with increasing molecular weight. Hence, it is necessary to find the molecular weight that renders ideal material properties for a finished polymer product, having flow properties that make it easy to shape the material during the manufacturing process as well as imparting adequate strength.

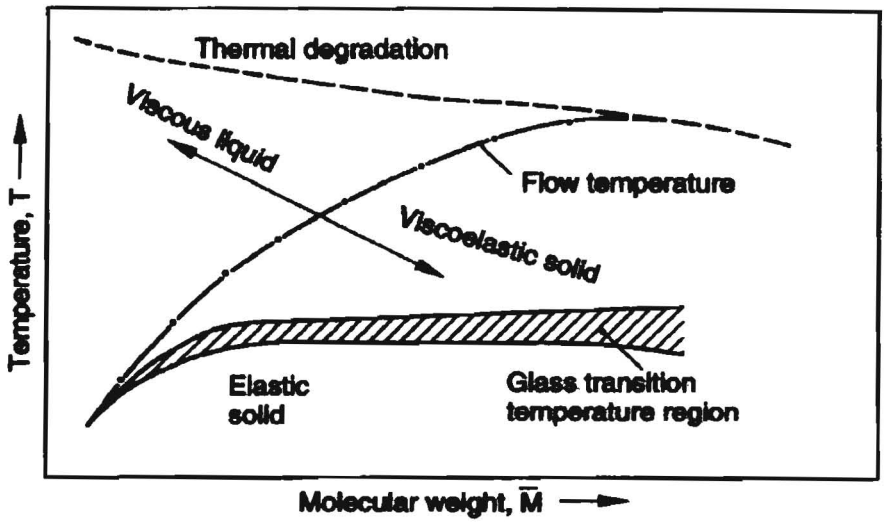

Figure 2.6 Illustration of the relationship between molecular weight, temperature and properties of a typical polymer [after ref. 11]

University of Cape Town

Most polymers exhibit a molecular weight distribution (MWD) such as that shown in Figure 2.7. For such a MWD function, we can define a number average and a weight average molecular weight. The number average is the first moment and the weight average is the second moment of the distribution function.

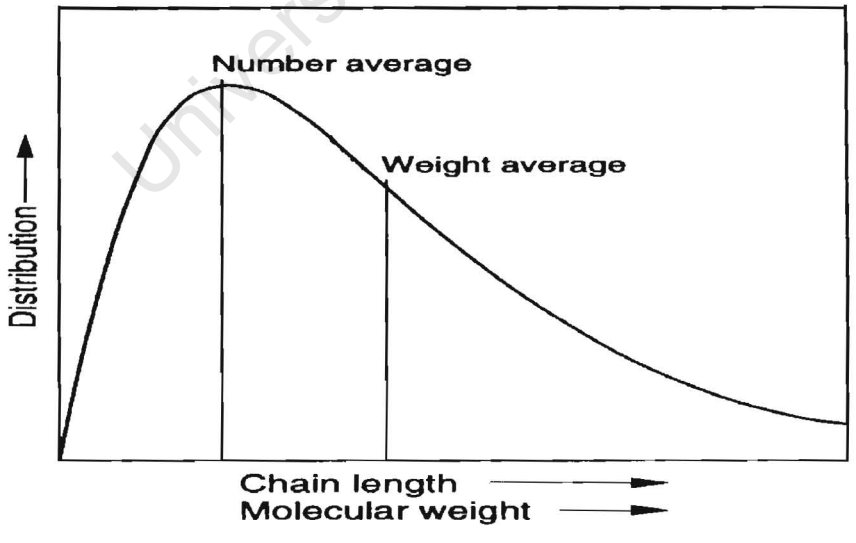

Figure 2.7 The molecular weight distribution of typical polymers [after ref. 11]

The number average is given by:

$$\overline{M_n} = \frac{\sum m_i}{\sum n_i} = \frac{\sum n_i M_i}{\sum n_i}$$

[Equation 2.2]

m_i is the weight, and n_i is the number of molecules with molecular weight M_i. The weight average is given by:

$$\overline{M_w} = \frac{\sum m_i M_i}{\sum m_i} = \frac{\sum n_i M_i^2}{\sum n_i M_i},$$

[Equation 2.3]

Figure 2.8 is a graphical representation of the relationship between the number average and the weight average on the properties of polymers. The arrows in the diagram indicate an increase in any specific properties. The MWD is a very important molecular parameter and is usually expressed as $\overline{M_w}/\overline{M_n}$. The MWD can be broad or narrow depending on the polymerisation conditions and the catalyst used. The MWD can also be controlled outside of a reactor with the use of peroxides that are commonly used to modify the MWD of polypropylenes[12]. These polypropylenes are known as "controlled rheology" (CR) polymers. With peroxide treatment the molecular weights is lowered and melt flow index (MFI) is increased. The MFI measures the rate of extrusion of thermoplastics at a defined temperature and load for a fixed period of ten minutes. For PP it is 230°C under a load of 21.6 N. Both the MWD and the MFI affect the impact strength differently. An increase in MFI decreases the impact strength, whilst a reduction in MWD (at constant MFI) increases the impact strength[13].

The amount of peroxide needed depends on several factors: (1) the MFI of the starting resin; (2) the desired MFI of the final resin; and (3) the antioxidant system used. The MWD of the degraded resin depends only on the starting MWD and the starting and ending MFI's.

University of Cape Town

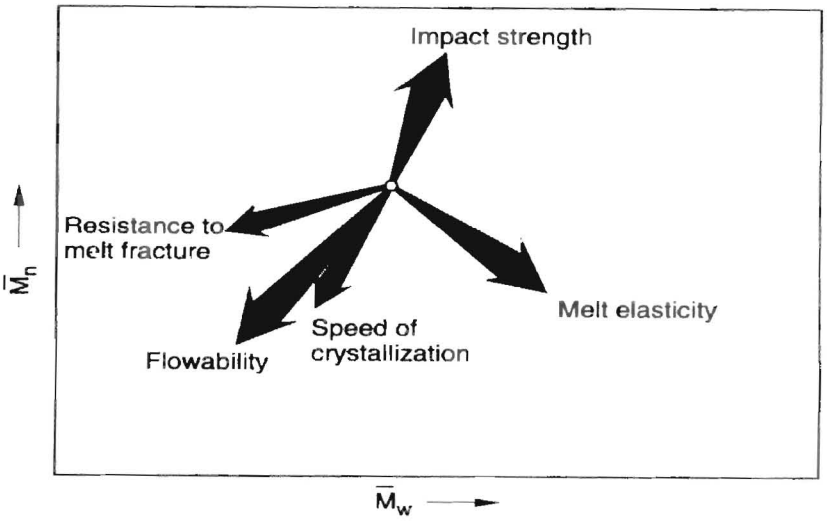

Figure 2.8 Influence of the number average and weight average on the properties of polymers [after ref. 11]

University of Cape Town

2.2 MANUFACTURING OF IMPACT COPOLYMERS

The processes that are used to manufacture polypropylene copolymers are based on the removal of the catalyst from the polymer and separation of the non-stereoregular atactic fraction. These processes also eliminate the use of hydrocarbon diluents by using either liquid or gaseous monomer as the polymerisation medium.

Processes using liquid monomer as the polymerisation medium are often divided into two categories: those using continuous stirred reactors and those using loop reactors. In either case, the use of liquid monomer as the polymerisation medium maximises the rate of the polymerisation reaction by providing a higher monomer concentration[14]. Processes using liquid monomer are often used to produce homopolymer PP and random copolymers with less than 5% ethylene. Liquid phase processes are not well suitable for the rubber phase in the liquid monomer. Consequently, the major producers of impact copolymers often use a hybrid process, consisting of homopolymerisation in the liquid phase followed by copolymerisation in the gaseous phase.

Some of the technologies provided by the major process licensors are: bulk slurry loop Spheripol PP technology (Montell), Univation PP technology (Union Carbide UNIPOL™), Novolen® PP technology (BASF), Innovene PP technology (AMOCO/Chisso) and Borstar PP technology. These processes are used to produce products with ultra high melt flow index homopolymers and high melt flow high impact copolymers, with the help of advanced fourth generation catalysts.

University of Cape Town

2.2.1 THE MONTELL SPHERIPOL PP PROCESS

The Spheripol process is widely used for the production of polypropylene copolymers using a hybrid process. The first stage of the process consists of polymerisation in liquid propylene monomer. Usually, two loop reactors are used in series to narrow the residence-time distribution of the catalyst. Polymerisation in liquid propylene results in extremely high productivities due to the high monomer concentration (~10 mol/l) and temperature (~70°C)[3]. In this process, the catalyst system (i.e. a high activity supported $TiCl_4/MgCl_2$), liquid propylene monomer and the hydrogen for molecular

weight control, are fed continuously to loop reactors for homopolymerisation, see Figure 2.9. The advantage of the loop reactor is that it offers low cost, high heat transfer and maintains a uniform temperature, pressure and catalyst distribution within the reactor. Reactor fouling is minimised by the use of the HY/HS* spherical form catalyst, with a narrow particle size distribution, coupled with high liquid velocities. The operating conditions are typically in the range of 60 to 80°C and 35 to 50 bars.

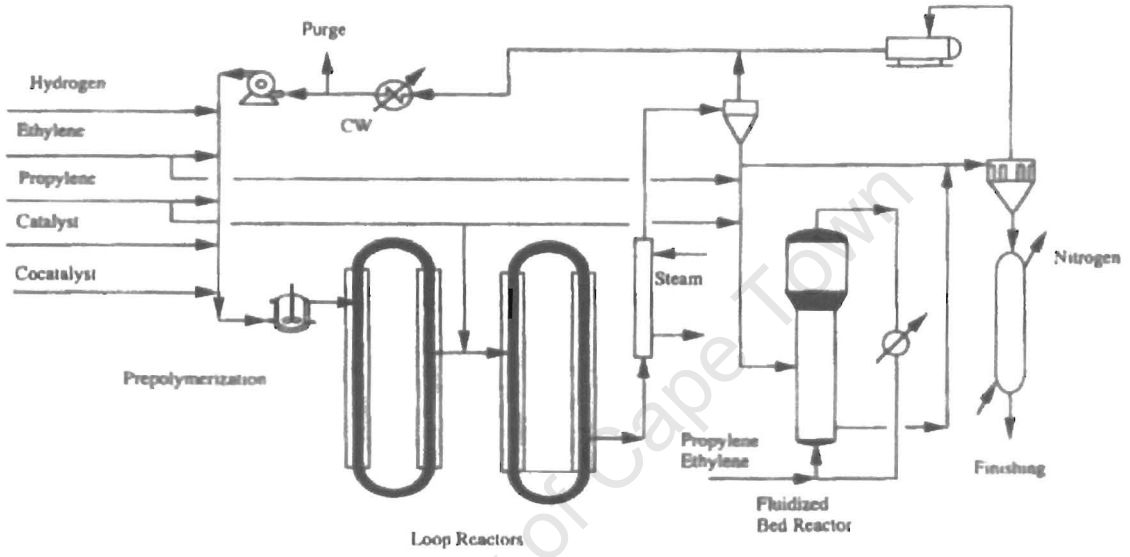

Figure 2.9 The Spheripol loop process [after ref. 15]

University of Cape Town

For the ethylene-propylene copolymer (EPR) stage, the Spheripol process utilises a gas-phase fluidised bed reactor (FBR), in series with the loop reactors. The gas-phase reactor allows the rubber to be retained in the porous particles. Fluidisation is maintained by adequate recirculation of the reacting gas (PP and PE), which also serves as the heat removal medium, via contact with cooling water in a recycling cooler. The liquid propylene/polymer suspension from the loop reactors is flashed to a gas/solid state prior to entering the second stage. The operating temperatures in the gas-phase reactors can be as high as 100°C with operating pressures of about 15 bars. Polymer exiting the polymerisation section passes through a low-pressure separator,

* HY/HS means high yield high stereospecific spherical catalyst

where the remaining monomer is separated for recycling, a steam treatment vessel to deactivate for the residual catalyst, and then lastly through a small fluid bed dryer[14].

2.2.2 THE UNION CARBIDE UNIPOL PROCESS

Union Carbide pioneered the use of the gas-phase fluidised bed reactor (FBR) for olefin polymerisation in the late 1960's, which was later adapted for the production of PP in 1985 by incorporating the Shell high activity catalyst (SHAC)[14]. The main features for this process are the two large fluid bed reactors with a wide upper section, separating the fluidised polymer from the recirculating gas as shown in Figure 2.10. One reactor is used for the production of homopolymers and a second reactor is used in series for the production of the ethylene-propylene copolymer rubber component of impact-modified copolymers. Polymer circulation resulting from the fluidisation maintains product uniformity and promotes heat transfer in the large polymer bed. The heat of reaction is removed by heat exchange between the recycle gas and cooling water. Operating temperatures for polymerisation is typically between 50°C and 100°C, with operating pressures of 30 bars in the homopolymer reactor and 20 bars in the copolymer reactor. Residence times range from 1 to 4 hours. The Union Carbide UNIPOL process employs a supported $TiCl_4/MgCl_2$ catalyst with productivities of up to 40 000g/g catalyst[3].

University of Cape Town

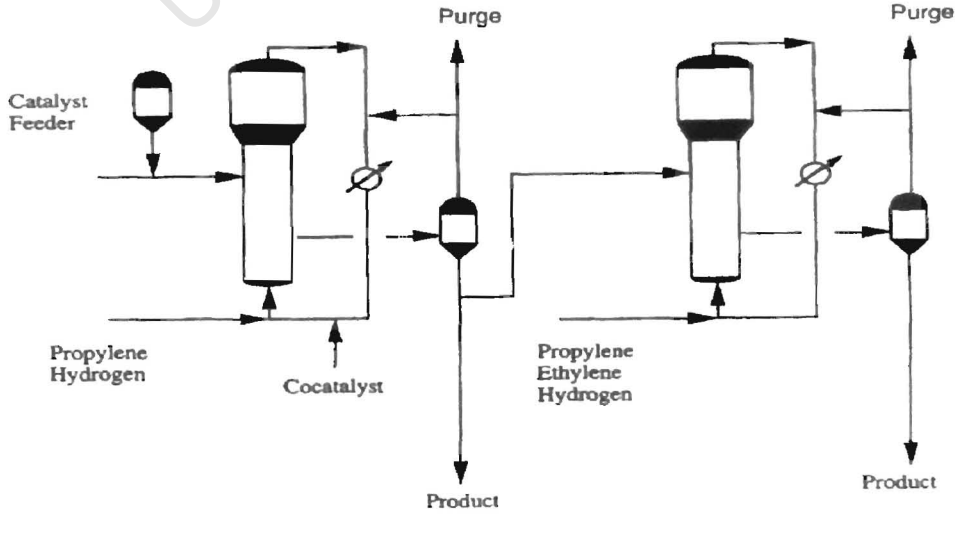

Figure 2.10 The Union Carbide fluidised-bed process [after ref. 15]

2.2.3 THE BASF NOVOLEN® PP PROCESS

The Novolen gas phase process was pioneered by BASF and has become more competitive by the use of high yield, high streospecific catalysts. The core of the process is two gas-phase vertical stirred bed reactors (VSBR) in which polymerisation is carried out continuously. A stirrer mechanically agitates the powder in each reactor. The production of impact copolymer requires two reactors connected in series (see Figure 2.11), the first is for homopolymerisation of propylene and the second for the copolymerisation of ethylene-propylene rubber. In the first reactor, liquid propylene together with the catalyst and co-catalyst system and hydrogen are fed into a reactor for homopolymerisation of PP. In the second reactor, only liquid propylene and ethylene are fed. Hydrogen is fed to each reactor to control the molecular weight. The flash heat exchange technology is used for cooling of the reactors, since the polymerisation reaction is exothermic. The polymerisation reaction and the heat exchange zone are separated in this system to avoid any wall fouling. The maximum heat exchange is achieved by flash evaporation of the liquid in the polymer bed, by injection of liquefied reactor gas mixed with fresh raw material into the reactor. Solids are removed from the reactor via a dip tube inserted into the powder bed. The pressure in the second reactor is always lower than the first reactor to permit solid transfer from the first reactor. The type of catalyst used for polymerisation in the Novolen® process, is TARGOR's PTK 4W® (an unsupported $TiCl_3$ and highly supported $TiCl_4/MgCl_2$ catalyst), a supported high yield, high tacticity system. This is suitable for the full Novolen® product range from high stiffness homopolymers to super high impact copolymers including all random copolymers[2].

University of Cape Town

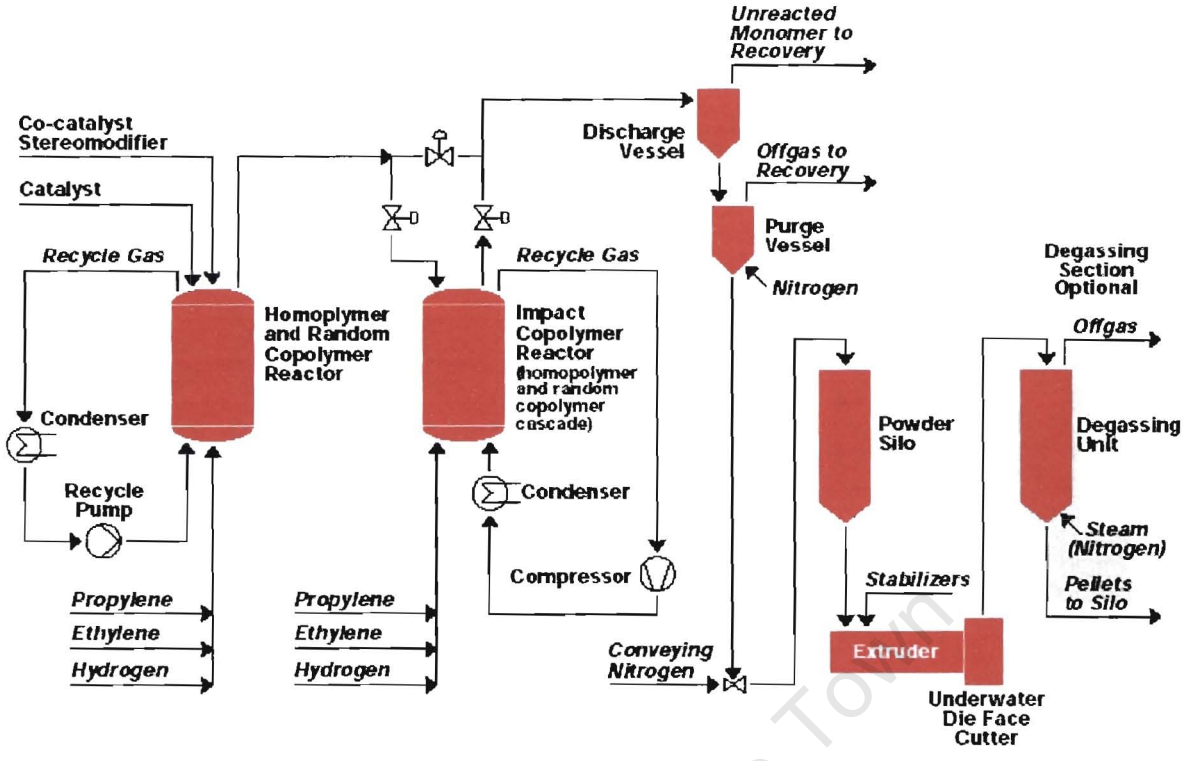

Figure 2.11 The BASF Novolen vertically stirred bed process

The pressure in the first reactor ranges from 20 to 35 bars and the second reactor operates in the range of 10 to 25 bars. First reactor temperatures range from 50 to 105°C and the second reactor temperature is usually in the range 40 to 90°C. Ethylene and hydrogen compromise up to 30 vol.% of the gas phase in the second reactor with propylene making up the remainder. Up to 40 wt.% of rubber phase has been claimed with the BASF process[3].

2.2.4 THE AMOCO/CHISSO INNOVENE PROCESS

This process uses two horizontal, mechanically agitated, multistage gas-phase reactors. This horizontal reactor design, where the polymer passes from one baffled zone to another in a pattern approaching plug flow, which behaves as a series of stirred reactors providing a narrow overall residence-time distribution of the catalyst particles and hence a more uniform copolymer content, see Figure 2.12.

University of Cape Town

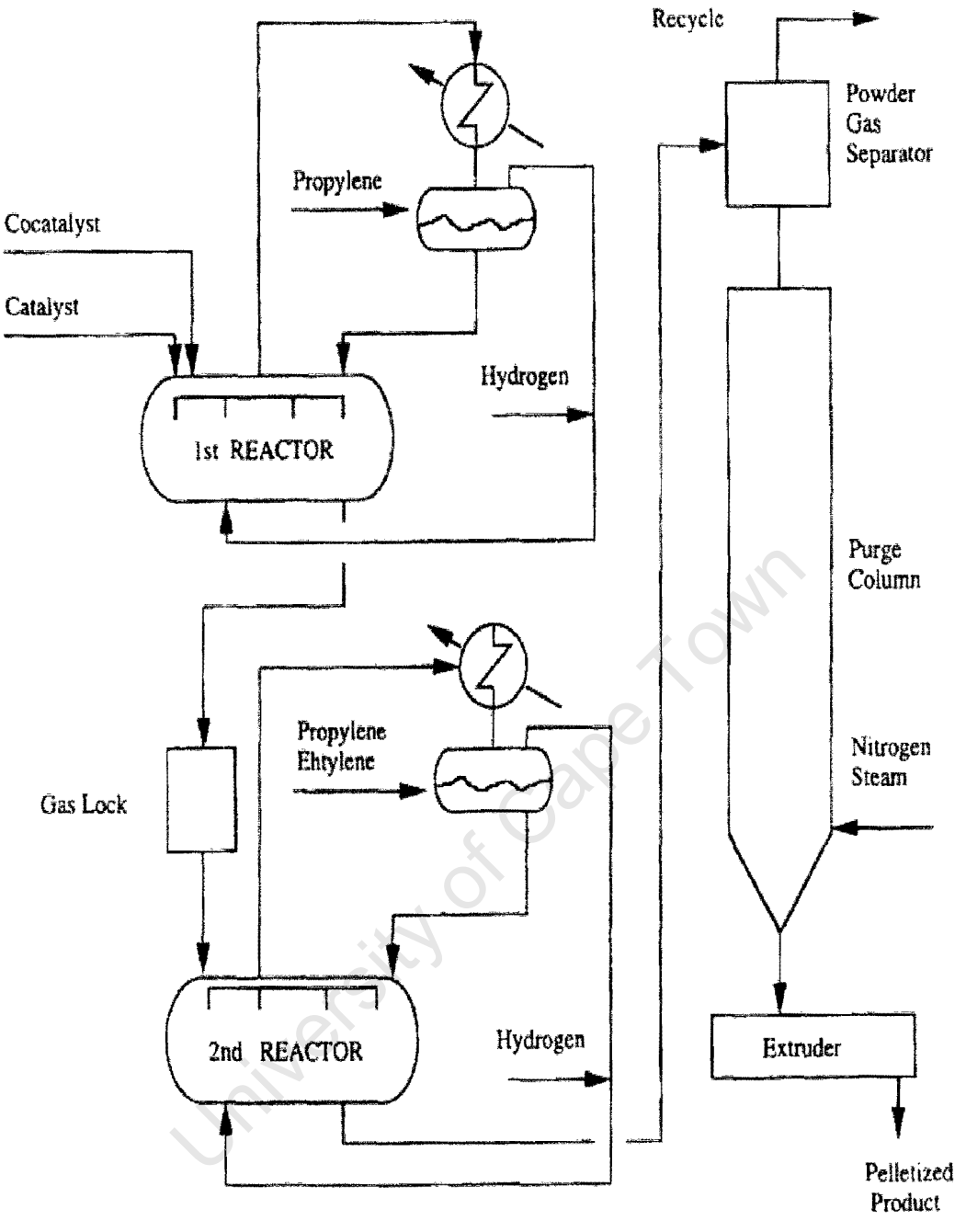

Figure 2.12 The AMOCO/Chisso Innovene horizontally stirred bed process [after ref. 15]

Polymer particle size and copolymer composition distribution can be significantly narrowed as compared to those from single stage stirred reactors. The total ethylene content in the product nominally ranges between 5.0 and 25.0 wt%. This translates to 12.5 to 62.5 wt% copolymer, assuming that the copolymer is 50 mol% ethylene[3]. In addition, the molecular weight distribution of the homopolymer can be broadened, by varying the hydrogen feed to each section of a reactor to provide different molecular

University of Cape Town

weights. As in other gas-phase processes, liquid monomer is fed to the polymer bed to facilitate heat removal. The operating conditions are also similar to other gas phase processes.

2.2.5 THE BORSTAR PROCESS

The Borstar PP process uses a combination of slurry loop and gas-phase reactors in series in order to increase production flexibility. This allows easy control of the breadth of the molecular weight and comonomer distribution. The formation of homopolymers and random copolymers is accomplished in the loop and gas-phase reactors, respectively. However, one or more smaller gas-phase reactors are often added when the production of heterophasic block copolymers is required. The process is designed to produce extremely high rubber contents and is usually built and operated in modular steps, as shown in Figure 2.13.

Propylene, ethylene and hydrogen are fed into the loop reactor together with the polymer-coated catalyst and co-catalyst, which comes from the pre-polymerisation step of the reaction. Polymerisation occurs in the reactor at high temperature conditions of 80 to 95°C and a pressure of 55 bars. These conditions are very close to the supercritical conditions of propylene. The polymer concentration in the slurry is typically 50 wt.%. The residence time is typically 0.7 hour in the loop reactor.

For the production of random copolymer, the slurry from the loop reactor is fed directly to the first gas-phase fluidised bed reactor and reacts with ethylene that is added. The reactive polymer/catalyst particles are fluidised and cooled with circulation gas. This circulation gas is cooled to remove the heat of reaction. Fresh propylene, ethylene and hydrogen are fed to the circulation gas line. The reactor is typically operated at 80 to 95°C and at 22 to 35 bars. The residence time distribution is in the region of 1.7 hours.

University of Cape Town

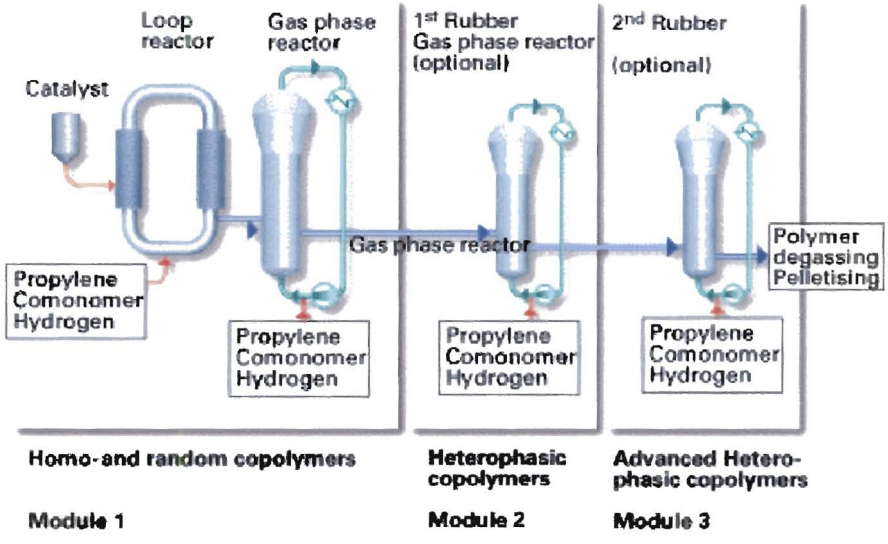

Figure 2.13 The Borstar modulated reactor [after ref. 16]

From the first gas-phase reactor, the polymer either enters the polymer degassing section or, in case of heterophasic copolymer production, the second gas-phase reactor. The second reactor is also a fluidised bed reactor and is used to produce the rubber phase of heterophasic copolymers. The operating conditions are in the temperature range of 70 to 80 °C and pressures of 15 to 20 bars. Fresh propylene, ethylene and hydrogen are fed to the circulation gas line. The circulation gas is cooled to remove the heat of reaction. The polymer outlet system is continuous, and the residence time distribution is in the region of 0.7 hour[3].

University of Cape Town

2.3 Physical Properties of Polypropylene Copolymers

2.3.1 Morphology of Injected Moulded Polypropylene

The injection moulding process is one of the most commercially important fabrications for moulding a broad spectrum of thermoplastics and provides an additional illustrative example of a strong interrelationship between structure, processing, morphology and final polymer properties. In the injection moulding process, molten polymer is injected into a cold mould cavity with geometry of the desired shape. The final morphology of a moulded part is a direct result of flow processes during mould filling and subsequent solidification[17].

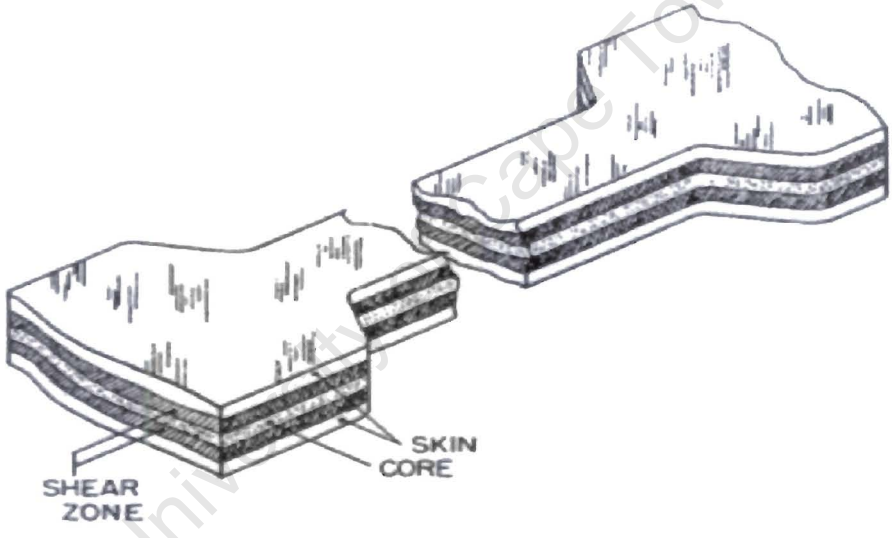

Figure 2.14 Skin-core morphology of injection moulded articles [after ref. 17]

Injection mouldings of iPP exhibit "skin-core" macrostructures and frozen-in orientations, which are sensitive to moulding conditions. The "skin-layer" in Figure 2.14 is due to the highly oriented flow-induced microstructure which is frozen-in by crystallisation. The morphology becomes spherulitic moving away from the part surface towards the "core-layer". The effective cooling rate is much lower in the "core layer", allowing more time for relaxation of the flow-induced orientation prior to solidification. These factors lead to less orientation in the core layer relative to the skin layer. The spatial distribution of the orientation in an injection-moulded part is important because

of the sensitivity of properties to frozen-in orientation. Depending on the moulding conditions and flow pattern, a continuous decrease of orientation or a local orientation maxima moving away from the surface to the core is observed.

According to Kantz and co-workers, the thickness of the skin-layer varies inversely with temperature[17]. The thickness of the intermediate layer varies with injection pressure, in a complex manner. It is also observed that the preferred crystallite orientation in the skin and the intermediate layer exerts a profound effect on the mechanical properties. Tensile yield strength, impact strength and shrinkage increase with increasing combined thickness of the two oriented outer layers[17].

2.3.2 Effect of the Processing Conditions

The compounding/fabrication process, in addition to the relative chemical composition and molecular weight of the PP and EPR phases, determines the morphology of rubber-modified PP. The blend of rubber-modified PP separates into distinct phases, the PP homopolymer and the rubber phase. Recent advances in multistep polymerisation technologies have added a new dimension to the control of rubber-modified PP. These advances include the ability to polymerise the rubber phase directly in the homopolymer matrix, a choice of monomers and monomer ratio and molecular weight control. The resultant product yields an as-polymerised finely dispersed rubber phase, which allows for the tailoring of rubber phase morphology and interfacial tension.

The morphologies observed in rubber-modified PP's range from a dispersed to a continuous phase structure. The rubber phase has its own morphological characteristics resulting from its structure and melt processing and crystallisation history. Figure 2.15 shows TEM micrographs of the dispersed phase structure of a typical reactor polymerised rubber-modified PP homopolymer. The materials have approximately 14% rubber phase and were injection moulded at 193°C (Figure 2.15(a)) and 215°C (Figure 2.15(b)). The average rubber particle size has increased with increasing injection moulding temperature, whilst the impact properties decreased[6].

University of Cape Town

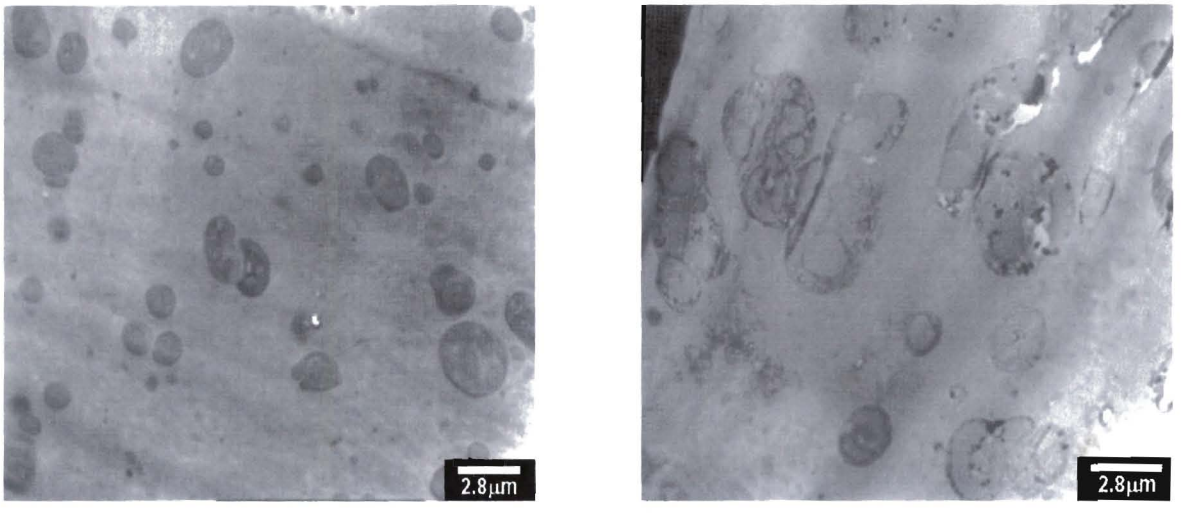

(a) (b)

Figure 2.15 TEM micrographs of reactor polymerised iPP/EPR injection moulded at: (a) 193°C with a five-minute barrel hold time, (b) 215°C with a ten-minute barrel hold time [after ref. 6]

University of Cape Town

The viscosity ratio ($\eta_r = \eta_{dispersed}/\eta_{matrix}$) of the blend is important in determining the effect of melt processing. This ratio is also an important factor governing dispersion in the reactor-produced blends. The change in the viscosity ratio in a reactor blend results in the change in a morphology as shown in Figure 2.16 for injection mouldings of low and high viscosity ratios.

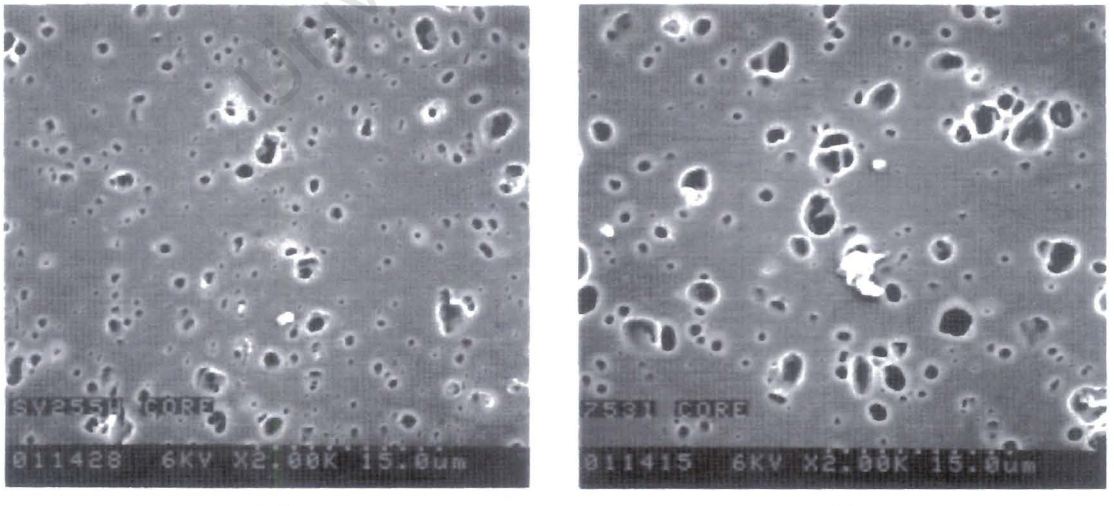

(a) (b)

Figure 2.16 SEM microphotographs of the reactor polymerised iPP/EPR with: (a) low viscosity ratio, (b) high viscosity ratio [after ref. 6]

A low viscosity ratio gives rubber particles of even distribution and small size. An increase in the viscosity ratio gives large particles of an uneven distribution, because the decrease in matrix viscosity reduces its ability to transfer shear stress to the rubber phase and break it apart[18].

2.3.3 Effect of the Modifying Phase

Rubber particles dispersed in the polymer matrix act as stress concentrators to initiate a transition of the deformation behaviour of matrices from highly localised shear yielding or crazing to extensive shear yielding or multiple crazing. The difference in the fracture behaviour can be examined by using scanning electron microscopy (SEM) and transmission electron microscopy (TEM). The rubber particles have two functions: it has to relieve the volume strain by cavitation and it has to act as stress concentrators[19]. Both the relieving of the volume strain and the stress concentrations are directly related to the rubber content[20].

The ductile-brittle transition (DBT) in polymer blends and composites is governed by morphological parameters such as rubber particles size and rubber content. For a given particle size, the DBT has been observed to occur at a certain critical particle content. For constant particle content, it is also seen at a certain critical particle size. It has been demonstrated that the particle size distribution is a crucial parameter in determining the DBT behaviour, and it must be emphasised that the critical values of particle size and content are functions of the particle size distribution.

Van der Wal and Gaymans studied the effect of particle size and they observed that for polypropylene-rubber blends, particles larger than 0.5 μm initiate crazes, while particles smaller than 0.5 μm initiate yielding when it comes to the deformation mechanisms involved. These are accompanied by stress whitening due to cavitation in the system. The larger the particles size the more easily will the cavities be expected to form. However, cavitation of the large particles proceeds differently from the small particles. The large particles contain several cavities situated near the interface with the matrix.

University of Cape Town

2.3.4 Toughening Mechanisms

The difference in toughening due to particle size may be attributed to the test method dependence associated with a change in the deformation mechanism. Therefore shear yielding and crazing have been proposed according to the different test methods[21,22,23]. In addition, the strain-rate and the specimen geometry also influence the deformation mechanism.

Different deformation mechanisms due to the fracture test method are possibly related to the disentanglement behaviour of the polymer chain in the deformation region. For crazing, molecular chains have to be disentangled during loading, as in low strain-rate tests, where there is enough time for chains to be disentangled. Crazing of toughened polymer can occur below some critical strain rate and at a high triaxial stress state that is satisfied by the presence of the notch tip. On the other hand, in the case of impact tests, where the test speed is much higher, there is not enough time to disentangle the polymer chain. Therefore, the deformation occurs in the mixed mode but the main deformation mechanism is shear yielding induced by the cavitations. However, the deformation mechanism of the toughened polymer is still ambiguous and contradictory results have been reported in the past[12].

University of Cape Town

2.3.5 Characterisation of Impact Copolymers

In order to optimise the mechanical and micro-mechanical properties of the polymer blend, it is better to understand the toughening mechanisms that occur during modification.

Optical Microscopy (OM) can the used to study the crystallisation of polymers including the rate at which the spherulites grow and the effects of modifiers on the crystallisation of the matrix. OM can also be used to observe gross features of the deformation processes such as the visualisation of shear bands and crazes and the size and shape of the plastic zone ahead of the crack tip.

Scanning Electron Microscopy (SEM) is useful for observing the fracture surfaces of the polymer. The deformation mechanisms of large rubber particles that have cavitated can be readily been seen in Figure 2.17 when using SEM. However, SEM cannot be

used to study crazing because it is a sub-surface feature. Instead, transmission electron microscopy (TEM), which requires great care for specimen preparation, is a much more useful technique to study the deformation below the fracture surface.

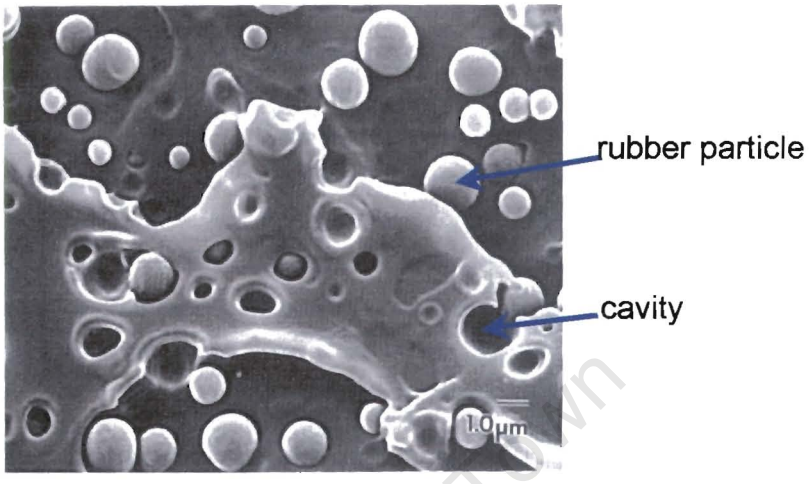

Figure 2.17 SEM micrograph of a notched Izod fracture surface of a polyacetal / polypropylene copolymer showing the dispersed rubber-particles [after ref. 24]

University of Cape Town

***Specimen Preparation for TEM Investigations*[25]:**

- **MICROTOMY**

Many polymer specimens are prepared for electron or optical microscopy by direct cutting of slices less than 100 nm thick. Generally, microtomy refers to sectioning of materials for observation in a microscope by transmitted light. This can be achieved using either glass or diamond cutting knives in an ultra-microtome.

Cryo-microtomy is the sectioning performed at low temperature to produce ultra-thin sections of polymer too soft for room temperature sectioning. Polymers with a T_g below room temperature are soft and can be hardened by cooling with liquid nitrogen, prior to sectioning. Cryo-microtomy gained popularity recently as a result of the ease of use of new commercial instruments. At low temperature such as –120°C, sectioning is more difficult and as a result a dry knife must be used. Dry sections are difficult to pick up without causing damage to the sections.

- **STAINING**

In TEM, image contrast is the result of variations in electron density among the structures present. This image contrast is the result of shadowing with heavy metals in a vacuum evaporator or staining, generally by addition of heavy atoms to specific structures.

Staining, involves the incorporation of electron dense atoms into the polymer, in order to increase the density and thus enhance contrast. Staining refers to either the chemical or the physical incorporation of heavy atoms. Most of the stains applied to the polymers are positive stains, meaning the region of interest is stained dark by either a chemical interaction or selective physical absorption.

Types of stains used in polymer blends

- *Osmium tetraoxides (OsO_4)* react with carbon-carbon double bonds in the unsaturated rubber phases enhancing the contrast in TEM by the increased electron scattering of the heavy atoms in the rubber compared to the unstained matrix. The reaction is important as it both fixes and stains the polymer. Fixation (shown by the reaction below) is a chemical crosslinking or bridging of the rubber, which causes hardening and increased electron density. Staining is also known to take place by selective absorption in both semicrystalline and amorphous polymers.

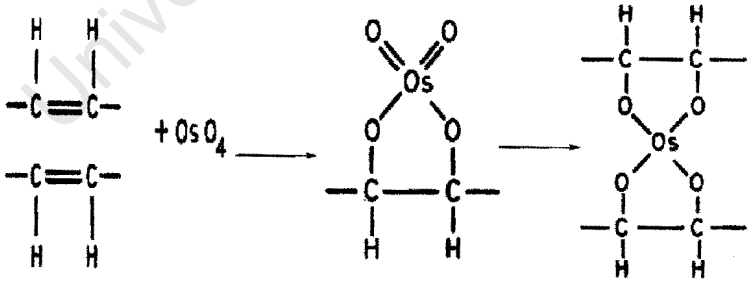

The staining reaction is slow, often taking days to weeks, when staining a block of material in an aqueous solution. OsO_4 is used to stain polymers with functional groups such as unsaturated hydrocarbons (-C=C-), alcohol's (-OH-), ethers (-O-) and amines ($-NH_2$).

- *Chlorosulphonic acid ($ClSO_3H$)* is used to enhance the lamellae structure of polyethylene. The soft bulk PE crystals cannot be sectioned, and is unstable in the electron beam due to radiation damage. The chlorosulphonation procedure

University of Cape Town

crosslinks, stabilises and stains the amorphous material in crystalline polyolefin's, permitting ultra-thin sectioning and stable electron microscopy observation.

- *Ruthenium tetraoxide (RuO_4)* is known to be a stronger oxidising agent than osmium tetraoxide and is supposedly superior for staining rubber. RuO_4 stains polymers containing both saturated and unsaturated hydrocarbons, ether, alcohol, aromatic or amine moieties. RuO_4 is very unstable, very expensive and not always available in a compound. Trent and other researchers found a way of easily preparing RuO_4 in the laboratory under a hood. The Trent method involved preparing the RuO_4 by oxidising the hydrated ruthenium dioxide ($RuO_2 \cdot xH_2O$) with sodium periodate ($NaIO_4$) as shown by the following reaction:

$$RuO_2 \cdot H_2O + 2NaIO_4 \rightarrow RuO_4 + 2NaIO_3 + 2H_2O$$

This reaction is completed in approximately 3-4 hours[26]. Another alternative of producing RuO_4 is using Montezinos method, which is to oxidise ruthenium trichloride ($RuCl_3$) with sodium hypochloride (NaClO) as shown by the following reaction[27,28]:

$$2RuCl_3 \cdot 3H_2O + 8NaClO \rightarrow 2RuO_4 + 8NaCl + 3Cl_2\uparrow + 3H_2O$$

In both processes the RuO_4 staining compound of 0.1 to 1.0% by weight can successfully be achieved.

A typical TEM microstructure of rubber- modified polypropylene is shown in Figure 2.18 below. The EPR rubber particles (a) are stained dark, the light polypropylene matrix (b) has a fine lamellae structure, whilst the polyethylene lamellae (c, arrowed) are much coarser.

University of Cape Town

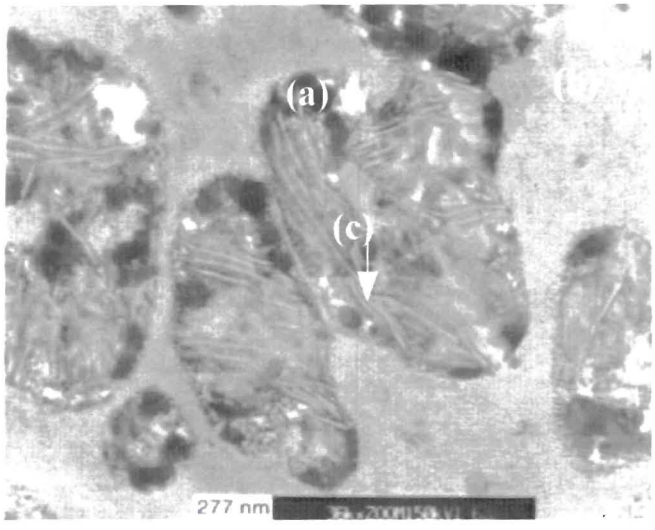

Figure 2.18 Typical TEM micrograph of rubber-modified PP with crystalline PE dispersed in the rubber phase [after ref. 6]

University of Cape Town

Wide Angle X-Ray Scattering (WAXS) is used to provide information pertaining to the degree of crystallisation and the orientation texture. Isotactic PP can crystallise in three different crystal modifications: the monoclinic α-form, the hexagonal β-form and the triclinic γ-form. In melt-crystallised iPP the predominant crystal structure is the α-modification[30].

The β-modification is observed only occasionally during crystallisation and it appears as a minor constituent of the PP. The hexagonal β-phase is identified by a strong maximum for the $(300)_\beta$ crystallographic plane occurring for the interplanar distance at 0.550 nm relative to the dominant α-phase. The relative amount of β-phase (K value) is determine by the ratio between the intensity I_β of the peak for the (300) diffracting plane and the intensities $I_{\alpha1}$, $I_{\alpha2}$, and $I_{\alpha3}$ of the (110), (040), and (130) planes respectively, as well as I_β of the $(300)_\beta$ crystallographic plane. Mathematically, the K value is given is given by:

$$K = \frac{I_\beta}{I_{\alpha1} + I_{\alpha2} + I_{\alpha3} + I_\beta}$$

[Equation 2.4]

According to Tjong and co-workers the addition of β-nucleating agents into the iPP homopolymer would result in an increase in the impact resistance and this improvement

in the impact properties is associated with the formation of microcrazes within the PP[29,30].

The γ-phase crystallinity is relatively uncommon for iPP homopolymer formed under typical commercial processing conditions and it is the least understood crystalline state for iPP[6]. More recent studies have demonstrated that the γ-form is produced at atmospheric pressure and elevated temperature for high molecular weight homopolymer and that it has the same diffraction pattern as the low molecular weight homopolymer. Its formation is also believed to be enhanced by the presence of copolymers into the iPP[31]. The X-ray diffraction patterns of the α- and γ-forms has been found to be similar in many respects, but the third strong reflection at the interplanar spacing 0.477 nm from the α-form is absent in the γ-form and is replaced by a line at 0.442 nm[32,33]. These characteristic peaks are found in the 2θ plot between the angles 18.0-19.0°, 15.0-16.0° and 19.2-20.5° for the α-, β-, and γ-crystals, respectively. Figure 2.19 below show the spectra of iPP.

Feng and co-workers used the wide-angle x-ray diffractometer to determine the compositional heterogeneity of the polypropylene-ethylene block copolymers, taking scan of fractions eluted at different temperatures[34]. Their results show that, for the higher temperature fractions, the crystalline peaks are sharp and distinctive, and that the amorphous background is small compared with those eluted at room temperatures.

University of Cape Town

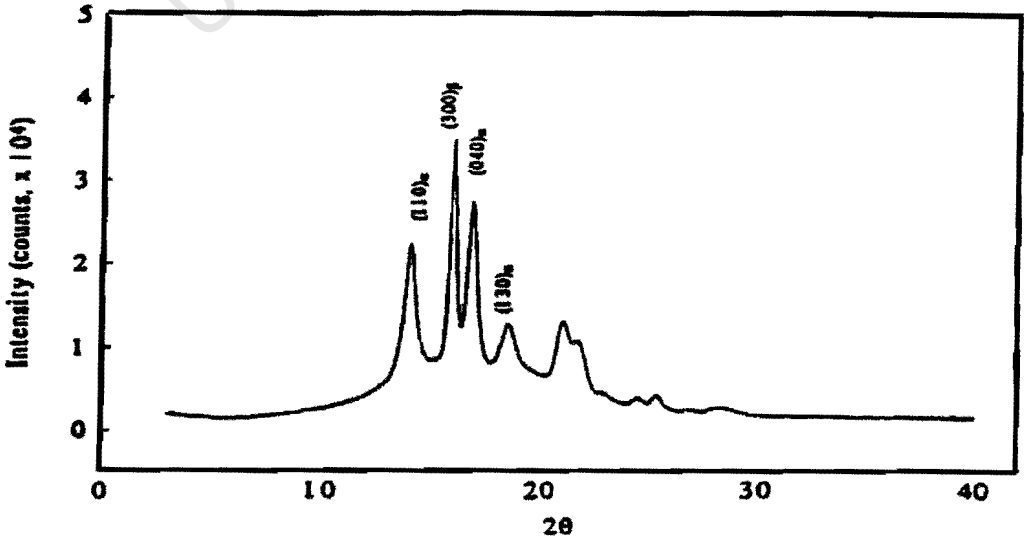

Figure 2.19 A typical WAXS diffratogram for polypropylene [after ref. 36]

Feng's results also show a clear peak of PE at about $2\theta = 23.4°$, which can be assigned to the (200) crystallographic plane of the PE crystal. This indicates the existence of long ethylene sequences in the copolymer fractions. In addition, the diffraction lines at 14.15° $(110)_\alpha$, 16.05° $(300)_\beta$, 16.75° $(040)_\alpha$ and 18.60° $(130)_\alpha$ show the characteristics of iPP.

WAXS can also be used to measure the volume fraction crystallinity, X_c, (equation 2.5) from the ratio of the areas under the crystalline and amorphous reflections, A_c and A_a respectively, as shown in Figure 2.20:

$$X_c = \frac{A_c}{A_c + A_a}$$

[Equation 2.5]

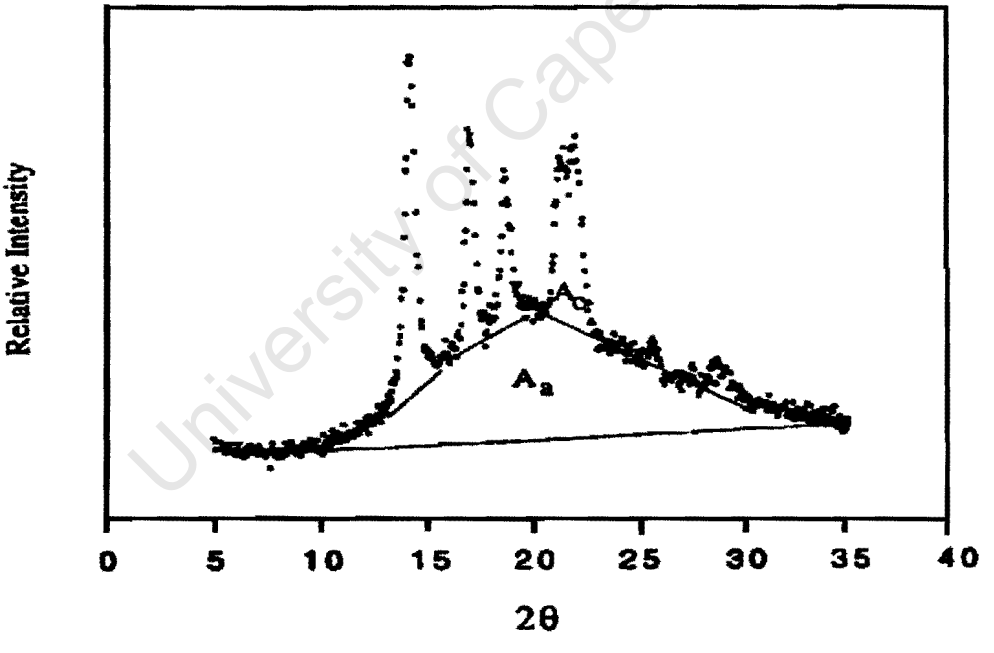

Figure 2.20 WAXS diffractogram showing the calculation method for crystallinity [after ref. 33]

The accuracy of the results obtained using the above mentioned method is limited by the difficulties in estimating the contribution on the amorphous background.

Fourier Transform Infrared Spectroscopy (Ft-IR) is used in the characterisation of the polymer, especially the chain structure and structural homogeneity of an iPP/EPR

University of Cape Town

copolymer. The monomer composition of the ethylene-propylene copolymer samples can be determined by means of Fourier transform infrared spectroscopy in the mid-infrared (4000-350 cm^{-1}) and near infrared (10000-4000 cm^{-1}) regions. The PE/PP ratio in the known copolymer composition can be determined from the mid-IR and near-IR and the different bands can be used in the analysis depending on the amount of PE present. The ethylene content can be estimated using the empirical formula based on the IR spectrum:

$$\ln A_{1150}/A_{720} = 2.98 - 0.060*C_2$$

[Equation 2.6]

where A_{1150} and A_{720} are the absorptions at the wavelengths of 1150 and 720 cm^{-1} respectively and C_2 is the mole percentage of ethylene in the polymer[10].

2.3.6 Characteristics of the Elastomer in Polymer Modification

The most important elastomers in the impact modification of polypropylene are the ethylene-propylene rubber (EPR) and ethylene-propylene-diene-monomer (EPDM)[10,12-14,17-20,35,36,37]. The important factors that determine the effectiveness of copolymers are:

- *Amount of rubber content*: The extent of impact enhancement increases with rubber content. It is known that the modulus and yield stress decreases with increasing rubber content while the ductile-brittle transition shift to lower temperatures[20,38]. Figure 2.21 shows the effect of rubber content on modulus and yield strength for a PP-EPDM blend.

  Microscopic studies show how the morphology of rubber particles changes with the rubber content. Three types of dispersed morphologies can be observed: (1) rubber particles dispersed in a continuous PP matrix, when the rubber content is lower than the PP content and when the two components have the same melt viscosities, (2) co-continuous PP and rubber phases, in the intermediate composition range when the melt viscosity of the rubber is lower than that of the PP. (3) at higher rubber content, PP particles will be dispersed in the continuous rubber phase[39]. Figure 2.22 below show examples of dispersed rubber particle morphologies as discussed above in systems (1) and (2).

University of Cape Town

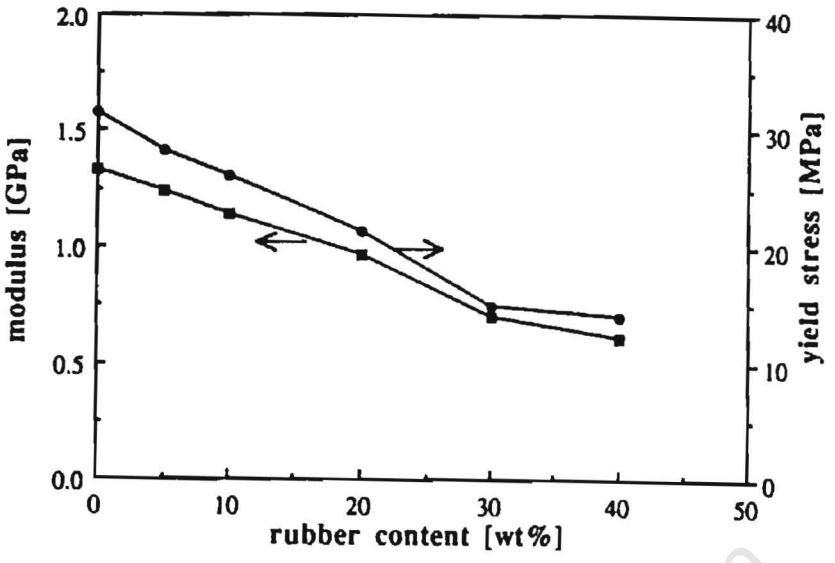

Figure 2.21 The tensile modulus and tensile yield stress as a function of the rubber content for PP-EPDM blends. ■ modulus and ● yield stress [after ref. 20]

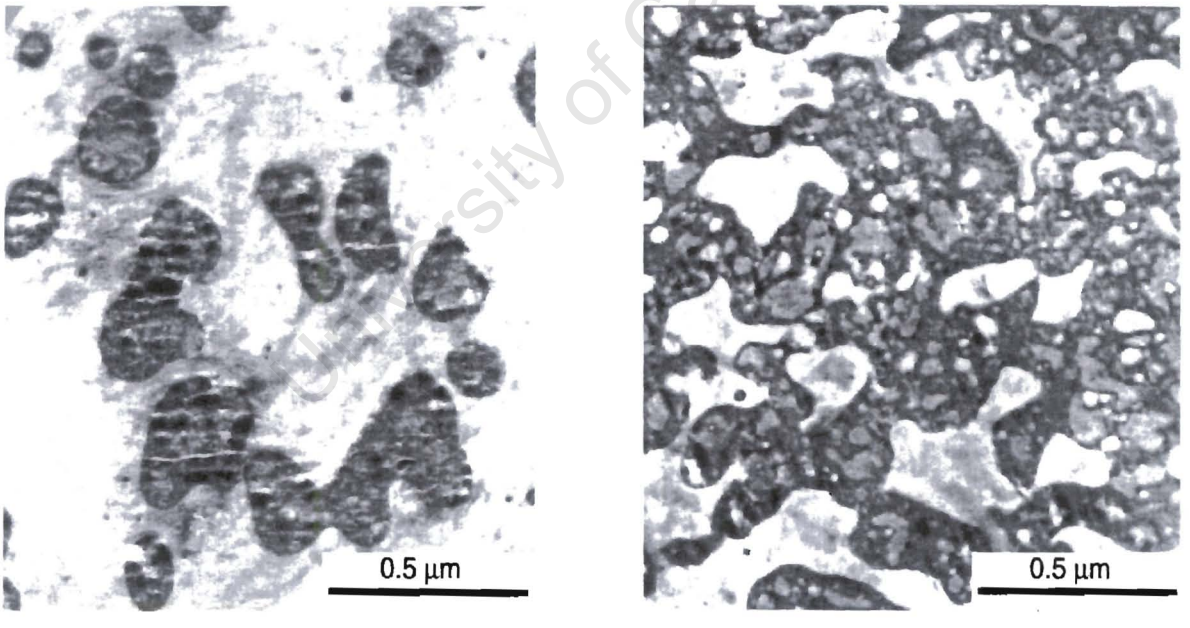

Figure 2.22 TEM micrographs of: (a) rubber particles dispersed in the PP matrix for 83% PP-17% EPR and (b) co-continuous PP and rubber phases for 35% PP-65% EPR [after ref. 39]

University of Cape Town

- *Particle size and distribution*: The impact characteristics can be influenced by the rubber particle size, principally through the effect of initiation and termination of crazing and shear yielding. It is well known that, for a particular polymer blend, there is a critical particle size that yields optimum toughness. For PP/EPR the critical particle size is thought to be about 0.4 μm to yield optimum toughness[6]. It has been shown that the particle size distribution considerably influences the impact strength of the material. It is well known that agglomerated rubber particles cannot toughen polymers. Hence, the morphology of well-dispersed particles is expected in all the polymer blends[22]. However, according to Liu and co-workers, there is another morphology of particle distribution that has a much better toughening efficiency than well-dispersed morphology. This morphology is called a pseudo-network morphology, whereby the rubber particles are randomly dispersed in the polymer matrix[22,23,47].

- *Chemical affinity for the PP matrix*: The blending of two immiscible polymers rarely results in a material with favourable properties. The polymer typically segregates into macroscopic domains that have high interfacial tension and poor interfacial adhesion. The resulting material will have poor mechanical properties. For the polymer blends, the interfacial adhesion is critical for the effective action of the impact-modified polymer. An attractive approach to improving interfacial adhesion is to employ an interfacial agent, such as a graft or block copolymer, whose parts are compatible with the different phases in the blend. The introduction of these interfacial agents reduces the interfacial tension and promotes interfacial adhesion. The results of the improvement in adhesion are a more stable, finer dispersion of the minor components and a great improvement in the mechanical properties. Also, for polypropylene impact copolymer blends at a fairly high level of ethylene, polyethylene crystallinity begins to show within the rubber phase. As a consequence, the rubber particle shrinks more during cooling, which then reduces the stress that otherwise would build up in the matrix, and the tendency to give a stress-whitening effect is reduced. Therefore, the adhesion and impact values reach a maximum. At still higher ethylene contents, the rubber becomes stiffer, the dissimilarity between the higher ethylene content in the EPR and the PP matrix increases, adhesion is lost and the impact strength falls. The maximum impact

University of Cape Town

strength occurs at about 50 to 60% ethylene in the rubber and falls off rapidly on either side of this range.

2.3.7 Thermal Properties of Polymers

Dynamic Mechanical Analysis (DMA) is a technique that characterises the viscoelastic properties i.e. properties relative to both the solid and liquid characteristics that change with temperature, time and frequency. To measure the viscoelastic properties, a DMA applies a sinusoidal force to a sample and then measures the resulting sample deformation or strain. The sample strain response lags behind the input stress wave with respect to time and the lag is known as the phase angle. The storage modulus, E', measures the ability of a material to store energy and is related to the stiffness of the material. The loss modulus, E", is the energy dissipated by the sample because of molecular motion and reflects the damping characteristics of materials. The loss tangent is given by the ratio, tan δ = E" /E'.

The DMA can be used to determine the thermal properties of blends of polymers, which may or may not be miscible. For a completely immiscible polymer, two peaks of the glass transition temperature (T_g) that corresponds to the parent copolymers can be seen[40,43], as seen Figure 2.23 below. When the difference between the two peaks is small there is good cohesion between the two phases and therefore better impact properties.

University of Cape Town

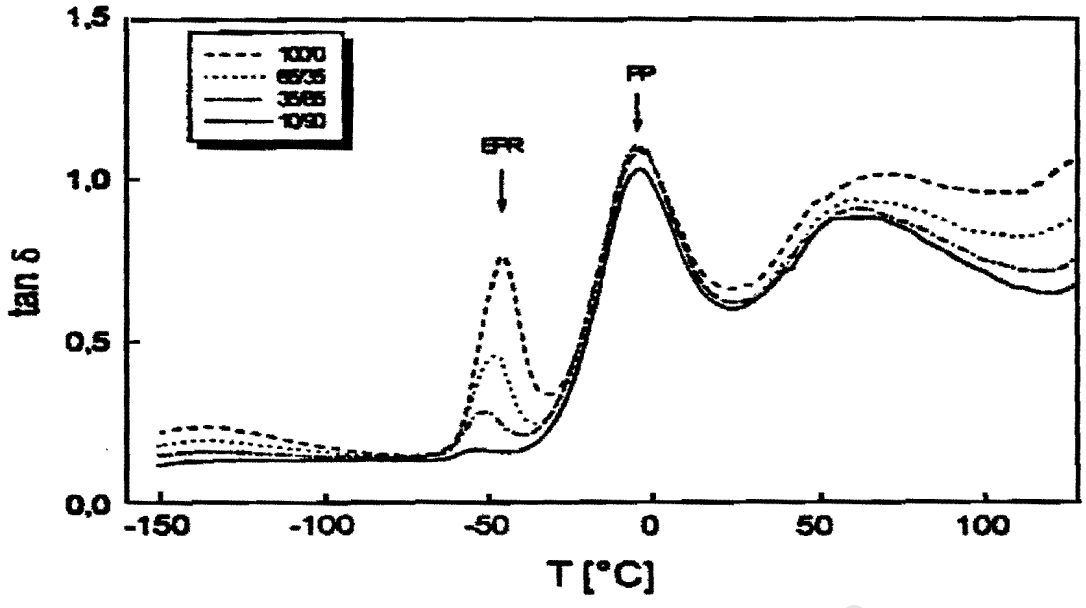

Figure 2.23 DMA spectrum of iPP/EPR blends with different compositions. The arrows indicate the T_g positions of the EPR and PP [after ref.41]

Since it is well known that melt-crystallised iPP exhibits α-, β-, and γ-relaxations at the temperature range from –150 to 150°C, Feng and co-workers[42] have investigated the molecular relaxation of iPP homopolymer and its copolymers. The α-relaxation is generally attributed to the crystalline phase and appears as a shoulder at the temperature range of 35 to 90°C, the β-relaxation correspond to the transition from the glassy to the rubber-like state and occurs at 0°C and is the dominant peak. The γ-relaxation is usually assigned to the local mode relaxation in the amorphous phase and it occurs at –100°C. Figure 2.24 below shows the DMA spectrum of iPP and its copolymers. Feng's results show three relaxations in the iPP homopolymer and random copolymer, as compared to four relaxation processes appearing for block copolymers. In the block copolymer there is another transition that appears at about –50°C and is attributed to the β_2-relaxation. This transition suggested that there is an EPR component existing in the block copolymer and because of the existence of the EPR component, the breaking energy of the block copolymer is much higher than that of iPP.

University of Cape Town

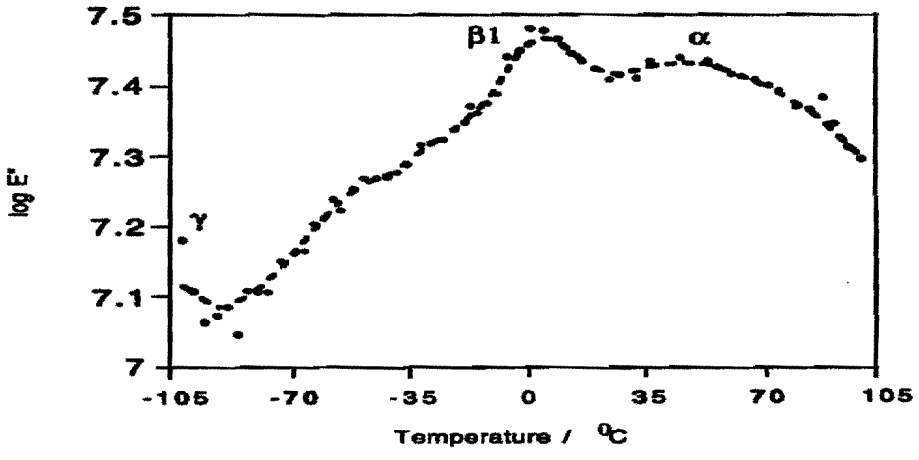

(a)

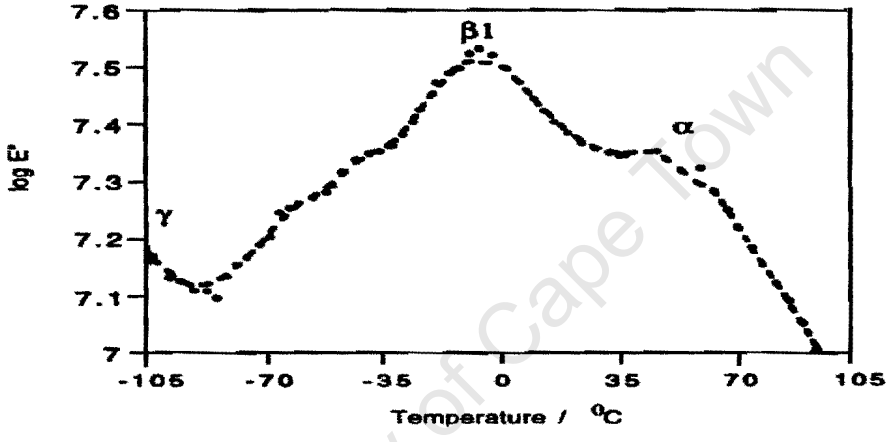

(b)

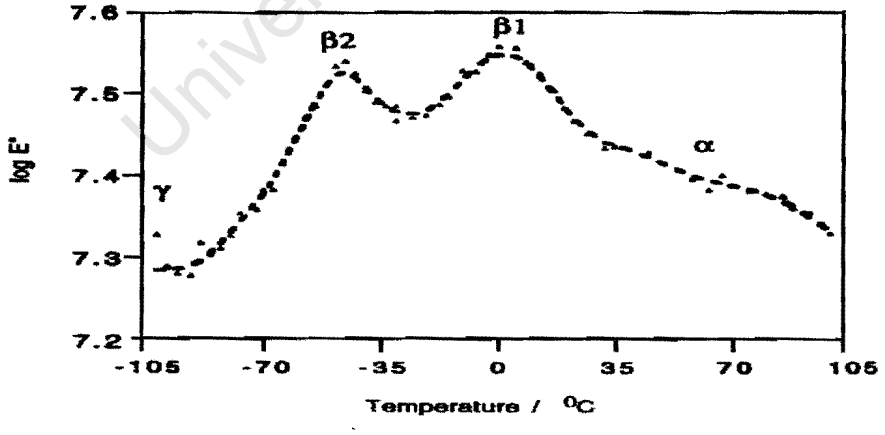

(c)

University of Cape Town

Figure 2.24 DMA spectra of iPP and its copolymers: (a) iPP, (b) random PP copolymer and (c) block PP copolymer [after ref. 42]

Differential scanning calorimetry (DSC) is a technique that is used to measure the heat flows into (endothermic) or out of (exothermic) a material as it undergoes phase changes. It is used to measure the heat capacity of a material. DSC is useful to compare materials to assess their similarities or to investigate the effect of additives on the thermal properties of polymer materials[43].

2.4 DUCTILE-BRITTLE TRANSITION

One of the functions of the impact test, especially the Izod and Charpy test, is to determine whether or not a material experiences a ductile to brittle transition with decreasing temperature and, if so, the range of temperature over which it occurs. The ductile-to-brittle transition (DBT) is related to the temperature dependence of the measured impact energy absorption. The temperature at which the ductile to brittle transition takes place is called the ductile-brittle transition temperature, (T_{db}). This transition temperature depends on matrix and blend morphology and test conditions. The deformation mechanisms proceed differently below and above the ductile to brittle transition and changes with test speed. Figure 2.25 shows clearly these effects on the schematic diagram of a DBT for polymers.

University of Cape Town

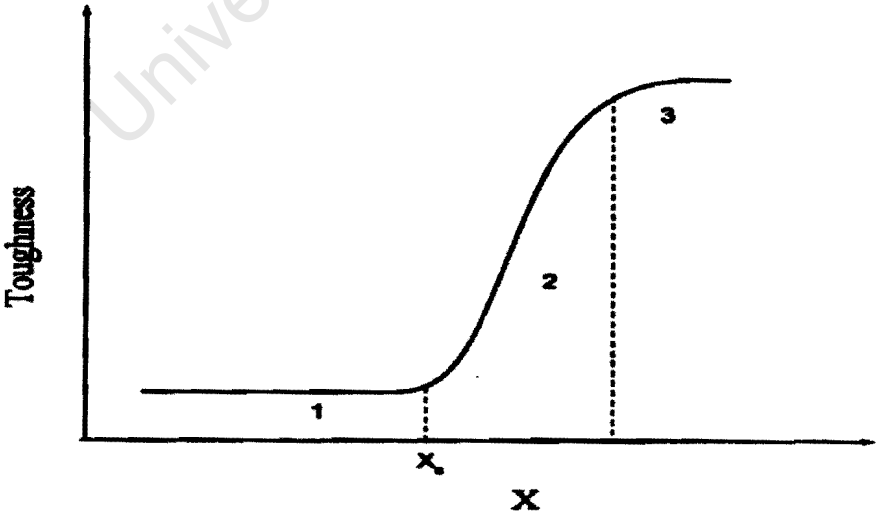

Figure 2.25 Schematic illustration of the ductile-to-brittle transition behaviour [after ref. 44]

The regions 1, 2 and 3 in this diagram correspond to brittle, transition and ductile regimes, respectively[44]. X denotes the different parameters that affect the DBT. X_c is a critical value of X at which the DBT occurs.

2.4.1 Effect of Morphological Parameters on the Ductile to Brittle Transition

Presently, most efforts have been made in producing tougher polymers. One of the ways for toughening plastics is to add a dispersed, elastomeric phase into a polymer matrix. However, toughened polymers exhibit a ductile behaviour only under a certain range of temperatures and loading rates. A ductile system can become brittle when the temperatures are lowered or the loading rate is increased.

The morphological parameter that affects the ductile to brittle transition of toughened polymers is the rubber particle size and volume fraction. During 1985 Wu suggested the criterion of critical matrix ligament thickness for rubber toughening, where the effects of average rubber particles size and rubber volume fraction have been formulated as the effect of average matrix ligament thickness[45,46]. Figure 2.26 shows a schematic presentation of two rubber particles in the matrix, where ID is interparticle distance (also called the matrix ligament thickness), d is the diameter of the rubber particles and L is the distance between the centres of the rubber particles. The ductile to brittle transition occurs when the average matrix ligament thickness equals its critical value. A blend is tough when the average matrix ligament thickness is thinner than the critical value; a blend is brittle when the average matrix ligament thickness is thicker than its critical value[22,47].

University of Cape Town

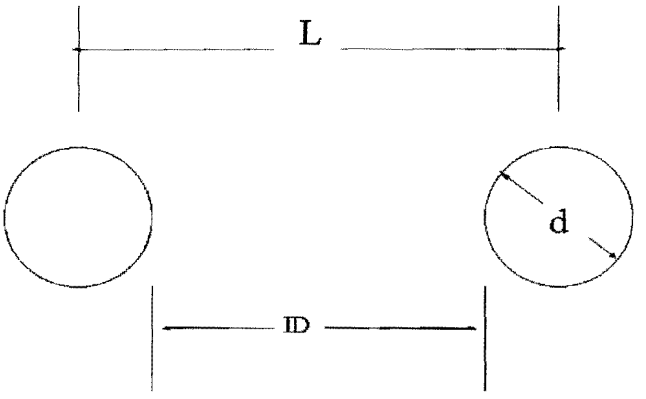

Figure 2.26 Schematic representation of the rubber particles and the matrix ligament [after. 45]

The ID for rubber-toughened polymers can be obtained from equation 2.7:

$$ID = d\left[\left(\frac{k\pi}{6V_r}\right)^{\frac{1}{3}} - 1\right]$$

[Equation 2.7]

where V_r is the rubber volume fraction and k is a geometric constant dependent on the lattice type. The volume fraction V_r of the rubber particles is be given by:

$$V_r = \frac{w_r\rho_m}{w_r\rho_m + (1-w_r)\rho_r}$$

[Equation 2.8]

where w_r, ρ_r and ρ_m refers to the weight fraction of the rubber particles, the density of the rubber particles and the density of the matrix, respectively.

Jiang and co-workers have shown using PP/EPDM, that the transition from brittle to ductile behaviour can be achieved either by decreasing the ID or by decreasing the tensile speed, i.e. they have an equivalent effect on the ductile to brittle transition of PP/EPDM blends[44,48]. Figure 2.27 shows the relationship between fracture energy and ID.

University of Cape Town

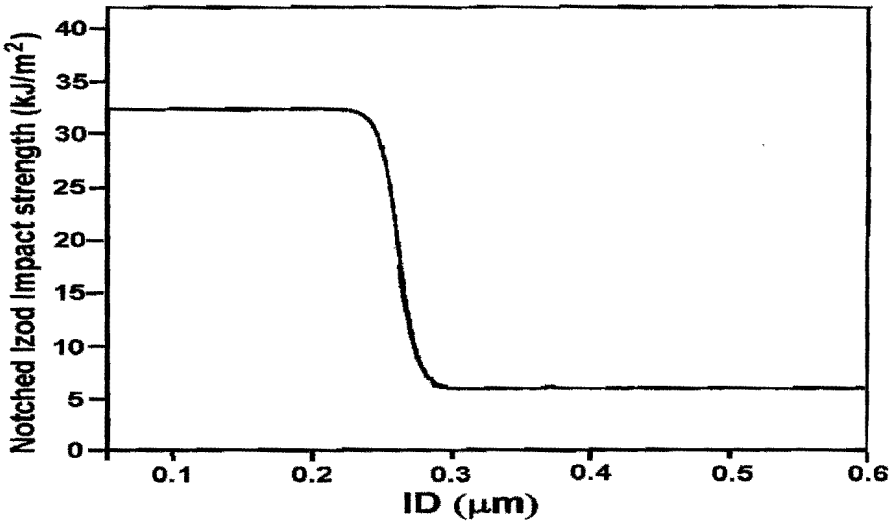

Figure 2.27 Variation of impact strength with ID for rubber modified PP blends [after ref. 44]

There are at least two different types of morphology of polymer/rubber blends that are effective in the rubber toughening mechanism. One is the pseudo-network morphology, where the rubber particles are randomly dispersed in the polymer matrix, as shown in Figure 2.28(a). Another type is the well-dispersed particle morphology, shown in Figure 2.28(b), which is very common in most polymer blends. The flocculated particles morphology is shown in Figure 2.28(c). The last two morphology types give a small value for the critical matrix ligament thickness because of the nearly close packed structure.

University of Cape Town

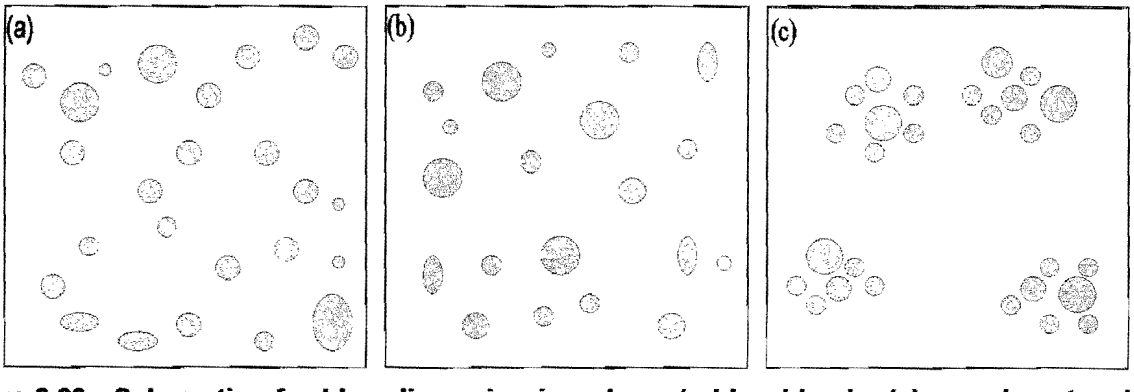

Figure 2.28 Schematic of rubber dispersion in polymer/rubber blends: (a) pseudo-network, (b) well-dispersed and (c) flocculated particle morphology. The filled region represents the rubber phase

It has been shown that the well-dispersed morphology is effective in obtaining super toughened polymer blends, but this might differ or change depending on the type of system used to toughen the polymer.

2.5 End Use Properties of the Impact Copolymers

Isotactic polypropylene and its copolymers have evolved its own set of characteristics properties to serve their associated markets. The homopolymers represent the simplest structures and the narrowest properties range, while the impact copolymers exhibit a rapidly growing range of structures, properties and complexities of manufacture. The key properties that define the major characteristics for the designer of a functional part are: (1) modulus; (2) tensile strength; (3) impact strength; (4) hardness; and (5) maximum temperature used. With these properties, and the melt flow index that determine processability, the vast majority of mechanical parts may be designed and fabricated.

When considering the physical and mechanical properties of the copolymer, it should be borne in mind that the polymer morphology provides a critical bridge between polymer structure, polymer processing and end use properties as shown in Figure 2.29 below. The important structural properties of the PP chain include the molecular weight and molecular weight distribution, composition in copolymers and details of the intra-chain architecture that include comonomer distribution in random, heterophasic and graft copolymers. Important processing parameters include the melt processing conditions, orientation, thermal history, the addition of nucleators and additives and post-synthesis reaction relating to polymer degradation of the molecular weight. Understanding the effects of these structural and processing variables on PP morphology is essential, because it is the morphology which provides the most direct link with polymer properties.

University of Cape Town

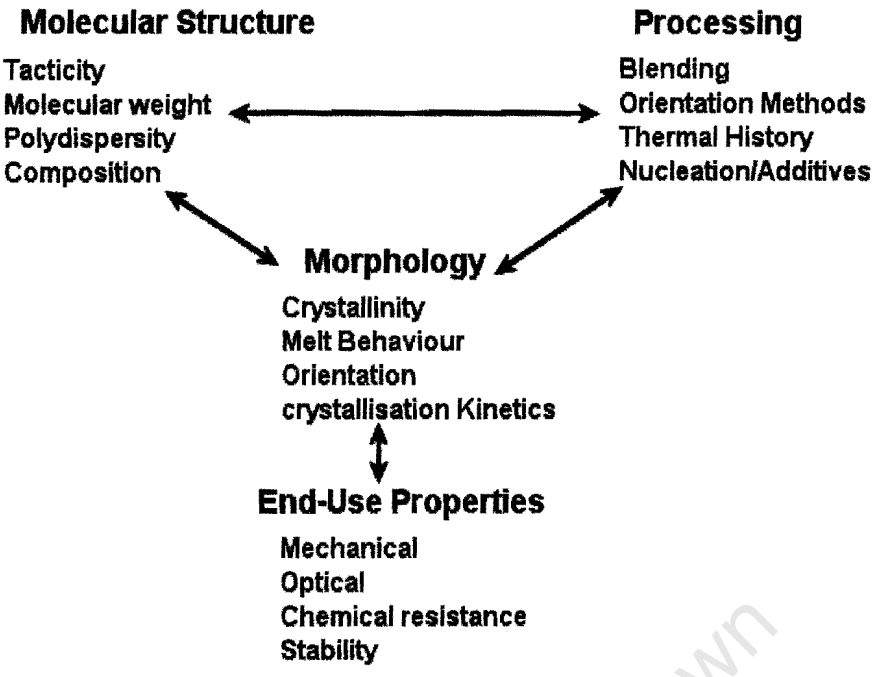

Figure 2.29 The interrelationship between the polymer structure, processing, morphology, and end-use properties.

University of Cape Town

2.5.1 Mechanical Properties

The main reason for the development of the impact copolymers is the improvement in the low temperature impact strength. This is achieved with a polymer structure where the rubber phase, usually the ethylene-propylene copolymer rubber (EPR) is uniformly dispersed within the PP homopolymer matrix. The introduction of the EPR component, characterised by a very low modulus, while increases the impact strength, causes a lowering of the product stiffness, hardness and tensile strength, as illustrated in Figure 2.30. The improvement in the impact strength is directly related to both the amount and the particle size of the EPR component. In addition, the best compromise between the stiffness and the impact is related to the degree of dispersion.

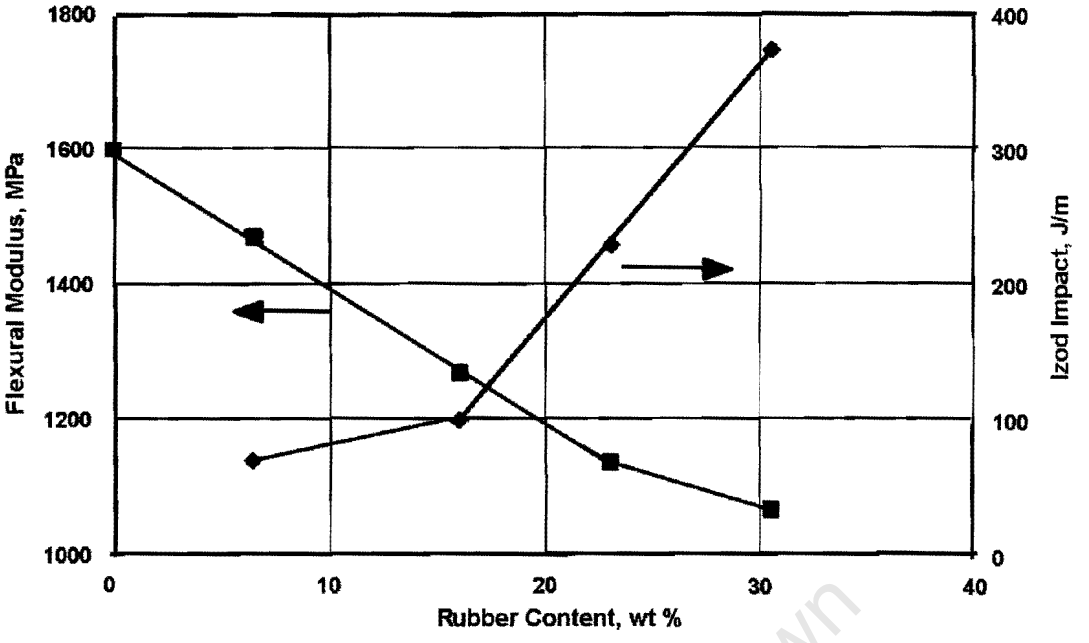

Figure 2.30 Effect of EPR phase in the iPP matrix on stiffness and impact strength [after ref. 49]

The effectiveness of the toughening mechanism of the polymer is determined by the nature of the rubbery phase, as well as by its amount, size and distribution within the matrix. The nature of the rubber determines the deformation behaviour of the dispersed particles and their ability to absorb and redistribute the energy, while the concentration and particle size define the probability of both initiating crazes and intercepting the fracture path. This mechanism operates best at the temperatures above the glass transition temperature of the rubber phase[49].

University of Cape Town

CHAPTER THREE

EXPERIMENTAL TECHNIQUES

3.1 MATERIALS USED

Thirty different grades of poly (propylene-ethylene) copolymers were investigated in this research project. These polymers are copolymers with isotactic polypropylene (iPP) as the matrix and ethylene-propylene rubber (EPR) as the dispersed phase. These grades, which are shown in Table 3.1, are used in a comparative study in this theses and are produced using different manufacturing processes such as BASF Novolen® PP technology (Sasol Polymers), Univation PP technology/Union Carbide UNIPOL™ (DOW Chemicals), AMOCO/Chisso Innovene PP technology (BP Chemicals), Montell Spheripol PP technology (Basell) and Borstar PP technology (Borealis). See section 2.2 for the description of each process. The ethylene content for these copolymer grades ranges between 5.9% and 15.0%, while their melt flow indices (MFI) varied from 0.4 g/10 min to 79.0 g/10 min.

Some of the physical and mechanical properties of these copolymers supplied by Sasol Polymer appear in Appendix A. The copolymer grades are differentiated from one another by a deciphered code. An example of the coding is shown in Table 3.2. An example of such coding can be explained using sample #20: Sasol grade 2448TC, is a controlled rheology grade, high MFI of about 50g /10 min, medium impact copolymer containing a nucleating agent.

University of Cape Town

3.1.1 SAMPLE PREPARATION

The copolymer samples tested were supplied by Sasol Polymers and were prepared by an injection moulding process as per the standards dictated in the ASTM D4101 and ISO 1873-2 standards. Samples were injection moulded into the desired shape at an injection speed of 50 mm/s and a pressure of 50 bars to fill the mould. A barrel temperature of 230°C was used. The mould wall temperature was kept constant at

30°C and the cooling time was set for 10 seconds. The samples were left for at least 48 hours prior to testing.

Table 3.1 The matrix shows the range of the polymers used.

Sample #	PP Manufacturing Technology	Sample name	MFI (g/10min)	Ethylene content (wt%)
1	Innovene	BP K7506	5.9	6.1
2	Spheripol	Basell EPC30R	6.5	7.3
3	Novolen	Sasol 2349MC	8.0	7
4	Innovene	BP K8512	12.0	5.9
5	Spheripol	Basell HEXP280	20.0	6.2
6	Borstar	Borealis BH345MO	44.0	7.6
7	Innovene	BP B8101	0.4	8.5
8	Univation	DOW SRC7-467	0.7	8.7
9	Spheripol	Basell EPD60R	0.8	8.9
10	Novolen	Sasol 2502G	1.0	11.5
11	Innovene	BP K7002	1.2	8.2
12	Spheripol	Basell EPQ30RF	1.5	8.8
13	Univation	DOW 7C62N	7.0	8.8
14	Innovene	BP K7312	14.0	7.0
15	Spheripol	Basell EPV31RA	28.0	8.3
16	Innovene	BP K9935	34.0	9.2
17	Univation	DOW SRD7-664	34.0	10.0
18	Spheripol	Basell EPH71HA	46.0	8.0
19	Innovene	BP K8550	49.0	8.4
20	Novolen	Sasol 2448TC	50.0	10.0
21	Univation	DOW SRD7-665	68.0	7.8
22	Spheripol	Basell EPS31HP	1.2	11.2
23	Spheripol	Basell EPC31H	7.0	12.9
24	Novolen	Sasol 2648M	8.0	11.5
25	Spheripol	Basell HEXP2000	15.0	15.0
26	Spheripol	Basell EPF31HR	17.0	10.8
27	Innovene	BP K9020	18.0	12.2
28	Novolen	Sasol 2648RC	24.0	12.4
29	Spheripol	Basell EPL31UA	73.0	11.4
30	Spheripol	Basell HEXP2023	79.0	10.7

University of Cape Town

Table 3.2 Deciphered codes used to differentiate the Sasol copolymer grades from one another

Polypropylene type	1	Homopolymer
	2	Block copolymer
	3	Random copolymer
Additive agent	0	General additive package
	4	Nucleating additive package
Target melt flow index (MFI)	H	2.0 g/10 min
	K	3.5 g/10 min
	L	5.5 g/10 min
	M	8.5 g/10 min
	N	12.0 g/10 min
	P	16.0 g/10 min
	R	21.0 g/10 min
	T	45.0 g/10 min
Last letter (in some cases)	C	Controlled rheology grade

University of Cape Town

3.2 Morphological Characterisation

3.2.1 Transmission Electron Microscopy (TEM)

3.2.1.1 Block Trimming

Prior to examination in the TEM, injected moulded discs were cut into small blocks that can fit into a sample holder in the Reichert Ultracut S (Leica) ultra-microtome. They were then trimmed with a razor blade to the required shape and size (critical for TEM use) under a stereomicroscope. The sides of the block were cut at an oblique angle to provide a square or trapezoidal shaped block face of about 1.00 mm^2 or less, see Figure 3.1. Smaller block faces are better for TEM viewing since they are easy to section and they minimise pressure on the blade.

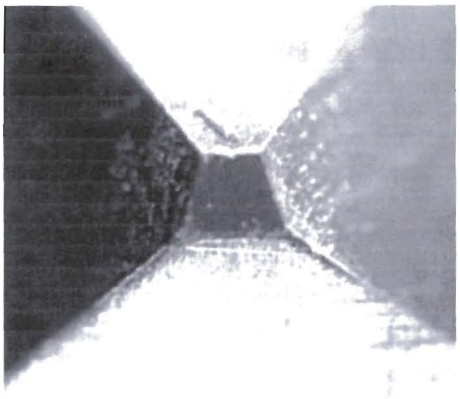

Figure 3.1 Photograph showing trapezoid shaped face of a trimmed block of polymer ready to be sectioned (viewed from top)

3.2.1.2 STAINING

After trimming the samples to the required size and shape, the samples were then treated with the concentrated chlorosulphonic acid for four to six hours at room temperature. They were then rinsed thoroughly with concentrated sulphuric acid and then in water. Chlorosulphonic acid is used to harden the blocks so that sectioning is easier and at the same time enhancing the lamella texture of polyethylene by staining it. Chlorosulphonic acid reacts vigorously with water and emits toxic fumes when they are mixed, so that proper precautions must be taken not to mix the two. The blocks were dried and then stained with ruthenium tetraoxide (0.5 wt. % RuO_4) vapour for a period of 2 to 24 hours. RuO_4 was prepared by oxidation of hydrated ruthenium dioxide ($RuO_2 \cdot xH_2O$) using sodium periodate ($NaIO_4$), as shown by the reaction below:

$$RuO_2\,(0.6g) + 2NaIO_4\,(4.0g) \rightarrow RuO_4 + 2NaIO_3$$

A RuO_4 stain is used to selectively increase the electron scattering of the polymer and thus aid contrast and resolution between the rubber particles and the matrix. In order to maximise diffusion of the stain in the block; the RuO_4 solution was buffered at a pH of 7.2 with sodium cacodylade (2.14g $Na(CH_3)_2AsO_2 \cdot 3H_2O$ in 100ml). Sodium cacodylade is carcinogenic and care must be taken when using handling it. The blocks were then thoroughly rinsed with distilled water and left to dry.

University of Cape Town

3.2.1.3 ULTRA-THIN SECTIONING

The stained samples were then ultra-thin sectioned at room temperature on a Reichert Ultracut S (Leica) ultramicrotome (see Figure 3.2) using either a DuPont® diamond or a glass knife fitted with water trough. The water was used to trap the ultra-thin sections that were being sectioned to about 70 nm to 200 nm. The aim of this preparation was to obtain sections that truly represent the original bulk structure and which are thin, flat and undeformed. These polymer sections must have contrast in order to form images that can be interpreted. Experience of operation is required to obtain such sections of polymer consistently.

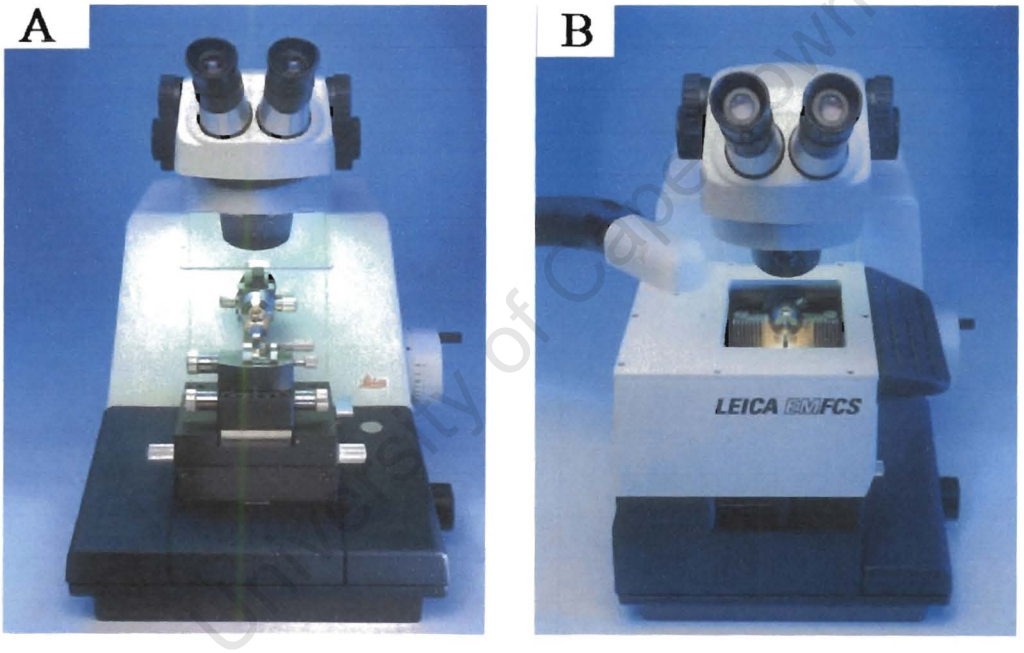

Figure 3.2 The microtoming machine used to section the copolymer samples: (a) room temperature setup and (b) cyogenic setup with an LEICA EMFCS attachment.

A factor to consider for TEM sectioning is the orientation of the specimen in the trimmed block, which is important for structural interpretation. In addition, approaching the specimen block with the knife requires a combination high quality stereomicroscopy, bright adjustable lighting and precision motion control. Figure 3.3 illustrates the precision motion of microtoming. The sectioned ribbons are then recovered onto the appropriate copper grid for viewing in the TEM. This was achieved by manipulating the

sections on the water surface using an eyelash probe. The polymer sections are captured onto a grid using a small pair of forceps. A JEOL JEM-200CX TEM operating at a voltage of 120 kV or 200 kV was used to investigate the morphologies of the rubber particles.

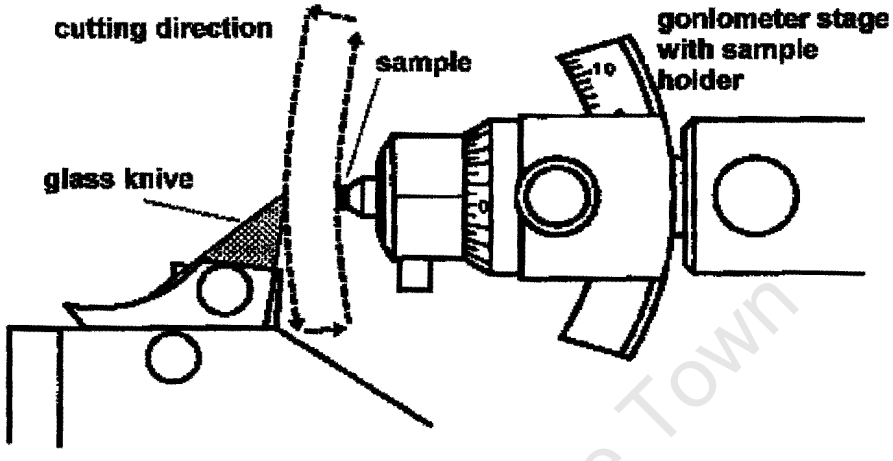

Figure 3.3 Illustration of the precise motion of microtoming.

University of Cape Town

3.2.2 Scanning Electron Microscopy (SEM)

SEM analysis was carried out on the cryogenically fractured surfaces obtained from both deformed and undeformed specimens in a direction perpendicular and parallel to the melt flow. For this purpose, the samples where first notched, followed by immersing them into liquid nitrogen for a period of about 30 minutes before they were fractured. The fractured samples were then mounted onto aluminium stubs using a mixture of glue and carbon dag to make them conductive. The fractured surfaces were then etched using heptane at 70 °C for 30 minutes in order to remove the rubber particles. They were then cleaned with methanol for 5 minutes in an ultrasonic bath. They were then sputter coated with gold/palladium for 10 minutes at a voltage of 2 kV and a current of 16 mA to render them conductive. To minimise electron charging from the specimen, a conducting silver dab path was made between the specimen top surface and the aluminium stub.

A LEO STEREOSCAN 440 SEM operating at a acceleration voltage of 10 kV was used to quantify the particle size and particle size distribution of the polymer blends. From

the SEM micrographs, the particle size and particle spacing were determined using the Joyce Loebl Image Analysis Software package. The particle size was measured across the perimeters of a particle and the particle spacing was measured form centre-to-centre of the particles. The number average particle size (D_n) and the weight average particle size (D_w) were determined. These averages are defines as:

$$D_n = \frac{\sum n_i d_i}{\sum n_i} \text{ and } D_w = \frac{\sum n_i d_i^2}{\sum n_i d_i}$$

[Equation 3.1]

where n_i is the number of particle, and d_i is the diameter of the EPR particle size.

3.3 THERMAL PROPERTIES

3.3.1 DYNAMIC MECHANICAL THERMAL ANALYSIS

The viscoelastic responses of the copolymer grades were determined at the Polymer Institute in the University of Stellenbosch using the Perkin-Elmer DMA7e analyser. The tests were carried out in order to determine the glass transition temperature (T_g) of the grades. Temperature scans of between –150 to 150°C was performed using a frequency of 1Hz and a heating rate of 5°C / min. The test specimens were taken from the injected moulded samples. The parallel plate-measuring configuration, which measures the materials' response to the applied constant static stresses over the temperature range, was used. The results were recorded as loss modulus, storage modulus or tan delta as a function of temperature. The DMA was also use to determine the stiffness of the polymer by applying static forces of about 1mN at a scanning rate of 1 mN/min to the polymer in the compression mode. The materials were scanned at a force range of between 2000 mN to 10000 mN.

3.3.2 DIFFERENTIAL SCANNING CALORIMETRY (DSC)

The DSC analysis of the copolymer grades was carried out in order to assess the effect of the ethylene content on the thermal properties of the polymer blends. Special emphasis was paid to measuring the heat flow (enthalpy, ΔH_m) into and out of the

University of Cape Town

polymers samples. The tests were performed using the NETZSCH STA 409C Thermal Analyser, which has a sample carrier that measures both the thermogravimetry (TG) and differential scanning calorimetry (DSC) response simultaneously.

3.3.2.1 CALIBRATION OF THE DSC

In order to correlate the specimen temperature to that temperature measured by the thermocouples of the DSC, the DSC was first calibrated using a series of high purity melting standards wires such as: Indium (In: 156.63°C), Tin (Sn: 231.93°C), Aluminium (Al: 660.37°C), Silver (Ag: 961.23°C) and Gold (Au: 1064.42°C) obtained from Goodfellow. The procedure for calibration is mentioned somewhere else[50].

3.3.2.2 DSC RUNS OF THE COPOLYMER GRADES

Tests were run using two aluminium crucibles with a lid on the sample and the reference crucibles. The reference crucible was always kept empty during the tests. The samples were heated at a temperature range of 20°C to 250°C, and then cooled back to 20°C. A heating and cooling rate of 5°C / min were used. The tests were run in a dynamic atmosphere of argon flowing into the furnace chamber at the rate of 50 ml/min. Firstly, the baseline correctional curve was established by heating two empty aluminium crucibles at the same conditions mentioned above and then the same correctional curve was used when running the DSC curves for the copolymer grades samples. The samples had a mass average of between 5.0 mg to 10.0 mg. The melting and recrystallisation enthalpies [ΔH_m (J/g)] were measured from the areas under the peaks in order to the estimate percentage crystallinity, X_c, of the blends by using the value of enthalpy [ΔH_o]:of 100% crystalline iPP to be 209J/g.

$$X_c = \frac{\Delta H_m}{\Delta H_o}$$

[Equation 3.2]

University of Cape Town

3.4 PHYSICAL PROPERTIES OF THE COPOLYMER GRADES

3.4.1 WIDE ANGLE X-RAY SCATTERING (WAXS)

The presence of crystallinity in the polypropylene copolymers was detected using the wide-angle x-ray scattering (WAXS) facility at iThemba Laboratory for Accelerator-Based Sciences. A Bruker AXS was used to obtain the WAXS patterns using a Ni-filtered CuKα radiation source (λ_{Cu} = 1.5418Å). The surfaces of the samples were firstly polished to obtain a smooth surface. The scanning range covered was from 5 to 35° with the sample holder rotating at 30 rpm. A step size of 0.1° at 2 second intervals was used. All the scans were taken at room temperature. The crystallinity of the copolymer was determined from the WAXS using the following equation:

$$X_c = \frac{A_c}{A_c + A_a}$$

[Equation 3.3]

where A_c and A_a are the areas under the crystalline and amorphous peaks from the WAXS patterns, respectively. The areas were subtracted by the software package supplied with the x-ray machine. The relative amount of the hexagonal β-amount (K value) was determined from the WAXS patterns using the following equation:

$$K = \frac{I_{(300)\beta}}{I_{(110)\alpha} + I_{(040)\alpha} + I_{(130)\alpha} + I_{(300)\beta}}$$

[Equation 3.4]

where I_α's and I_β are the relative intensity for the α- and β-forms.

The apparent crystal size (D) for the (110), (130) and (040) crystallographic planes were calculated using the Scherrer equation:

$$D_{hkl} = \frac{K\lambda}{\beta_0 \cos\theta_{hkl}}$$

[Equation 3.5]

where β_0 is the half width in radians of the reflection corrected for the instrument, λ is the incident x-ray wavelength used at 1.5418Å, and K is the shape factor set to unity.

University of Cape Town

3.4.2 FOURIER TRANSFORM INFRA-RED SPECTROSCOPY (FTIR)

Fourier transformation infrared spectroscopy analysis for the sample grades was performed at the Cape Technikon using Ft-IR Spectrum 1000 Perkin-Elmer spectrometer. Spectrums were taken at the 4000 to 350 cm^{-1} mid-IR region. The spectral accumulation was done at a resolution of 8.0 cm^{-1} and a step size of 0.1 cm^{-1}. The spectral averaging was done with 10 scans of which each run was duplicated to see if the peaks observed are correct or consistent. The machine was continuously purged with nitrogen to minimise absorbance readings of the atmospheric gas during testing. The background scan was done in air i.e. without any sample attached to the sample holder. The samples were prepared by means of hot pressing the samples between two microscope glass slides at a temperature of about 240°C and allowing them to be air-cooled.

3.5 MECHANICAL TESTING

Izod impact tests, shore hardness tests and tensile tests for the grades were all performed at Sasol Polymers and their results are shown at Appendix A.

University of Cape Town

3.5.1 IMPACT TESTING

3.5.1.1 TENSILE IMPACT TESTING

The double edge notch tensile impact test was carried out using a Zwick Pendulum Impact Tester shown in Figure 3.4 below. The tests were performed in accordance to the ASTM D1822* standard test methods. Tensile impact samples were milled from the injection moulded disc samples in a direction parallel and perpendicular to the melt flow as illustrated in Figure 3.5 below. The sample dimensions were 10 x 3 mm with a 2 mm deep 45° V-notch on each side of the bars. All the tests were performed at room temperature. The testing parameters are as follows: a hammer of 5.4J; a release angle

* ASTM D1822: Test Method for Tensile Impact Energy to Break Plastics and Electrical Insulating Materials

of 124.5°; impact speed of 3.54 m/s; gauge length of 2.5 cm; yoke mass of 60g. The impact resistance results were recorded as kJ/m^2 units. At least five tests were performed for each impacted copolymers grade.

Figure 3.4 Zwick Pendulum Impact Tester

University of Cape Town

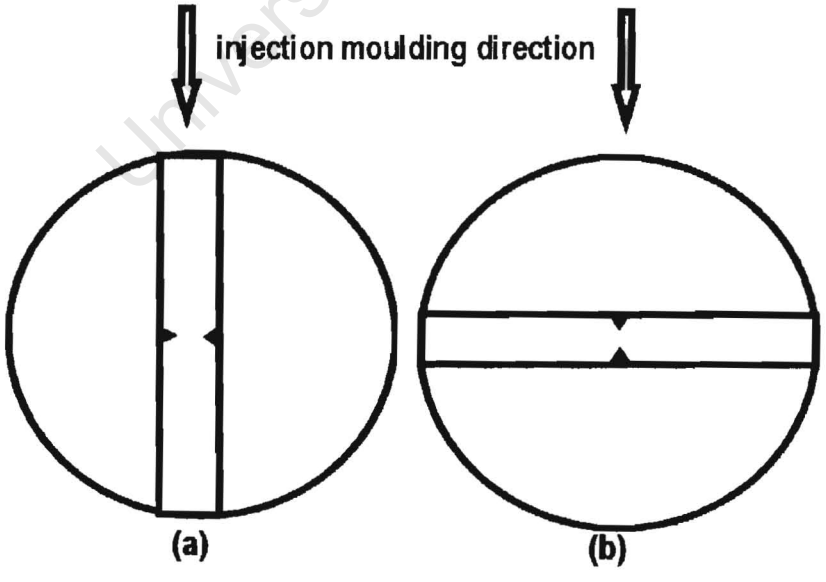

Figure 3.5 Illustration of the injected moulded disc from which the double edge tensile impact samples were obtained in the direction: (a) parallel and (b) perpendicular to the melt flow.

3.5.1.2 DROP WEIGHT IMPACT TESTING

The drop weight impact tests were performed using the in-house built drop weight impact tester located in the Centre for Materials Engineering. In order to obtain meaningful results, the load cell of the drop weight impact tester was calibrated, the procedure for calibration being mentioned somewhere esle[38]. The tests were performed at room temperature and at –20°C, and all the impact tests were performed in such a way to ensure that the impactor fully penetrates and causes complete damage to a sample. The weight of the impactor used was 3.10 kg. The drop height was kept constant throughout the impacting procedure and the impact speed was calculated to be 4.445 m/s for the samples impacted at room temperature and 3.968 m/s for the samples impacted at –20°C. The samples were tightly clamped into a sample holder in such way to minimise vibration of the sample during impacting. The impacted samples were square injected moulded plaques of dimension 100 x 100 x 3 mm.

For the low temperature impact tests, a copper-cooling disk was placed onto the section of the polymer surface that was to be impacted, ensuring direct contact with the sample. See Figure 3.6 for the low temperature set-up. The liquid nitrogen coolant was allowed to flow from the storage Dewar flask through the disk and pumped back into the Dewar flask. The operational procedure for the use of the copper-cooling disk system are as follows: the targeted temperature is set from the Gefran unit temperature controller; the liquid nitrogen is pumped from the storage Dewar flask, the flow rate of the liquid nitrogen is controlled by power supply connected to the pump, which further allows for the ease of the temperature regulation.

The disk was placed onto the polymer specimen for a period of about 15 minutes to allow the temperature of the sample to equilibrate to the desire target temperature. The temperature was set to about –10°C lower than the desired temperature, so as to accommodate for sample heating upon the removal of the disk from the sample surface. The sample temperature was monitored using an infrared thermal device, whereas the cooling disk temperature was monitored by a thermocouple attached to the Gefran unit temperature controller. The actual impact was done when the temperature readings between the thermocouple and the infrared thermal device were within ±1°C of each other and within ±1°C of the target temperature.

University of Cape Town

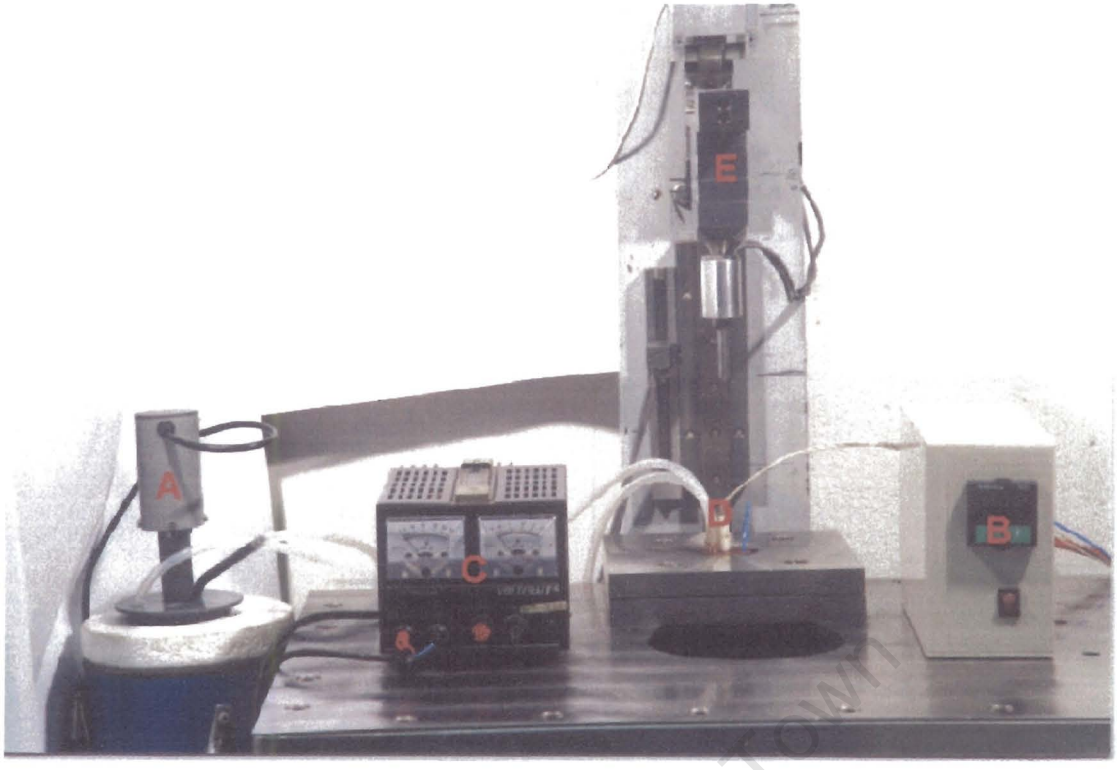

Figure 3.6 **The cooling apparatus set-up used for the low impact temperature tests: (a) pump and Dewar flask; (b) Gefran unit temperature controller; (c) power supply; (d) copper-cooling disk attached with heating element and thermocouple; and (e) the impactor**

University of Cape Town

CHAPTER FOUR

EXPERIMENTAL RESULTS

4.1 INTRODUCTION

The results of the materials characterisation and analysis of the different copolymer blends are presented in this chapter. Various correlation factors were established and in the case where there were common denominators, care was taken not to repeat any correlation between the two dependent variables. The results are presented in the following order:

1. **Thermal Analysis**
2. **Physical Analysis**
3. **Mechanical Behaviour**
4. **Morphological Characterisation**

University of Cape Town

4.2 THERMAL ANALYSIS

4.2.1 DIFFERENTIAL SCANNING CALORIMETRY (DSC) RESULTS

It is well known that the crystallinity of semi-crystalline polymers plays a significant role in determining the mechanical properties, especially the impact response of polymers. The addition of a second phase such as rubber may affect the crystallinity of iPP. It has been reported that the secondary phase such as ethylene-propylene rubber (EPR) acts as a nucleating agent reducing the crystallinity of PP[51]. It was noticed that the crystallinity of iPP is independent of the EPR content, but EPR does reduce the spherulitic size[52]. The effect of the secondary phase material on the crystallinity depends on the composition of the blend and the structure and morphology of the second phase. DSC analyses were carried out on the copolymer grades supplied (see Table 3.1) in order to evaluate to what extent the ethylene content affect the crystallinity of the iPP and the melt properties of the iPP. Table 4.1 shows the thermal properties obtained from DSC during the melting and recrystallisation cycles.

The effect of the ethylene content on the average melting temperature T_m, is not apparent from these results since the melt point for all the grades are in the range of 160.0–168.0°C, which is within the iPP melting temperature range. The recrystallisation temperature in the range 110.0-120.0°C is also expected from literature results. The higher enthalpy values obtained in the recrystallisation cycles are due to iPP chains ordering.

The effect of the ethylene content on the percentage crystallinity during the melting cycle is shown in Figure 4.1 below. The grades are grouped together according to their manufacturing technologies. The general trend observed, is that, the degree of crystallinity decreases with increasing ethylene content. This trend is more marked with the BP grades, whilst the other grades show some scattering in the trend.

University of Cape Town

Table 4.1 DSC results showing the melting temperature (T_m), crystallisation temperature (T_c) and percentage crystallinity ($\%X_c$). The standard deviations appear in brackets. Information on manufacturing technologies appear in Table 3.1

Sample #	Melting			Recrystallisation		
	ΔH_m (J/g)	T_m (°C)	$\%X_C$	ΔH_m (J/g)	T_c (°C)	$\%X_C$
1	94.3	168.1	45.1 (2.2)	98.7	114.8	47.2 (1.2)
2	76.9	166.3	39.8 (1.2)	83.0	113.6	39.7 (1.5)
3	85.3	166.4	40.8 (0.8)	92.3	120.4	44.2 (1.2)
4	85.5	161.3	40.9 (0.3)	88.3	114.7	42.3 (1.6)
5	104.3	163.9	49.9 (1.0)	101.2	121.9	48.4 (2.5)
6	97.9	167.6	46.9 (1.6)	110.0	121.2	52.6 (1.1)
7	77.4	168.4	37.0 (1.9)	87.3	110.9	41.8 (0.2)
8	71.2	166.9	34.0 (3.2)	84.2	109.4	40.3 (1.2)
9	74.1	166.8	35.5 (2.6)	84.2	110.3	40.3 (1.2)
10	77.1	167.8	36.9 (2.2)	85.0	113.1	40.7 (0.9)
11	86.4	167.5	41.3 (2.2)	99.2	119.1	47.5 (1.0)
12	71.9	165.9	34.4 (1.9)	82.4	108.7	39.4 (1.0)
13	76.6	166.3	36.6 (0.5)	95.2	109.0	45.5 (1.1)
14	91.5	166.4	43.8 (1.8)	100.0	120.1	47.9 (2.3)
15	94.1	162.1	45.0 (2.3)	96.1	118.0	46.0 (1.1)
16	83.6	161.6	40.0 (0.8)	93.7	115.5	44.8 (1.4)
17	94.6	164.5	45.3 (1.7)	108.7	121.4	52.0 (1.1)
18	83.6	160.8	40.0 (1.5)	88.1	120.6	42.2 (1.8)
19	88.1	162.8	42.1 (1.8)	100.2	119.0	48.0 (0.9)
20	82.2	164.1	39.3 (2.4)	95.0	120.7	45.5 (1.6)
21	95.3	165.5	45.6 (2.6)	102.2	118.4	48.9 (1.7)
22	84.6	164.4	40.5 (1.7)	91.5	121.9	43.8 (1.1)
23	84.2	167.2	40.3 (0.5)	94.9	122.8	45.4 (1.4)
24	83.8	167.8	40.1 (2.7)	92.9	120.5	44.4 (2.4)
25	78.2	166.2	37.4 (2.2)	80.9	121.6	38.7 (1.1)
26	84.5	167.2	40.4 (5.4)	87.6	122.8	41.9 (1.6)
27	77.1	163.8	36.9 (1.8)	86.2	112.1	41.3 (0.3)
28	84.0	167.5	40.2 (1.5)	93.3	119.1	44.7 (1.9)
29	73.3	162.8	35.1 (2.7)	84.6	120.7	40.5 (1.4)
30	93.7	163.6	44.8 (1.9)	94.5	121.0	45.2 (1.6)

University of Cape Town

Using the data in Table 3.1 and Table 4.1 it would appear in Figure 4.2 that the melt flow index has no significant effect on the degree of crystallinity, since the degree of crystallinity is almost constant over the whole range of MFI. Therefore, the crystallinity of the iPP matrix does not depend on the molecular weight, but may very well depend on other molecular weight parameters such as the molecular weight distribution.

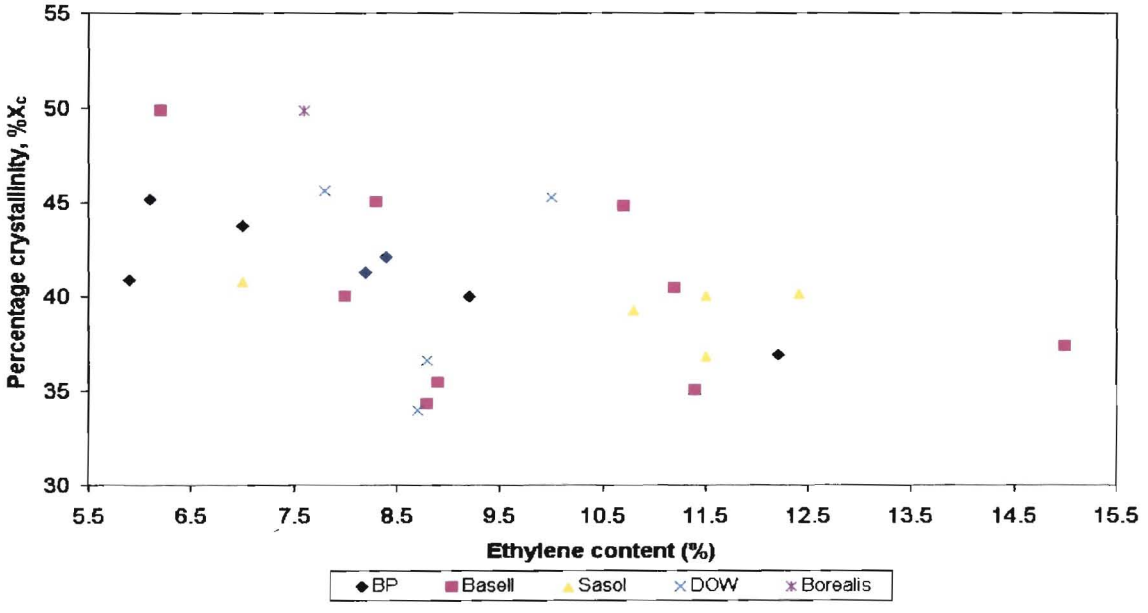

Figure 4.1 Illustration of the effect of percentage ethylene content on percentage crystallinity of the copolymer grades

University of Cape Town

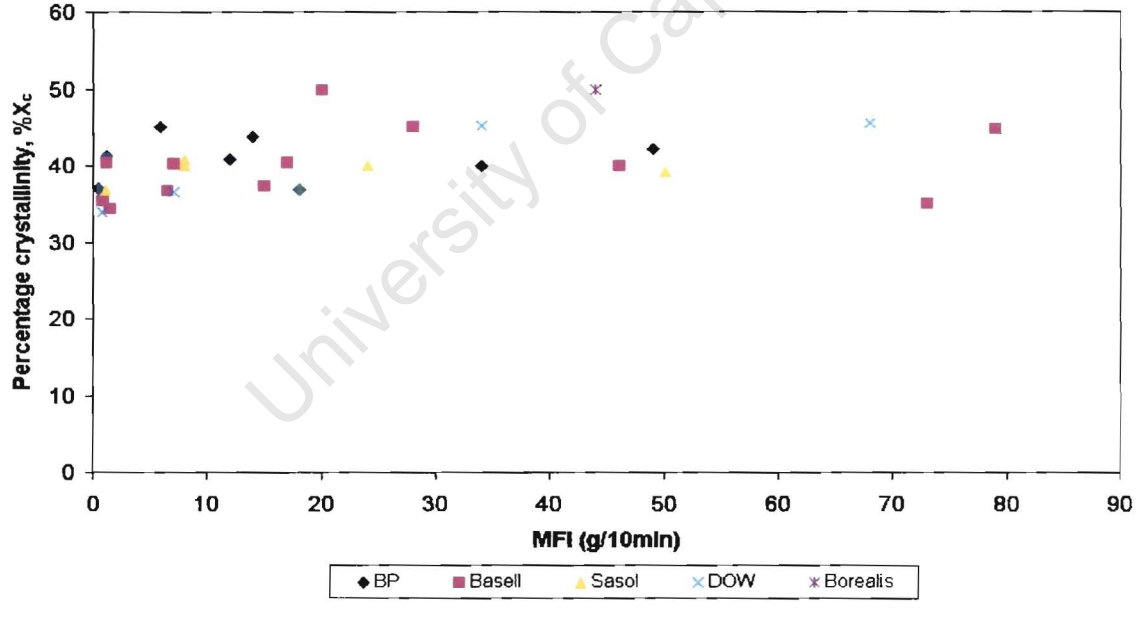

Figure 4.2 Illustration of the effect of melt flow index (MFI) on percentage crystallinity of the copolymer grades

4.2.2 DYNAMIC MECHANICAL ANALYSIS (DMA) RESULTS

The dynamic mechanical spectrums of the polypropylene grades from which glass transition temperatures, T_g and the stiffness (modulus) values were obtained from are shown in Figure 4.3 to Figure 4.5. The stiffness at three selected temperatures, the T_g's for EPR and iPP and the molecular relaxations i.e. the β_1– and β_2–relaxations for iPP and EPR, respectively, are listed in Table 4.2 below. The stiffness values were obtained from the storage modulus (E′) curves; the T_g's from the loss modulus curves and the molecular relaxations from the peaks of the loss modulus (E″) curves. Table 4.2 shows that T_g's measured from tan δ peaks are about 5°C higher than those measured from loss modulus peaks. The tan δ curves are shown in the Appendix C. As shown by most curves, there are clear and well-separated peaks for β_1 and β_2, which indicates a clear phase separation between the two existing phases, i.e. between EPR and iPP. Sample #28 shows a broad peak and little or no phase separation at all.

Table 4.2 The T_g and relaxation values from DMA runs of selected copolymer grades

Sample #	Stiffness (GPa)			T_g (°C)		Molecular relaxation (°C)	
	23°C	0°C	-20°C	EPR	iPP	(β_2)	(β_1)
1	1.90	2.49	2.71	-44	2	-50	-2
2	1.58	2.17	2.60	-55	10	-60	-10
10	1.34	1.92	2.42	-42	9	-47	-5
12	1.30	1.84	2.21	-44	5	-50	0
17	2.02	2.39	2.56	-52	15	-55	-6
18	2.48	2.77	2.91	-47	11	-50	7
21	2.43	2.73	3.07	-48	2	-55	-3
24	1.86	2.47	2.76	-38	12	-40	0
28	2.04	2.20	2.16	-	-	-44	-4
29	2.55	2.77	2.85	-31	16	-32	14
30	2.23	2.74	2.93	-55	9	-56	4

University of Cape Town

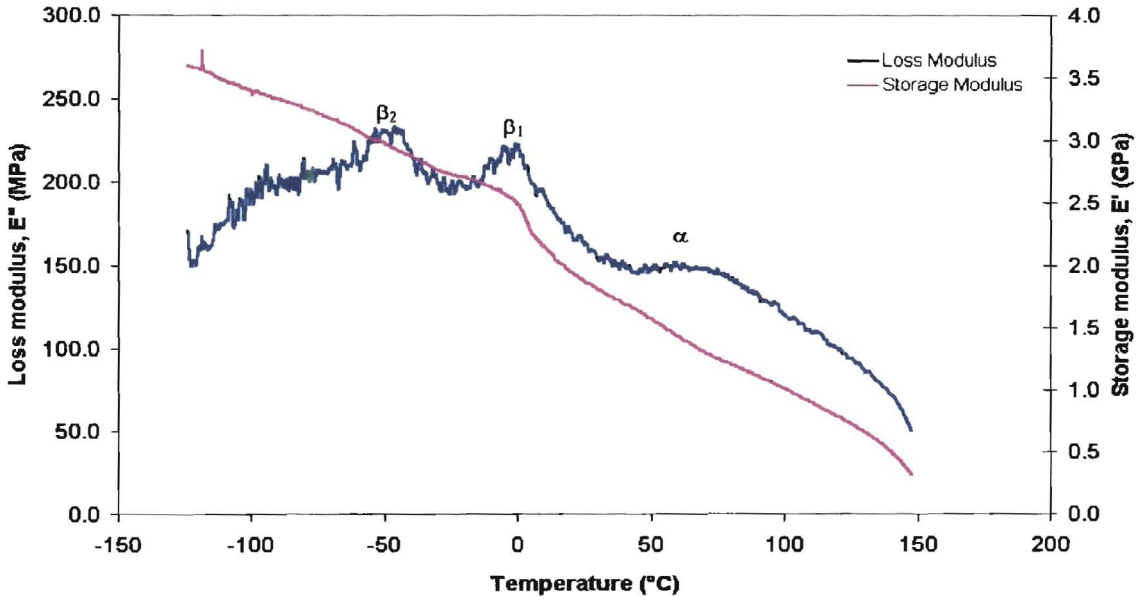

Sample #1: BP grade: C_2 = 6.1%, MFI=5.1 g/10 min

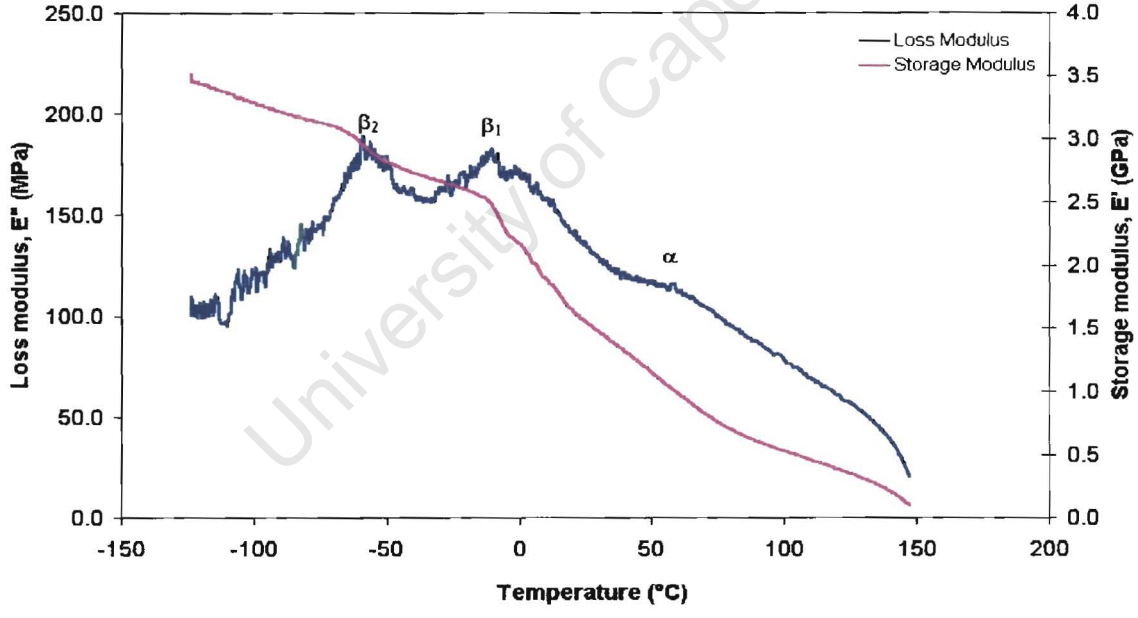

Sample #2: Basell grade: C_2 = 7.3%, MFI=6.5 g/10 min

Figure 4.3 Loss modulus (E″) and storage modulus (E′) versus temperature for the samples with ethylene contents of less than 8%

The loss and storage modulus plots of the grades with ethylene content less than 8% are shown in Figure 4.3. Sample #1 shows a slightly higher stiffness value than sample

University of Cape Town

#2. Also, the β_2-relaxation peak for sample #2 is shifted to lower temperatures than that of sample #1 by a margin of 10°C, which would gives this copolymer better impact properties over sample #1.

Figure 4.4 show the modulus curves of the samples with percentage ethylene content of between 8 and 10%. The stiffness decreases with increasing ethylene content, as was expected, with negligible effect of the MFI on the stiffness. Sample #18 and #21 show an increase in the peak value of the α-relaxation, which appears more pronounced rather than a shoulder found in other samples. The β_1- relaxation temperature for sample #18 is much higher than samples with similar ethylene contents. The peak height of the β_1-relaxation for samples #12 and 21 are slightly higher than that of their β_2-relaxations.

University of Cape Town

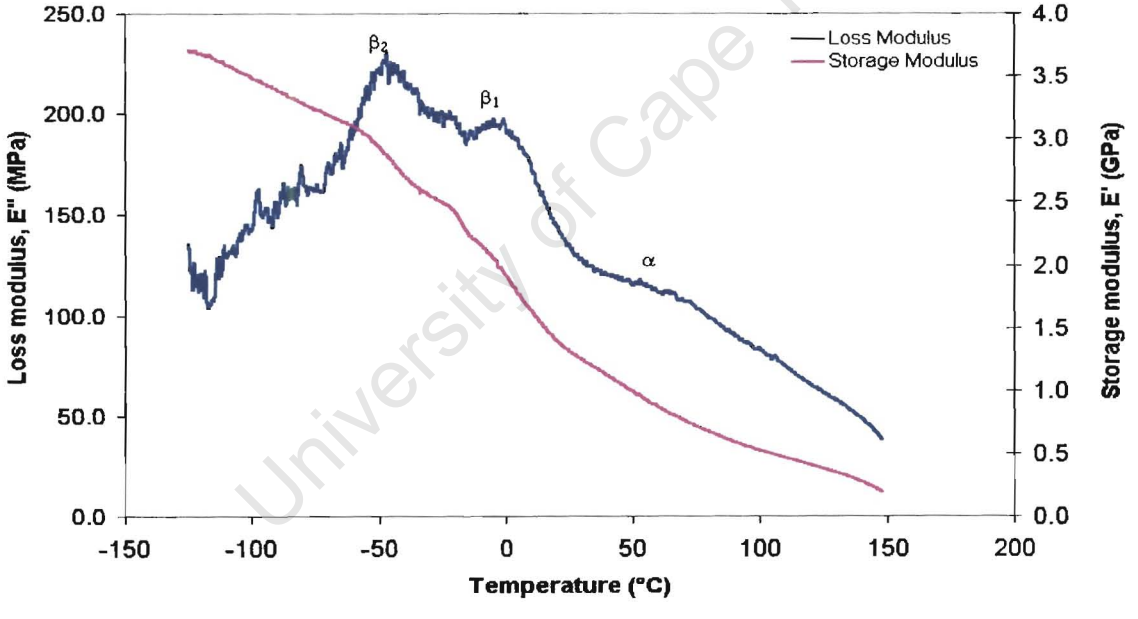

Sample #10: Sasol grade: C_2 = 6.1%, MFI=5.1 g/10 min

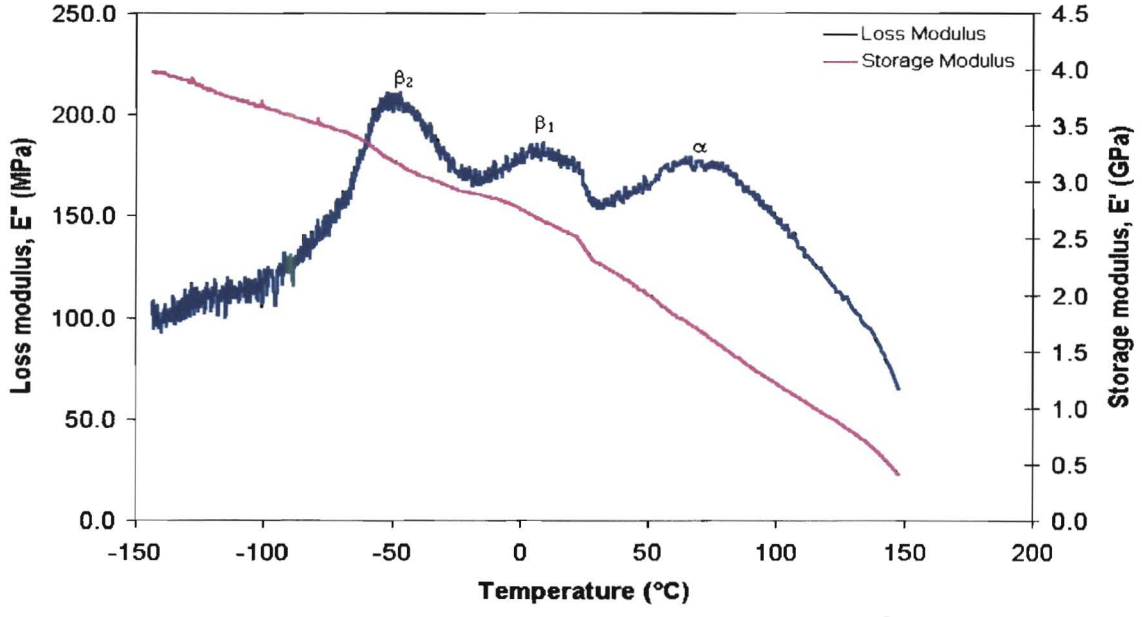

Sample #18: Basell grade: C_2 = 8.0%, MFI= 46.0 g/10 min

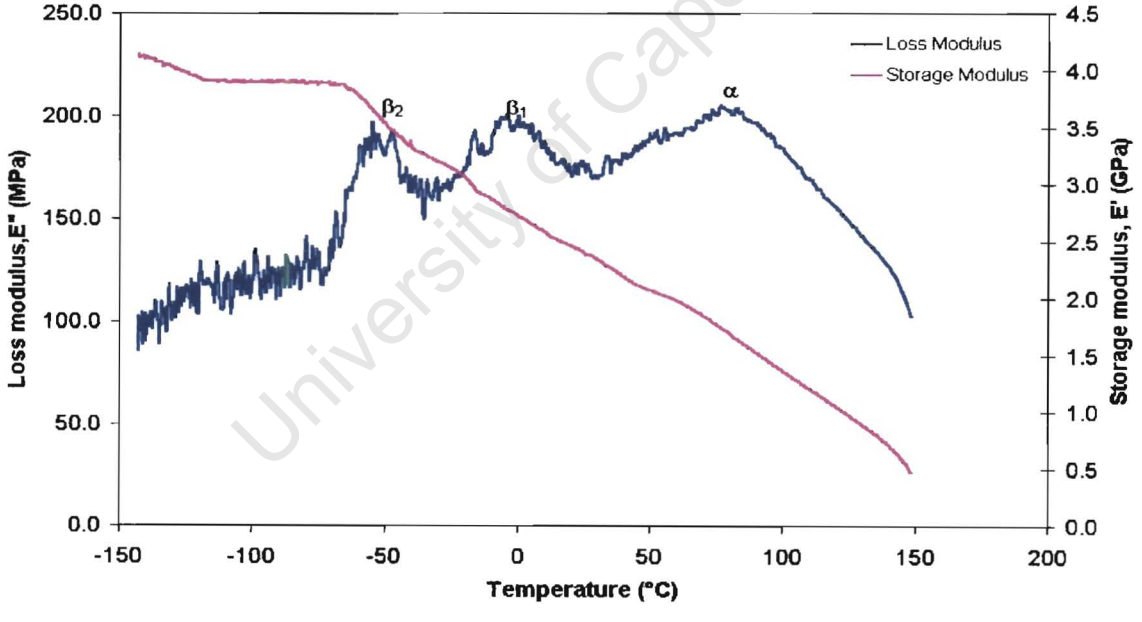

University of Cape Town

Sample #21: DOW grade: C_2 = 7.8%, MFI= 68.0 g/10 min

Figure 4.4 Loss modulus (E″) and storage modulus (E′) versus temperature for samples with ethylene contents between 8-10%

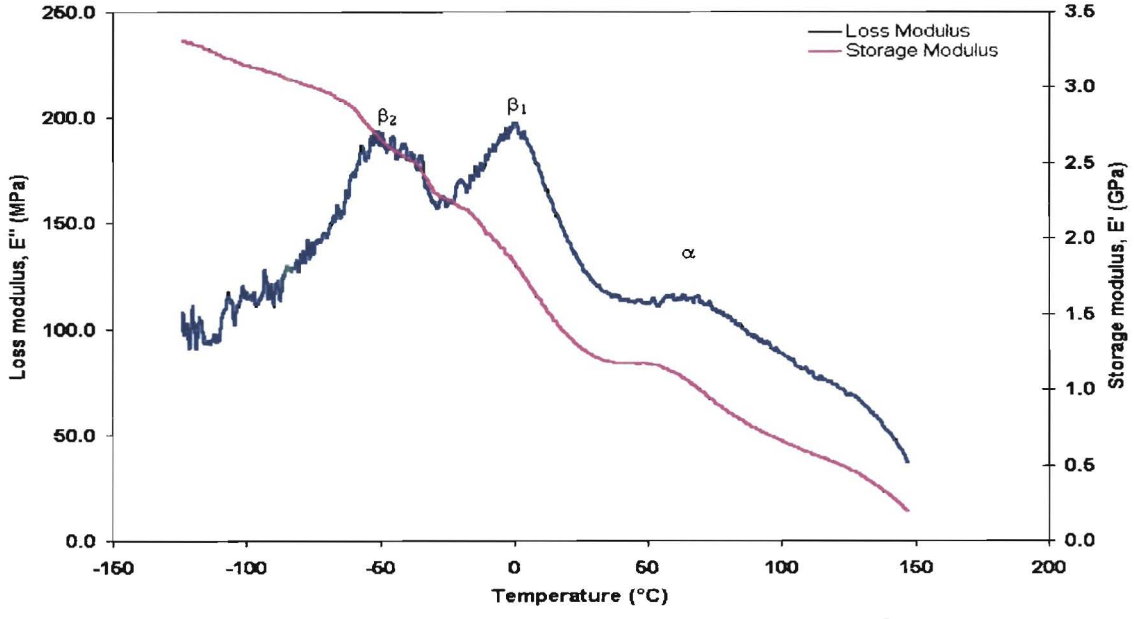

Sample #12: Basell grade: C_2 = 8.2%, MFI=1.5 g/10 min

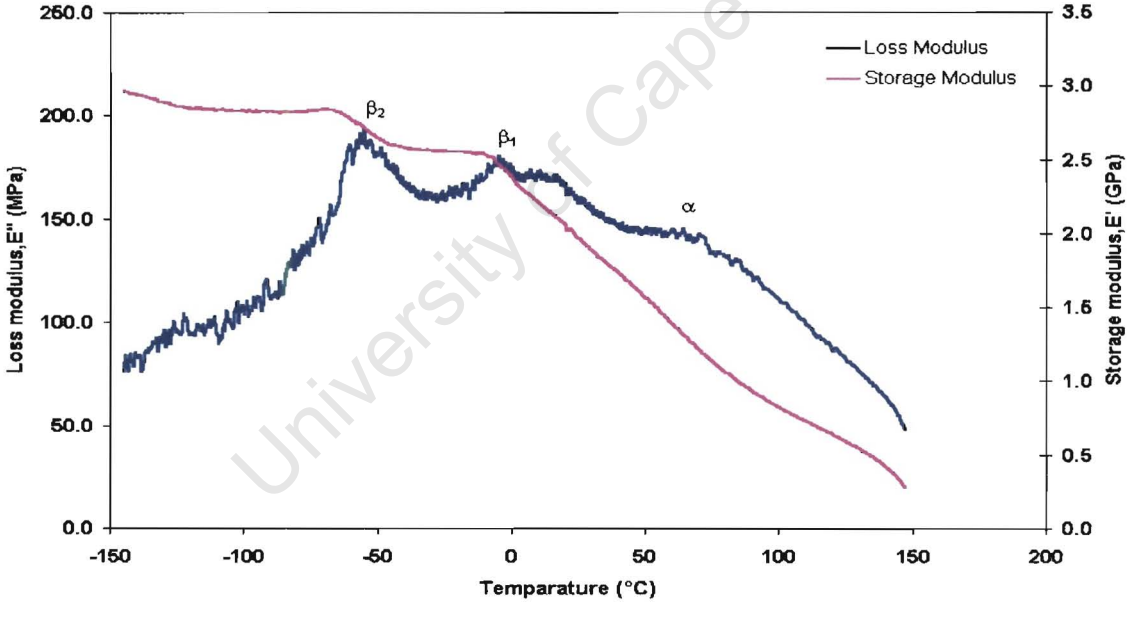

Sample #17: DOW grade: C_2 = 10.0%, MFI=34.0 g/10 min

University of Cape Town

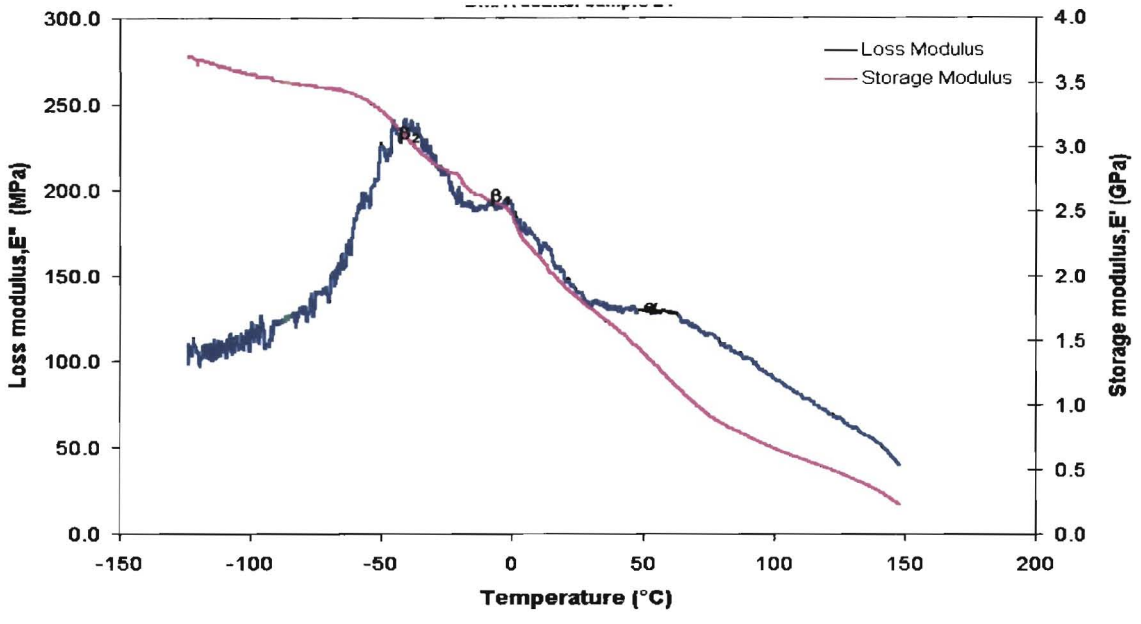

Sample #24: Sasol grade: C_2 = 8.0%, MFI=11.5 g/10 min

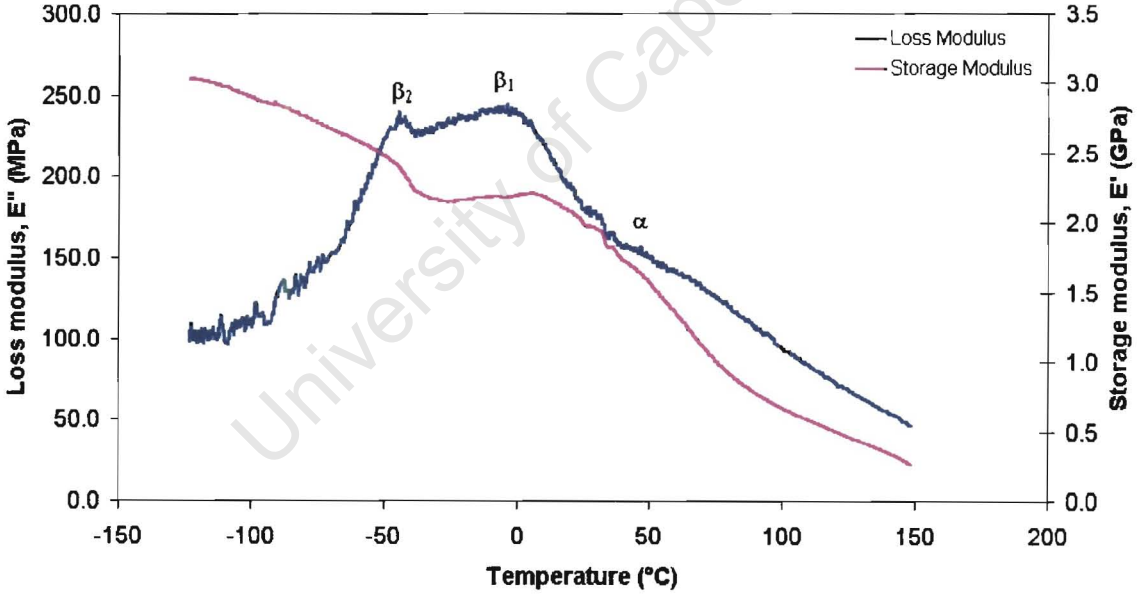

Sample #28: Sasol grade: C_2 = 12.4%, MFI=24.0 g/10 min

University of Cape Town

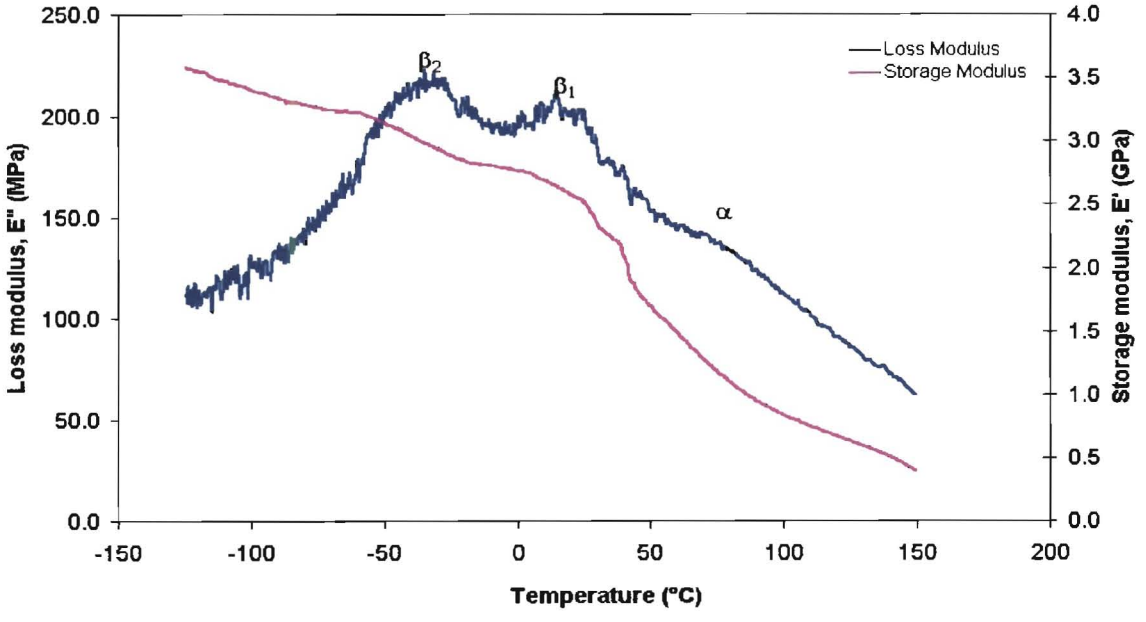

Sample #29: Basell grade: C_2 = 11.4%, MFI=73 g/10 min

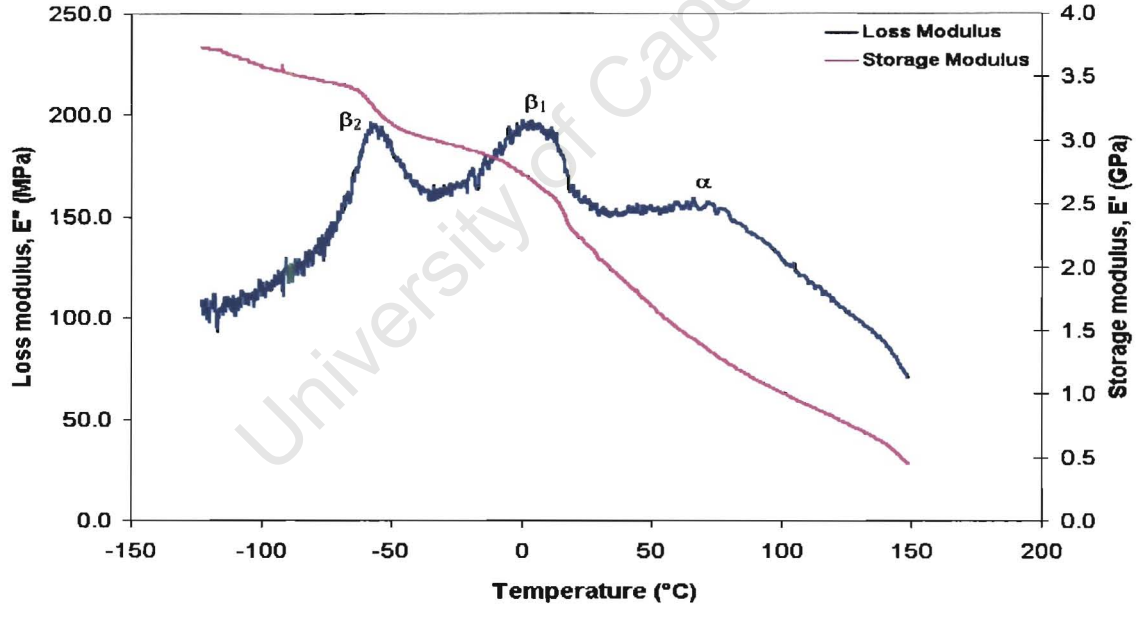

Sample #30: Basell grade: C_2 = 10.0%, MFI=79 g/10 min

Figure 4.5 Loss modulus (E″) and storage modulus (E′) versus temperature for samples with ethylene contents greater than 10%

The value of the stiffness obtained from the DMA stress-strain curves at different temperature are shown in Table 4.3 below. The results, with the exception of sample

University of Cape Town

#1, show that the stiffness decreases with increasing temperature. At 0°C the modulus values appear to show a minimum. This could be because at 0°C the β-relaxation of iPP shows a transition from the glassy to the rubber-like state. Since the DMA static stress-strain curves were measured in the region of linear viscoelasticity, this transition resulted in a lowering of the stiffness at 0°C. The plots for the static stress against static strain at the different temperatures are shown in Figure 4.6(a) to Figure 4.6(c), and the stiffness values were obtained from the slopes of the curves.

Table 4.3 The modulus data results obtained from the dynamic mechanical analysis static stress-static stress plots

Samples #	Modulus (GPa)		
	23 °C	0 °C	-20 °C
1	1.390	0.422	1.010
3	0.746	0.652	0.818
10	0.415	0.384	0.568
17	0.547	0.502	0.763
20	0.320	0.358	0.494
24	0.274	0.588	0.621
28	0.414	0.442	0.689
29	0.509	0.403	0.634
30	0.808	0.470	0.824

University of Cape Town

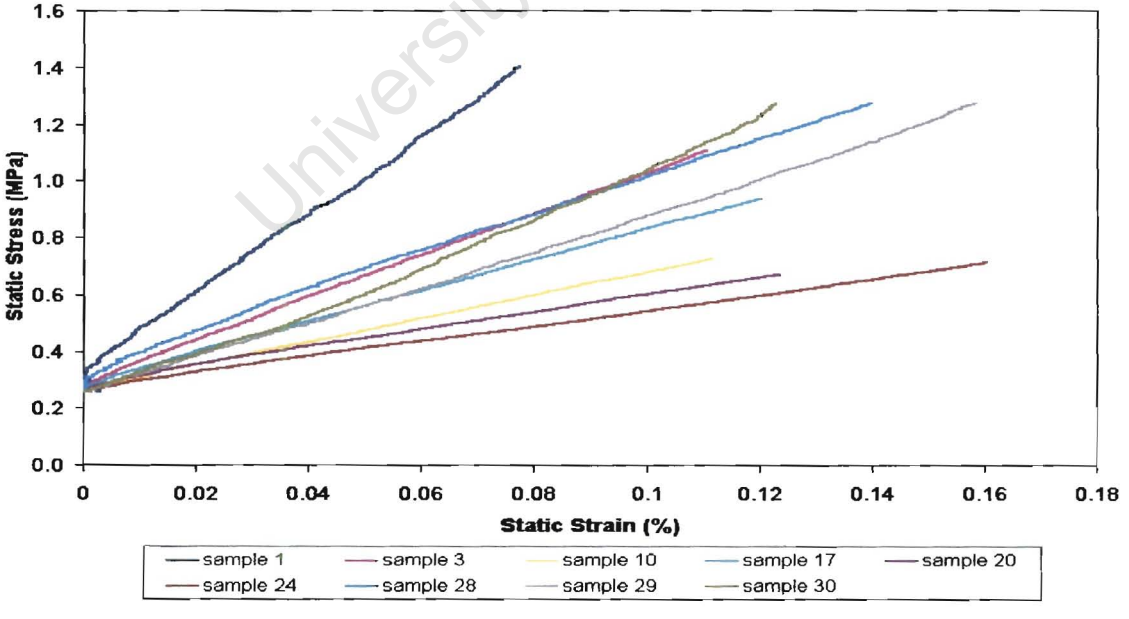

(a)

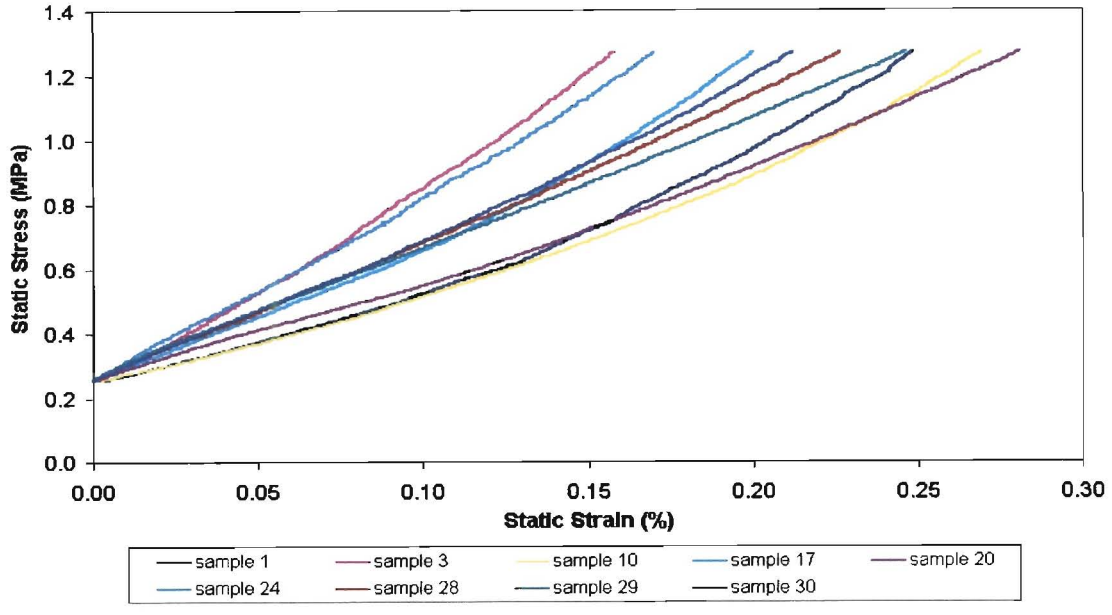

(b)

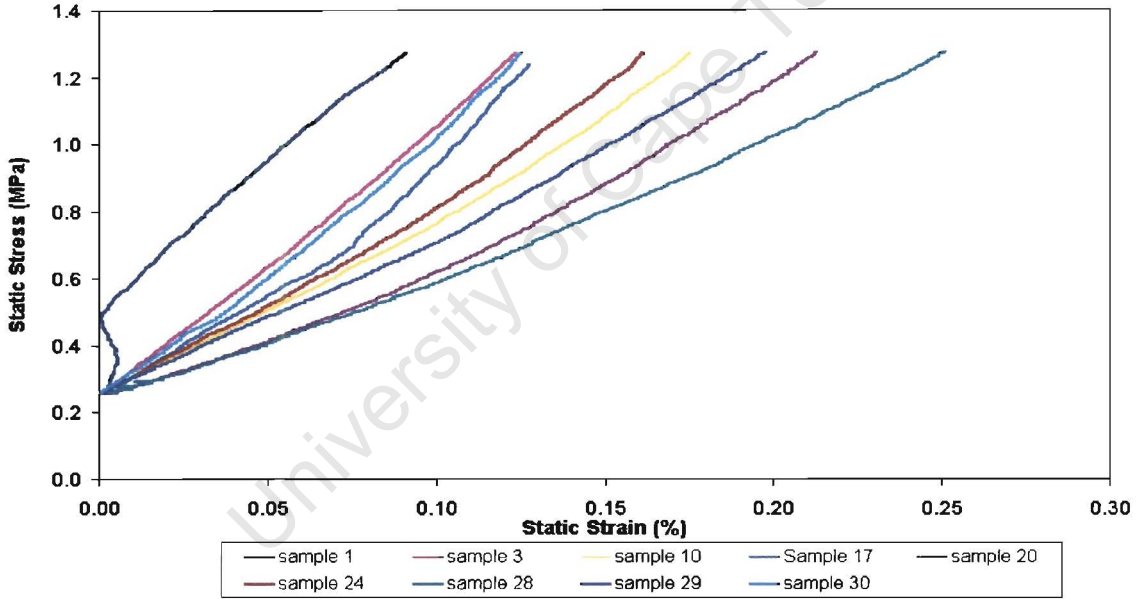

(c)

University of Cape Town

Figure 4.6 DMA plots illustrating the static stress-static strain behaviour of the copolymer grades as obtained at: (a) 23°C, (b) 0°C and (c) –20°C

Figure 4.6 shows the illustrations of the dynamic mechanical analysis static-stress against static-strain curve obtained at 23°C, 0°C and –20°C. There seems to be a decrease in the stiffness values with an increasing ethylene content of the samples. These results are more consistent compared with those obtained from the storage

modulus curves, since the expect behaviour is for the stiffness to decrease with increasing ethylene content. Sample #1 seems to be much stiffer compared with other samples tested at both 23°C and –20°C (see Figure 4.6(a) and (c)) although the contrary is observed at 0°C where sample #1 has a lower stiffness value. The results at 0°C are not consistent with the expected trend, since it would be expected for the stiffness to decreases with increasing temperatures.

4.3 Physical Analysis

4.3.1 Fourier Transform Infrared (FT-IR) Results

All the copolymer grades were analysed using Ft-IR and the spectrum results are shown in the figures below. For this project, the region of interest is the absorbance from 1350 to 350 cm^{-1}, since this region gives a better indication of the polyethylene peaks within the PP matrix. Figure 4.7 shows the reliability of the Ft-IR instrument by comparing the peaks obtained from a single sample after two runs. It was observed that the tests are reproducible and there is not much difference in terms of intensity and number of peaks observed between the two runs. The spectrums in Figures 4.8 to 4.10 are grouped in accordance with the relevant samples' ethylene content range. Figure 4.8 is for the samples with ethylene contents below 8%, Figure 4.9 for the samples with the ethylene contents of between 8 and 10%, and Figure 4.10 is for samples with ethylene contents greater than 10%. The values for the ethylene content of each sample are tabulated in Table 3.1 of the experimental techniques section. The 730 and 720cm^{-1} peak absorptions are characteristic of the PE doublet and an increase in their intensity is an indication of an increase in PE chain length. The ability of PE to crystallise is determined by the PE content. The 668 cm^{-1} absorption peaks is due to the carbon dioxide (CO_2) vapour absorption from the atmosphere and its presence affects the intensity of the PE absorption peaks. The rest of the peaks are attributed to the iPP absorption peaks.

University of Cape Town

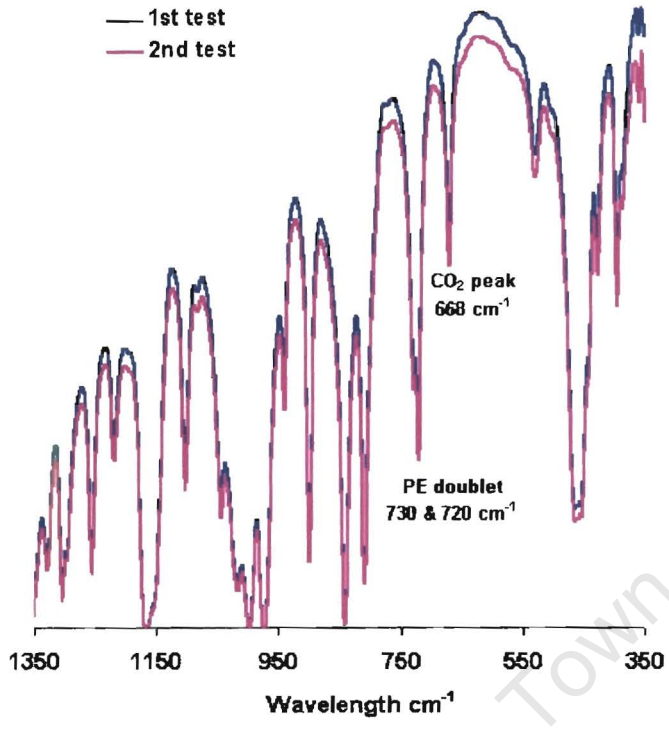

Figure 4.7 **The Ft-IR spectrum of sample number 14, showing the reproducibility of the test**

From Figure 4.8, it is clear that spectrums of samples #1, 2 and 4 show the same kind of characteristics in that there is no peak at 668 cm^{-1} due to the absorption of atmospheric CO_2 vapour. The presence of the CO_2 vapour peak interferes with the intensity of the PE doublet, as it has been noticed by Skaare and co-workers on work done on ethylene-propylene copolymers[53]. The spectrums of samples # 3, 5 and 6 show similarities, except for the intensity of the PE doublet at 720 cm^{-1}, which is dominating in sample # 3.

University of Cape Town

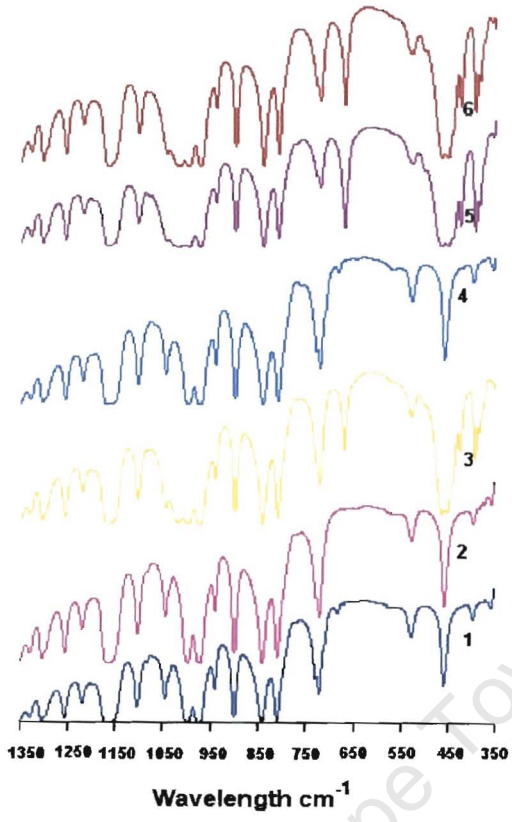

Figure 4.8 Ft-IR spectrums for samples with ethylene contents below 8%

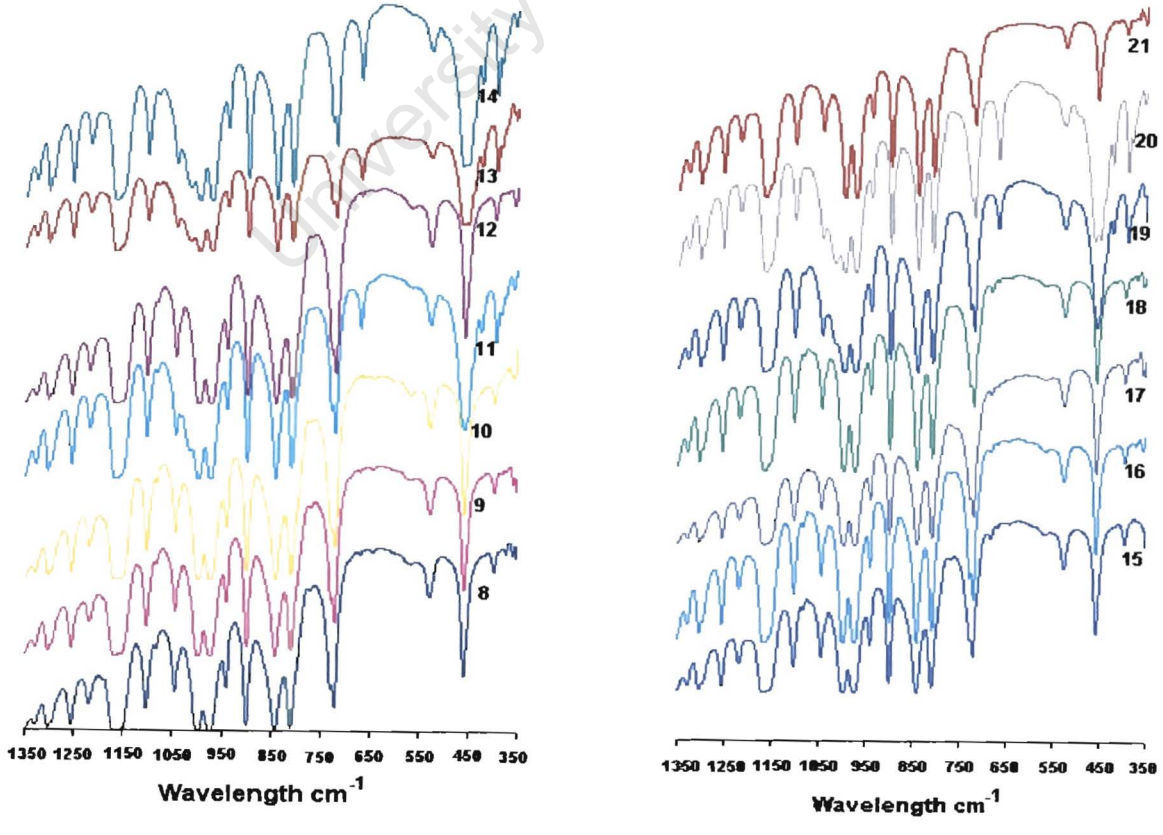

Figure 4.9 Ft-IR spectrums for samples with ethylene contents between 8 and 10%

University of Cape Town

Figure 4.9 shows the Ft-IR spectrums for samples #8 to 21, which have ethylene contents of 8 to 10%. The spectrum's for samples # 11, 13, 14, 19 and 20 show the characteristic CO_2 vapour band peak at 668 cm^{-1} absorption, whilst the rest of the samples do not show this peak. It can be seen that the intensities of the PE peak at the absorbance of 730 and 720 cm^{-1} differ from sample to sample.

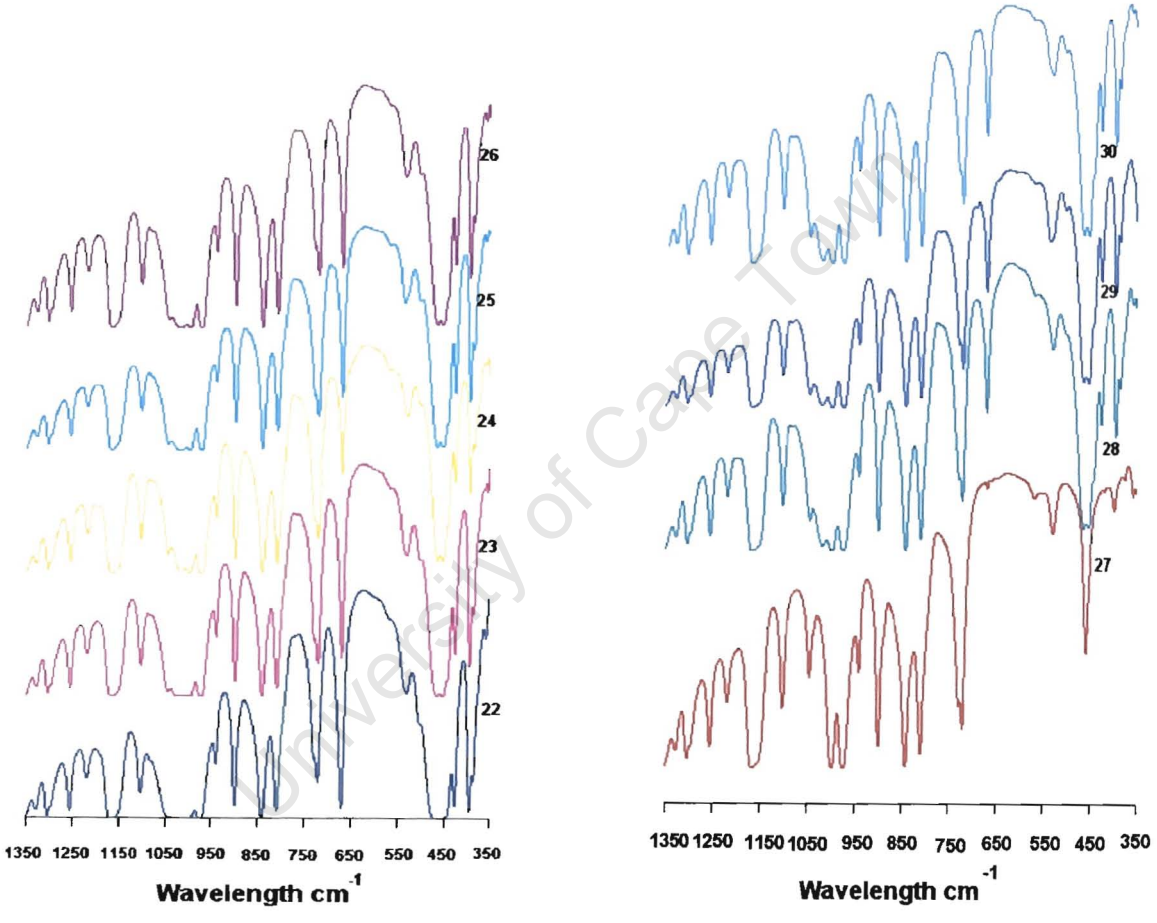

Figure 4.10 Ft-IR spectrums for samples with ethylene contents greater than 10%

Figure 4.10 shows the Ft-IR spectrums of samples # 22 to 30 with ethylene content greater than 10%. The PE doublet absorbance is affected by the presence of the CO_2 vapour absorbance at 668 cm^{-1} except for sample #27, which does not have the CO_2 absorption band. It is noted that sample #27 is a BP grade. This suggests that at ethylene content above 10%, there is an excessive amount of atmospheric CO_2 being absorbed by the copolymer grades during processing.

University of Cape Town

4.3.2 WIDE-ANGLE X-RAY SCATTERING (WAXS) RESULTS

The summarised results of the β-content (K-value) and degree of crystallinity, $\%X_c$, obtained from the WAXS is shown in Table 4.4. In addition, some of the selected x-ray scattering patterns are shown in Figures 4.11 to 4.13, with the relevant characteristic peaks of the $(110)_\alpha$, $(130)_\alpha$ and $(040)_\alpha$ crystallographic planes occurring at 14.15°, 16,75° and 18.60 respectively, indicated. The peak at 2θ = 16.10° is assigned to the (300) crystallographic plane of the β-crystal. This peak appears as a shoulder or is completely absent in some copolymer grades. In only a few of the grades it appears intense as it is mentioned in some of the literature. From these observations, it can be concluded that the proportion of the β-crystal depends on its presence of a β-nucleating agent and on the processing conditions of the copolymer grades.

University of Cape Town

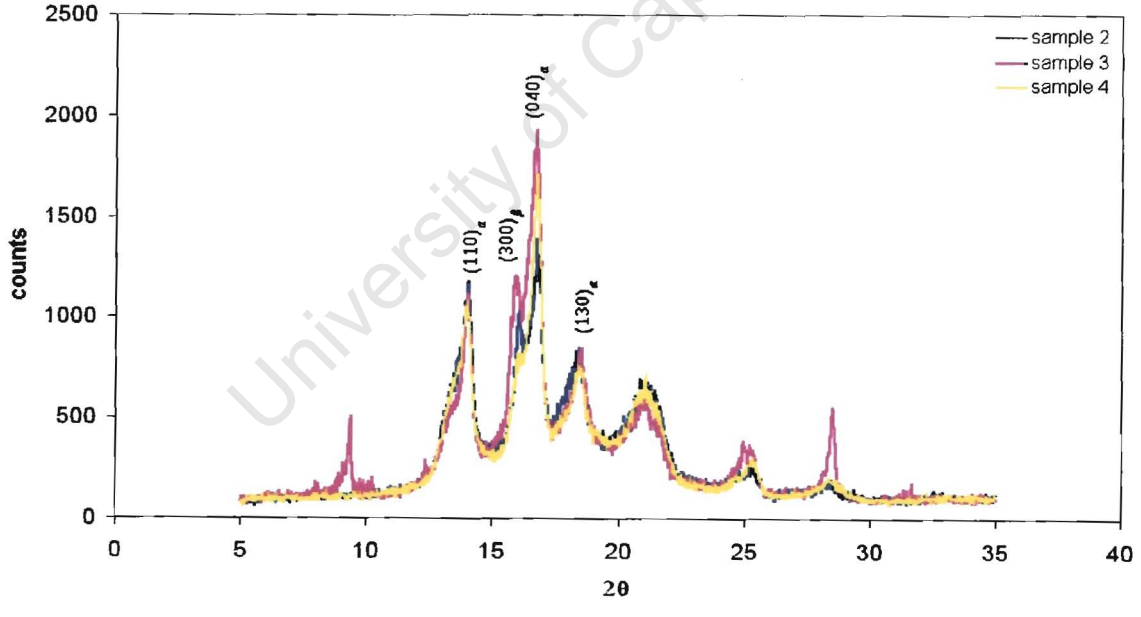

Figure 4.11 Illustration of the WAXS scans of some of the selected grades with ethylene contents below 8%

Table 4.4 The WAXS results showing the overall copolymer crystallinity and the K-values of the β-form

Sample #	X_c (%)	K-value
1	57.8	0.29
2	51.8	0.23
3	54.4	0.30
4	50.1	0.19
5	66.5	0.32
6	47.3	0.24
7	-	-
8	51.2	-
9	60.7	0.24
10	51.2	0.38
11	60.4	0.44
12	57.2	0.30
13	-	-
14	53.8	0.17
15	52.8	0.26
16	49.0	-
17	49.1	-
18	51.9	0.18
19	46.8	-
20	48.1	-
21	57.7	-
22	58.7	0.35
23	53.0	0.23
24	52.1	0.22
25	50.4	0.22
26	53.9	0.23
27	94.3	-
28	52.8	-
29	-	-
30	51.1	0.25

University of Cape Town

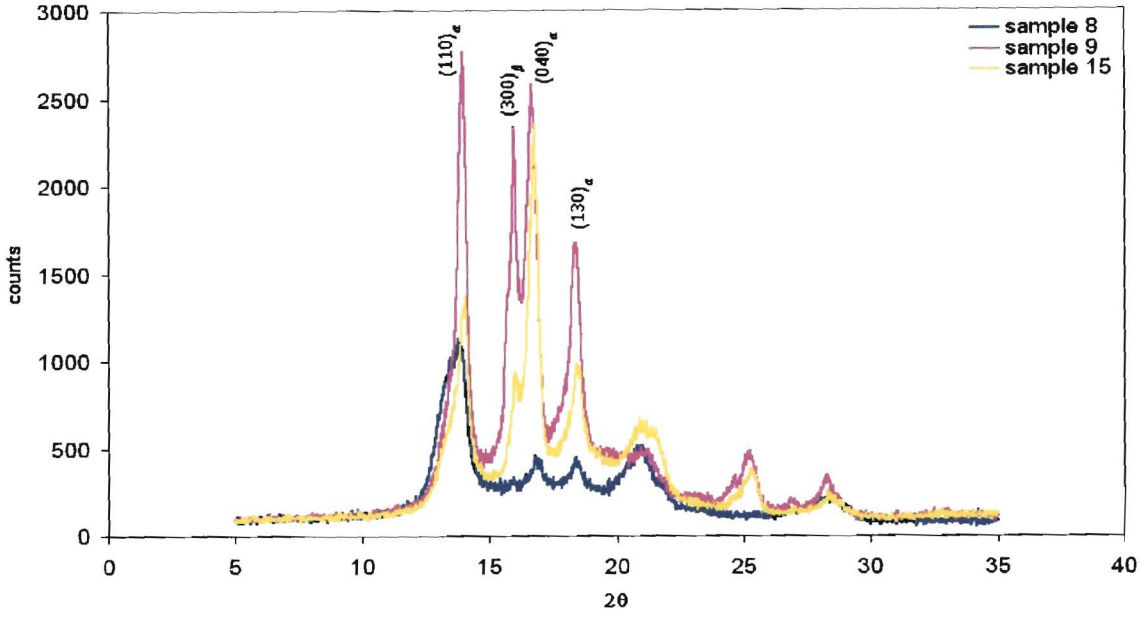

Figure 4.12 Illustration of the WAXS scans of some of the selected grades with ethylene contents between 8 and 10%

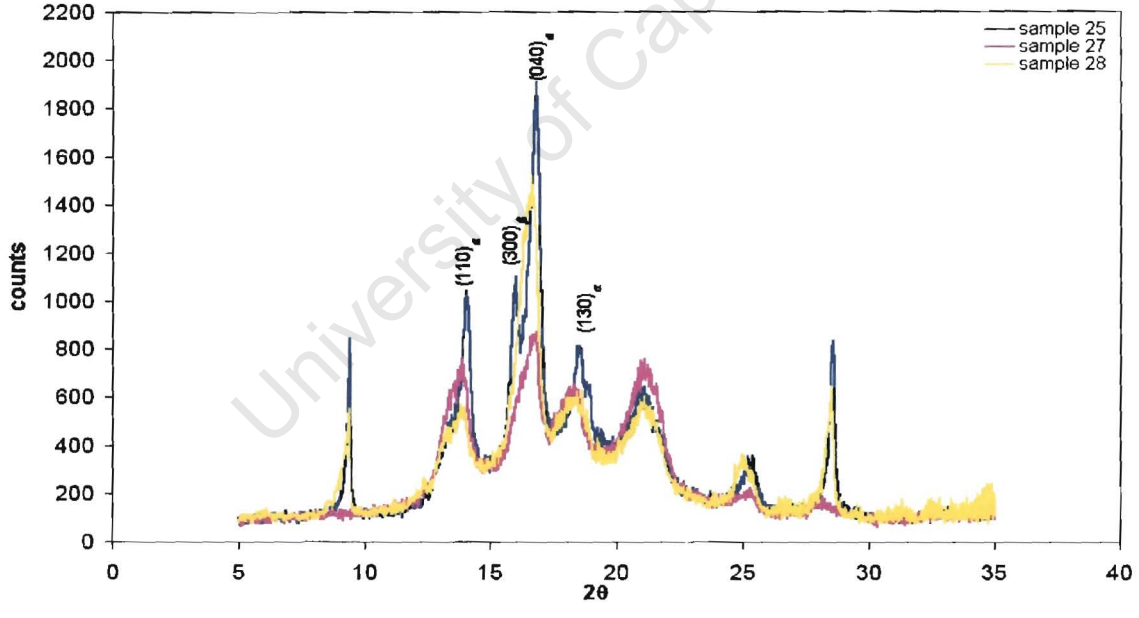

Figure 4.13 Illustration of the WAXS scans of some of the selected grades with ethylene contents above 10%

Figure 4.11 shows the WAXS scans for the grades with ethylene contents below 8%. The samples showed in these scans show the presence of the $(300)_\beta$ crystallographic plane and its intensity increase from sample #2 to sample #4. Sample #3 show the

University of Cape Town

presence of a peak at $2\theta = 9.5°$ and at $2\theta = 28.5°$. The peak at $2\theta = 9.5°$ is absent in samples #2 and 4. In addition, the peak at $2\theta = 28.5°$ is less intense in samples #2 and 4 compared with that found in sample #3. Figure 4.12 show the WAXS scans for the grades with ethylene contents between 8 and 10%. Sample #8 shows the presence of only α-crystal peaks with the $(110)_\alpha$ crystallographic peak dominating. Samples #9 and 15 shows the presence of the $(300)_\beta$ crystallographic peak, which is more intense in sample #9 than in sample #15. The intensity of the crystallographic peaks in sample #8 is quite low compared with other grades within this ethylene content range, with the peak at $2\theta = 25.5°$ being absent in sample #8. Figure 4.13 shows the WAXS for the samples with ethylene contents above 10%. Only sample #25 shows the presence of the $(300)_\beta$ crystallographic peak, whilst in samples #27 and 28 it is absent. Sample #27 shows the absence of the crystallographic peaks at $2\theta = 9.5°$ and $2\theta = 28.5°$. The WAXS scans did not show the presence of the ethylene peak at $2\theta = 23.4°$ due to the (200) crystallographic plane, suggesting that the polyethylene chain is not long enough to crystallise in these grades.

University of Cape Town

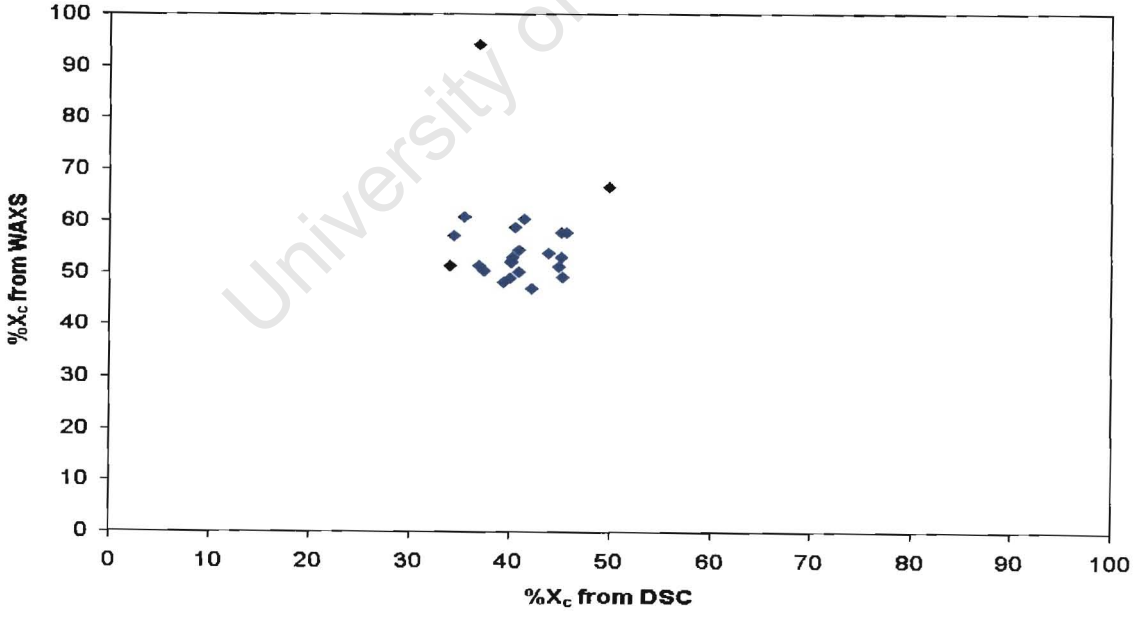

Figure 4.14 Comparisons between the percentage crystallinity, $\%X_c$ determined from DSC and WAXS

The degree of crystallinity obtained from DSC and WAXS when plotted against one another, shows no apparent correlation as shown by Figure 4.14. In addition, the

degree of crystallinity obtained from WAXS is higher than that calculated from the DSC scans. This can be attributed to the difficulties or accuracy when calculating or estimating the amorphous phase area from the crystalline peak area in WAXS scans in order to calculate percentage crystallinity.

Figure 4.15 shows the effect of ethylene content on the degree of crystallinity using the WAXS method. There is no apparent trend observed from these plots, except in the DOW grades where the crystallinity decreases with increasing ethylene content. Most of the grades from the other manufacturing technologies show an almost constant crystallinity over the whole range of ethylene content. Figure 4.16 show that the ethylene content does not have any apparent effect on the K-value of the copolymer grades. Most of the copolymer grades from the manufacturing technologies, except for grades from DOW, do show the presence of β-crystals within them. This could mean that there is a possibility that during processing, the β-nucleating agent was not used in the DOW copolymer grades, and the processing condition did not favour the formation of β-crystals.

University of Cape Town

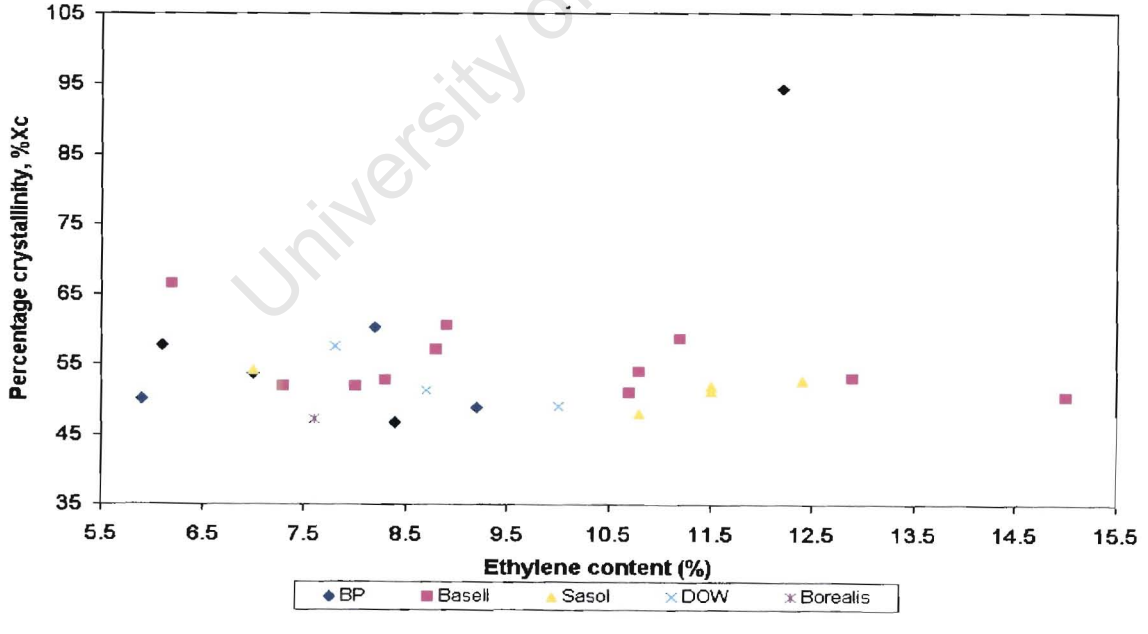

Figure 4.15 Effect of ethylene content on the percentage crystallinity of the copolymer grades.

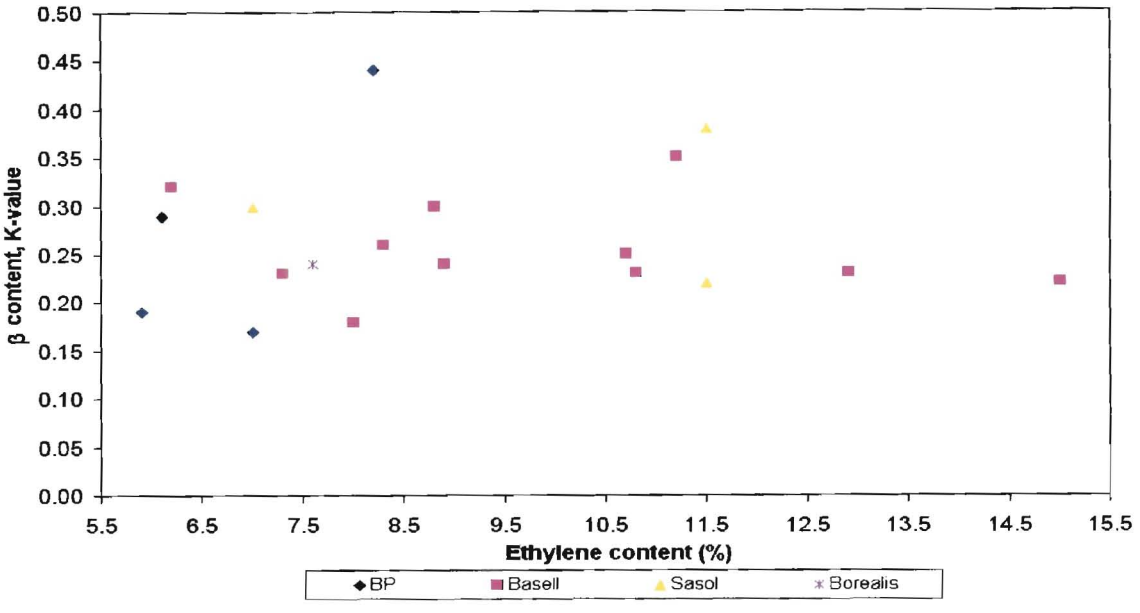

Figure 4.16 **Effect of ethylene contents on the β-content, K-value of the copolymer grades.**

The apparent crystal size or D- values calculated from the WAXS of the copolymer grades are shown in Table 4.5, together with the ratio between the $D_{(110)}$ values and the $D_{(040)}$ values. The data shows that the apparent crystal size of the iPP phase crystallised in the presence of the EPR phase is higher in the direction perpendicular to the (040) crystallographic plane and lower in the (110) crystallographic plane in most of the copolymer grades. The effect of the ethylene content on the $D_{(110)}$/ $D_{(040)}$ ratio is shown in Figure 4.17. The BP grades seem to have a close to constant crystal size ratio over the whole range of ethylene content whilst both the Sasol and Basell grades show scattering in their plotted data points. On other the hand, the DOW grades show an apparent decrease in their crystal size ratio with increasing ethylene content.

University of Cape Town

Table 4.5 The crystallite size (D) of polypropylene copolymers

Sample #	$D_{(110)}$ (Å)	$D_{(040)}$ (Å)	$D_{(130)}$ (Å)	$D_{(110)}/D_{(040)}$ (-)
1	84.5	130.3	73.2	0.64
2	92.7	144.7	59.7	0.64
3	99.2	142.8	80.9	0.69
4	90.2	179.0	73.3	0.50
5	116.0	116.4	105.3	1.00
6	59.7	122.7	41.1	0.49
7	-	-	-	-
8	77.3	51.2	61.3	1.51
9	178.9	171.4	159.9	1.04
10	144.1	97.6	85.1	1.48
11	158.7	437.6	150.2	0.36
12	195.0	201.4	198.6	0.97
13	-	-	-	-
14	119.6	188.9	125.5	0.63
15	109.1	208.7	171.5	0.52
16	93.5	178.5	115.3	0.52
17	87.1	96.8	57.2	0.90
18	85.5	201.9	219.9	0.42
19	78.9	99.5	46.3	0.79
20	110.5	38.9	55.3	2.84
21	79.5	41.6	51.1	1.91
22	195.4	134.6	180.8	1.45
23	208.4	142.3	71.4	1.46
24	102.8	164.4	86.8	0.63
25	103.8	161.8	57.4	0.64
26	87.9	144.7	67.1	0.61
27	79.9	90.1	39.7	0.89
28	61.3	103.3	47.2	0.59
29	-	-	-	-
30	245.5	138.9	52.8	1.77

University of Cape Town

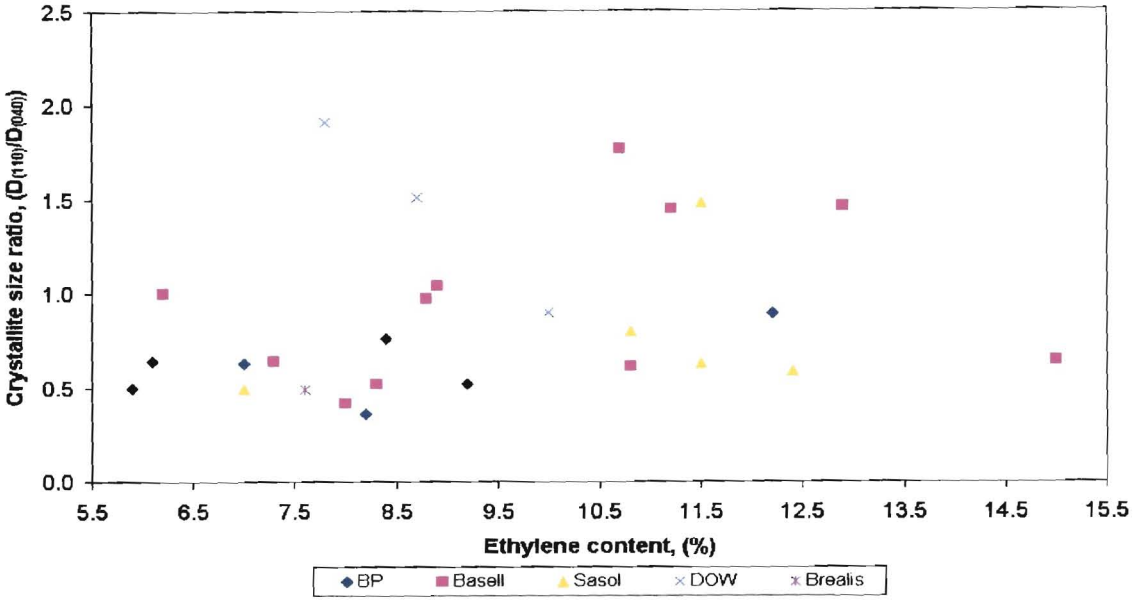

Figure 4.17 Effect of ethylene content on the $D_{(110)}/ D_{(040)}$ ratio of the copolymers

University of Cape Town

4.4 Mechanical Behaviour

4.4.1 Effect of the Material Parameters on Mechanical Properties

Material parameters such as the ethylene content, MFI and the crystallinity are known to affect to some extent the mechanical properties of polypropylene copolymers. These parameters can be correlated with mechanical properties such as the impact strength, yield strength, tensile modulus, hardness and ductility. Table 4.6 shows the three material parameters as they are grouped in percentage ethylene content ranges.

The data of the mechanical properties such as impact strengths (Izod impact, tensile impact and drop weight impact), hardness, tensile modulus, tensile yield strength and percentage elongation of the grades are shown in Appendix A.

Table 4.6 Selected material parameters of ethylene content, MFI and percentage crystallinity that affect the mechanical properties

Sample #	C_2 range	Ethylene content (%)	MFI (g/10min)	$\%X_C$ (melt)
1	C_2 <8%	6.1	5.9	43.6
2		7.3	6.5	39.2
3		7.0	8.0	41.0
4		5.9	12.0	40.7
5		6.2	20.0	49.8
6		7.6	44.0	47.1
7	C_2 = 8 – 10%	8.5	0.4	34.3
8		8.7	0.7	33.2
9		8.9	0.8	33.2
10		11.5	1.0	45.7
11		8.2	1.2	39.0
12		8.8	1.5	33.8
13		8.8	7.0	36.9
14		7.0	14.0	41.7
15		8.3	28.0	42.4
16		9.2	34.0	39.5
17		10.0	34.0	43.1
18		8.0	46.0	39.9
19		8.4	49.0	41.4
20		10.0	50.0	38.5
21		7.8	68.0	45.4
22	C_2 > 10%	11.2	1.2	40.3
23		12.9	7.0	40.5
24		11.5	8.0	40.0
25		15.0	15.0	36.9
26		10.8	17.0	38.0
27		12.2	18.0	35.9
28		12.4	24.0	40.8
29		11.4	73.0	38.9
30		10.7	79.0	44.7

University of Cape Town

4.4.2 Effect of the Melt Flow Index (MFI) on Mechanical Properties

Table 4.7 show the matrix of the copolymer grades that are considered to have the same melt flow index ranges. Figure 4.18 and Figure 4.19 below shows the effect of the melt flow index (MFI) on the impact strength behaviour of the copolymers tested. The effect of the MFI on the impact strength was established by considering only the tests done at room temperature, given that none of the copolymers undergo any transition at this temperature. In addition, the effect of MFI on impact strength was established by plotting data of the tests performed at –20°C. It is clear that the MFI of the copolymer grades has a significant effect on the impact strength as shown by the

figures below. At room temperature the Izod and tensile tests show the same kind of behaviour, where the impact strengths decrease rapidly until it reaches a value of about 10 g/10min and then more gradually with increasing MFI. The difference between the Izod impact test and the tensile impact test is that the Izod impact test shows a ductile to brittle transition in the plot, whilst this transition is not so apparent with the tensile impact results. The drop weight impact results on the other hand, shows a somewhat slightly different behaviour in Figure 4.18(c) below, considering that only a few copolymer grades were tested. Therefore, the correlation between drop weight impact, Izod and tensile impact strength still needs to be established.

Table 4.7 The matrix of samples with the same MFI range but different ethylene contents

Sample #	MFI ranges	Ethylene content%
11	MFI < 2	8.2
7		8.5
8		8.7
12		8.8
9		8.9
22		11.2
10		11.5
1	MFI = 3 - 10	6.1
3		7.0
2		7.3
13		8.8
24		11.5
23		12.9
4	MFI=10-18	5.9
14		7.0
27		12.2
25		15.0
26		17.0
5	MFI=18-40	6.2
6		7.6
15		8.3
16		9.2
17		10.0
28		12.4
21	MFI > 40	7.8
18		8.0
19		8.4
30		10.7
20		10.8
29		11.4

University of Cape Town

The low MFI polymers have relatively high ethylene contents so that the trend becomes a little distorted, since the high ethylene content tends to push the impact strength to high values. These conditions are good if one is trying to optimise the impact strength to stiffness ratio of the materials with low MFI. However, at a high MFI the ethylene content makes no significance difference on the impact properties of the copolymer grades, as indicated by the figures below.

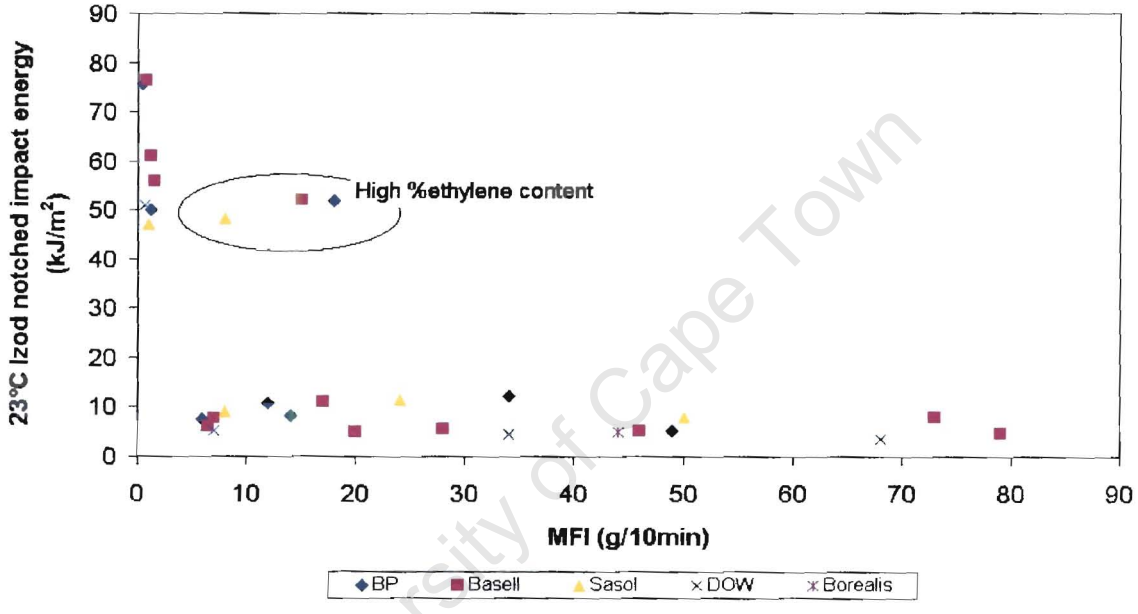

(a)

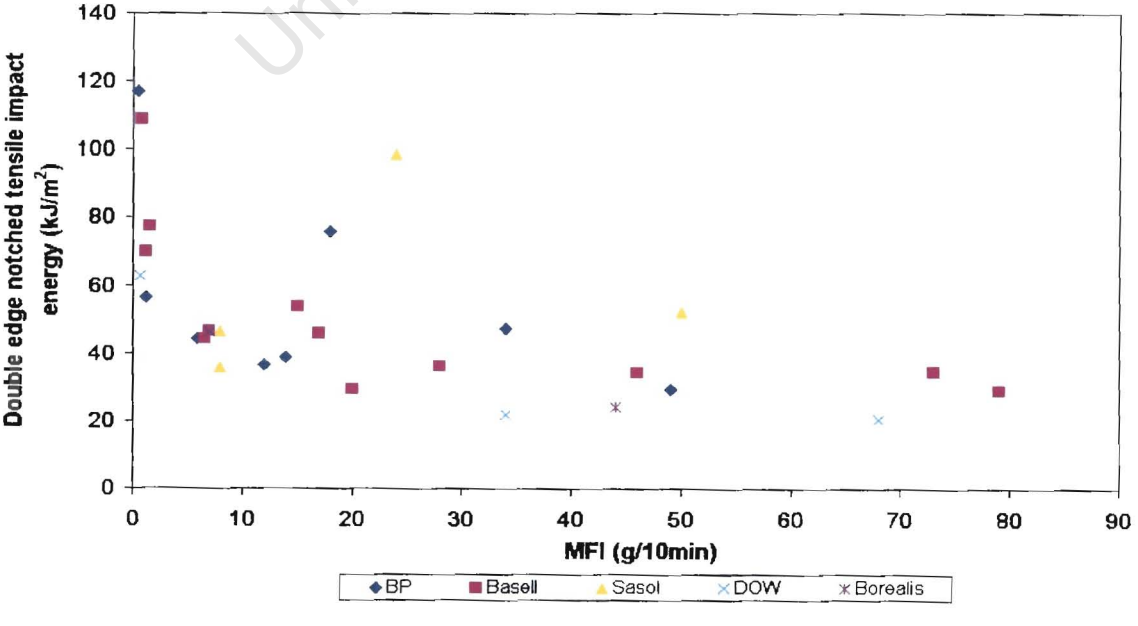

(b)

University of Cape Town

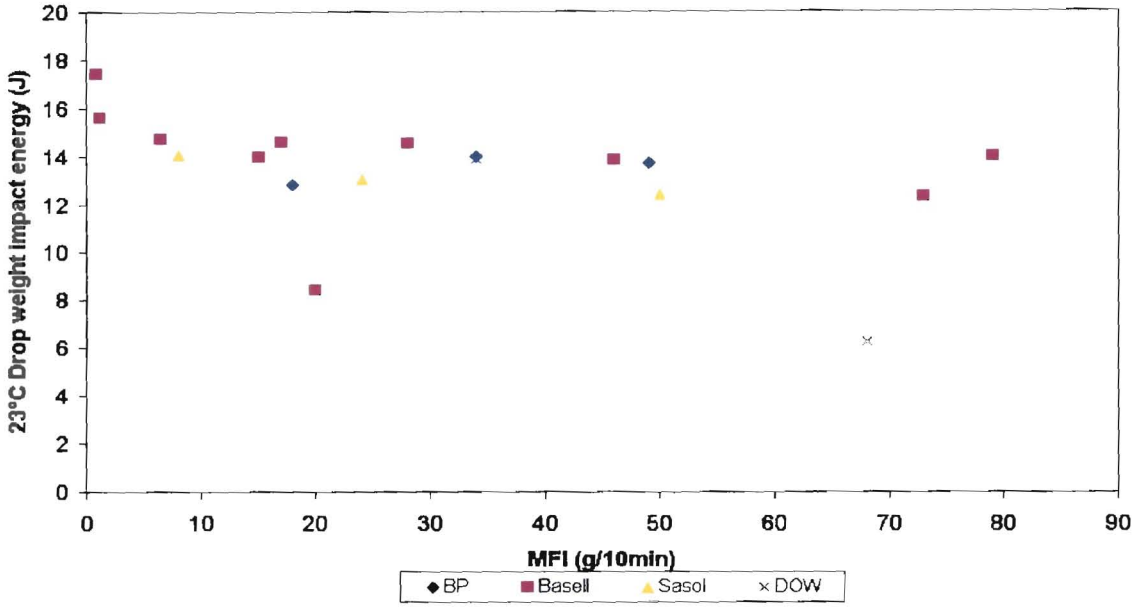

(c)

Figure 4.18 Illustration of the effect of the melt flow index (MFI) on the impact strength of the copolymer grades at room temperature: (a) Izod impact, (b) tensile impact, and (c) drop weight impact tests

University of Cape Town

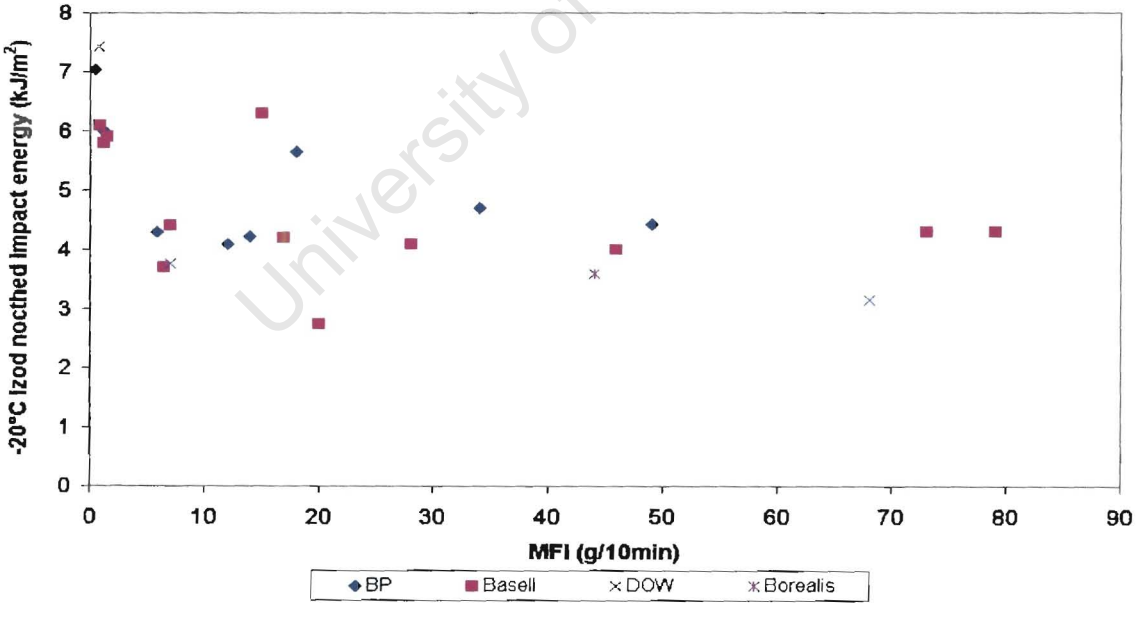

(a)

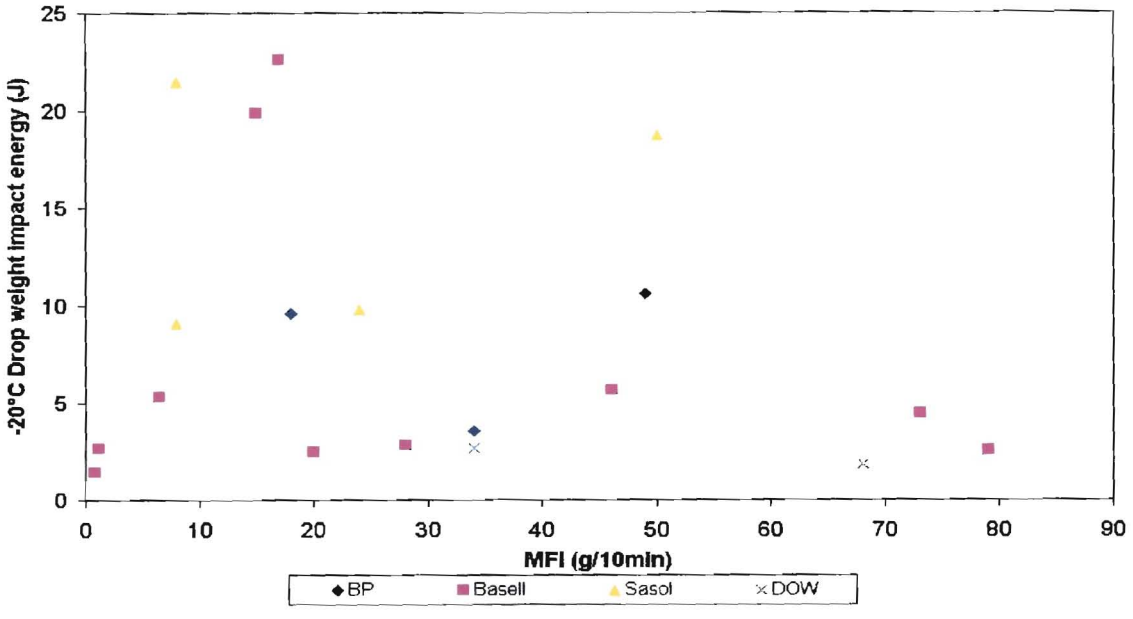

(b)

Figure 4.19 Illustration of the effect of the melt flow index (MFI) on the impact strength of the copolymer grades at –20°C: (a) Izod Impact and (b) drop weight impact tests

University of Cape Town

At low temperatures, a similar trend is in Figure 4.19(a) is observed from the Izod impact curve. The decrease in impact strength with the increasing MFI is not as pronounced as when tested at room temperature. The low temperature data from the drop weight impact results seems not to follow any distinct trend at all as shown in Figure 4.19(b) above, as there is no distinct trend and some grades show an increase in impact energy at –20°C.

Figures 4.20 to 4.22 show the effect of MFI on the yield strength, modulus, and hardness, respectively. A plot of the yield strength and stiffness against melt flow index shows a scattering of the data points over the whole range of MFI. This suggests that the MFI does not have any effect on the yield strength and modulus. The Sasol grades have on average the lowest yield strength, modulus and hardness values over the entire MFI range, compared with the other copolymers grades. The BP grades have the highest hardness values, whilst the Sasol grades have the lowest values. The Basell grades have somewhat intermediate values of hardness over the whole MFI range as indicated in Figure 4.22 below. From this figure it would appear that the melt flow index (molecular weight) does not have any effect on the hardness of the copolymer grades.

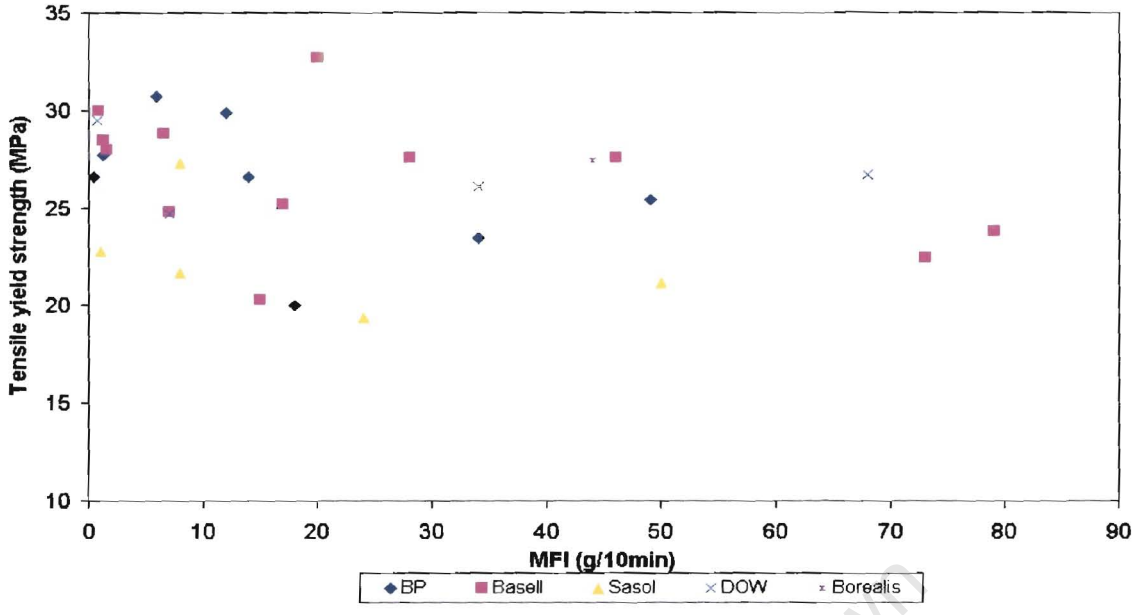

Figure 4.20 Illustration of the effect of the melt flow index (MFI) on the tensile yield strength of the copolymer grades

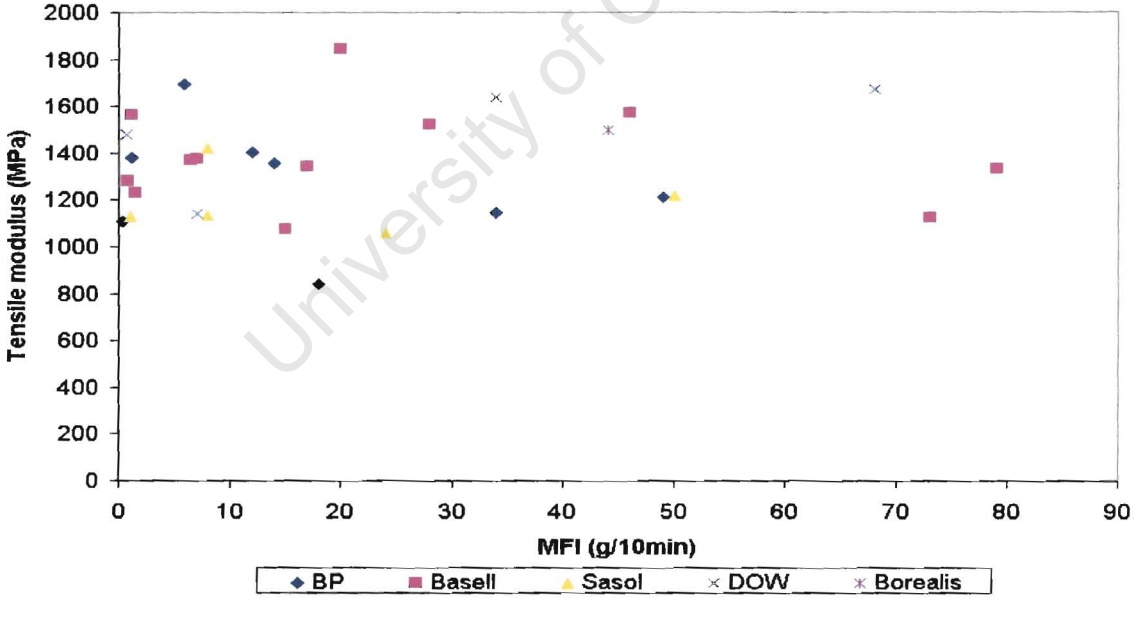

Figure 4.21 Illustration of the effect of the melt flow index (MFI) on the tensile modulus of the copolymer grades

University of Cape Town

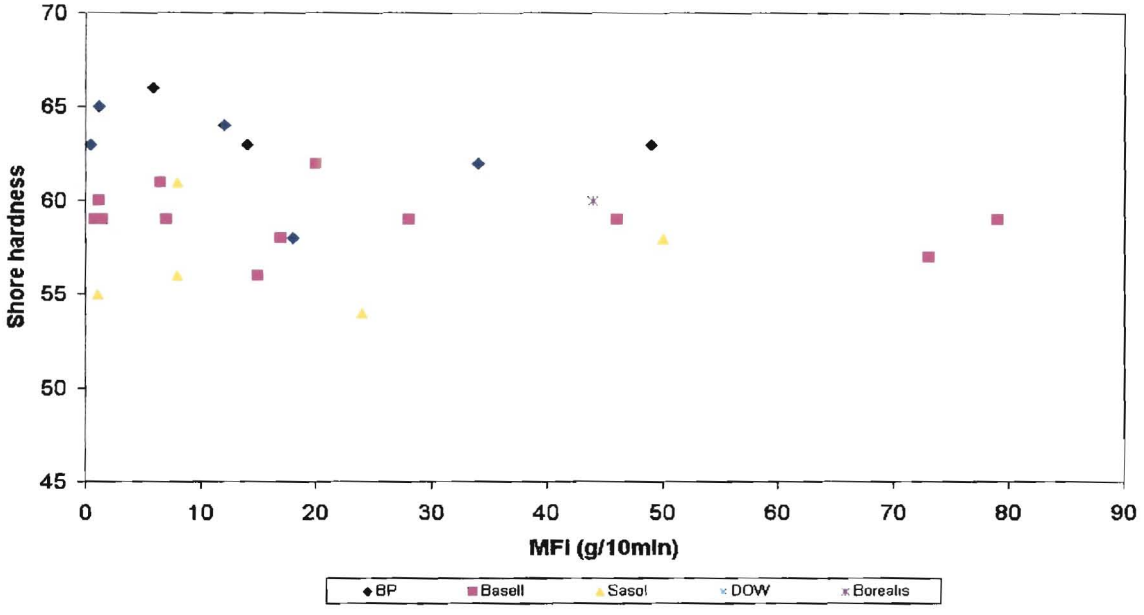

Figure 4.22 Illustration of the effect of the melt flow index (MFI) on the Shore hardness of the copolymer grades

Figure 4.23 shows that the Sasol grades are much more ductile over the whole MFI range, followed by the BP and the Basell grades, with the DOW grades being the less ductile. There is generally a decrease in the percentage elongation of the grades until an MFI of 20 g/10min, followed by the steady decreases in ductility. This behaviour can be seen with the Basell grades.

University of Cape Town

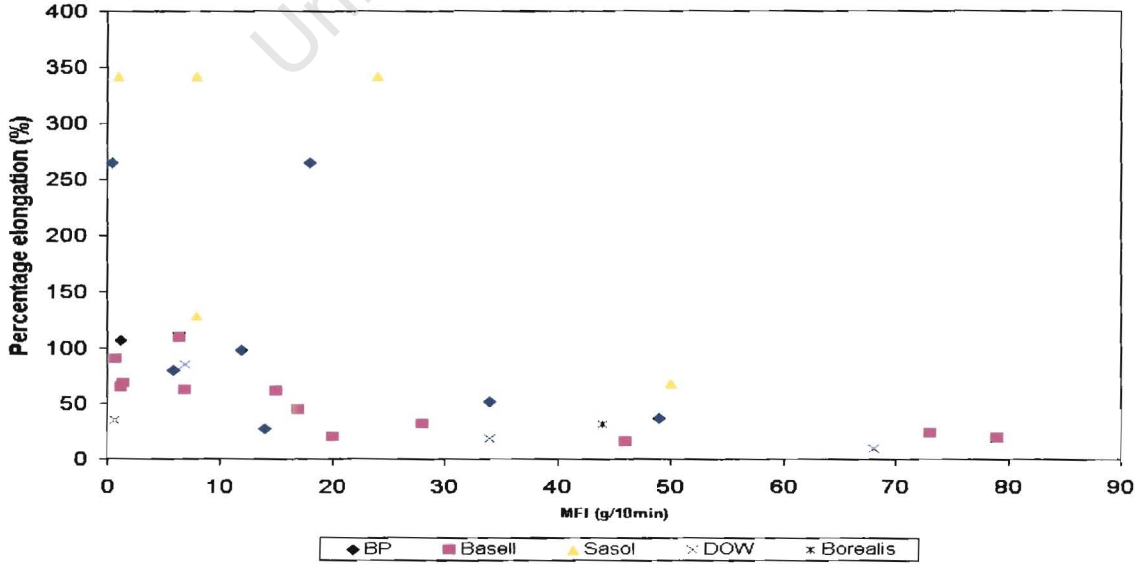

Figure 4.23 Illustration of the effect of the melt flow index (MFI) on percentage elongation of the copolymer grades

4.4.3 Effect of Ethylene Content on Mechanical Properties

The plots of the effect of the ethylene content on the impact strength are shown in the Figure 4.24 below. In the previous section it was observed that a low melt flow index has a significant effect on the impact strength of the copolymers. On the contrary, the ethylene content does not have a significant effect on the impact strength, specifically with the copolymer grades with a high melt flow index. However, ethylene content does show a significant influence within the copolymer grades of a low melt flow index. Therefore, in order to make sense out of the results about the influences of the ethylene content on impact strength, plots of the ethylene content against the impact strength is therefore shown from the data of the copolymer grades with melt flow indices of less than 30 g/min.

Figure 4.24(a) to Figure 4.24(c) below show the plots of effect of ethylene content on the impact properties for the samples with MFI's of 30 g/10min and lower for room temperature tests. Most of the grades show an increase in the Izod and tensile impact energy at ethylene content around of 8.5%. This indicates that there is transition from ductile-to-brittle behaviour with increasing ethylene content at about 8.5% ethylene. For the drop weight impact tests, because of the limited number of sample grades with melt flow indices of less than 30 g/10 min, this transition could not be seen or determined. Nevertheless, the trend of the Basell grades shows an increase of impact strength up 9% ethylene content, followed by a slight decrease in impact strength.

University of Cape Town

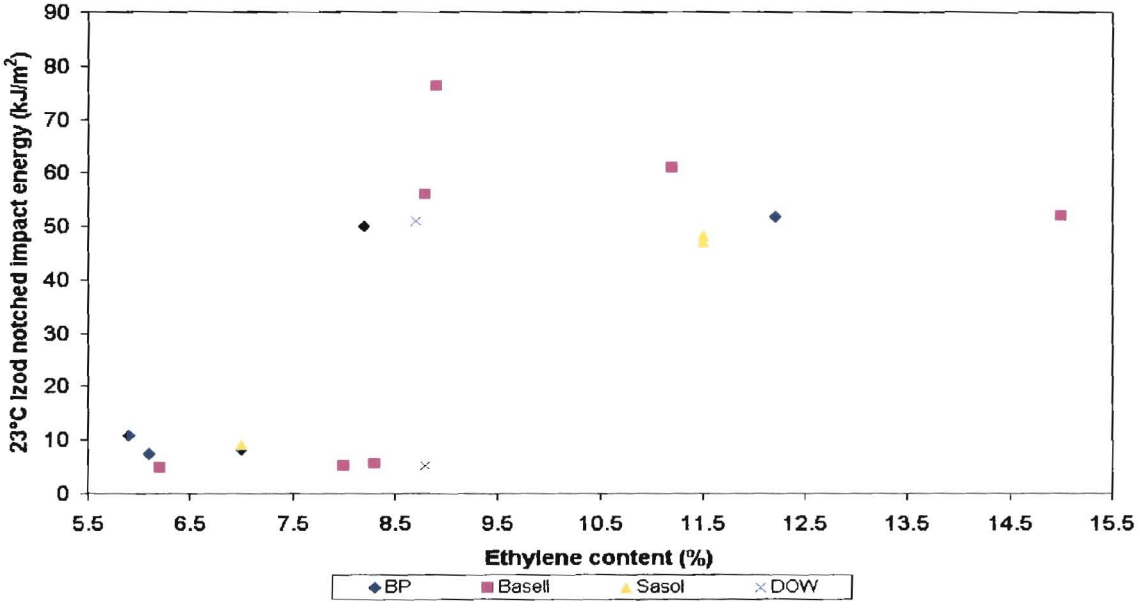

(a)

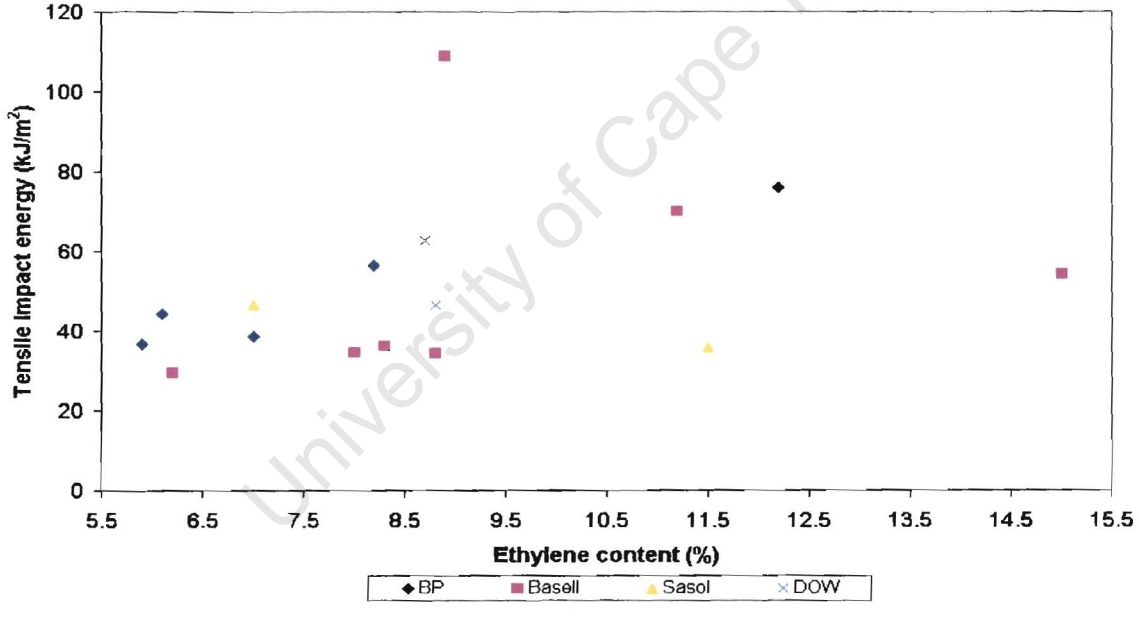

(b)

University of Cape Town

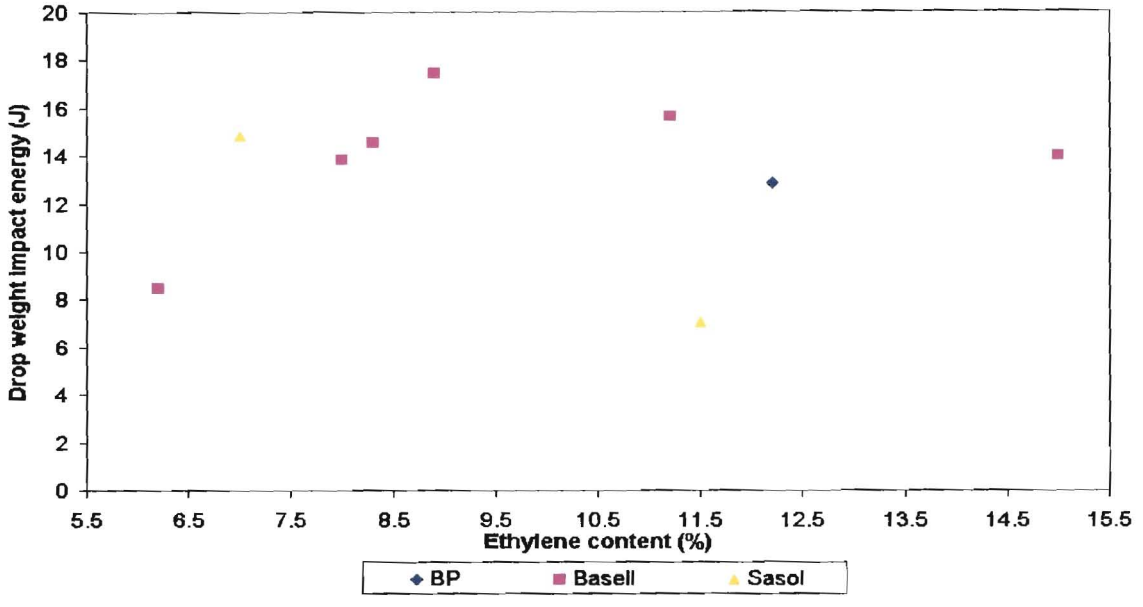

(c)

Figure 4.24 Illustration of the effect of the ethylene content on impact energy for samples with MFI < 30 g/10min; (a) Izod impact, (b) tensile impact, and (c) drop weight impact

Figure 4.25 below shows the effect of the ethylene content on the impact strength of the copolymers grades with melt flow indices of below 30 g/10 min at a temperature of –20°C. At this temperature, only the Izod impact test indicates that the impact energy increases with ethylene content, while the drop weight data doesn't seem to follow any particular trend.

University of Cape Town

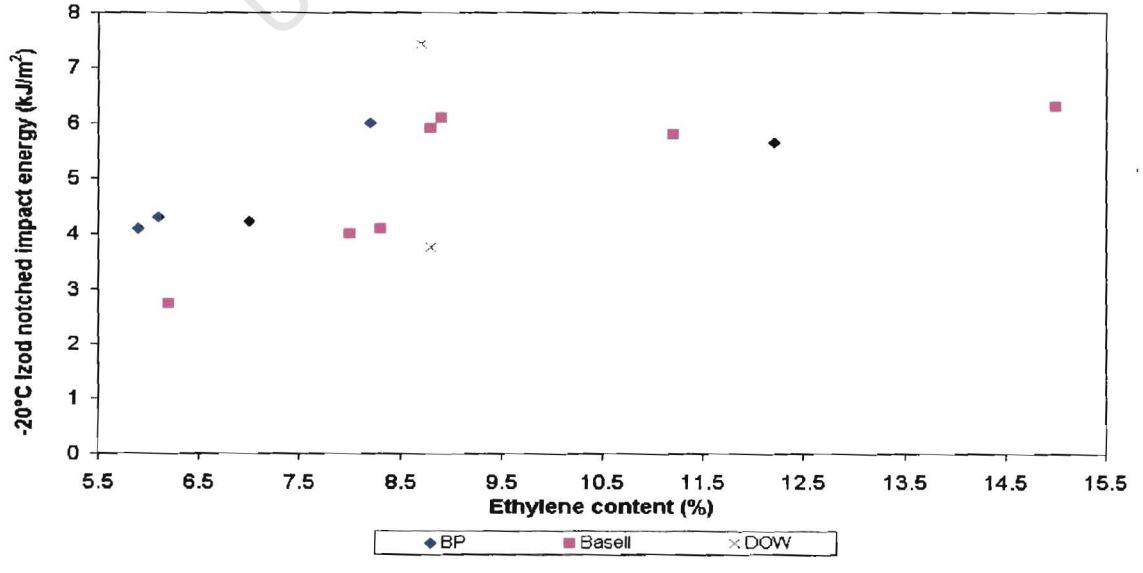

(a)

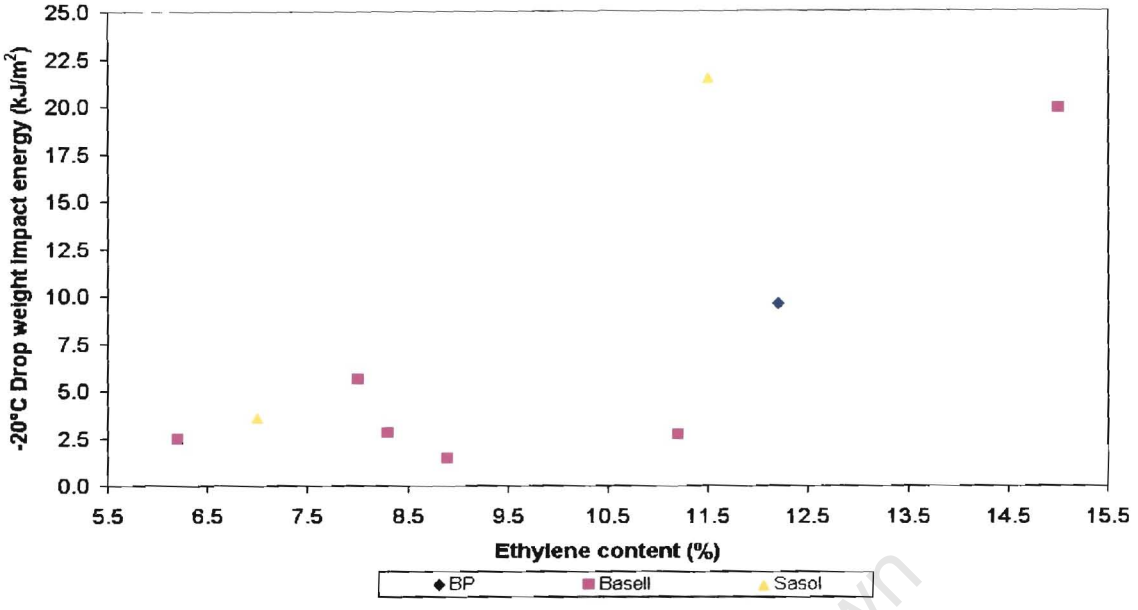

(b)

Figure 4.25 Illustration of the effect of the ethylene content on the impact strength of the copolymer grades at –20°C; (a) Izod impact and (b) drop weight impact tests

Figures 4.26 to 4.28 shows the effect of the ethylene content on the yield strength, tensile modulus and hardness, respectively. The general behaviour observed is that the yield strength, modulus and the hardness decrease with increasing ethylene content. From Figure 4.26, it is clear that the Basell grades have higher yield strengths and tensile modulus than other grades. In Figure 4.28 it is observed that BP grades have higher hardness than the Basell grades. The Sasol grades have both lower values for the hardness and stiffness compared with the other grades.

University of Cape Town

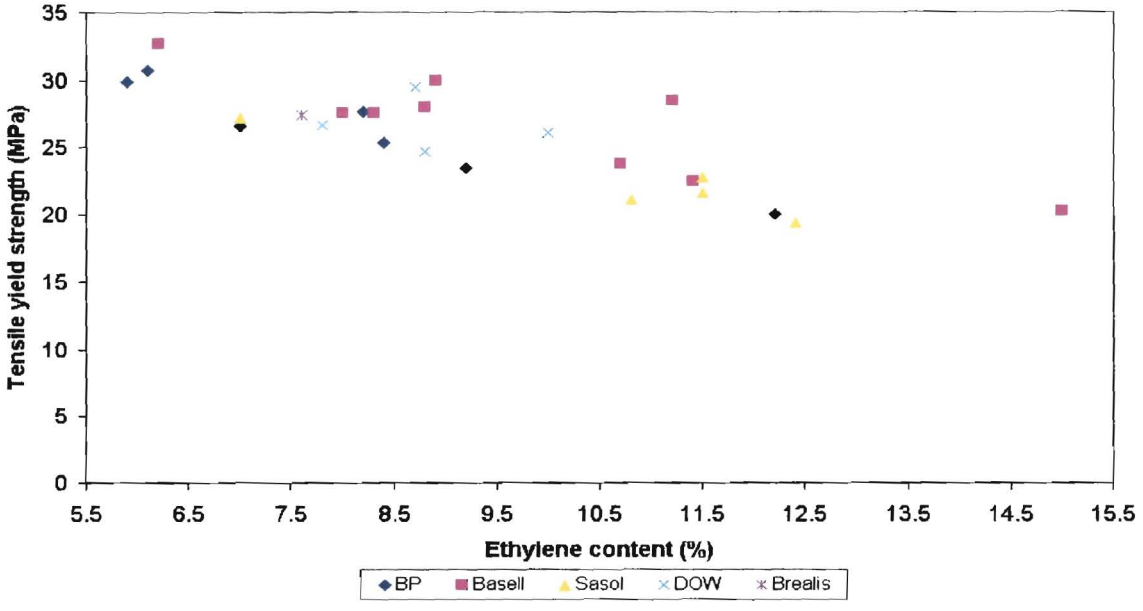

Figure 4.26 Illustration of the effect of percentage ethylene content on the yield strength of the copolymer grades

University of Cape Town

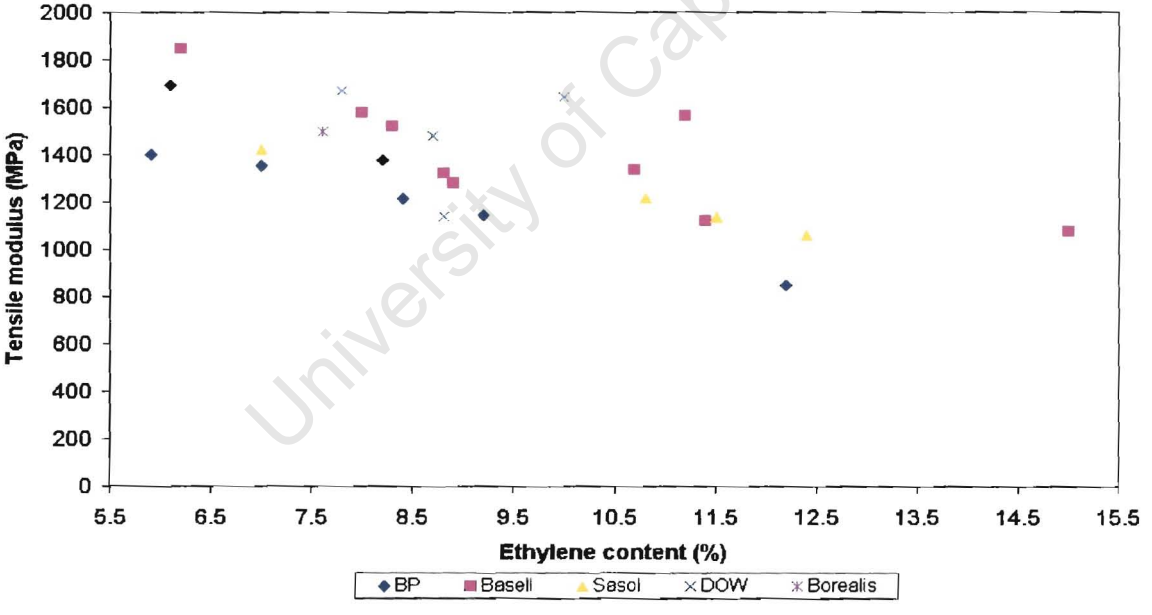

Figure 4.27 Illustration of the effect of percentage ethylene content on the tensile modulus of the copolymer grades

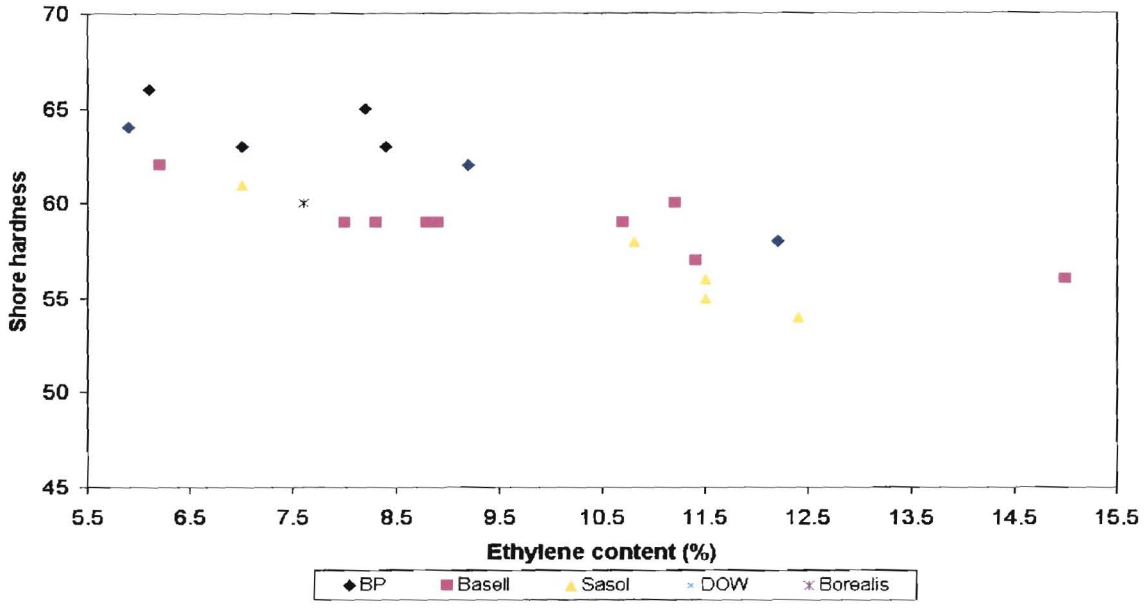

Figure 4.28 Illustration of the effect of percentage ethylene content on the shore hardness of the copolymer grades

The effect of the ethylene content on the ductility of the copolymer grades is shown in Figure 4.29. There is no particular trend observed from this plot, although it would commonly be expected that the ductility of the material to increase with increasing ethylene content, since the stiffness and the hardness decrease with increasing ethylene content.

University of Cape Town

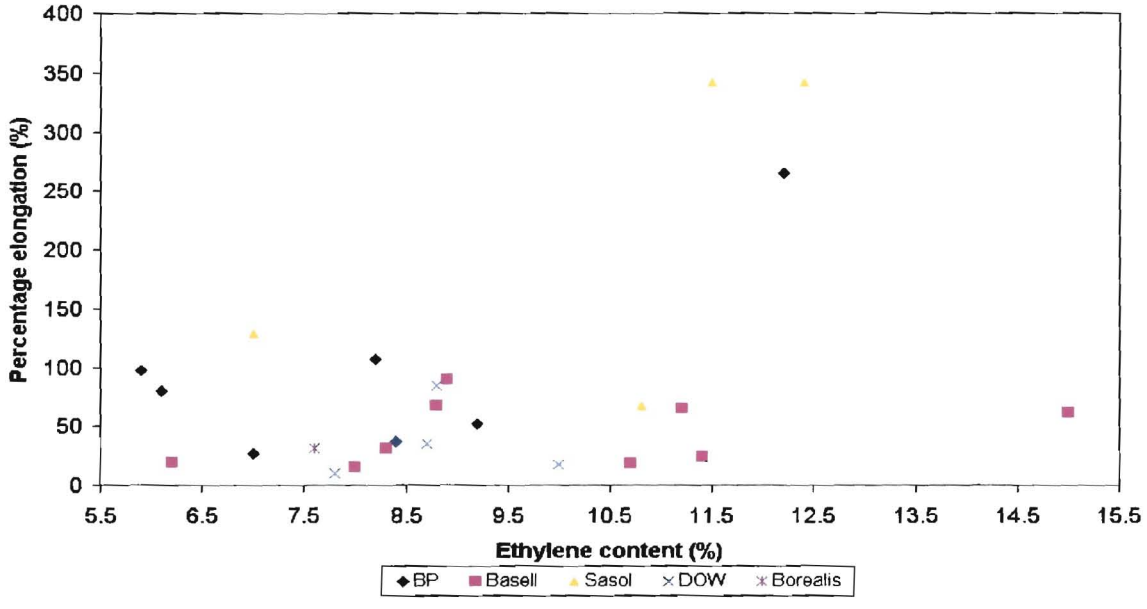

Figure 4.29 Illustration of the effect of percentage ethylene content on the percentage elongation of the copolymer grades

4.4.4 Effect of Percentage Crystallinity on Mechanical Properties

The effect of the degree of crystallinity on the impact strength results is shown in Figure 4.30(a) to Figure 4.30(b) below. The results show that the impact strength decreases with increasing percentage crystallinity. The Izod and tensile impacts show a reasonable correlation with crystallinity. Except for a few samples, there are trends observed within the BP, Basell and DOW grades. The Sasol grades have impact energy independent of the percentage crystallinity. The DOW grades seem to have lower percentage crystallinity and impact strength compared other grades.

University of Cape Town

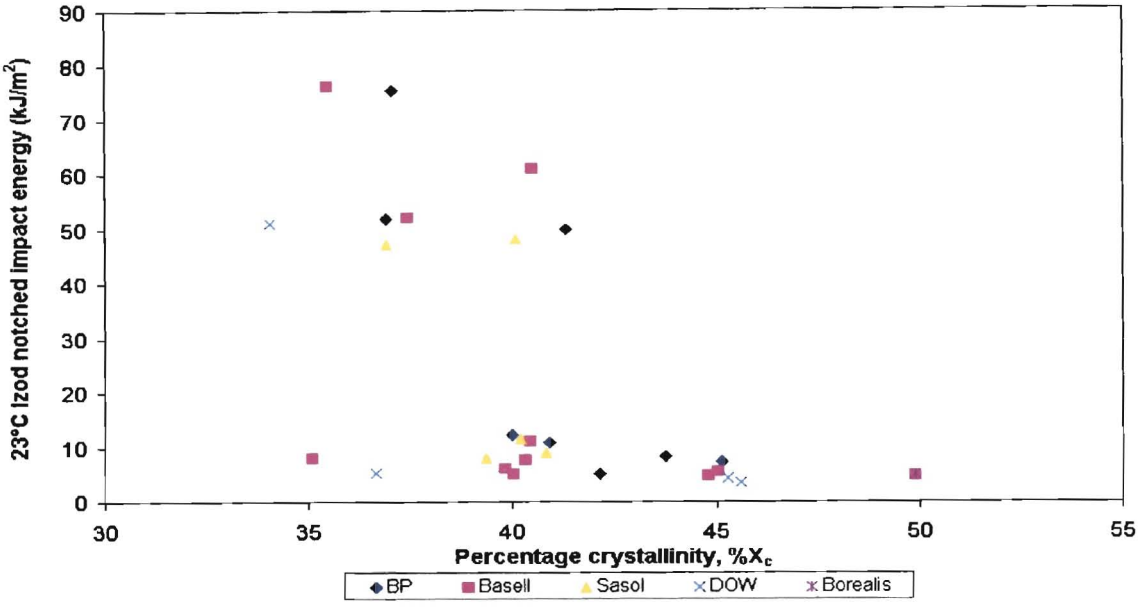

(a)

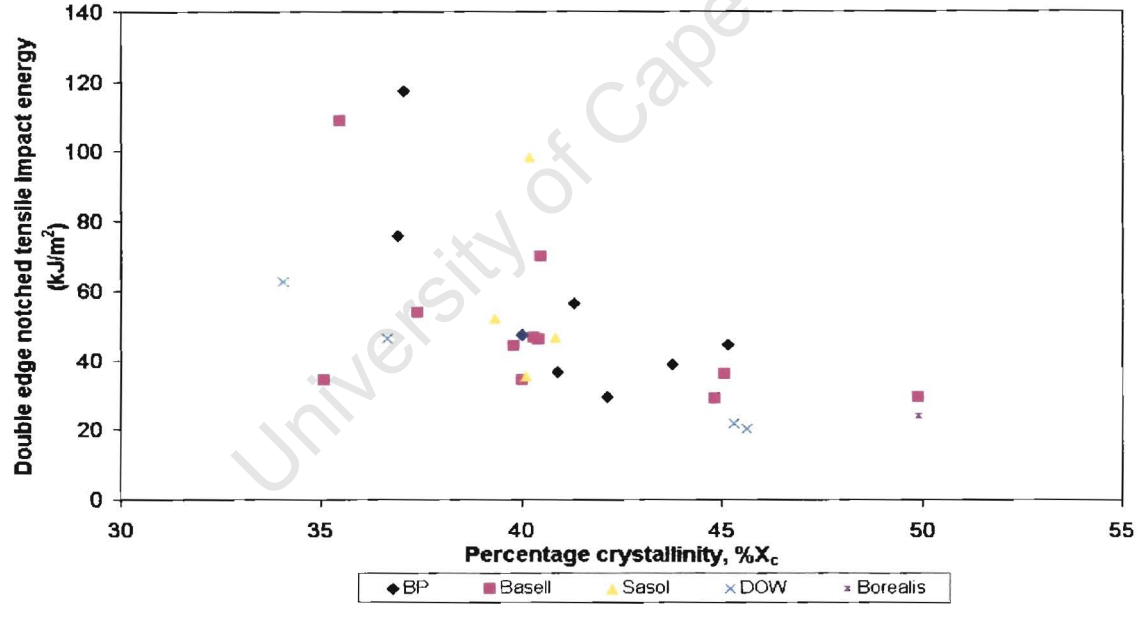

(b)

University of Cape Town

Figure 4.30 Illustration of the effect of percentage crystallinity on the impact strength of the copolymer grades; (a) Izod impact, (b) tensile impact

The effect of the degree of crystallinity on the modulus, yield strength and hardness are shown in Figures 4.31 to 4.33. The plots show that the modulus, yield strength and hardness increase with increasing degree of crystallinity. Figure 4.33 show that the BP

grades have the highest hardness values, the Sasol grades the lowest, and the hardness of the Basell grades lie midway between these over the whole range of crystallinity.

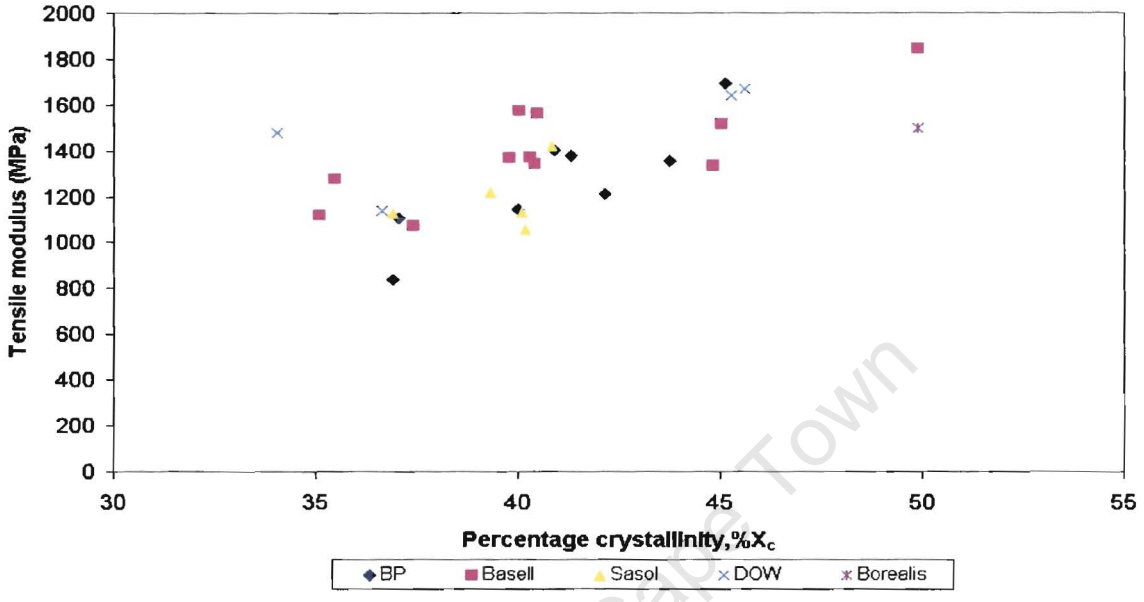

Figure 4.31 Illustration of the effect of percentage crystallinity on the tensile modulus of the copolymer grades

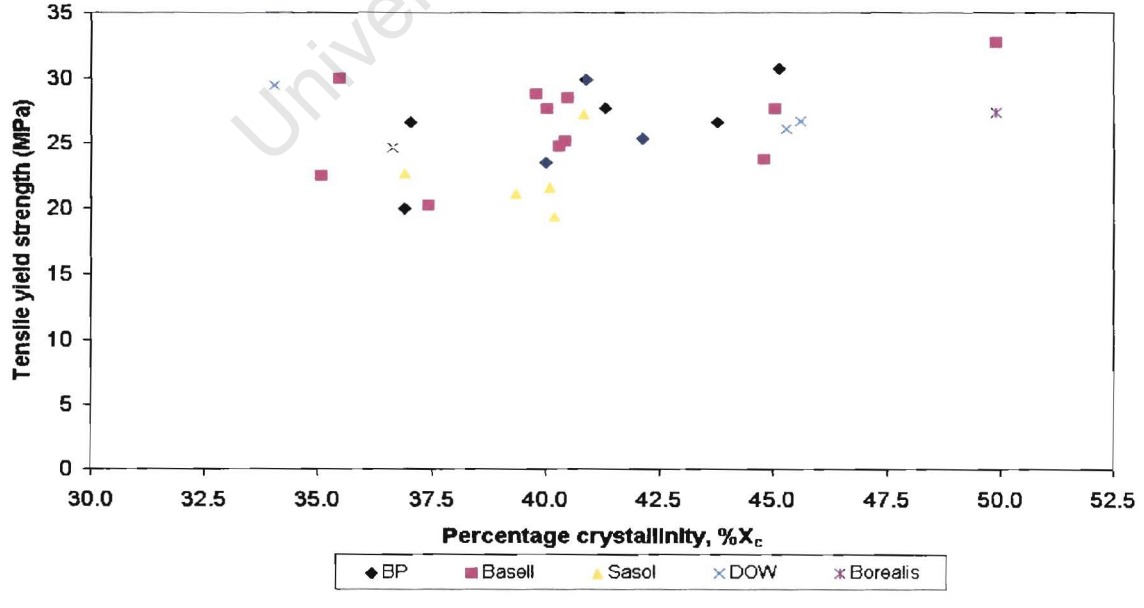

Figure 4.32 Illustration of the effect of percentage crystallinity on the yield strength of the copolymer grades

University of Cape Town

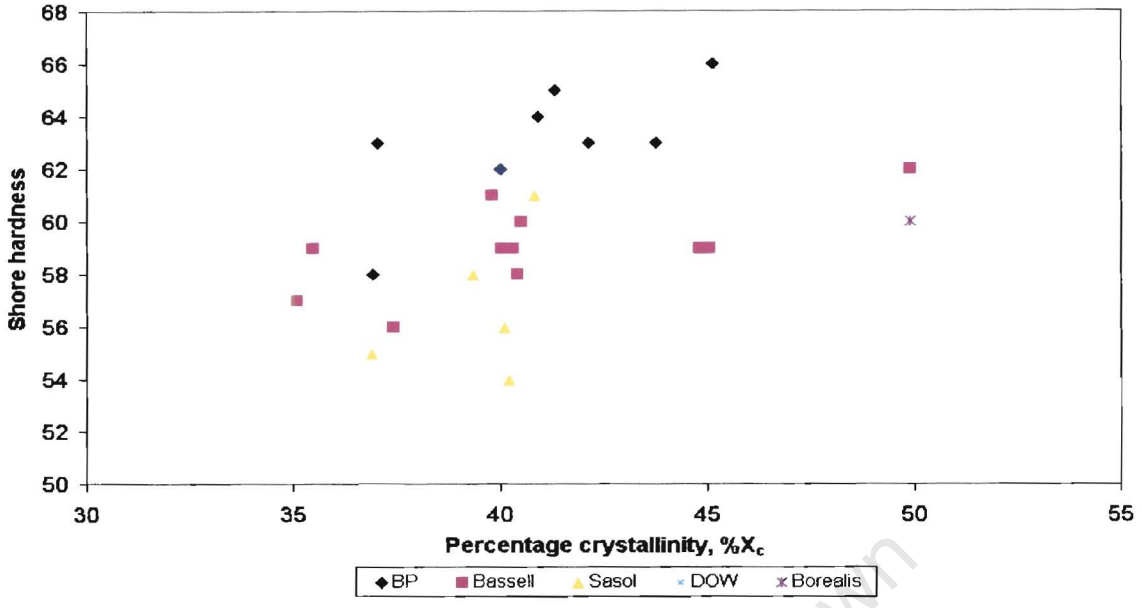

Figure 4.33 Illustration of the effect of percentage crystallinity on the shore hardness of the copolymer grades

The effect of the degree of crystallinity on the ductility is shown in Figure 4.34 below. There seems to be no distinct trend observed from the plots, therefore, the degree of crystallinity has no significant effect on the ductility of the copolymer grades.

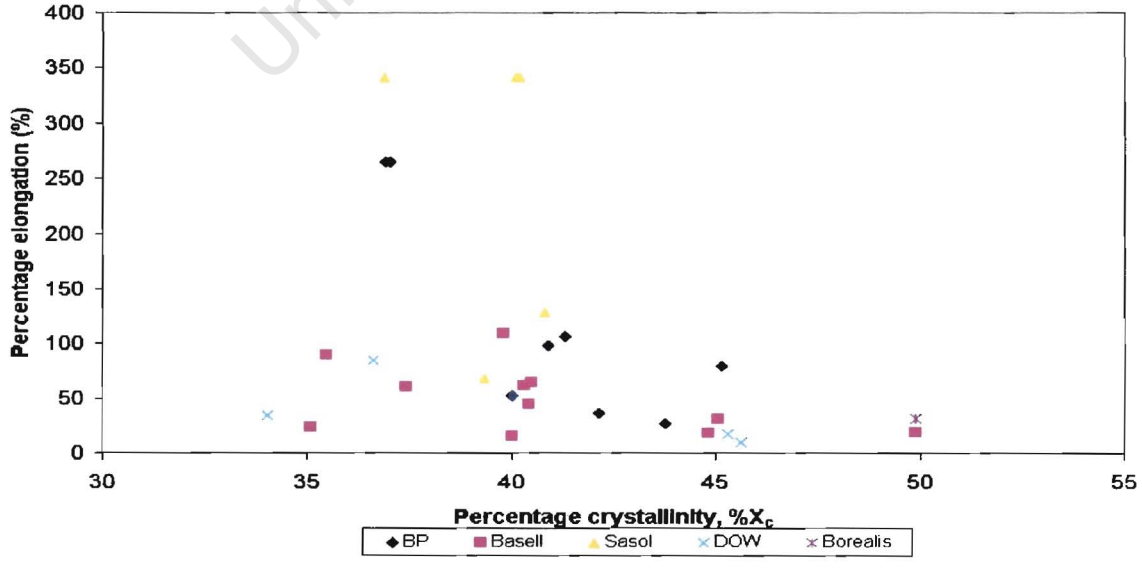

Figure 4.34 Illustration of the effect of the degree of crystallinity content on percentage elongation of the copolymer grades

University of Cape Town

4.5 Morphological Characterisation

4.5.1 Scanning Electron Microscopy (SEM)

Scanning electron microscopy micrographs of the etched grades are shown in Figure 4.35 to Figure 4.37. The micrographs are arranged according to their relevant percentage ethylene content ranges. All the micrographs presented here are taken at the same magnification of x500. As it can be seen from these micrographs, the etching process only dissolved the rubber phase, leaving pores on surface of the polymers, from which the particle size, particle size distribution and interparticle distance were measured and quantified. It is generally known that the average particle size depends on the viscosity ratio between the dispersed phase and the matrix. Therefore, the higher the viscosity ratio the lower the particle size would be, or vice versa. Nevertheless, from this work the values of the viscosity ratio were not available so this comparison could not be made.

According to Kim and co-workers, in order to improve toughness of the polymers the optimal internal phase morphology of the modifier, should be studied together with particle size and interparticle distances[19]. Therefore, the results of the average weight particle size (D_w), particle size distribution (D_w/D_n) and interparticle distance (ID) for all the grades tested are summarised in Table 4.8. These values were obtained from SEM micrographs by image analysis systems averaging at least 250 rubber particles holes. The D_w/D_n ratio is a measure of the particle size distribution. The distribution broadens with increasing D_w.

University of Cape Town

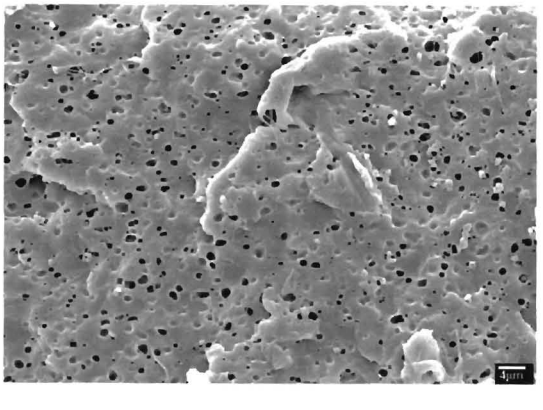

Sample #1: C_2= 6.1%, MFI= 5.9 g/10 min

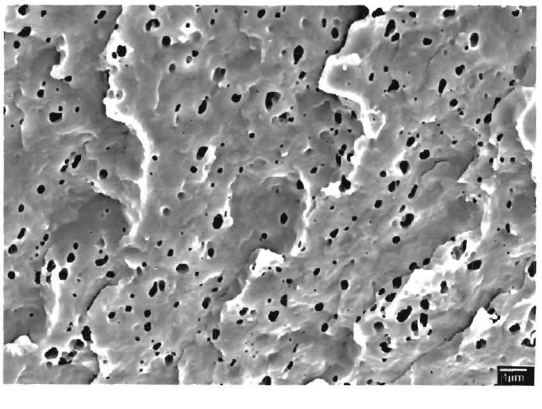

Sample #2: C_2= 7.3%, MFI= 6.5 g/10 min

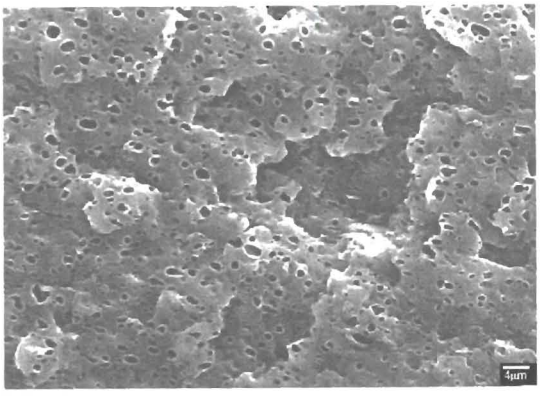

Sample #3: C_2= 7.0%, MFI= 8.0 g/10 min

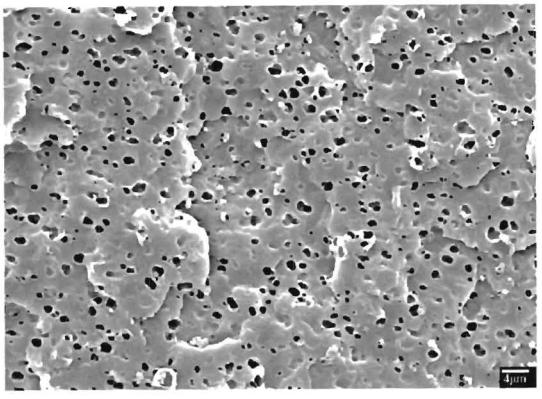

Sample #4: C_2= 12.0%, MFI= 5.9 g/10 min

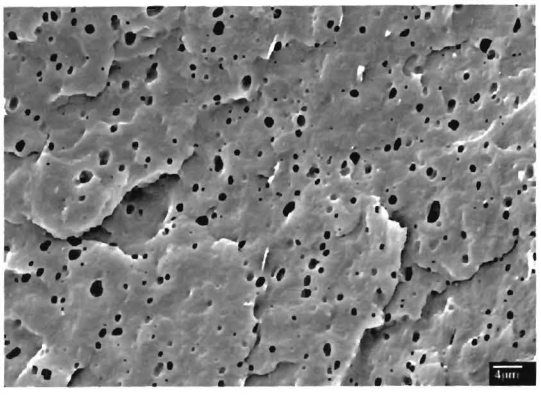

Sample #5: C_2= 6.2%, MFI= 20.0 g/10 min

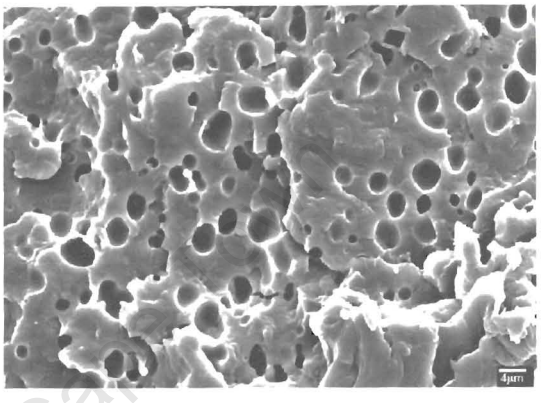

Sample #6: C_2= 7.6%, MFI= 44.0 g/10 min

Figure 4.35 SEM micrographs for the sample grades with percentage ethylene contents of less than 8%

University of Cape

Table 4.8 shows that most of the samples shown in Figure 4.35 have an average weight rubber particle size of the order 1.0 μm to 1.7 μm, except for sample #6 which have a particle size of greater than 2.5 μm. Unfortunately, sample #6 is the only sample grade supplied using the Borstar process. Therefore, further comments and observations regarding this grade will be dealt with at the later stages of the discussion. Figure 4.36 shows the samples with ethylene contents ranging between 8 and 10%. Samples #7 and 9 have average weight rubber particle sizes of 0.52 μm and 0.19 μm, respectively. These values are not only the smallest in this ethylene content range, but also of all the grades examined. Sample #17 manufacture by DOW have the largest particle size of 4.51 μm, while sample #13 also produced by DOW shows long elongated particles, which are oriented in the direction parallel to the melt flow. These kinds of rubber particle morphologies are well known to reduce the impact strength of the copolymers, since they act as stress raisers instead of stress concentrators during

the impact event and they cannot stop the propagating crack during fracture of materials due to their unidirectionality.

Table 4.8 Particle size distribution of iPP/EPR copolymers. D_n is the number average particle size, D_w is the weight average particle size and ID is the interparticle distance

Sample #	D_n (μm)	D_w (μm)	D_w/D_n	ID(μm)	ID/D_w
1	0.91	1.06	1.16	1.61	1.52
2	1.03	1.27	1.23	2.18	1.72
3	1.34	1.68	1.25	1.98	1.18
4	0.88	1.03	1.17	1.82	1.77
5	0.99	1.17	1.18	1.97	1.68
6	2.56	2.95	1.15	3.85	1.31
7	0.43	0.52	1.21	0.93	1.79
8	1.43	1.81	1.27	2.82	1.56
9	0.15	0.19	1.27	0.30	1.58
10	1.05	1.25	1.19	1.45	1.16
11	1.30	1.51	1.16	2.18	1.44
12	0.91	1.06	1.16	1.74	1.64
13	1.05	1.45	1.38	1.54	1.06
14	1.45	1.71	1.18	2.33	1.36
15	1.58	1.81	1.15	2.46	1.36
16	1.13	1.28	1.13	1.88	1.47
17	3.24	4.51	1.39	5.40	1.20
18	1.16	1.35	1.16	2.06	1.53
19	1.83	2.11	1.15	2.96	1.40
20	0.65	0.85	1.31	1.17	1.38
21	1.96	2.42	1.23	5.08	2.10
22	0.74	0.85	1.15	1.44	1.69
23	1.34	1.63	1.22	2.11	1.29
24	0.63	0.75	1.19	1.29	1.72
25	1.26	1.56	1.24	2.11	1.35
26	0.81	0.96	1.19	1.34	1.40
27	0.76	0.86	1.13	1.16	1.35
28	0.91	1.07	1.18	1.56	1.46
29	0.79	0.91	1.15	1.34	1.47
30	2.90	3.43	1.18	4.75	1.38

University of Cape Town

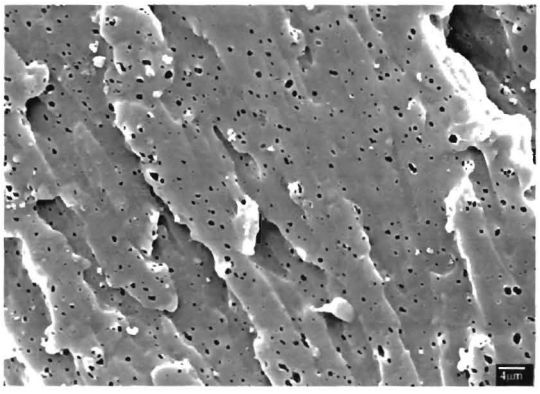

Sample #7: C_2= 8.5%, MFI= 0.4 g/10 min

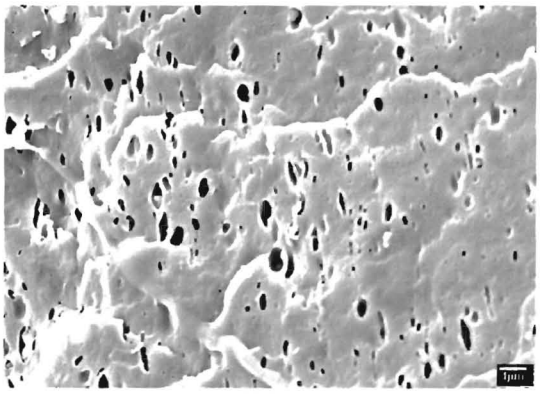

Sample #8: C_2= 8.7%, MFI= 0.7 g/10 min

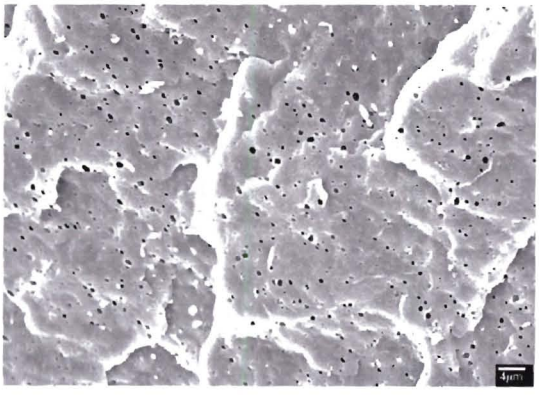

Sample #9: C_2= 8.9%, MFI= 0.8 g/10 min

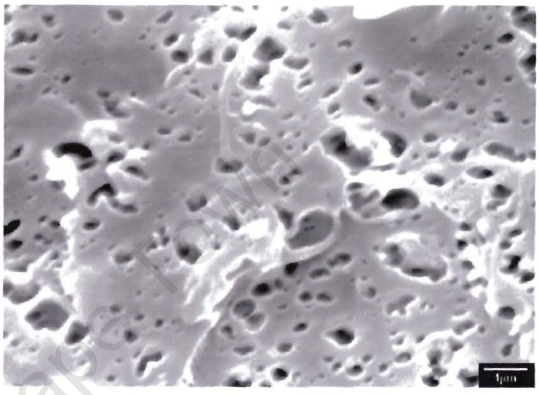

Sample #10: C_2= 11.5%, MFI= 1.0 g/10 min

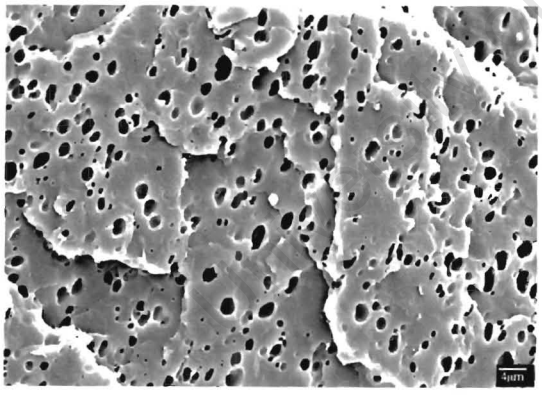

Sample #11: C_2= 8.2%, MFI= 1.2 g/10 min

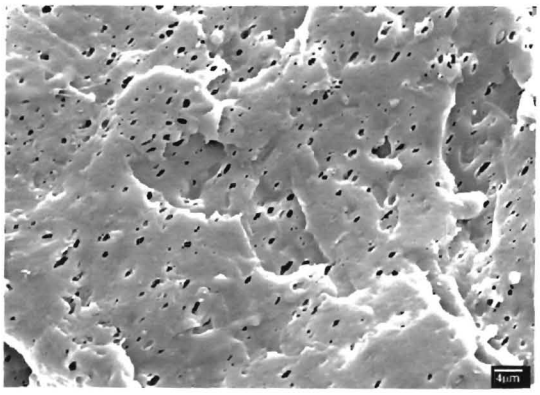

Sample #12: C_2= 8.8%, MFI= 1.5 g/10 min

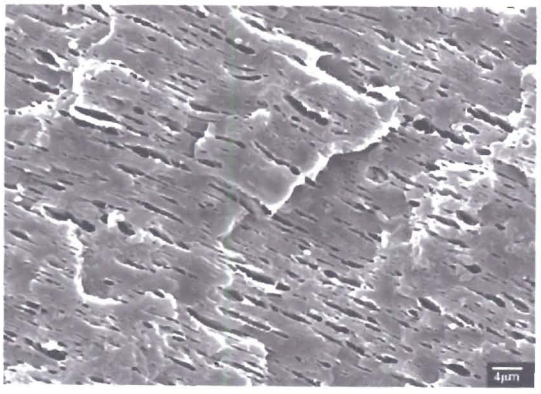

Sample #13: C_2= 8.8%, MFI= 7.0 g/10 min

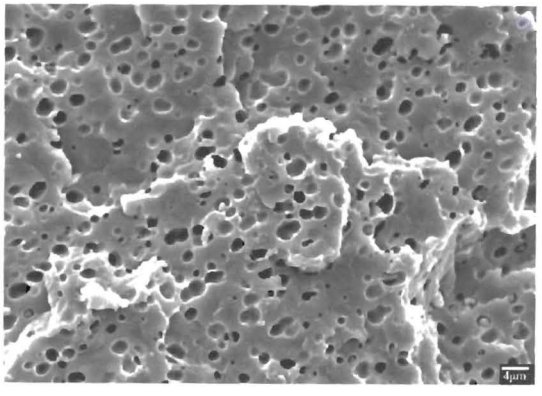

Sample #14: C_2= 7.0%, MFI=14.0 g/10 min

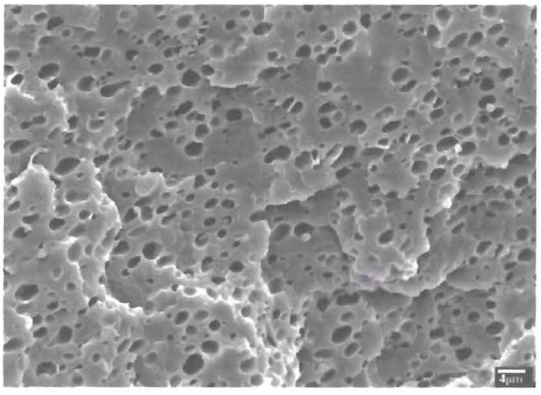

Sample #15: C_2= 8.3%, MFI=28.0 g/10 min

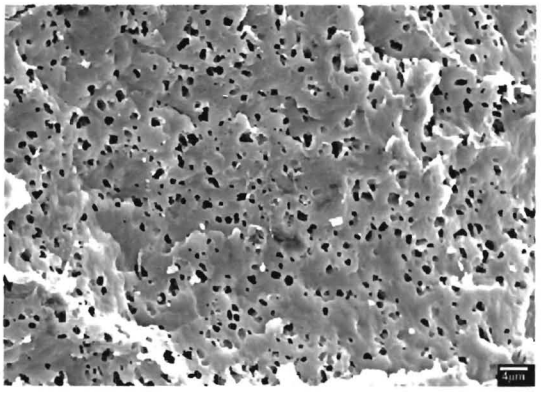

Sample #16: C_2= 9.2%, MFI=34.0 g/10 min

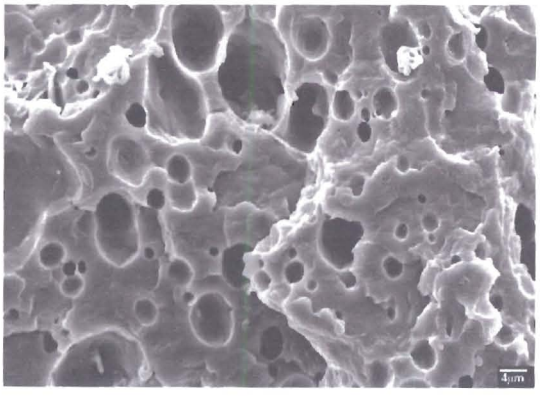

Sample #17: C_2= 10.0%, MFI=34.0 g/10 min

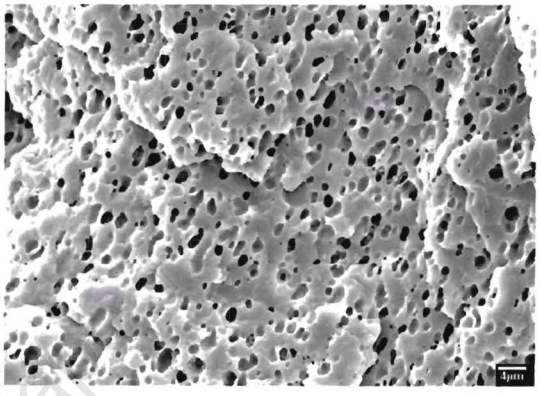

Sample #18: C_2= 8.0%, MFI=46.0 g/10 min

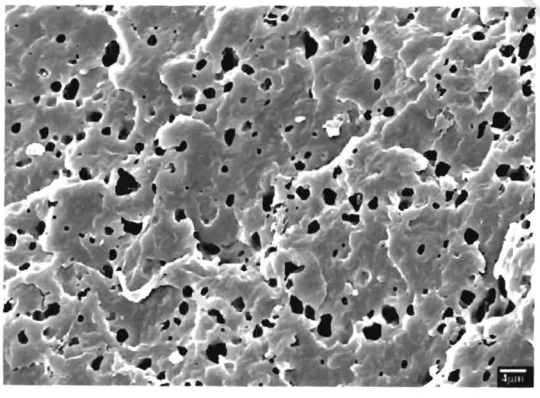

Sample #19: C_2= 8.4%, MFI=49 g/10 min

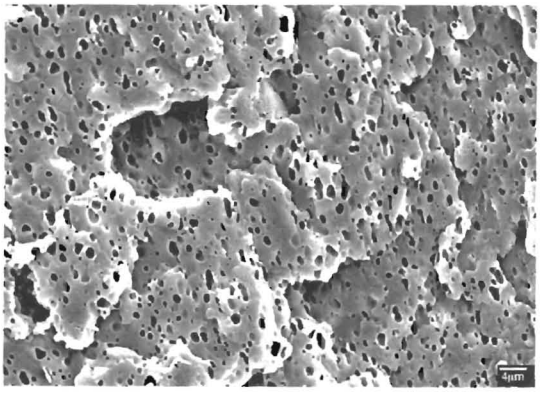

Sample #20: C_2=10.0%, MFI=50.0 g/10 min

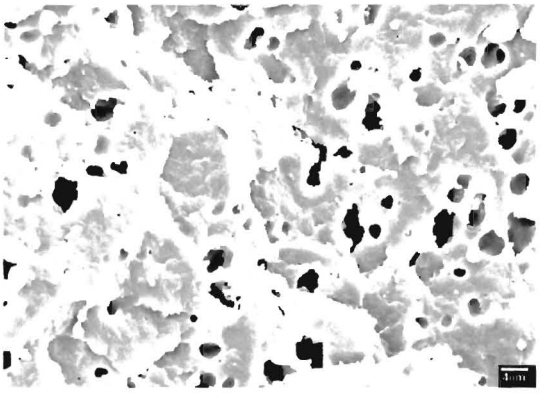

Sample #21: C_2=7.8%, MFI= 68.0 g/10 min

Figure 4.36 SEM micrographs for the sample grades with percentage ethylene contents of between 8 and 10%

Figure 4.37 show the samples with ethylene contents greater than 10%. Table 4.8 shows that most of the grades have average weight particle sizes of ±1.0 μm, except for samples #23, 25 and 30. Sample #30 produced by Basell has the largest average particle size of about 3.43 μm in this ethylene content range.

University of Cape Town

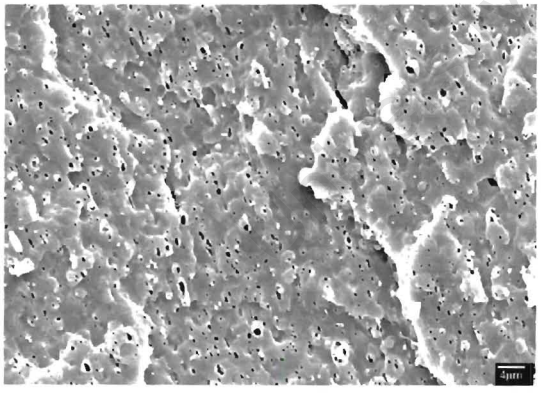

Sample #22: C_2=11.2%, MFI= 1.2 g/10 min

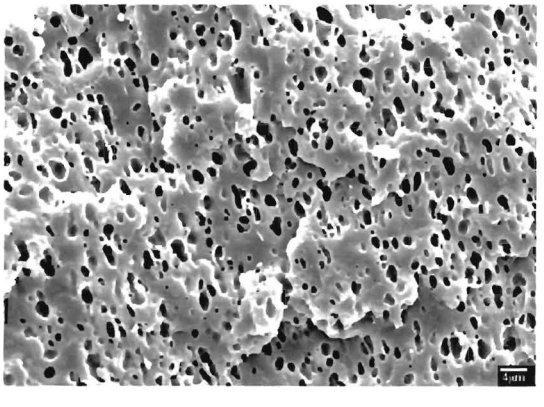

Sample #23: C_2=12.9%, MFI= 7.0 g/10 min

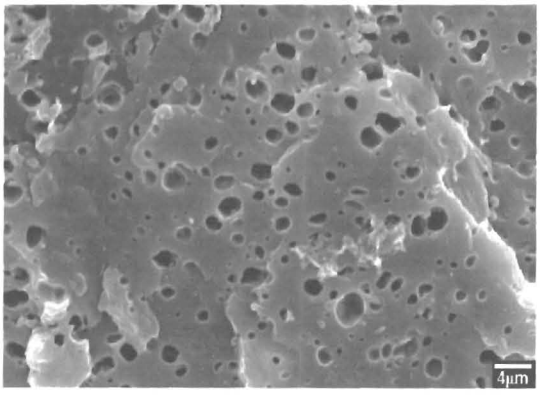

Sample #24: C2=11.5%, MFI= 8.0 g/10 min

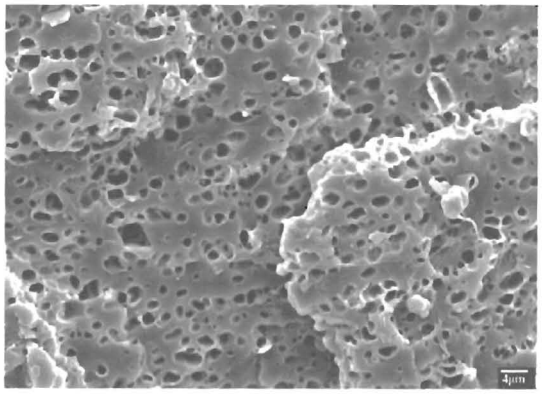

Sample #25: C2=15.0%, MFI= 15.0 g/10 min

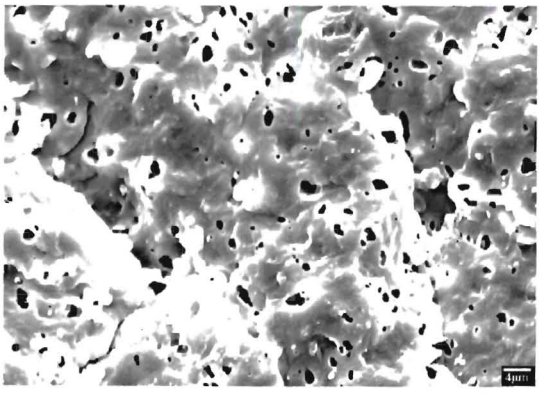

Sample #26: C2= 10.8%, MFI= 17.0 g/10 min

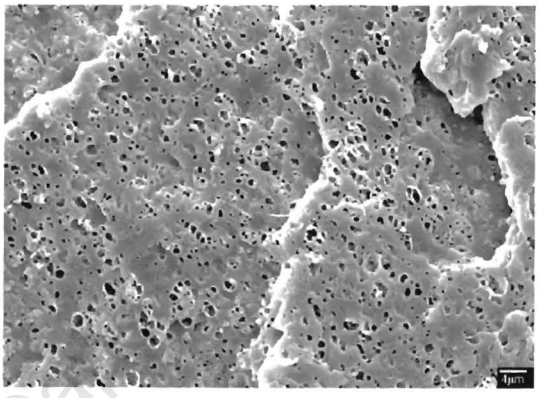

Sample #27: C2=12.2%, MFI= 18.0 g/10 min

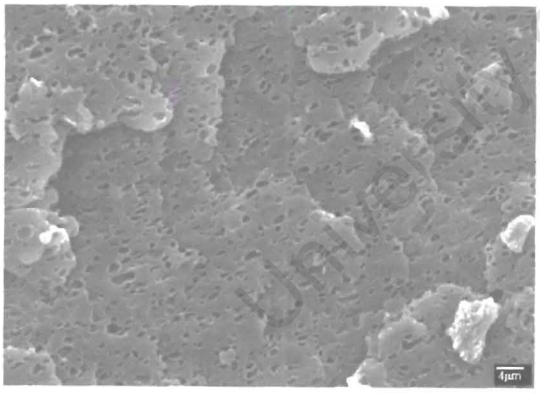

Sample #28: C2= 12.4%, MFI= 24.0 g/10 min

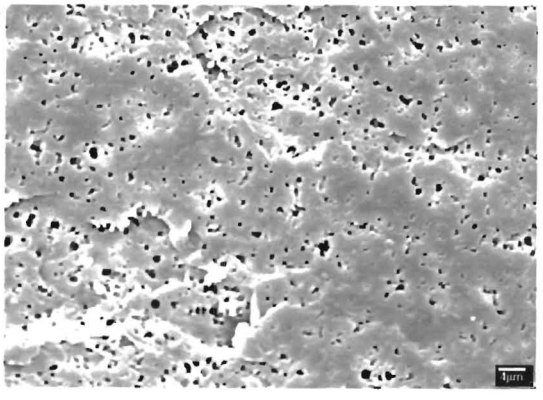

Sample #29: C2=11.4%, MFI= 73.0 g/10 min

University of Cam

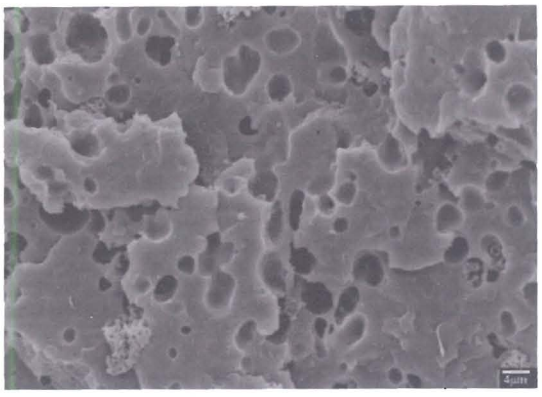

Sample #30: C2=10.7%, MFI= 79.0 g/10 min

Figure 4.37 SEM micrographs for the sample grades with percentage ethylene contents of greater than 10%

The effect of ethylene content on the average particle size is illustrated in Figure 4.38. In practice, it would be expected that the average particle size to decrease with increasing ethylene content. However, this kind behaviour is not observed here since all the copolymer grades have relatively low percentage ethylene contents. Therefore, the average weight particle size of copolymer grades is independent of ethylene content and processing conditions and it amounts to about 1.0 μm on average. Figure 4.39 shows the average interparticle distance for the copolymer grades as a function of ethylene content. It is also observed that the interparticle distance is independent of ethylene content. Generally, it would be expected for the interparticle distance to gradually decrease with increasing ethylene content until it reaches a certain ethylene content level. This analogy in the rubber particle size distribution can be understood by considering an increase in ethylene content, which will lead to an increase in the rubber particle size and at the same time a decrease in the interparticle distance. Nevertheless, this is not always the case since rubber particle do tend to agglomerate or coalesce during processing, making the size of the particle bigger than would normally be expected even at lower ethylene contents. In addition, it is known that rubber particle size is a function of the viscosity ratio, which will determine if the particles will coagulate or easily disperse. At the same time, viscosity decreases with increasing shear rate during processing of the copolymer grades.

University of Cape Town

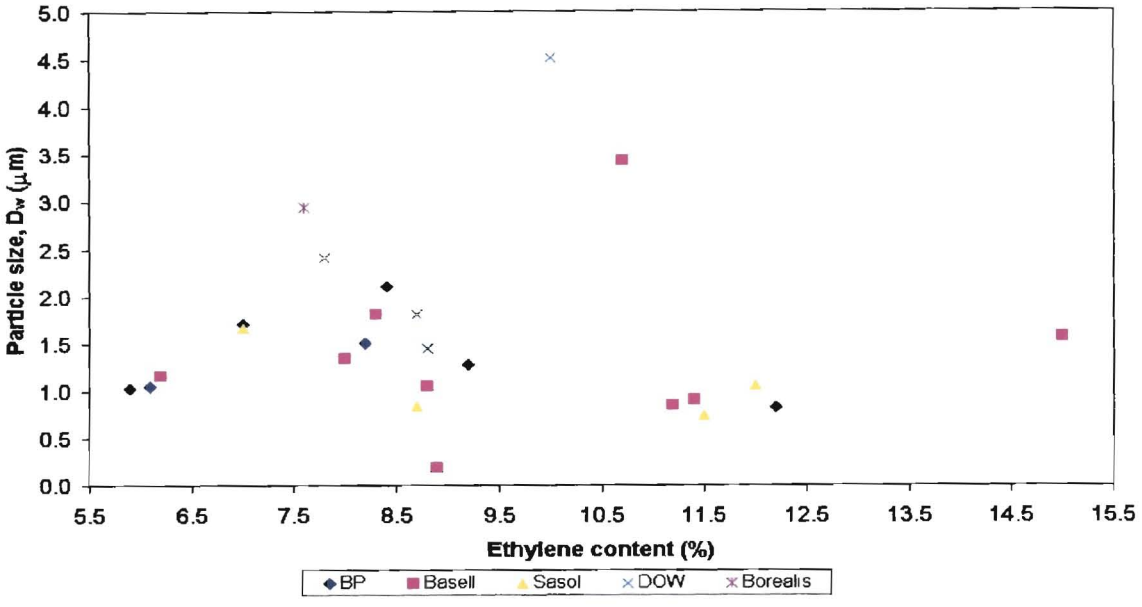

Figure 4.38 Illustration showing the effect of ethylene content on the particle size

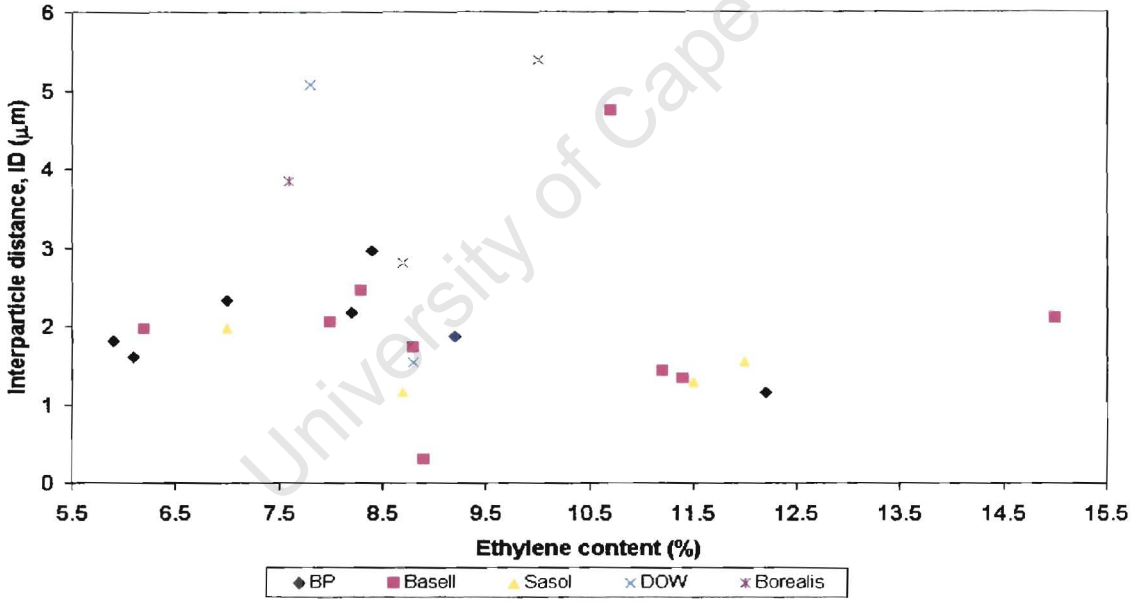

Figure 4.39 Illustration showing the effect of ethylene content on the interparticle distance

Figure 4.40 shows the ratio of interparticle distance to average particle size (ID/D_w) on the ethylene content. In this ethylene content range (i.e. 5.9 – 15%), both the BP and DOW grades show an exponential decrease in the ID/D_w ratio with increasing ethylene content, while the other grades show scatter in their plotted data. The ID/D_w value amounts to about 1.50 on average for all the grades produced using the different manufacturing processes. Since the EPR particle act as stress concentrators during

University of Cape Town

deformation, this value of ID/D_w is small enough to allow overlapping of the stress fields around adjacent rubber particles during the deformation process. Therefore, voids will be easily being produced and the multiple cavitations process will take place in the rubber particles.

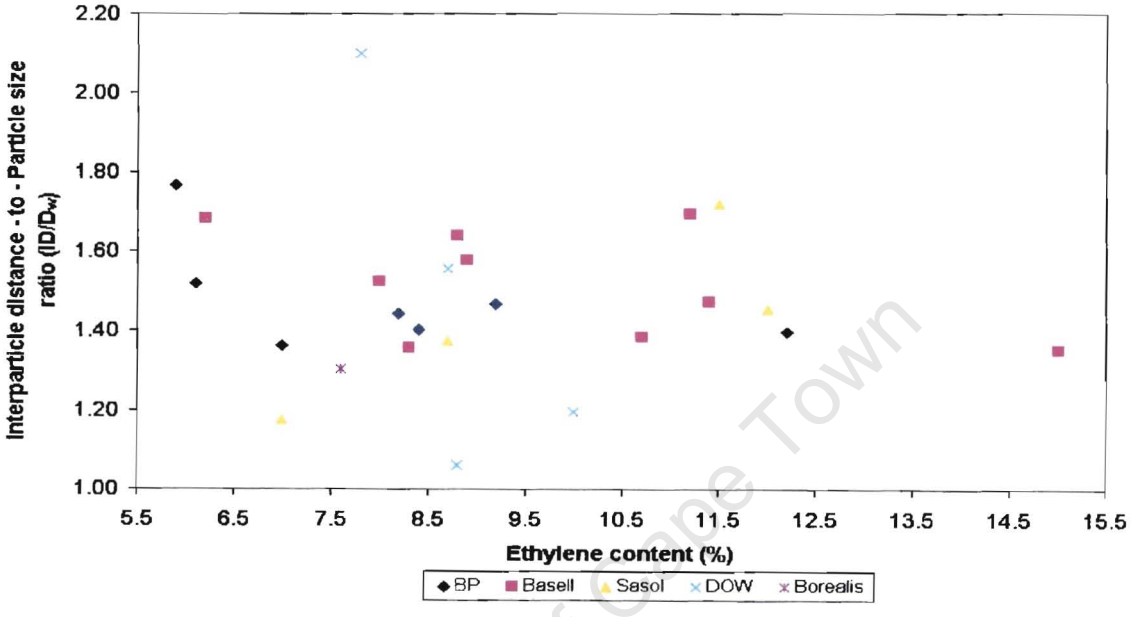

Figure 4.40 Illustration showing the effect of ethylene content on the interparticle distance-to-particle size ratio

The effect of MFI on the particle size plotted in Figure 4.41 shows that there is no particular trend observed. There is a huge amount of scattering of the data plotted at around MFI's of 35 g/10 min and above. This behaviour is not enough to make any conclusive remarks about the effect of MFI on the average weight particle sizes.

University of Cape Town

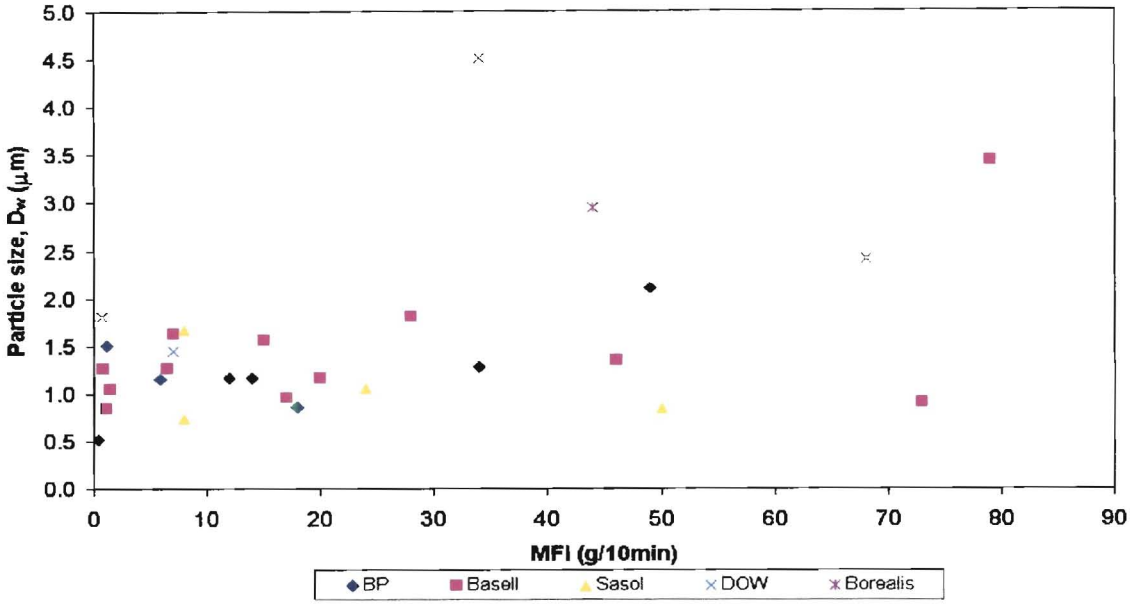

Figure 4.41 Illustration showing the effect of MFI on the average particle size

University of Cape Town

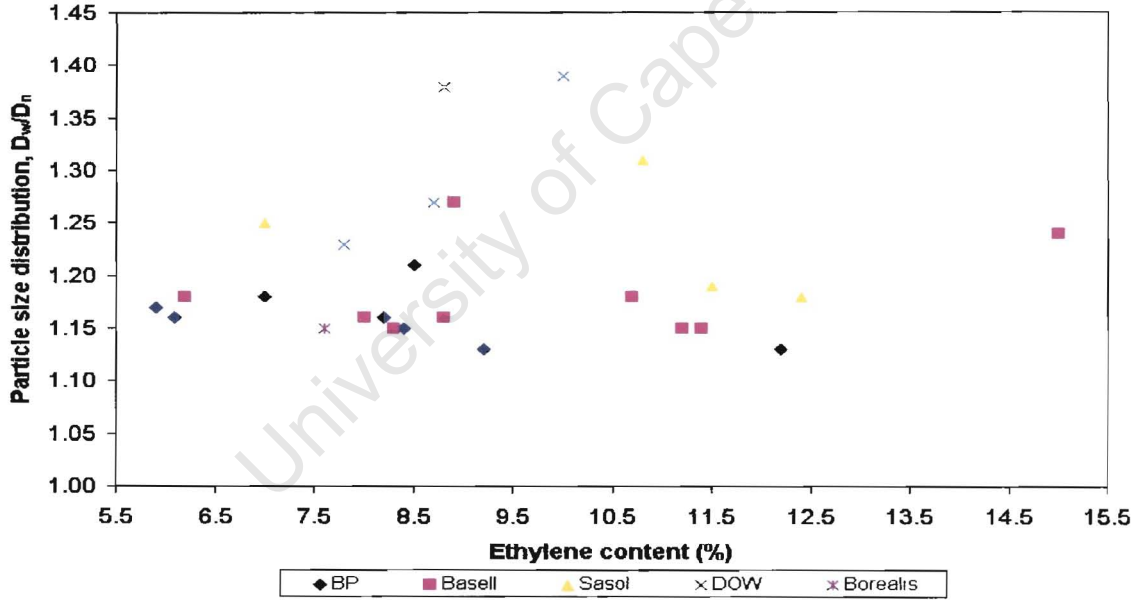

(a)

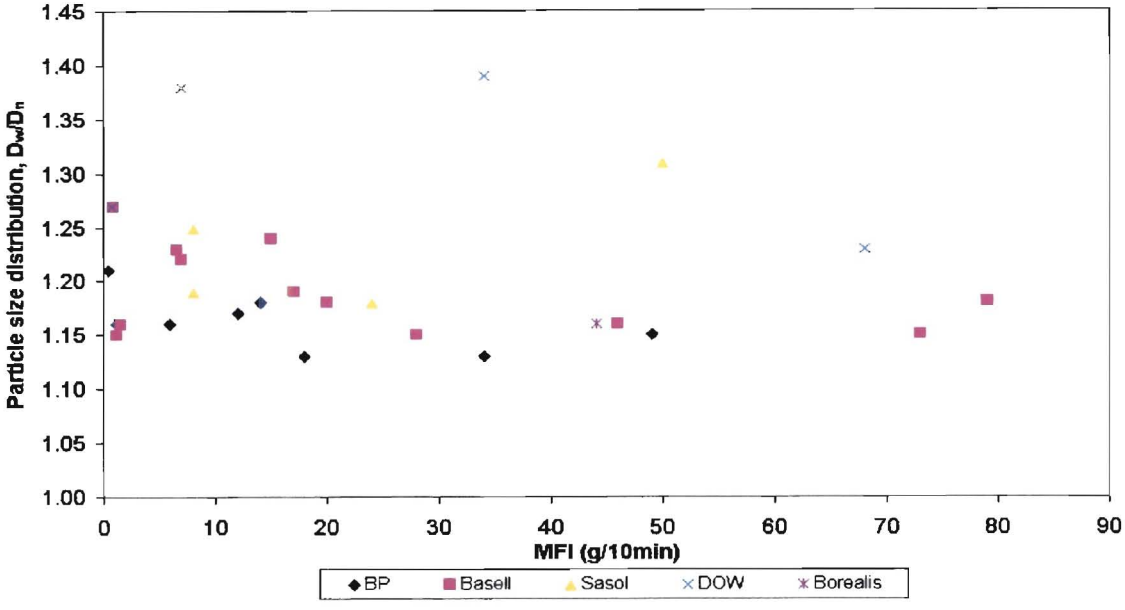

(b)

Figure 4.42 Illustration showing the dependence of particle size distribution on the: (a) ethylene content and (b) MFI

University of Cape Town

The effect of ethylene content and MFI on the particle size distribution is shown in Figure 4.42(a) and Figure 4.42(b), respectively. In both cases, the particle size distribution shows a similar kind of behaviour. It is clear from the plots that the BP grades have a constant particle size distribution over the whole range of ethylene content and MFI. The BP, Basell and Sasol grades have a narrow particle size distribution of about 1.18 on average, whilst the DOW grades show a broad particle size distribution over the whole range of ethylene content.

4.5.2 TRANSMISSION ELECTRON MICROSCOPY (TEM)

Typical micrographs obtained from TEM imaging are shown in Figures 4.43, 4.44, 4.46 and 4.47 below. These micrographs show the microstructure of ethylene-propylene rubber (EPR) particles dispersed in the isotactic polypropylene matrix, which is not possible to see using scanning electron microscopy (SEM). From the TEM micrographs, the rubber particles appear dark due to the staining with ruthenium tetraoxide (RuO_4). In the phase structure, characteristics of ternary microstructures are clearly visible: the matrix of the semicrystalline iPP; the amorphous ethylene-propylene

rubbery phase (this area appears shiny dark); and semicrystalline polyethylene (PE) inclusions in the particles. The manufacturing and processing conditions for these copolymer grades control the number, size and the crystallinity of PE inclusions within the rubber phase. Figure 4.43 below shows a typical microstructure of the iPP/EPR obtained from TEM imaging.

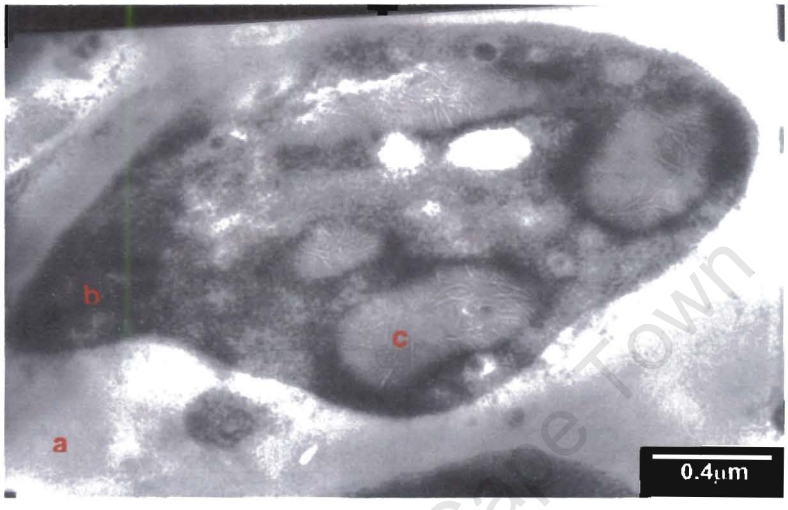

Figure 4.43 TEM image of a typical rubber particle: (a) isotactic polypropylene matrix, (b) ethylene-propylene rubbery phase and (c) polyethylene inclusion showing the lamellae structure

University of Cape Town

From the figures below, the micrographs image on the left hand side show how the rubber particles are distributed within the matrix. The images on the right hand side are taken at a higher magnification and they represent the morphology within the ethylene-propylene rubber particle. TEM micrographs are not well suited to determine true particle size, particle size distribution and interparticle distance because these micrographs usually contain only very few rubber particles. Therefore, the quantitative characterisation of the dispersed rubber particles was performed using SEM micrographs.

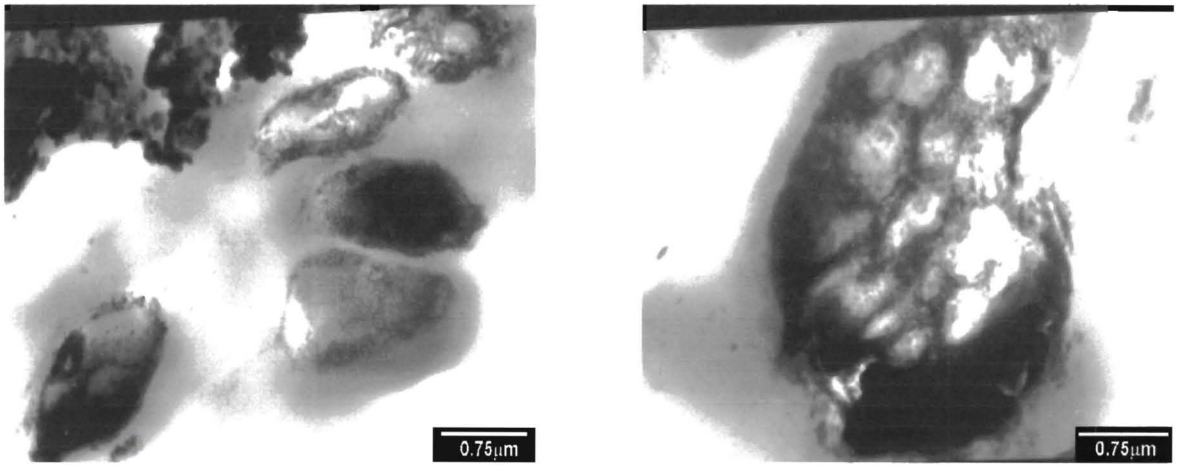

Sample #2: Basell grade

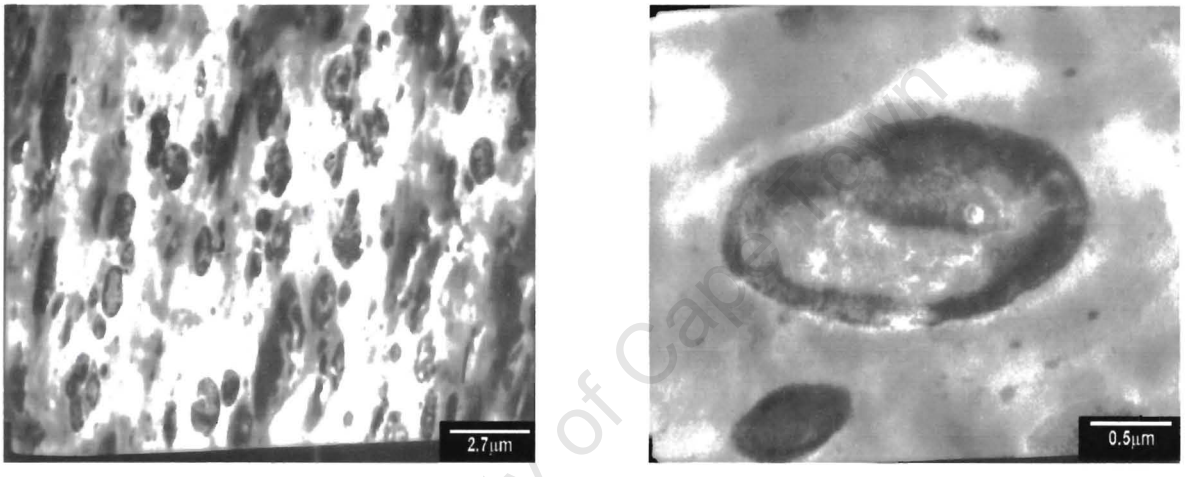

Sample #3: Sasol grade

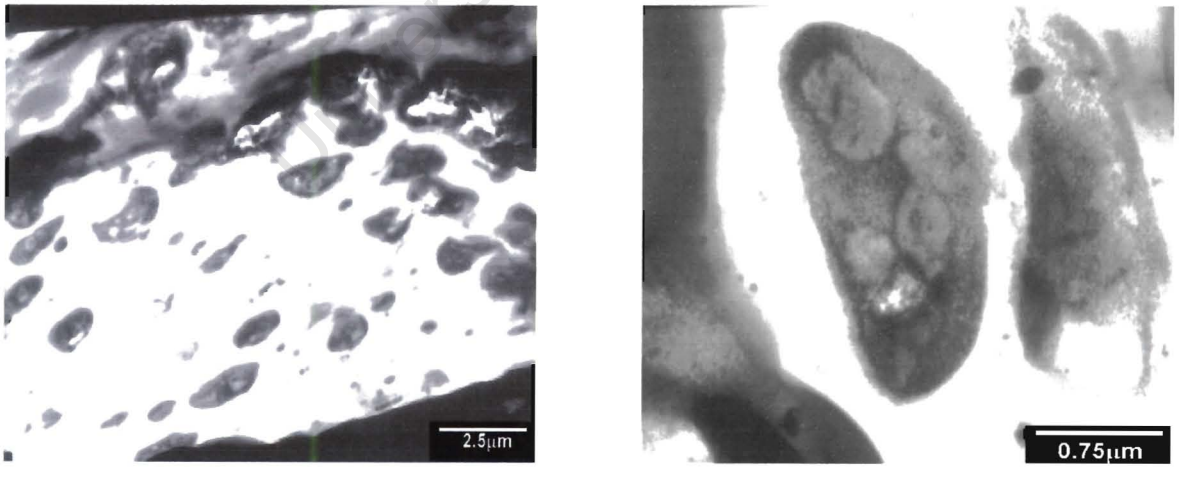

Sample #4: BP grade

University of Cape Town

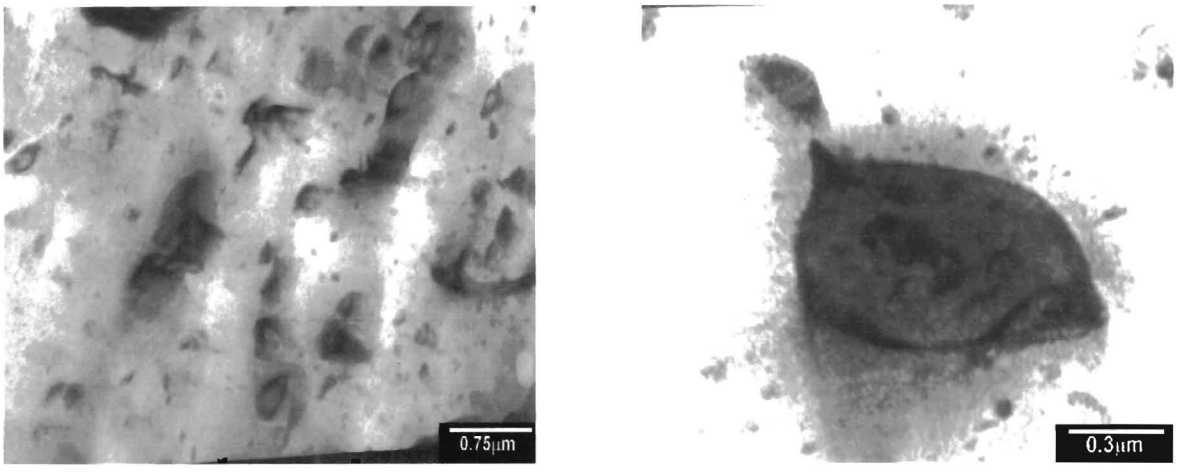

Sample #5: Basell grade

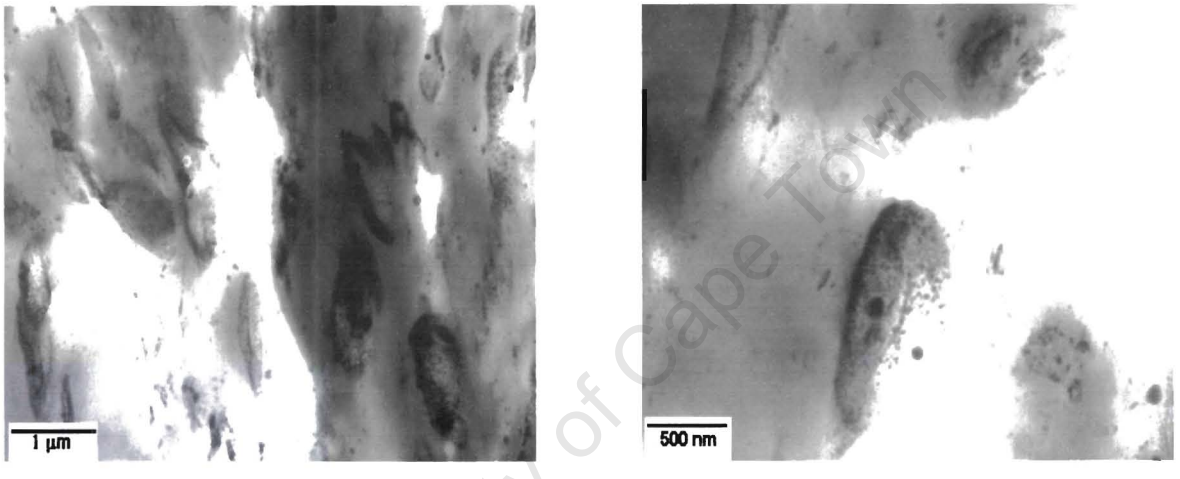

Sample #6: Borealis grade

Figure 4.44 TEM micrographs of samples with ethylene contents below 8%

University of Cape Town

Typical TEM micrographs for samples #2, 3, 4, 5 and 6, that have ethylene contents below 8% are shown in Figure 4.44 above. Sample #2 seems to have many polyethylene inclusions in its rubber particles, sample #3 and 4 have only few numbers inclusions within their rubber particles, whilst sample #5 seems to have only single inclusions within their rubber particles. It can be seen that shape, structure and size of the rubber particles differ from grade to grade and this can be attributed to the processing and manufacturing conditions of the copolymer grades.

In Figure 4.45 the energies from different impact tests are compared for each copolymer grade. Figure 4.45(a) illustrates the impact strength of samples with the ethylene contents below 8%. At this ethylene content range, the BP grades (samples # 1 and 4) and the Sasol grades (sample #3) are superior in impact strength. TEM

micrographs for the Sasol (sample #3) and BP (sample #4) grades in Figure 4.45(a) show similarities in morphology between these grades and this may explain their similar impact behaviour.

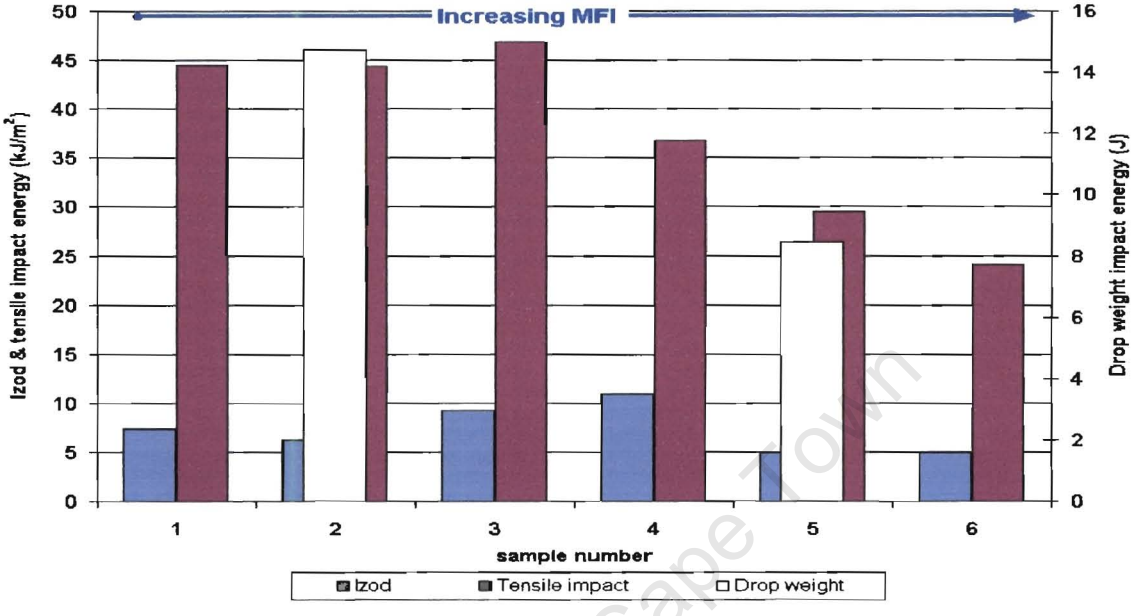

(a)

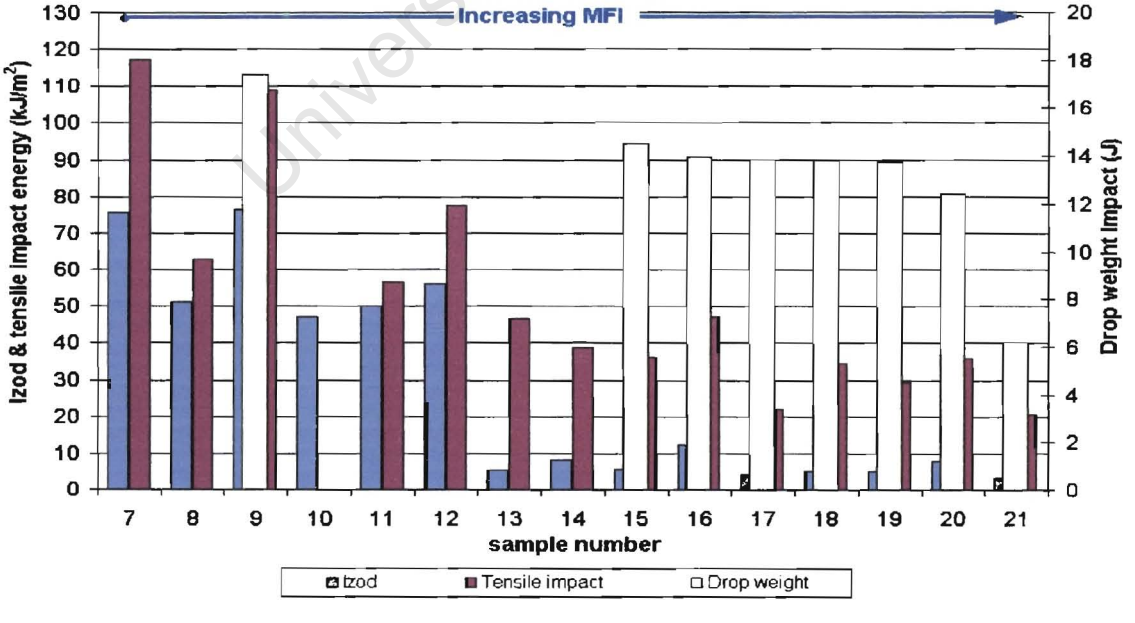

(b)

University of Cape Town

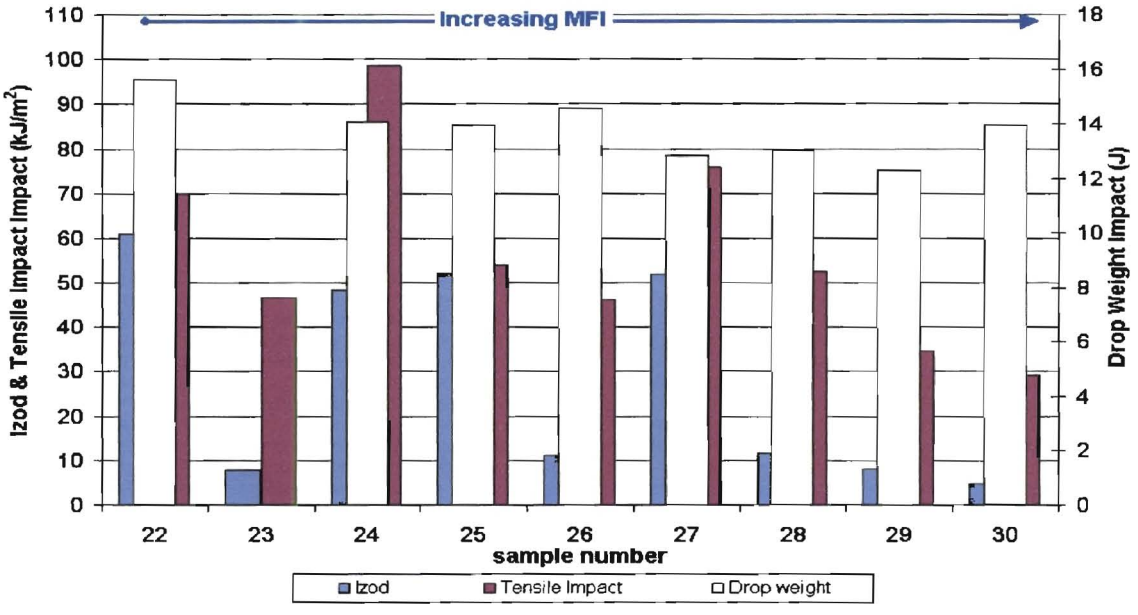

(c)

Figure 4.45 Bar graphs showing the difference in impact energy of different copolymer grades performed at room temperature: (a) samples with ethylene contents below 8%, (b) samples with ethylene contents between 8 - 10%, and (c) samples with ethylene contents above 10%

University of Cape Town

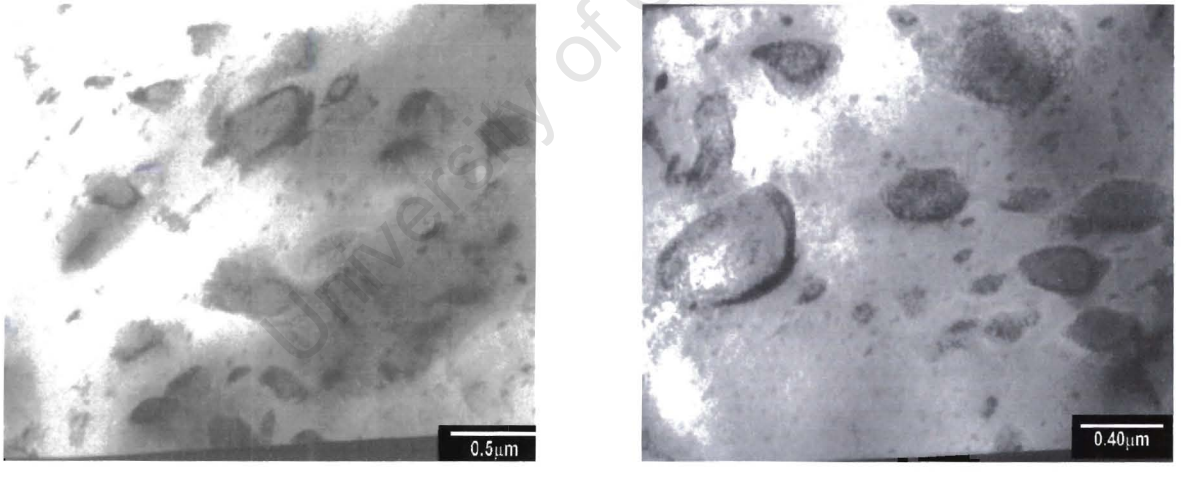

Sample #9: Basell grade

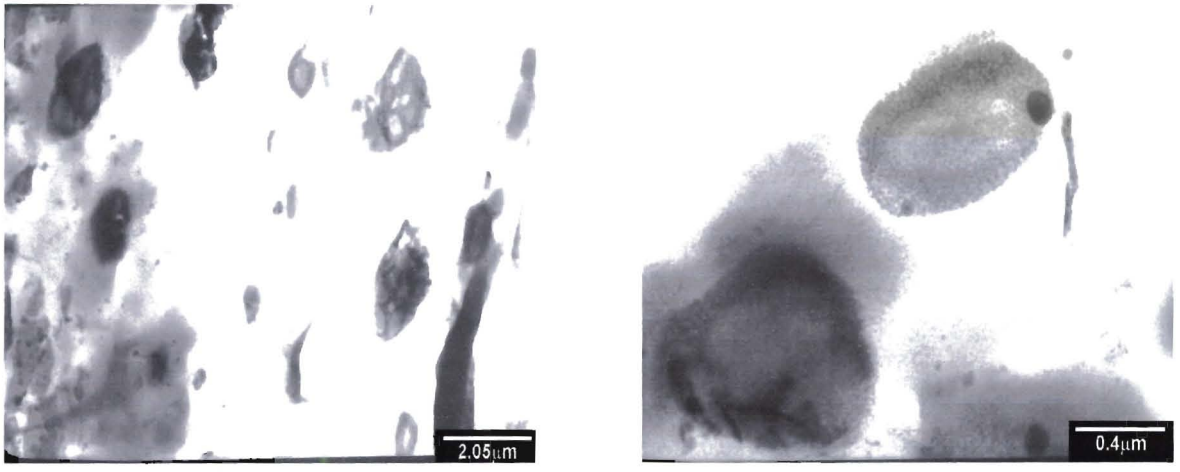

Sample #15: Basell grade

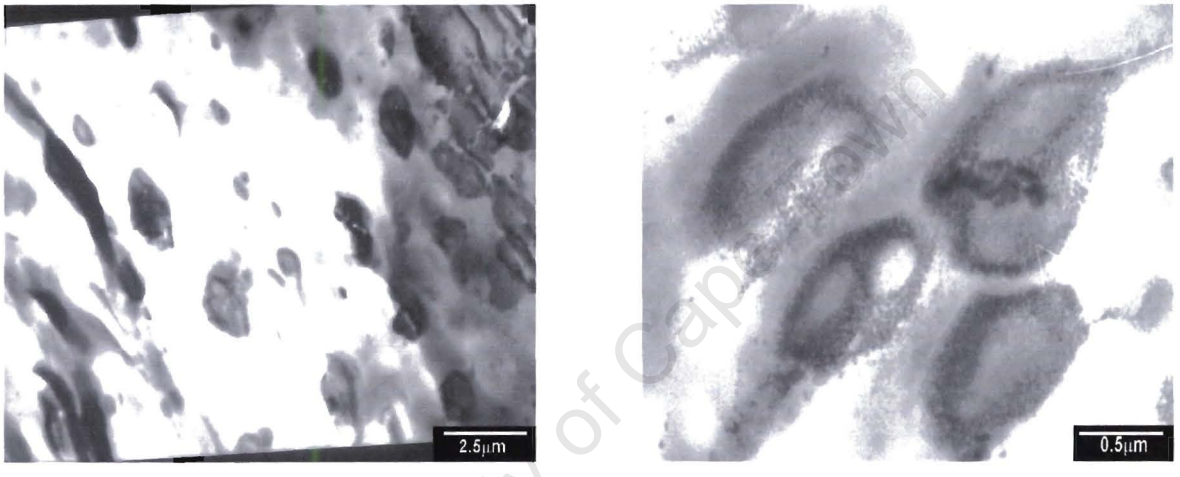

Sample #16: BP grade

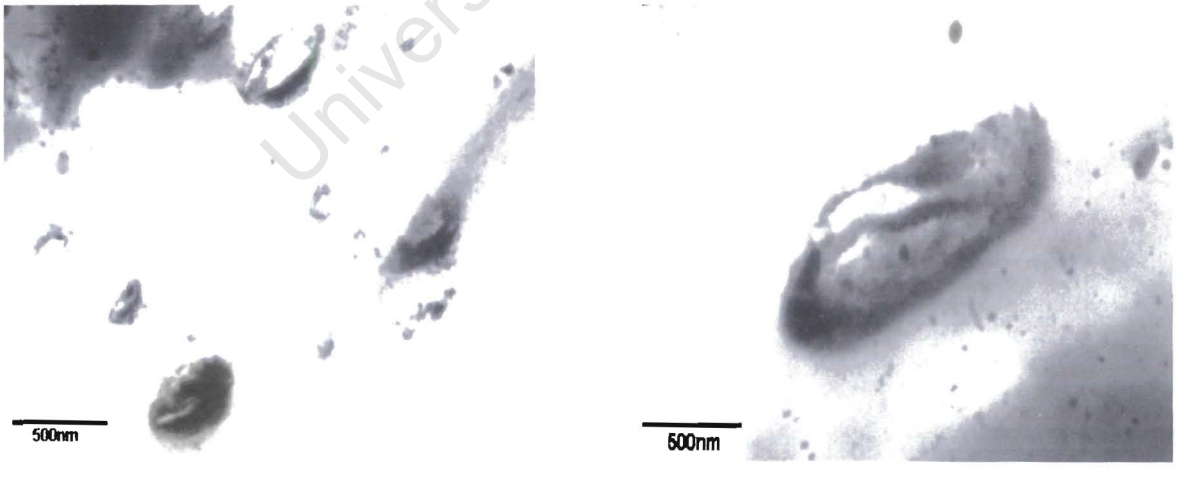

Sample #17: DOW grade

University of Cape Town

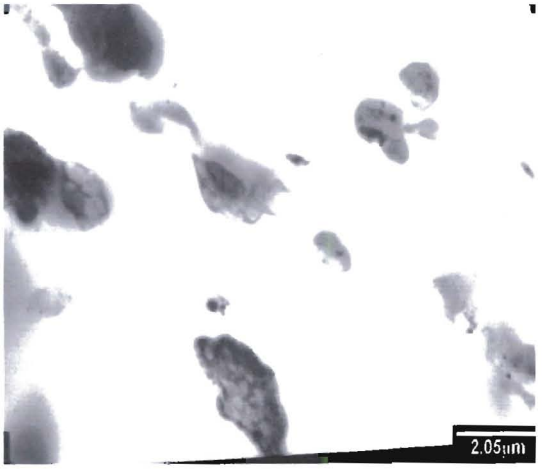

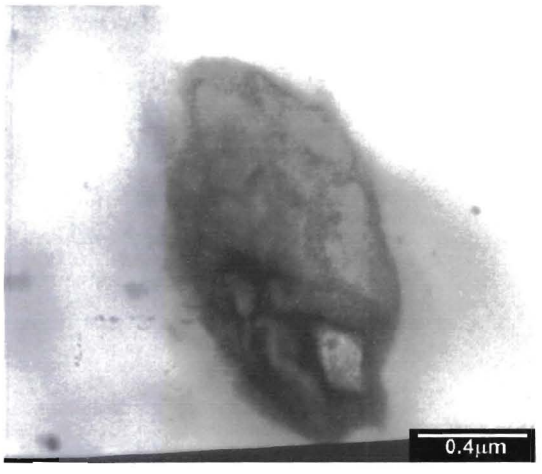

Sample #19: BP grade

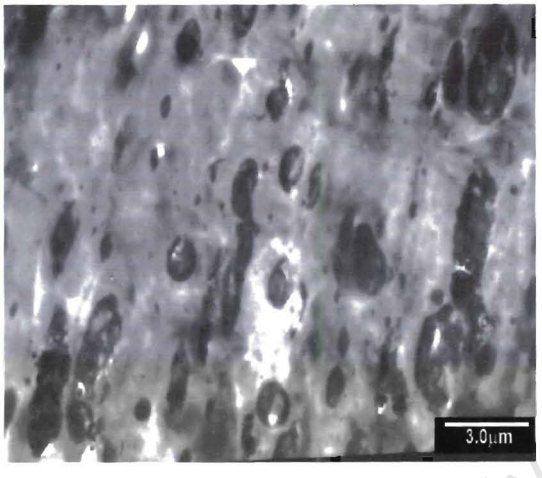

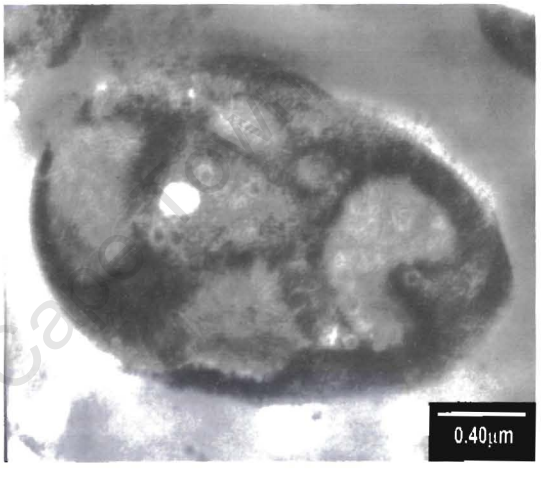

Sample #20: Sasol grade

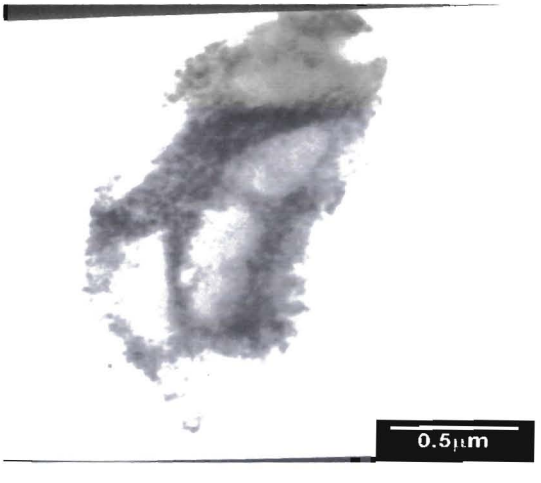

Sample #21: DOW grade

Figure 4.46 TEM micrographs of the samples with ethylene contents between 8 and 10%

Figure 4.46 show the TEM micrographs of samples with ethylene contents between 8 and 10%. The microstructure of sample #9 is similarities to that of sample #5, both of

which grades are produced by the Basell process. From Figure 4.45(b) it can be seen that the BP grades (samples #7, 11, 14, 16 and 19) and the Basell grade (sample #9) have superior impact strengths in this ethylene content range. The Sasol grades (samples #10 and 20) have somewhat lower impact strengths. For both BP grade (sample # 7) and Basell grade (sample #9) it was shown in Table 4.8 that they have small average rubber particle sizes over this ethylene content range. The high impact strength of these grades can be attributed to both their particle size and low MFI. If we compare, pair-wise DOW grade (samples #8) and Basell grade (sample #9) which have similar ethylene contents and MFI's (Table 3.1), then it would appear that the Basell grade have superior impact strengths (Figure 4.45 (b)) because of the smaller rubber particles size of 0.19 μm compared with 1.81 μm found in the DOW grades. The same analogy of the effect of particle size on impact strength can be drawn between the BP grade (sample #16) with an average particle size 1.28 μm, compared to the DOW grade (sample #17) with an average particle size 4.5 μm.

It is generally known that PP blends with smaller rubber particle sizes are tougher and more ductile than those with larger particles, probably because the former represent a more efficient way of the rubbery phase promoting crazing and shear yielding. This does not necessarily mean that, the smaller the particle size the better the toughening effect. This is because the dimension of the propagating crack depends on the fracture ligament at the end of the crack[54]. If the fracture ligament is greater than the size of a particle, then smaller particle wont be effective in preventing the crack from propagating, leading to premature failure of the material.

University of Cape Town

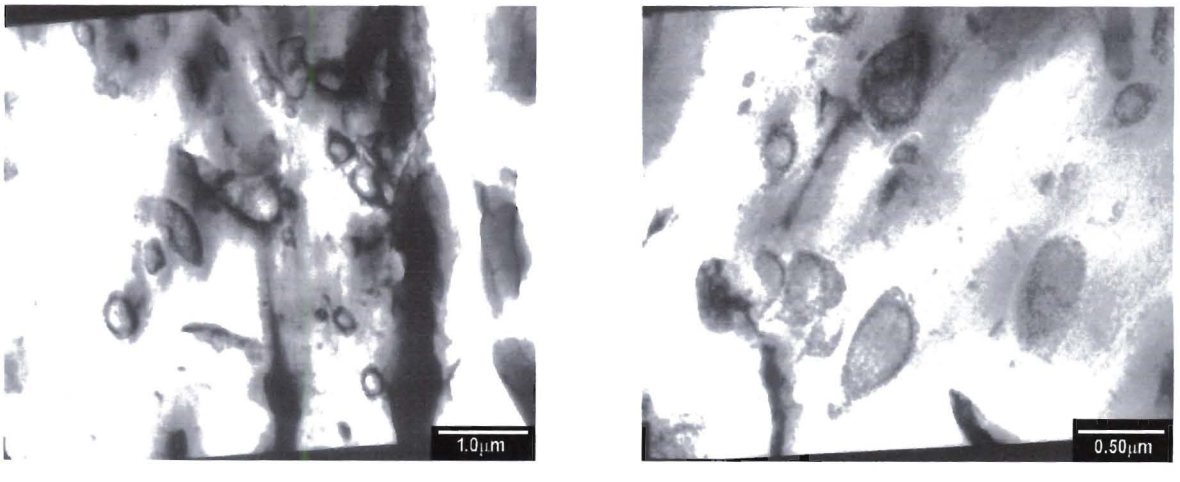

Sample #22: Basell grade

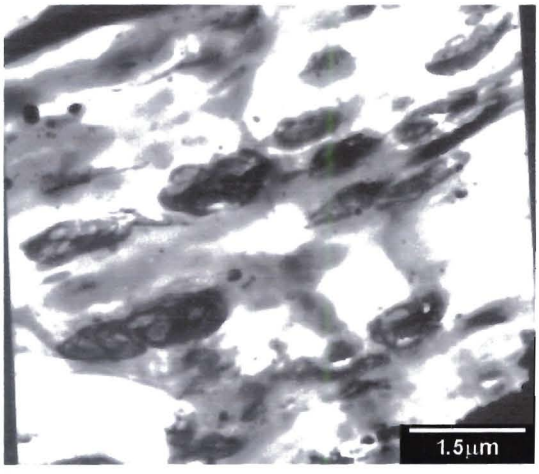

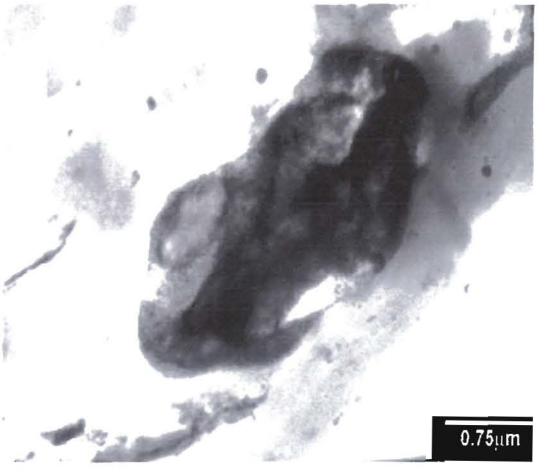

Sample #24: Sasol grade

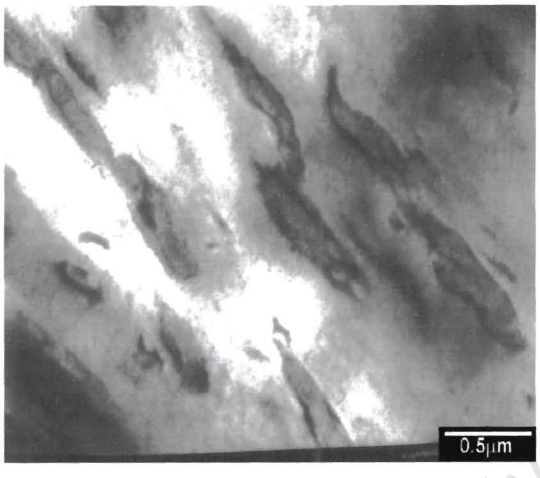

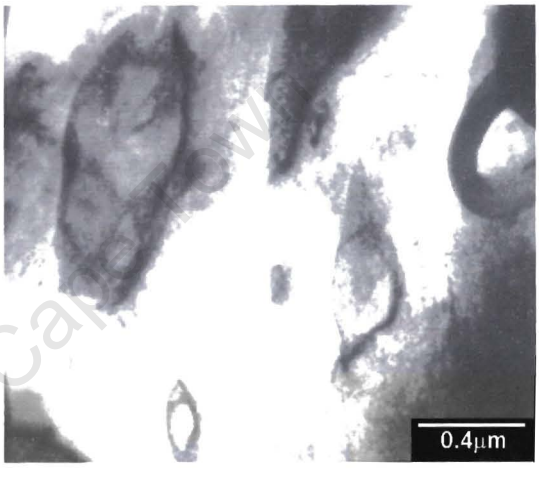

Sample #26: Basell grade

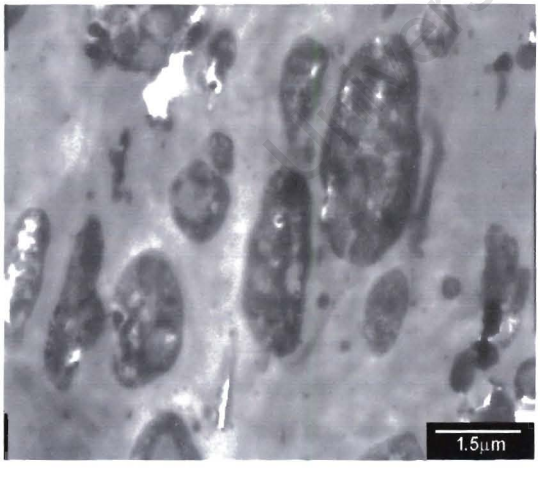

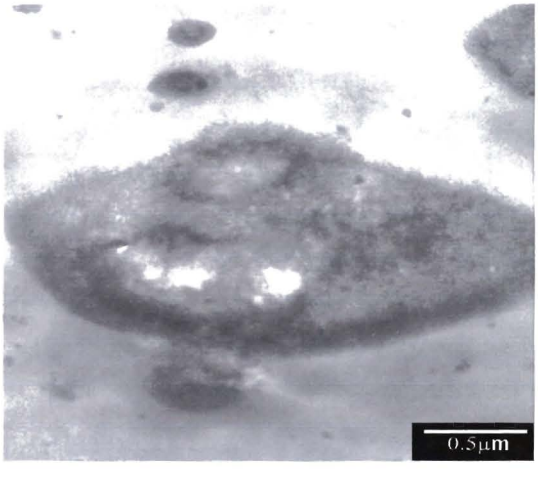

Sample #28: Sasol grade

University of Cape Town

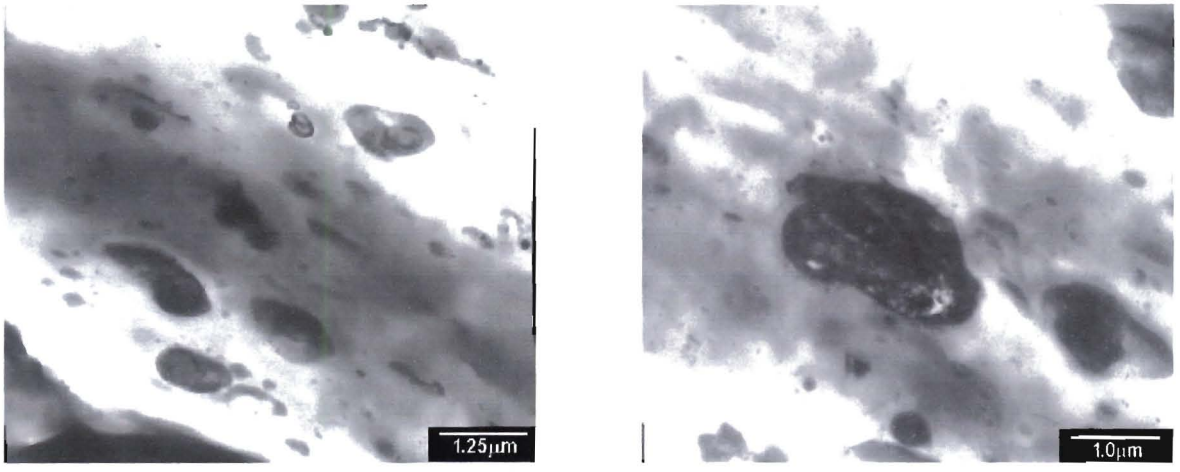

Sasol grade 2540H

Figure 4.47 TEM micrographs of samples with the ethylene contents greater than 10%

Figure 4.47 shows the microstructures for samples with ethylene contents above 10%. The Sasol grades (sample #3, 20, 24, 28 and grade 2540H) have several inclusions within the rubber particles whilst the Basell grades (sample #22 and 26) have only few inclusions within them. If we compare the impact strengths together with the MFI, ethylene content and particles size (Table 4.8) of samples #26, 27 and 28 then it would appear that the lower particle size of 0.86 μm for the BP grade, gives it relatively good Izod, Tensile and drop weight impact strengths. Figure 4.45(c) also indicates that the Sasol grade 2648 M (sample #24), also has favourable impact values and again, this may be attributed to its relatively small rubber particle size of 0.75 μm. The Basell samples #23 and #30 have relatively low Izod impact values and this may be due to their relatively large particle sizes of 1.63 μm and 3.43 μm, respectively (Table 4.8).

University of Cape Town

CHAPTER FIVE

DISCUSSION

5.1 INTRODUCTION

The morphology of copolymer grades plays a key role in determining the micro- and macro-mechanical behaviours of polymers. The production of poly (propylene-ethylene) copolymer is currently achieved in-situ, by reactor copolymerisation of ethylene-propylene rubber (EPR) into a previously polymerised isotactic polypropylene (iPP) homopolymer matrix. This leads to rubber particles being finely dispersed within the matrix, resulting in copolymers with improved impact strength especially at low temperatures. In addition, slight variations in the polymerisation processes introduce more variation in the morphology. This investigation is a technological benchmark exercise to compare how the different manufacturing technologies affect both the morphology and the mechanical behaviour of copolymer grades. Of particular interest, are the effects of ethylene content and melt flow index on morphological parameters and impact properties. Hence, an understanding of these morphological parameters will lead to a better understanding of how different manufacturing technologies affect these parameters, and how to achieved a copolymer with optimum mechanical properties from existing technologies.

University of Cape Town

5.2 MECHANICAL PROPERTIES

5.2.1 EFFECT OF MATRIX PARAMETERS ON MECHANICAL PROPERTIES

The effect of matrix parameters such as the molecular weight distribution (MWD), melt flow index (MFI) and the degree of crystallinity (%X_c) on the mechanical behaviour of poly-(propylene-ethylene) copolymers have been studied by many researchers to optimise their performance[12,13,20]. It is well known that different parameters within polymeric materials affect the mechanical behaviour in an opposing ways; therefore,

care must be taken when trying to optimise certain physical and mechanical properties for a particular application.

The design of copolymers requires a compromise between stiffness and toughness. As impact strength and flowability are opposing factors, toughness decreases with increasing MFI. The effect of the MFI on impact strength of the copolymer grades was shown in Figure 4.18. These plots show three different impact tests, namely: Izod notched impact, double edge notched tensile impact and drop weight impact tests, all performed at room temperature. Both, the Izod notched and double edge notched tensile impact tests, showed similarity in their trends, whereby the impact strength decreases with increasing MFI. The only difference is that, the Izod impact showed an initial rapid decrease in impact strength at low MFI while tensile impact plot did not. A similar type of trend was found in the study conducted by Marcus, whereby an exponential decrease in impact strength with increasing MFI was observed. It was concluded that the molecular weight parameter outweighs the effect of the ethylene content at low MFI's and the independency of impact strengths on ethylene content at very high MFI was observed from the copolymer grades studied[13]. It is obvious that impact strength decreases substantially as the MFI increases, and levels off at an MFI of 8.5 g/10 min irrespective of the ethylene content level. At a low temperature of –20°C, the Izod impact test still shows effect of MFI on the toughness of the copolymer grades. However, the results from the drop weight impact tests did not show this clear trend. The impact data points were scattered when plotted against MFI. This can be attributed to the differences in the stress states experienced during the impact event. The sample in a drop weight impact experiences multi-axial stresses and in an Izod impact it experiences bi-axial stresses leading to different fracture behaviour, thus different toughness behaviour. The work conduct by Patil on a drop weight impact test indicates that, the toughness of the copolymers *increase* with decreasing temperature, and then drops drastically after a certain lower temperature, whilst the Izod impact strength results were decreasing continuously with decreasing temperature[38]. The same observations were made from this work in some grades. However, the results are not conclusive to point out which grades of copolymers and associated manufacturing technologies behaved in such a manner.

It was shown that the MFI has no significant effect on the tensile yield strength, tensile modulus and hardness of the materials shown in Figure 4.20 and Figure 4.22.

University of Cape Town

However, a study conducted by Sugimoto and co-worker on polypropylene showed that, increasing the molecular weight (or decreasing MFI) of the PP causes a drop in both tensile modulus and yield strength[55]. It is apparent that both molecular weight and crystallinity affect mechanical properties in positive ways. However, high molecular weight polymers have lower crystallinity and may account for the observations in this work. The Sasol grades were found to have lowest values of tensile yield strength, tensile modulus and Shore hardness over the whole range of MFI when compared with the other grades. The BP grades had the highest hardness values over the whole range of MFI. A low MFI of the matrix contributes to intrinsic toughness of the copolymer, but it also lowers the flowability considerably, which makes processing difficult. It seems that increasing the MFI of the copolymer grade is correlated with a decrease in percentage elongation. The Sasol grades was shown (Figure 4.23) to have the highest ductility over the whole range of MFI, followed by the BP and Basell grades, with DOW grades being least ductile.

It has been observed that the small strain properties, such as modulus, tensile yield strength and hardness depend on the degree of crystallinity and to a small extent on the molecular weight. The MWD affect crystallinity and the modulus-related properties in opposite ways since crystallinity is known to decrease with increasing MWD[55]. The impact strength and elongation with increasing crystallinity was found to decrease in Figure 4.30 and Figure 4.34, respectively. The BP grades had the highest hardness while the Sasol grades had the lowest hardness when plotted as a function of crystallinity. The Basell and DOW grades had hardness values between those of the Sasol and BP grades. The DOW grades had the lowest crystallinity and impact strength values when compared with the other grades. Most of the copolymer grades that had a nucleating agent added show an increased crystallinity and mechanical properties such as hardness, tensile modulus and yield strength. The addition of nucleating agents is known to increase the percentage crystallinity and crystallisation temperature[56]. Consequently, nucleators are particularly useful when increases in stiffness, upper use temperature, or an improvement in optical properties are desired in end-use properties.

University of Cape Town

5.2.2 Effect of Ethylene Content on Mechanical Properties

The incorporation of a rubber phase into the iPP matrix increases the toughness of the polymers. Since the rubber particles act as stress concentrators it initiates a multitude of deformation modes such as cavitation of the rubber phase followed by shear yielding or multiple crazing of the iPP matrix. Therefore, this would result in the toughness of the copolymer being increased. The deformation mechanism of polypropylene rubber blends has been studied extensively by many researchers[20,38,55,57,58,59]. The ductile to brittle transition (DBT) of the copolymers with increasing ethylene content is attributed to a critical rubber content of the system. The Izod notched and double edge notched tensile impact results in Figure 4.24 shows that the toughness of the copolymer grades increase significantly to a maximum energy at about 8.5% ethylene content, then followed by a slight drop in toughness for the Basell grades. On the other hand, the increase in impact strength was less dramatic in the drop weight impact tests. The DBT is dependent on the rubber particle size and for a system of iPP enhanced with EPR the critical particle size was found out to be 0.4 μm[6]. From the present investigation, the effect of particle size on DBT could not be determined, since it was demonstrated that particle size is independent from ethylene content.

The tensile yield strength, tensile modulus and hardness were observed to be decreasing with increasing ethylene content. Similar types of trends have been observed previously, and this decrease in the yield strength and modulus was found to exceed expectations based on the rule of mixtures[18]. This is because the rubbery phase plasticises the iPP matrix, leading to an easy slippering of molecules during low strain testing. This plasticising effect lead to a decrease in the yield strength, tensile modulus and hardness, at the same time increasing both impact strength and percentage elongation at break.

5.3 Physical Properties

5.3.1 DSC, WAXS and FTIR

The effect of ethylene content on the degree of crystallinity of the copolymer grades was studied using both differential scanning calorimetry (DSC) and wide-angle x-ray scattering (WAXS). The WAXS traces were found more useful in that information

University of Cape Town

pertaining crystallite size could be obtained in addition to percentage crystallinity. The two methods gave completely different values for crystallinity, and there was no correlation in the data obtained from these methods. The accuracy of WAXS crystallinity results is limited by difficulties in estimating the contribution of the amorphous background from the crystalline peaks. Although the DSC traces of copolymer grades showed a well defined peak for iPP separate peaks for polyethylene could not be observed or elucidated from the traces. It is generally known that the amount of the crystallisable polyethylene (PE) chains is very low for these particular copolymer grades. However, a study conducted by Mange using a DSC on poly (propylene-ethylene) copolymers, shows that when the ethylene content was relatively high at about 20%, separate endothermic peaks at 120°C attributed to crystallisable PE chains, can be observed. The percentage crystallinity of crystallisable PE chains was estimated to be about 0.5% for that particular grade[60]. In addition, WAXS traces did not show any presence of a PE peak, which would normally be found at 2θ = 23.4°, attributable to the (200) crystallographic plane. Techniques such as carbon-13 nuclear magnetic resonance (^{13}C NMR) spectroscopy and Fourier transform infrared (Ft-IR) spectroscopy can be useful in determining the chain structure and amount of crystallisable PE chains[10]. These techniques use fractionation methods such as solvent extraction or temperature rising elution fractionation (TREF) in order to determine the structural heterogeneity of the copolymer blends.

The Ft-IR results taken at the mid-infrared region (1350 to 350 cm^{-1}) show that more than ten PP bands and two PE bands at 730 and 720 cm^{-1} can be separated successfully. The intensities of the PE doublet indicate crystallisable PE chains within the copolymer. When the crystallinity of PE is small, the band at 730 cm^{-1} of the doublet is reduced to a shoulder of the band at 720 cm^{-1}, as is the case with most copolymer grades studied. The presence of the atmospheric CO_2 vapour band at 668 cm^{-1} was found to interfere with the intensity of the PE doublet, which then reduces the crystallinity of the PE chains. According to Skaare and co-workers the presence of atmospheric CO_2 vapour is due time to dry air purge the spectrometer, and its intensity diminishes with the length of purging time[53]. The intensity of PE doublet was observed to vary from grade to grade, and also to increase with increasing ethylene content as was shown in Figure 4.8 to Figure 4.10. At ethylene contents above 10%, it was observed that most of the spectrums show the presence of the CO_2 band that is even

University of Cape Town

more intense than the PE doublet band. Most of the BP grades did not show presence of the CO_2 band, which clearly indicates that the presence of CO_2 vapour in the grades was not introduced during infrared scanning time but could only have been introduced before i.e. during processing. Ft-IR has been demonstrated to be a useful technique to characterise the chain structure of the iPP copolymer grades since it gives results that have been confirmed by many other researchers through the use of TREF in conjunction with ^{13}C NMR[10,40,53]. For the purpose of this investigation the Ft-IR on its own was found to give satisfactory results, and as such no attempt was made to apply other methods such as TREF. Ft-IR clearly reveals the presence of the PE doublet band and how its intensity is affected by the presence of CO_2 vapour band.

The apparent crystal size of iPP was determined from the WAXS. It was observed that, in the direction perpendicular to (040) crystallographic plane, the crystal sizes were generally larger than crystals in the direction perpendicular to (110) crystallographic plane as shown by Table 4.5. When the ratio between the $D_{(110)}$ and $D_{(040)}$-crystal size is plotted against ethylene content, the data points show some scattering for the Sasol and Basell grades. The scattering was much less pronounced in the BP grades, with the crystal size ratio remaining fairly constant over the whole range of ethylene content. This suggests that in the BP grades, the crystal size together with its spherulite size, are independent of the ethylene content. In addition, that the DOW grades show an apparent decrease in the crystal size ratio over the whole range of ethylene content, (see Figure 4.17). The difference in crystal size of the grades can be attributed to the processing conditions and manufacturing technologies used for the copolymer grades.

The most predominate crystalline morphology of the melt crystallised iPP is the α-crystal phase and is most stable crystalline structure. The β-crystal phase is observed occasionally during crystallisation and appears as a minority constituent of iPP. Some researchers have reported that iPP, which have high levels of the β-crystal, exhibit lower values of modulus and yield stress, but higher values of impact strength and elongation at break[29-34]. From this work the relative amount of β-crystal, i.e. the K-value was determined and found to range between 0.17 and 0.44. Most of the DOW grades did not show the presence of the β-crystal, and have consequently shown a poor ductility and crystallinity compared with other grades. This could be because in most of the DOW grades nucleating agents were not used to enhance their crystallinity.

University of Cape Town

The effect of ethylene content on the relative amount of the β-crystal was determined and was found not to influence the amount of the β-crystal phase. All the grades with the β-crystal had shown good impact strengths.

Since all the grades were produced under the same injection moulding conditions, the difference in the β-content can be attributed to fluctuations in processing variables such as reactor temperature and pressure and the formulation and activity of the catalytic system used. In general, the addition of nucleating agents improves the degree of crystallinity, which then leads to improvement in the stiffness and yield strength of the copolymers by enhancing the relative amount of β-crystals.

5.4 MICROSTRUCTURAL ANALYSIS

5.4.1 SEM AND TEM

These analyses were carried out in order to determine to what extent the particle size, interparticle distance and particle size distribution have an effect on the micro- and macro-mechanical properties of the copolymer grades. In addition, the analyses were also intended to determine differences in the rubber particle morphology in the different copolymer grades manufactured using different technologies.

The effect of ethylene content and MFI on the average weight particle size and interparticle distance was determined. It was observed that both ethylene content and MFI have no significant effect on the particle size and interparticle distance depending on type manufacturing technology used (see Figure 4.38 and Figure 4.41). However, when the ratio of the interparticle distances to average particle size (ID/D_w) is plotted against ethylene content, a trend was observed from BP and DOW grades but not with other grades. Both the BP and DOW grades showed an exponential decrease in the ID/D_w ratio with increasing ethylene content. The Sasol grades showed an increase in the ID/D_w ratio with increasing ethylene content. The overall observation was that the copolymer grades had a relatively small ID/D_w ratio, which would allow for an overlapping of stress fields around adjacent rubber particle during the deformation process. Therefore, voids will easily be produced and a multiple cavitation process will take place in the rubber particle of these grades. The average weight particle size (D_w)

University of Cape Town

in most grades was about 1.0 μm on average, with the Sasol grades having a D_w of 0.75 to 1.68 μm, BP a D_w of 0.52 to 2.11 μm, Basell a D_w of 0.19 to 3.43 μm, DOW a D_w of 1.45 to 4.51 μm and Borealis grade a D_w of 2.98 μm. The interparticle distance (ID) was found to be about 2.0μm on average in most copolymer grades. However, some of the DOW grades had higher interparticle distances of above 5.0 μm.

The Sasol, Basell and BP grades seem to have a small particle size on average over the whole range of ethylene content compared with the DOW grades. The BP grades seem to have a constant narrow particle size distribution over the whole range of ethylene content and MFI, followed by the Basell and Sasol grades. The DOW grades show a broad particle size distribution.

TEM was used to study the phase morphology of the isotactic polypropylene modified with ethylene-propylene block copolymer in more detail, as shown in Figure 5.1. The microstructure shows a ternary system because the interfacial stress between the ethylene-propylene phase and iPP matrix is lower than that between the polyethylene phase and the iPP matrix. This interface develops as a rubber shell around the PE core. Even though iPP and the rubber phase are not miscible, there is a certain affinity that leads to good adhesion between the two phases. Thus, the rubber phase serves as a compatibiliser in addition to being an impact modifier.

University of Cape Town

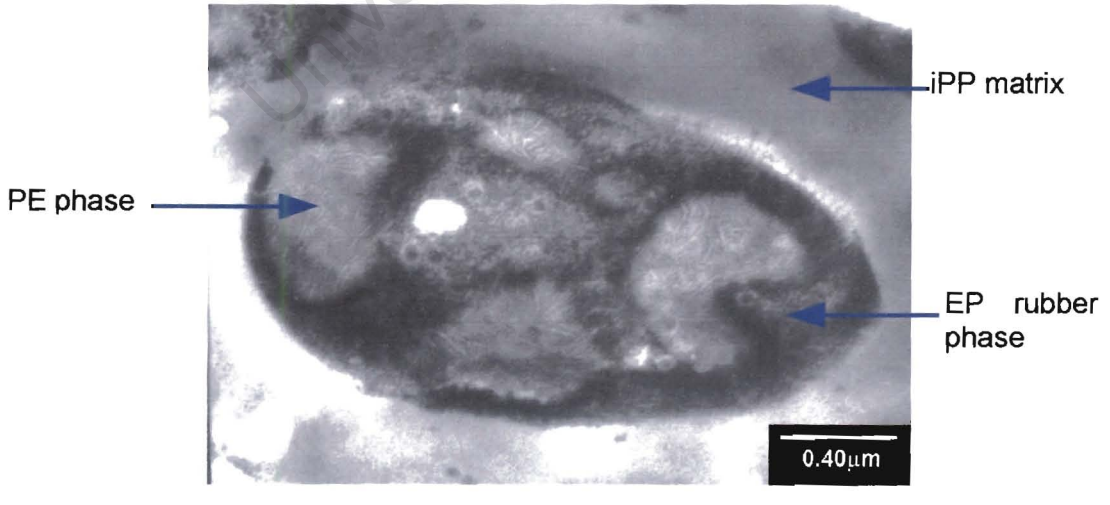

Figure 5.1 The phase morphology of ethylene-propylene copolymer showing a ternary structure

The rubber phase is composed of PE and PP units, which, in theory, are distributed statistically in equal amounts. The rubber phase composition influences glass transition temperature, T_g, its compatibility with the matrix, the amount of crystalline PE and shrinkage of the rubber phase during cooling. In general, the compatibility decreases with increasing ethylene content. Taking into account all these factors, a substantial improvement of the rubber phase morphology and thus impact strength can be achieved.

By varying the polymerisation and the subsequent processing conditions, this could lead to a product with very different properties. Figure 5.2 shows two similar kinds of morphologies, which are slightly different in the homogeneity of their rubber particle distribution, as shown in Figure 5.3. Sample #3 had a larger average particle size (D_w = 1.68 μm) and a broad particle size distribution (D_w/D_n = 1.25) compared with sample #4, which has a small average weight particle size (D_w = 1.03 μm) and a narrow particle size distribution (D_w/D_n = 1.17). In addition, there is competition between dispersion and coagulation, which plays a key role in the properties of the samples and adds further complications to the final morphologies. Sample #3 shows a microstructure with rubber particles that have coagulated, whilst sample #4 shows a well-dispersed rubber particle microstructure. As a consequence of this, the homogeneous sample #4 is observed to have a higher impact strength than inhomogeneous sample #3 when using the Izod impact test, although the reversed in impact results was observed when using the tensile impact test. This would suggest that different morphologies are favoured when different stress states are applied during the deformation processes.

Since both grades where processed under the same injection moulding conditions, the difference in their homogeneity could be traced back to their polymerisation conditions. Sample #3 is polymerised using the Novolen PP technology and sample #4 is polymerised using the Innovene PP technology. Nevertheless, this observation does not generalise the overall observed morphology between the two technologies. It is just an illustration of how different polymerisation conditions can affects the final morphologies of copolymer grades. In addition, there are some other factors, which would affect the final morphology of the copolymers grades. Factors such as the processing temperature, the pressure and the use of peroxide clipping to increase the MFI of the polymer were seen to affect the final morphology of the rubber particles. All these factors were found to disperse or agglomerate rubber particles.

University of Cape Town

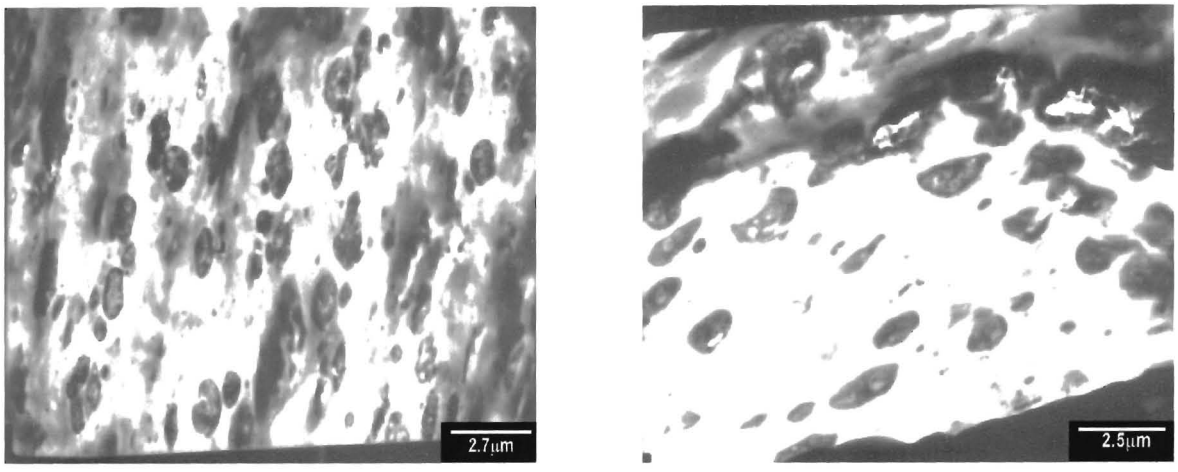

(a) (b)

Figure 5.2 Morphologies of two copolymer grades with ethylene content below 8%: (a) sample #3 and (b) sample #4

University of Cape Town

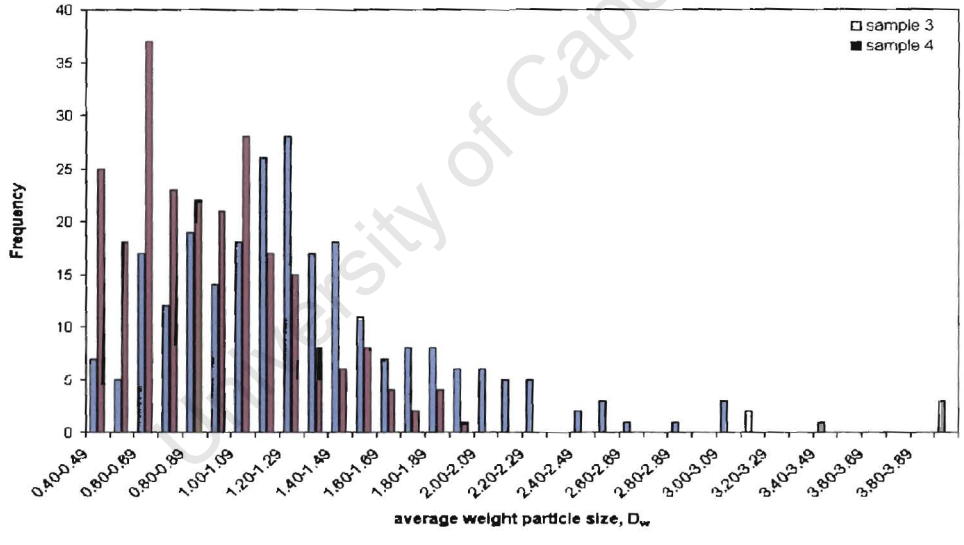

Figure 5.3 Illustration of difference between particle size distributions in two samples produced by different manufacturing technologies

Different microstructural morphologies were observed in the different copolymer grades studied. An overall observation is that the Sasol, BP, and DOW grades show rubber particles with several PE inclusions. In addition, the Sasol and BP grades are similar in their morphologies. The Basell grades generally show morphology of rubber particles with single or few inclusions within them. In addition, the number of inclusions in the

particle can be related to the agglomeration of small rubber particles to form a bigger one. Figure 5.4 illustrates how small rubber particles can coalesce to form a bigger particle as the rubber concentration increases.

It is observed that, the BP followed by the Sasol grades have overall higher toughness values compared with the Basell grades. This is attributed to presence of rubber particles with several inclusions. Kim and coworkers concluded that modifier particles with several inclusions have a higher toughening effect on PP/EPR blends[19]. This can be explained by systems that are modified with several inclusions dissipate more impact energy through multiple cavitation processes than those systems modified with single inclusions. The DOW grades seem to have poor toughness, even poorer than grades with the single inclusions in their rubber particles. This can be attributed to their broad particle size distribution and a large interparticle distance within their grades, which plays an important role in the toughening and micro-mechanical process during deformation.

University of Cape Town

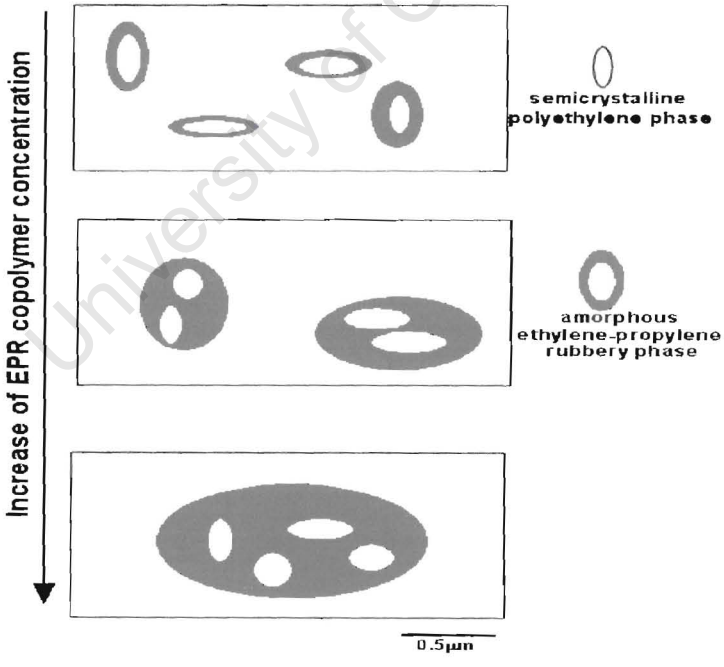

Figure 5.4 Illustration of the coalescence of small rubber particles to form a bigger particle [after ref. 19]

It is generally known that the average weight particle size is a function of the viscosity ratio between the rubber phase and the matrix. This was found to be correct if the rubber particle has a single polyethylene inclusion within a rubber phase. However, it was found that if the particles have several inclusions within the rubber phase, then the final average rubber particle size does not only depend on the viscosity ratio, because the average particle size is an aggregation of individual particles[19]. Therefore, when tailoring for copolymers with fine dispersed particle size distribution within the matrix, factors such as the MW of the EPR phase that is crucial to control the size of the rubber as well as the shear rate should be considered. These factors play an important role in achieving a microstructure that will give a copolymer with better impact properties.

5.5 Dynamic Mechanical Properties

From the DMA spectrums, the presence of β_2-relaxation indicates that the iPP and EPR phases are completely immiscible within the copolymer grades. The T_g values measured from DMA are frequency dependent. It is observed that the loss modulus and tan δ peaks of the β_1- component shifts to a lower or higher temperature or remain constant depending on the amount of ethylene content and type of copolymer grades. Similarly, the height and area under loss modulus curves of the β_1- and β_2- components change depending on the amount and type of copolymer grades. The increase in height and area under the loss modulus peak corresponds to total energy dissipated because of the viscoelastic relaxation of β_1. An increase of the loss modulus peak area was observed and found to be related to the amount of ethylene content. Some researchers suggest that there is a correlation between toughness and area under the loss modulus peak[42,61,62]. From this work, this correlation could not be determined.

The plots of storage modulus (E') as a function of temperature are shown in Figure 4.3 to Figure 4.5. Stiffness values were measured from the storage modulus curves at temperatures 23°C, 0°C and –20°C. These values were compared with values obtained from dynamic mechanical static stress-train curves measured in the region of linear viscoelasticity at the same temperatures and are shown in Table 4.3. Both methods show a decrease in stiffness with increasing temperature, though that the 0°C results from the static stress-strain shows some inconsistency with this decrease. DMA is a versatile technique to monitor stiffness under dynamic loading of the copolymers

University of Cape Town

over a wide temperature range, and can be used to correlate impact strength of the copolymers with their dynamic mechanical properties. This technique should be used in conjunction with other techniques such as DSC, to monitor the amount of crystallinity as it is being affected by ethylene content.

5.6 Effect of Manufacturing Techniques

The description of manufacturing technologies used in the production of copolymer grades investigated are mention in detail in section 2.2. These copolymer grades were polymerised in a two-stage process with Ziegler-Natta catalysts that are designed for suitable targeted copolymer grades and technologies used. The reactor conditions for polymerisation are different from one technology to the other, even during the production of different grades on the same plant.

The Sasol and BP grades where polymerised using the mechanically agitated gas-phase reactors, with Sasol's Novolen technology having vertical stirred bed reactors (VSBR's) and BP's Innovene technology having horizontal stirred bed reactors (HSBR's). Because of the continuous polymerisation nature of the process, factors such as reactor residence-time distribution and back mixing must be considered, since they both affect the final morphology of the copolymer grades. Both catalyst residence-time distribution and back mixing implies a natural distribution of polymer properties from polymer particle to particle, as they exit the process. The Innovene technology has proven to be the most effective, since from this work it was observed that the rubber particle size distribution was narrow over the whole range of ethylene content and MFI in all BP's copolymer grades. This could be attributed to the plug flow movement of polymer particles that minimised both back mixing and average particle residence-time distribution within the reactor by making sure that all the particles spend almost equal amounts of time inside the reactors.

The Novolen technology showed a broad particle size distribution, and this can be attributed to the back mixing and particle residence-time distributions within the reactor since it is not possible to quantify whether the particles spent equal amounts of time within the vertical reactors. Debling and co-workers made the same observations in their studies in the VSBR process only one stirred bed reactor is used for each stage of polymerisation leading to a broad particle size distribution. They suggested that to

University of Cape Town

narrow the particle size distribution, one must use additional copolymerisation reactors in series such as in the Innovene reactors[3]. Furthermore, the rubber particle morphology from two technologies showed some similarities with several number of PE inclusions which have proven to be effective for the toughening mechanism since they [rubber particles] dissipate more impact energy during deformation. Consequently, this has demonstrated that the BP copolymer grades to have overall better impact property than other the grades.

The Basell grades where produced using the Spheripol PP technology, which utilises two loop reactors and a gas-phase fluidised bed reactor (FBR). The particle distribution time and particle back mixing has been claimed to be a minimum when using this technology[2,4]. This could be true, since the rubber particles from this technology where found to have a constant narrow particle size distribution. TEM results showed that, the rubber particle morphology for the Basell grades to have a few number of inclusions of PE within them, which resulted in these grades having lower impact strength than the BP and Sasol grades.

The DOW grades where produced using Univation PP technology/ UNIPOL PP technology, which utilises two fluidised bed reactor in series for polymerisation. From what is observed from the DOW grades, this technology is problematic in controlling the reactor residence-time distribution, since most of their grades have a broad particle size distribution, a large particle size and large interparticle distance. This resulted in their grades having poor mechanical properties compared with the other grades. According to Debling and co-workers the poor grade morphology can be attributed to the catalyst size selection, where it was found that a significant fraction of small catalyst particles remain in the homopolymerisation reactor for long periods of time whereas many of the large catalyst particle leave quickly. This would affect the performance of the copolymerisation stage of the process and the product properties[3].

The Borealis grade was produced using the Borstar PP technology, which is more or less similar to the Spheripol PP technology, except that it is modulated through the introduction of other small gas-phase FBR's for polymerisation of heterophasic impact copolymers. The general performance for this grade was found to be reasonable compared with other copolymer grades that fell within the same ethylene content and MFI range. In order to explain these observations, TEM was found to be an extremely useful technique in illustrating the final rubber particle morphology of the copolymer

University of Cape Town

grades. It should be noted however, that the morphologies cannot satisfactorily be predicted during the polymerisation process since there are many factors that govern the final morphology of the rubber particles.

University of Cape Town

CHAPTER SIX

CONCLUSIONS

- The result shows that for the grades evaluated, the average weight particle size and interparticle distance are independent of the ethylene content and MFI. When the ratio of interparticle distance –to –particle size (ID/Dw) was plotted against ethylene content, a decreasing trend was observed within the BP and DOW grades, but not with the other grades. This ratio was considered to be small enough in all the grades to allow an overlapping of stress fields around adjacent rubber particles during the deformation process. Therefore, the size and dispersion of EPR particles can be improved through manipulation of its molecular weight and the viscosity ratio between the rubber phase and the matrix.

- Both the BP and Basell grades show a narrow rubber particle size distribution, which is attributed to the type of manufacturing technology used. The Sasol grades follow next and then lastly the DOW grades, which showed a broad particle size distribution within the matrix.

- TEM has proven to be a powerful tool to elucidate the morphological differences of the internal EPR phase microstructures of the different copolymer grades. A typical TEM micrographs show that the poly (propylene-ethylene) copolymer microstructure consists of a ternary system because the interfacial stress between the ethylene-propylene phase and the iPP matrix is lower than that between the polyethylene phase and the iPP matrix. This interface develops as a rubber shell around the PE core. The PE inclusions within the rubber phase differ from grade to grade. With the Sasol, BP and DOW grades there are several inclusions whilst the Basell grades only few inclusions were found.

- Grades with several numbers of PE inclusions appeared to have higher impact strengths than those with fewer inclusions. Most of these grades have an average particle size of about 1.0 μm. The results show that, during the deformation

University of Cape Town

process, different rubber morphologies (i.e. dispersion and coagulation) are favoured in order to obtain maximum impact energy under different stress states.

⌘ The BP grades were shown to be superior with the best balance between the strength and stiffness, followed by the Sasol and the Basell grades and lastly the DOW grades. The impact properties of the Borealis grades can be placed between those of the Basell and DOW grades since their performance was found to be fairly reasonable compared with the other grades.

University of Cape Town

RECOMMENDATIONS FOR FUTURE WORK

- The production of the poly (propylene-ethylene) copolymers is one of the complex yet interesting phenomena to study. Therefore, in order to understand the materials investigated, the reseacher should spend time on plants to see how the production of these copolymers comes about. This would lead to a better understanding, of the factors in processing to consider during his/her investigations.

- The use of TEM has proven itself to be a powerful tool in elucidating the internal morphologies of the poly (propylene-ethylene) copolymers grades. In the present study, the morphology of rubber was observed on undeformed copolymer grades. It is suggested that in subsequent TEM investigations, the investigator should concentrate more on both deformed and undeformed copolymer grades in order to understand the kind of deformation mechanisms involved in the different rubber morphologies.

- A comprehensive study on DMA should be conducted on different grades in order to understand effect of ethylene content on the viscoelastic properties of the copolymers. Also, the investigator should spend more time on understanding the correlation between impact strength and dynamic mechanical properties.

University of Cape Town

CHAPTER SEVEN

REFERENCES

1. P. Galli, S. Danesi, T. Simonazzi, *"Polypropylene Based Polymer Blends: Field of Application and New Trends"*, **Polym. Eng. Sci., 24 (1984)**, 544

2. B. Sole, *"Private communication"* Sasol Polymers

3. J. A. Debling, J. J. Zacca and W. H. Roy, *"Reactor Residence-Time Distribution Effects on the Multistage Polymerisation of Olefins-III. Multi-Layered Products: Impact Polypropylene"*, **Chem. Engng. Sci., 52 (1997),** 1969

4. T. Simonazzi, G. Cecchin and S. Mazzullo, *"An Outlook on Progress in Polypropylene-Based Polymer Technology"*, **Prog. Polym Sci. (1991)**, 303

5. D. C. Bassett, **Principles of Polymer Morphology,** Oxford Science Publications, New York, 1988

6. R. A Phillips and M. D. Wolkowics, "Structure *and Morphology*", In: **Polypropylene Handbook**, Ed., E. P. Moore, Jr., Hanser/Gardner Publications, Inc., Cincinnati, 1996, pp. 113

7. C. Hall, **Polymer Materials: An Introduction for Technologists and Scientists,** 2nd ed., MacMillan Education, London, 1989

8. J. Li, R. A. Shanks and Y. Long, *"Miscibility and Crystallisation of Polypropylene-Linear Low Density Polyethylene Blends"*, **Polymer, 42 (2001)**, 1941

9. Y. Masubuchi, *"Thermal Analysis of Shear Induced Crystallisation by the Shear Flow Thermal Rheometer: Isothermal Crystallisation of Polypropylene"*, **Polymer, 42 (2001),** 5023

10. Z-q. Fan, Y-q. Zhang, J-t. Xu, H-t. Wang and L-x. Feng, "*Structure and Properties of Polypropylene/Poly (Ethylene-Co-Propylene) in-situ Blends Synthesized By Spherical Ziegler-Natta Catalyst*", **Polymer, 42 (2001)**, 5559

11. T. A. Osswald and G. Menges, **Materials Science of Polymers for Engineers.** Hanser/Gardner Publications Inc, Cincinnati, 1995

University of Cape Town

12. A. van der Wal, J.J. Mulder, J. Oderkerk and R. J Gaymans, *"Polypropylene-Rubber Blends: 1. The Effect of the Matrix Properties on the Impact Behaviour"*, **Polymer, 39 (1998),** 6781

13. K. Marcus, *"Copolymer Project Part 1: A Statistical Study on the Correlation Between Mechanical and Molecular Parameters: BNP Copolymers"*, **Polifin Internal Report, 1997**

14. R. B. Lieberman and R. T. LeNoir; *"Manufacturing"*, In: **Polypropylene Handbook**, ed., E. P Moore, Jr. Hanser/Gardner Publications, Inc., Cincinnati, 1996, pp 287

15. J.J Zacca, J. A. Debling and W. H. Ray, *"Reactor Residence-Time Distribution Effects on the Multistage Polymerisation of Olefins-I. Basic Principles and Illustrative Examples, Polypropylene"*; **Chem. Engng Sci. 51 (1996),** 4859

16. http://www.borealisgroup.com

17. M. R. Kantz, H. D. Newman, Jr., and F. H. Stigale, *"The Skin-Core Morphology and Structure-Property Relationships in Injection-Molded Polypropylene"*, **J. Appl. Polym. Sci., 16 (1972),** 1249

18. L. D'Orazio, C. Mancarella, E. Martuscelli, G. Cecchin and R. Carrieri, *"Isotactic Polypropylene/Ethylene-Co-Propylene Blends, Effect of the Copolymer Microstructure and Content on Rheology, Morphology and Properties of Injection Moulded Samples"*, **Polymer, 40 (1999)**, 2745

19. G. -M. Kim, G. H. Michler, M. Gahleitner and J. Fiebig, *"Relationship Between Morphology and Micromechanical Toughening Mechanisms in Modified Polypropylenes"*. **J. Appl. Polym. Sci., 60 (1996),** 1391

20. A. van der Wal, R. Nijhof and R. J. Gaymans, *"Polypropylene-Rubber Blends: 2. The Effect of the Rubber Content on the Deformation and Impact Behaviour"*, **Polymer, 40 (1999),** 6031

21. K. Cho, J. Yang and C. E. Park., *"The Effect of Rubber Particle Size on the Toughening Behaviour of Rubber-Modified Poly(Methyl Methacrylate) with Different Test Methods"*, **Polymer, 39 (1998),** 3081

22. Z. H. Liu, X. D. Zhang, X. G. Zhu, Z. N. Qi, F. S. Wang, R. K. Y. Li and C. L. Choy, *"Effect of Morphology on the Brittle-Ductile Transition of Polymer Blends: 3. The Influence of Rubber Particle Spatial Distribution on the Fracture Behaviour of Poly (Vinyl Chloride)/ Nitrile Rubber Blends"*, **Polymer, 39 (1998),** 5027

University of Cape Town

23. Z. H. Liu, X. D. Zhang, X. G. Zhu, Z. N. Qi, F. S. Wang, R. K. Y. Li and C. L. Choy, *"Effect of Morphology on the Brittle-Ductile Transition of Polymer Blends: 4. Influence of the Rubber Particle Spatial Distribution in Poly (Vinyl Chloride)/ Nitrile Rubber Blends"*, **Polymer, 39 (1998),** 5035

24. P. A. Lovell, *"Rubber-Toughened Plastics: Strategies for their Preparation and Evaluation"*, **IUPAC Conference**, University Of Stellenbosch, *South Africa, 2001*

25. L. C. Sawyer and D. T Grubb, **Polymer Microscopy**, 2nd ed., Chapmen & Hall, London, 1996

26. J. S. Trent, *"Ruthenium Tetraoxide Staining of Polymers: New Preparative Methods for Electron Microscopy"*, **Macromolecules, 17 (1984),** 2923

27. D. Montezinos, B. G. Wells and J. L. Burns, *"The Use of Ruthenium in Hypochlorite as a Stain for Polymeric Materials"*, **J. Polym. Sci.: Polym. Lett. Ed., 23 (1985)**, 421

28. G. M. Brown and J. H. Butler, *"New Method for the Characterization of Domain Morphology of Polymer Blends Using Ruthenium Tetroxide Staining and Low Voltage Scanning Electron Microscopy (LVSEM)"*, **Polymer, 38 (1997),** 3937

29. S. C. Tjong, J. S. Shen and R. K. Y. Li, *"Mechanical Behavior of Injected Molded β-Crystalline Phase Polypropylene"*, **Polym. Eng. Sci, 36 (1996)**, 100

30. S. C. Tjong, J. S. Shen and R. K. Y. Li, *"Morphological Behaviour and Instrumented Dart Impact Properties of β-Crystalline-Phase Polypropylene"*, **Polymer, 37 (1996),** 2309

31. A. Turner-Jones, *"Development of the γ-Crystal Form in Random Copolymers of Propylene and Analysis by DSC and X-Ray Methods"*, **Polymer, 12 (1971)**, 487

32. R. A. Campbell, *"The Gamma Phase of High-Molecular-Weight Polypropylene: 1. Morphological Aspects"*, **Polymer, 40 (1993)**, 4809

33. Y. Feng, X. Jin and J. N. Hay, *"Crystalline Structure of Propylene-Ethylene Copolymer Fraction"*, **J. Appl Polym Sci., 68 (1998),** 381

34. Y. Feng and J. N. Hay, *"The Measurement of Compositional Heterogeneity in a Polypropylene-Ethylene Block Copolymer"*, **Polymer, 39 (1998)**, 6723

35. Y. Yokoyama and T. Ricco, *"Toughening of Polypropylene by different Elastomeric Systems"*, **Polymer, 39 (1998)**, 3675

University of Cape Town

36. J.C. Randall, *"Sequence Distribution versus Catalyst Site Behavior of in Situ Blends of Polypropylene and Poly (ethylene-co-propylene)"*, **J. Polym. Sci.,: Part A: Polym. Chem., 36 (1998),** 1527

37. J. Karger-Kocsis, A. Kalló, A. Szafner, G. Bodor and Zs. Sényei, *"Morphological Study on the Effect of Elastomeric Impact Modifiers in Polypropylene Systems"*, **Polymer, 20 (1979),** 37

38. R. Patil, *"An Investigation into the Impact Fracture Behaviour of Poly (Propylene-Ethylene) Copolymers using an Instrumented Low Temperature Drop Weight Impact Tester"*, **MSc Thesis**, University Of Cape Town, 2001

39. Y. Marchal, B. Oldenhove, D. Daoust, R. Legras and F. Delannay, *"Characterization of the Fracture Toughness of Rubber-Toughened Polypropylene Thin Plates"*, **Polym. Eng. Sci., 38 (1998),** 2063

40. C. Hongjun, L. Xiaolie, M. Dezhu, W. Jianmin and T. Honsheng, *"Structure and Properties of Impact Copolymer Polypropylene.II. Phase Structure and Crystalline Morphology"*, **J. Appl. Polym Sci., 71 (1999),** 103

41. J. U. Starke, G. H. Michler, W. Grellmann, S. Seidler, M. Gahleitner, J. Fiebig and E. Nezbedova, *"Fracture Toughness of Polypropylene Copolymers: Influence of Interparticle Distance and Temperature"*, **Polymer, 39 (1998)** 75

42. Y. Feng, X. Jin and J. N. Hay, *"Dynamic Mechanical Behavior Analysis for Low Ethylene Content Polypropylene Copolymers"*, **J. Appl. Polym. Sci., 68 (1998)**, 395

43. S. Díez-Gutiérrez, M. A. Rodríguez-Pérez, J. A. De Saja and J.I Velasco, *"Dynamic Mechanical Analysis of Injection-Moulded Discs of Polypropylene and Untreated and Silane-Treated Talc-Filled Polypropylene Composites"*, **Polymer, 40 (1999)**, 5354

44. W. Jiang, S. C. Tjong and R. K. Y. Li, *"Brittle-Tough Transition in PP/EPDM Blends: Effects of Interparticle Distance and Tensile Deformation Speed'*, **Polymer, 21 (2000)**, 3479

45. S. Wu, *"Phase Structure and Adhesion in Polymer Blends: A Criterion for Rubber Toughening"*, **Polymer, 26 (1985),** 1855

46. S. Wu, *"A Generalised Criterion for Rubber Toughening: The Critical Matrix Ligament Thickness"*, **J. Appl. Polym. Sci., 35 (1988),** 549

University of Cape Town

47. Z. H. Liu, X. G. Zhu, Q. Li, Z. N. Qi and F. S. Wang, *"Effect Of Morphology on the Brittle Ductile Transition of Polymer Blends: 5. The Role of CaCO3 Particle Size Distribution in High Density Polyethylene/ CaCO3 Composites"*, **Polymer, 39 (1998)**, 1863

48. W. Jiang, C-h. Liu, Z-g. Wang, L-j. An, H-j. Liang, B-z. Jiang, X-h. Wang and H-x. Zhang, *"Brittle-Tough Transition in PP/EPDM Blends: Effects of Interparticle Distance and Temperature"*, **Polymer, 39 (39)**, 3285

49. D. Del Duca and E. P Moore, Jr., *"End-use Properties"*, In: **Polypropylene Handbook**, ed., E. P Moore, Jr., Hanser/Gardner Publications, Inc., Cincinnati, 1996, pp 237

50. M. Sello, *"NETZSCH STA 409C Thermal Analyser Calibration Report"* Centre for Materials Engineering, University of Cape town, 2002

51. G. -X. Wei, H. –J. Sue, J. Chu, C. Huang and K. Gong, *"Toughening and Strengthening of Polypropylene using the Rigid-Rigid Polymer Toughening Concept: Part I. Morphology and Mechanical Property Investigations"* **Polymer, 41 (2000)**, 2947

52. C. J. Chou, K. Vijayan, D. Kirby, A. Hiltner and E. Baer, *"Ductile-to-Brittle Transition of Rubber-Modified Polypropylene. Part 1: Irreversible Deformation Mechanisms"*, **J. Mater. Sci., 23 (1988)**, 2521

53. L.E. Skaare, P. Klaeboe and C. J. Nielsen, *"Spectroscopic Studies of Ethylene-Propylene Copolymers in the Near- and Mid-Infrared Regions"*, **Vibrational Spectroscopy, 3 (1992),** 23

54. J. Z. Liang and R. K. Y. Li, *"Rubber Toughening in Polypropylene: A Review"*, **J. Appl. Polym. Sci., 77 (2000),** 409

55. M. Sugimoto and M. Ishikawa, *"Toughness of Polypropylene"*, **Polymer, 36 (1995)** 3675

56. T. Xu, J, Yu and Z. Jin, *" Effect of Crystalline Morphology on the Impact Behavior of Polypropylene"*, **Materials & Design, 22 (2001)** 27

57. W. G. Perkins, *"Polymer Toughness and Impact Resistance"*, **Polym. Eng. Sci., 39 (1999),** 2445

58. A. van der Wal, A. J. J. Verheul, R. J. Gaymans, *"Polypropylene- Rubber Blends: 4. The Effect of the Rubber Particles Size on the Fracture Behaviour at Low and High Test Speeds"*, **Polymer, 40 (1999)**, 6057

University of Cape Town

59. P. Gensler, C. J .G. Plummer, C. Crein and H. –H. Kausch, *"Influence of the Loading Rate on the Fracture Resistance of Isotactic Polyprpopyne and Impact Modified Isotactic Polypropylene"*, **Polymer, 41 (2000),** 3809

60. S. Mange, *"Structure-Property Relationships in Poly-(Propylene-Ethylene) Copolymers"*, **MSc Thesis**, University of Cape Town, 1999

61. S. H. Jafari and A. K. Gupta, *"Impact Strength and Dynamic Mechanical properties Correlation in Elastomer-Modified Polypropylene"*, **J. Appl. Polym. Sci., 78 (2000)**, 962

62. P. I. Vincent, *"Impact Strength and Mechanical Losses in Thermoplastics"*, **Polymer, 15 (1978),** 111

University of Cape Town

Sample No.	Sample Name	MFI	Tensile yield	% elongation	Tensile modulus	Notched Izod 23C	Notched Izod 0C	Notched Izod -20C	Shore Hardness	Nucleated ?	CR / no CR
		g/10min	MPa	%	MPa	kJ/m2	kJ/m2	kJ/m2			
1	BP K7506	5.9	30.7	80	1693	7.43	4.9	4.3	66	yes	no
2	Basell EPC30R	6.5	28.8	110	1370	6.2	5	3.7	61	yes	no
3	Sasol 2349MC-7697Y	8	27.3	129	1422	9.2			61	yes	no
4	BP K8512	12	29.9	98	1402	10.9	5.3	4.1	64	yes	yes
5	Basell HEXP280	20	32.7	20	1845	4.85	3.3	2.75	62	yes	yes
6	Borealis BH345MO	44	27.4	32	1500	4.9	3.7	3.6	60	yes	yes
7	BP B8101	0.4	26.6	265	1108	75.6	36.9	7.03	63	no	no
8	DOW SRC7-467	0.7	29.5	35	1480	51.1	15.2	7.43		no	no
9	Basell EPD60R	0.8	30	90	1280	76.4	29	6.1	59	no	no
10	Sasol 2502G-7795Y	1	22.8	342	1133	47.3			55	no	no
11	BP K7002	1.2	27.7	107	1378	50	7.9	6	65	no	no
12	Basell EPQ30RF	1.5	28	68	1230	56	8.4	5.9	59	no	no
13	DOW 7C50H	7	24.7	85	1140	5.28	4.25	3.76		no	no
14	BP K7312	14	26.6	27	1355	8.25	5.65	4.23	63	yes	yes
15	Basell EPV31RA	28	27.6	32	1520	5.6	4.8	4.1	59	yes	yes
16	BP K9935	34	23.5	52	1145	12.3	5.9	4.7	62	no	yes
17	DOW SRCD7-664	34	26.1	18	1640	4.38	4.2			yes	?
18	Basell EPH71HA	46	27.6	16	1575	5.2	4.4	4	59	yes	yes
19	BP K8550	49	25.4	37	1213	5.06	4.99	4.43	63	yes	yes
20	Sasol 2448TC-7759Y	50	21.2	68	1220	8.05			58	yes	yes
21	DOW SRD7-665	68	26.7	10	1670	3.55	3.47	3.14		yes	yes
22	Basell EPS31HP	1.2	28.5	65	1565	61	11.2	5.8	60	yes	no
23	Basell EPC31HR	7	24.8	62	1375	7.75	5	4.4	59	yes	no
24	Sasol 2648M-7750Y	8	21.7	342	1138	48.4			56	yes	no
25	Basell HEXP2000	15	20.3	61	1075	52.1	8.4	6.3	56	yes	no
26	Basell EPF31HR	17	25.2	45	1345	11.1	5.4	4.2	58	yes	yes
27	BP K9020	18	20	265	842	51.9	39.8	5.65	58	no	yes
28	Sasol 2648RC-7779Y	24	19.4	342	1060	11.6			54	yes	yes
29	Basell EPL31UA	73	22.5	24	1120	8.1	5.4	4.3	57	yes	yes
30	Basell HEXP2023	79	23.8	19	1335	4.8	4.7	4.3	59	yes	no

University of Cape Town

Sample No.	Sample Name	MFI	Tensile impact	Drop Weight
		g/10min	kJ/m2	J
1	BP K7506	5.9	44.45	
2	Basell EPC30R	6.5	44.40	14.723
3	Sasol 2349MC-7697Y	8	46.88	
4	BP K8512	12	36.77	
5	Basell HEXP280	20	29.49	8.451
6	Borealis BH345MO	44	24.07	
7	BP B8101	0.4	117.26	
8	DOW SRC7-467	0.7	62.77	
9	Basell EPD60R	0.8	108.94	17.421
10	Sasol 2502G-7795Y	1		
11	BP K7002	1.2	56.47	
12	Basell EPQ30RF	1.5	77.65	
13	DOW 7C50H	7	46.54	
14	BP K7312	14	38.77	
15	Basell EPV31RA	28	36.18	14.531
16	BP K9935	34	47.30	13.963
17	DOW SRCD7-664	34	21.83	13.887
18	Basell EPH71HA	46	34.46	13.829
19	BP K8550	49	29.39	13.729
20	Sasol 2448TC-7759Y	50	35.91	12.417
21	DOW SRD7-665	68	20.47	6.226
22	Basell EPS31HP	1.2	69.95	15.62
23	Basell EPC31HR	7	46.81	
24	Sasol 2648M-7750Y	8	98.66	14.1
25	Basell HEXP2000	15	53.96	13.969
26	Basell EPF31HR	17	46.27	14.605
27	BP K9020	18	75.87	12.836
28	Sasol 2648RC-7779Y	24	52.68	13.047
29	Basell EPL31UA	73	34.61	12.293
30	Basell HEXP2023	79	29.21	13.983

University of Cape Town

APPENDIX B: DSC CURVES

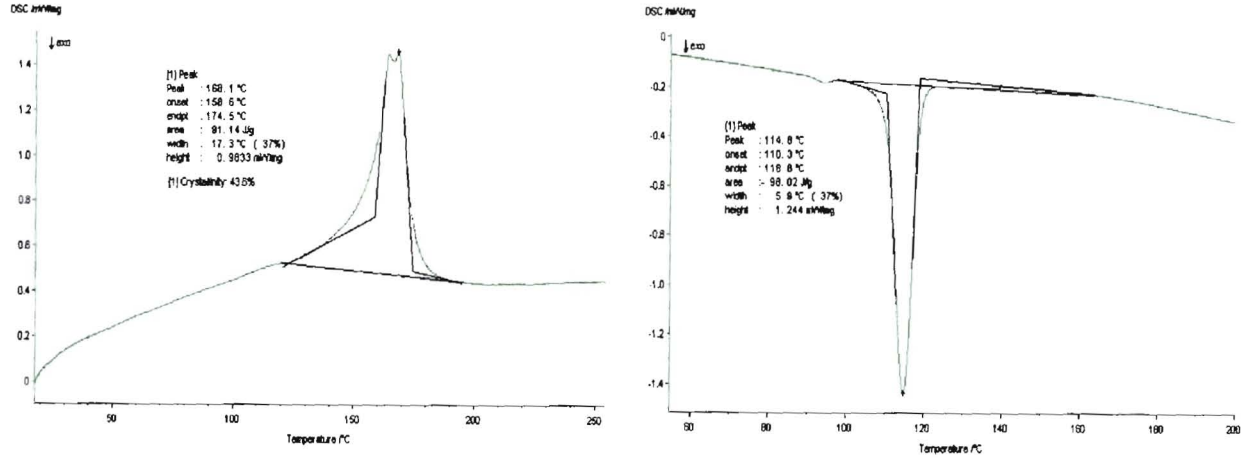

sample #1

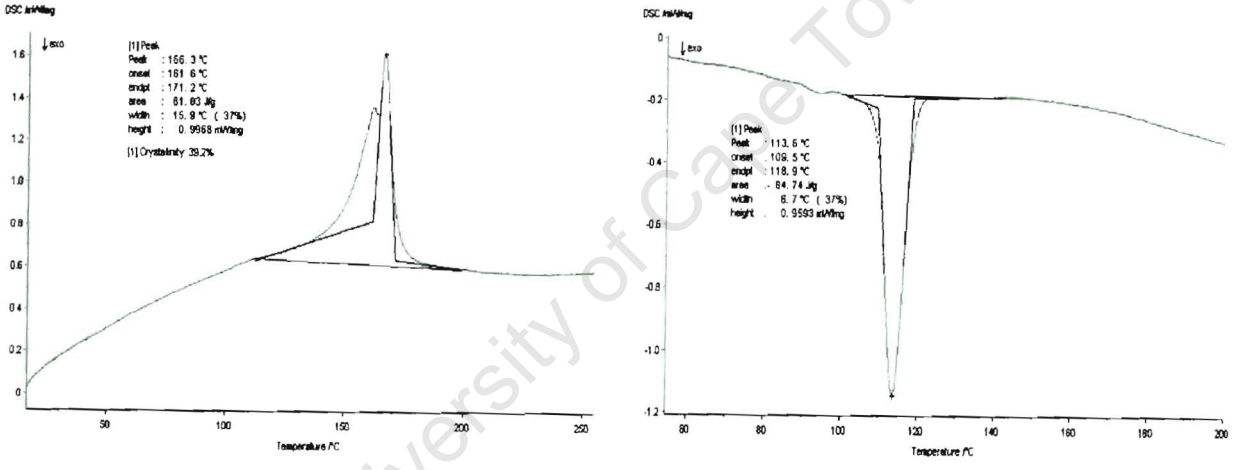

sample #2

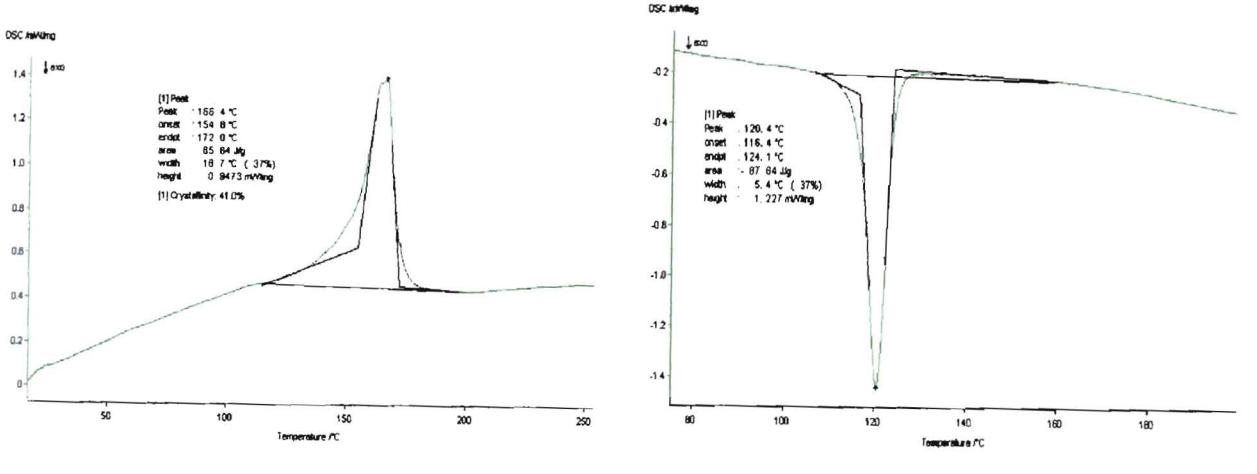

sample #3

University of Cape Town

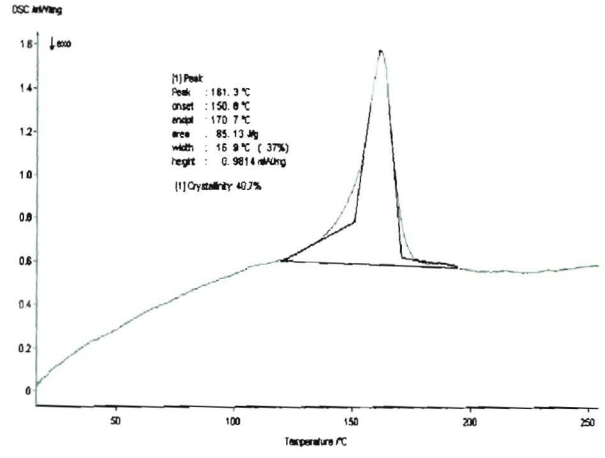

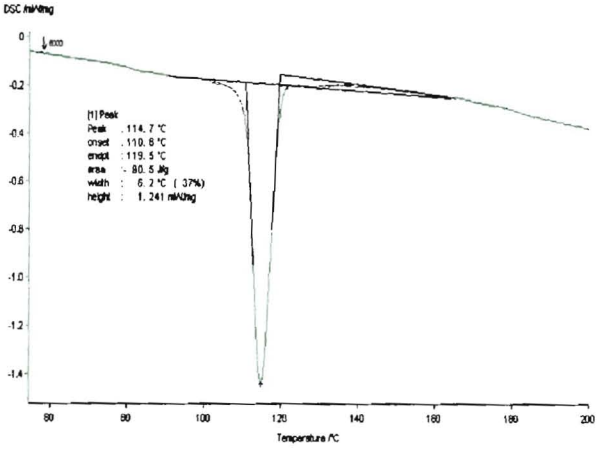

sample #4

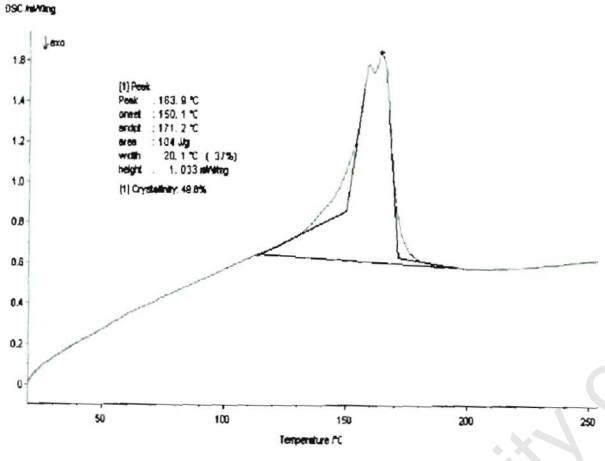

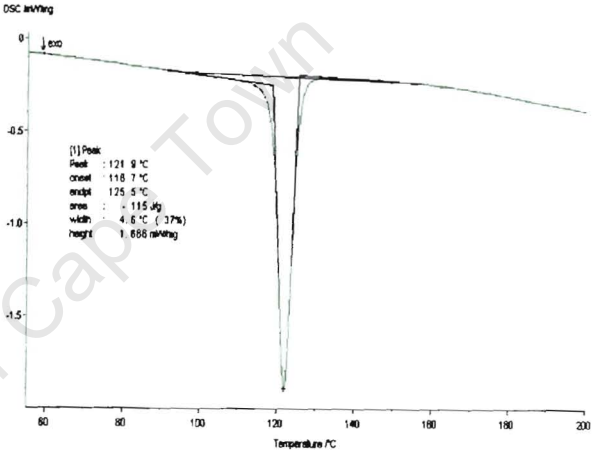

sample #5

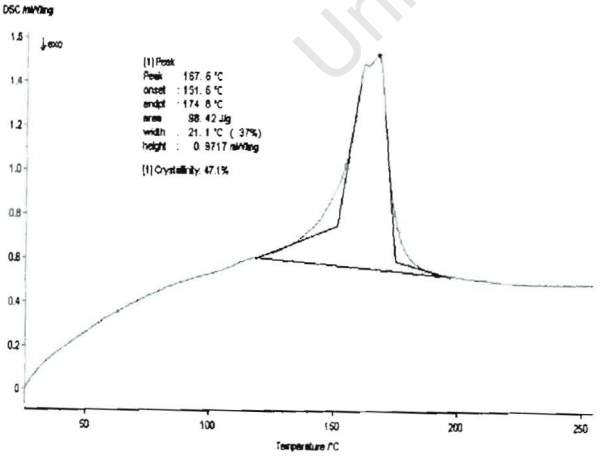

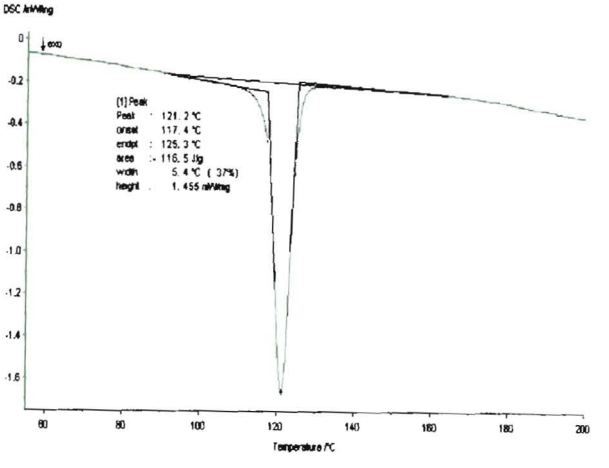

sample #6

University of Cape Town

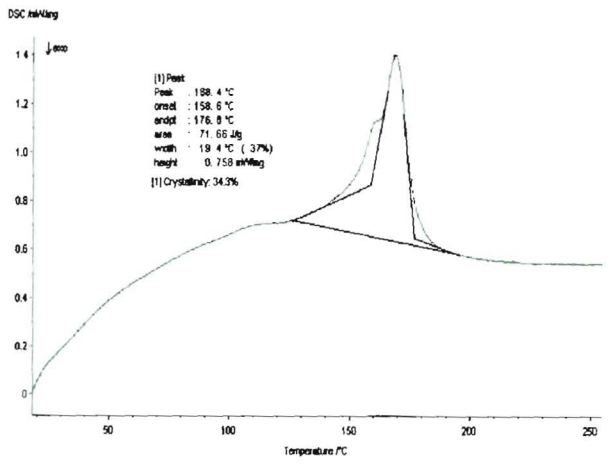

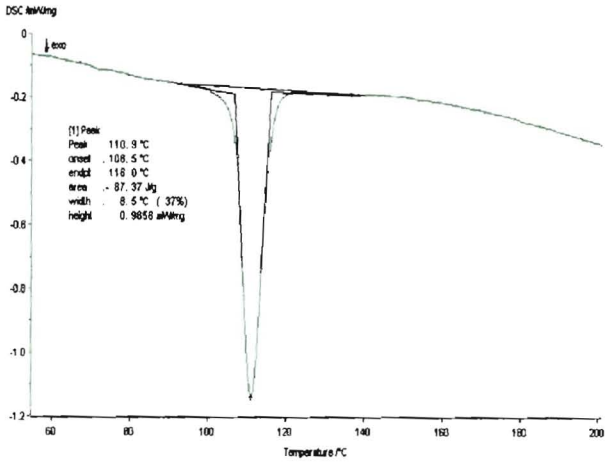

sample #7

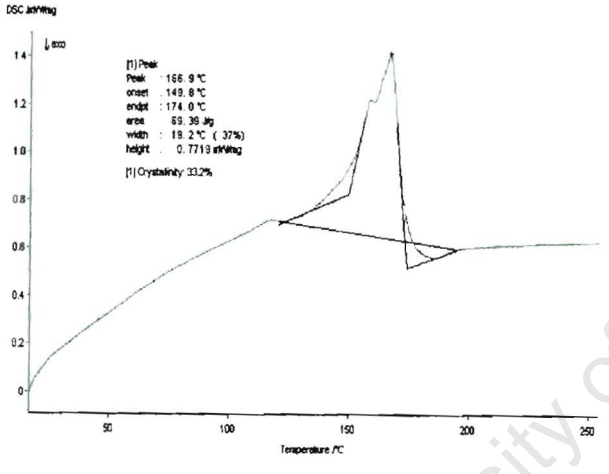

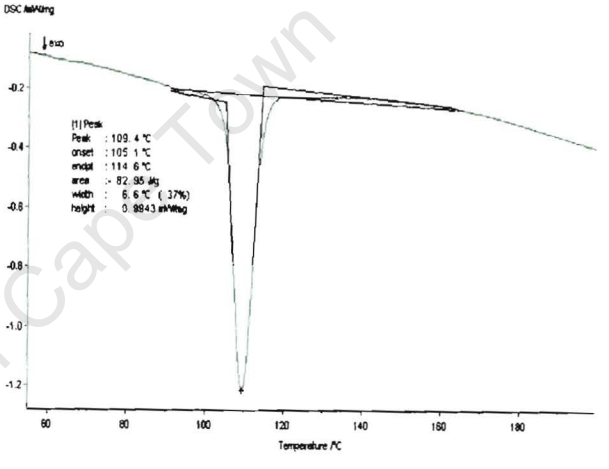

sample #8

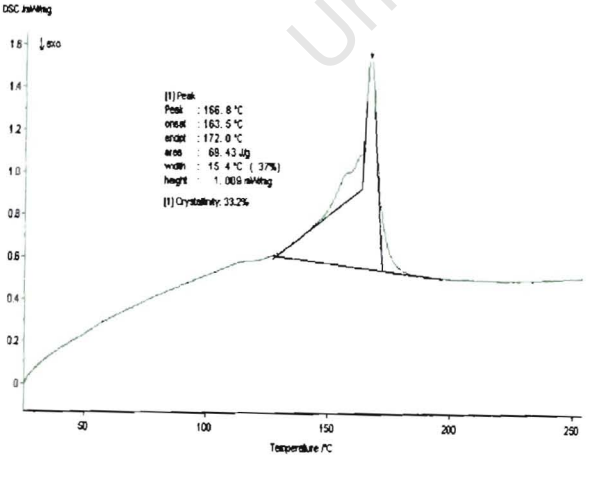

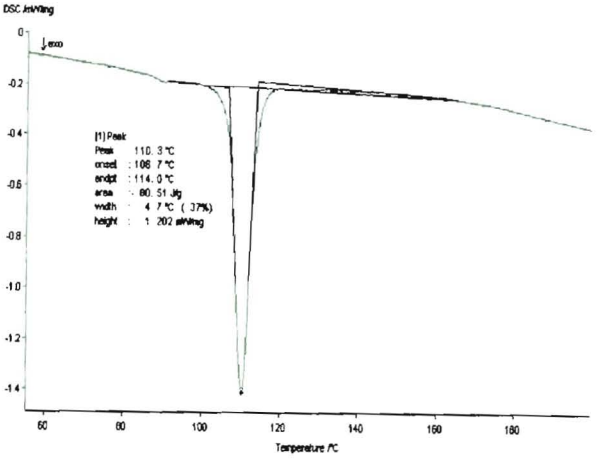

sample #9

University of Cape Town

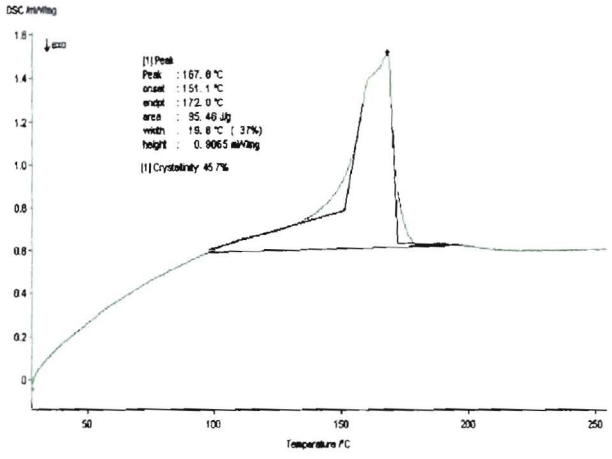

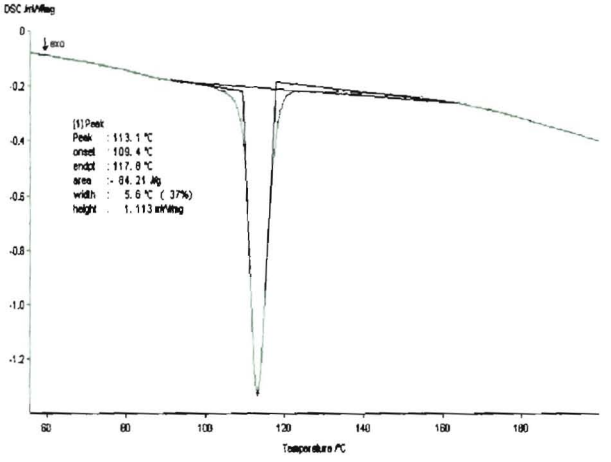

sample #10

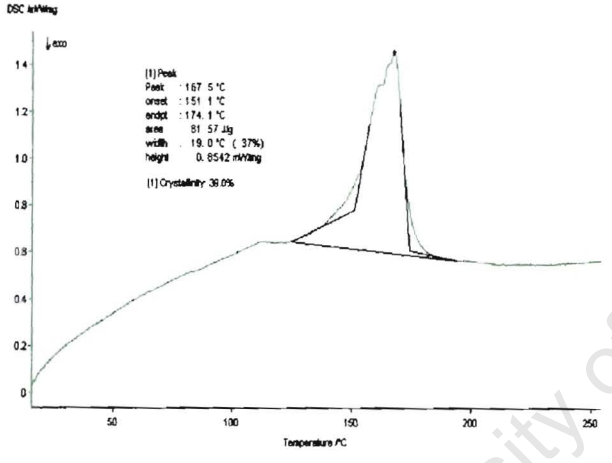

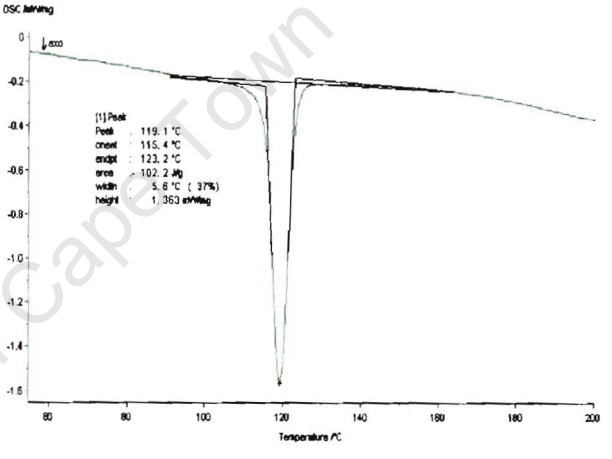

sample #11

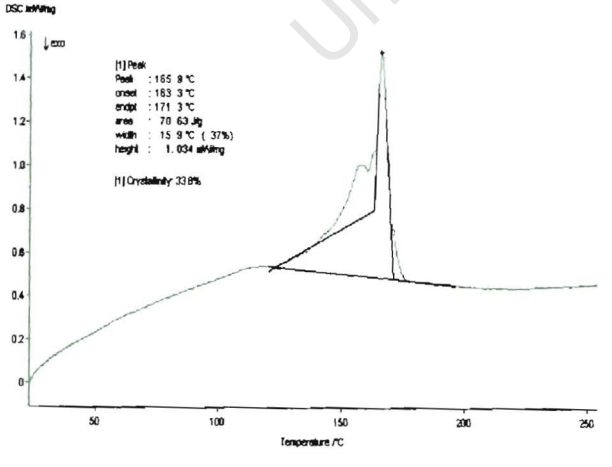

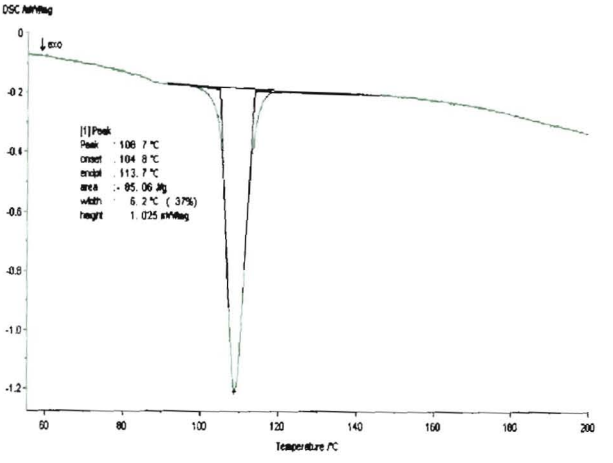

sample #12

University of Cape Town

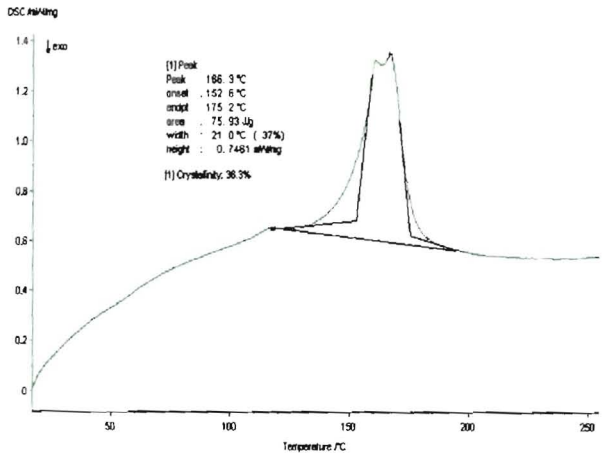

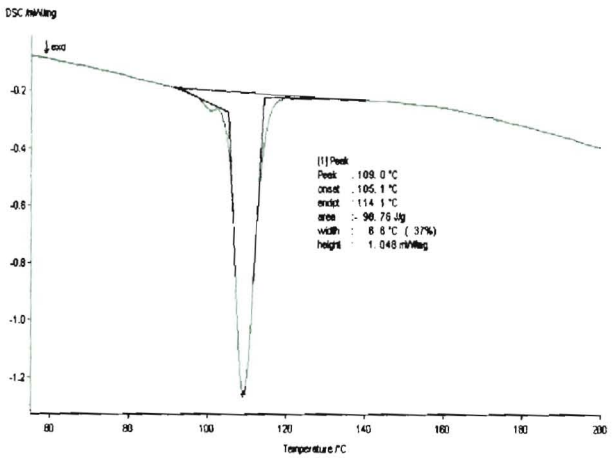

sample #13

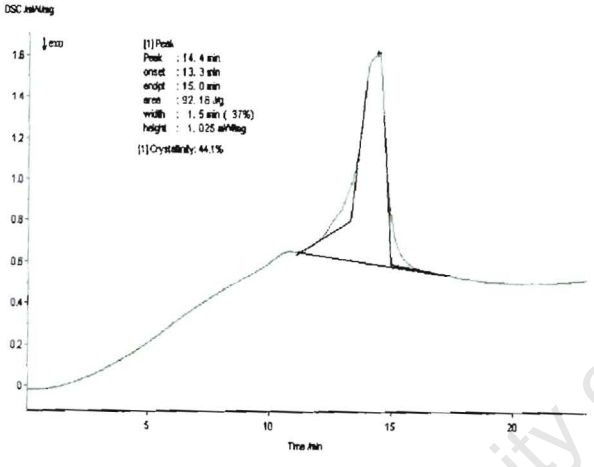

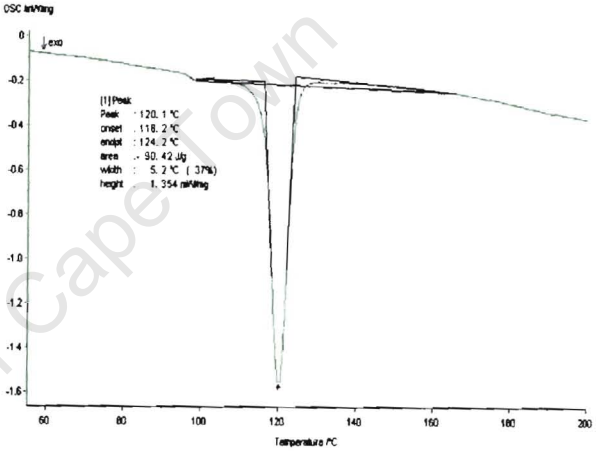

sample #14

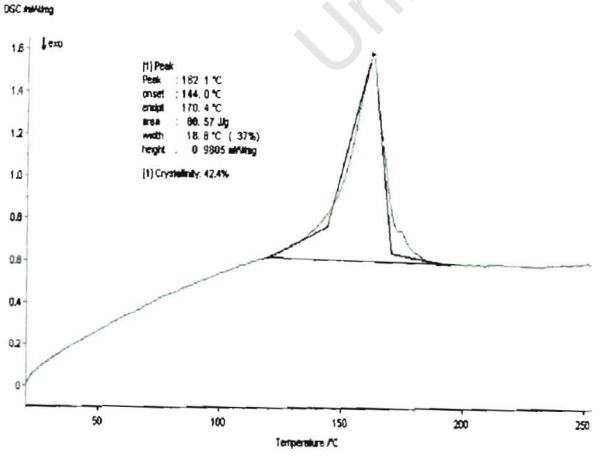

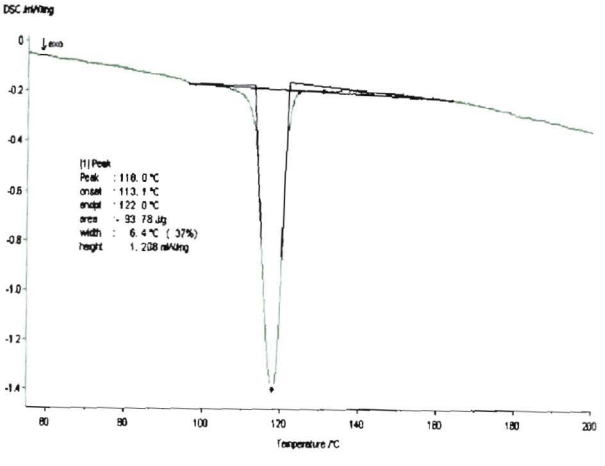

sample #15

University of Cape Town

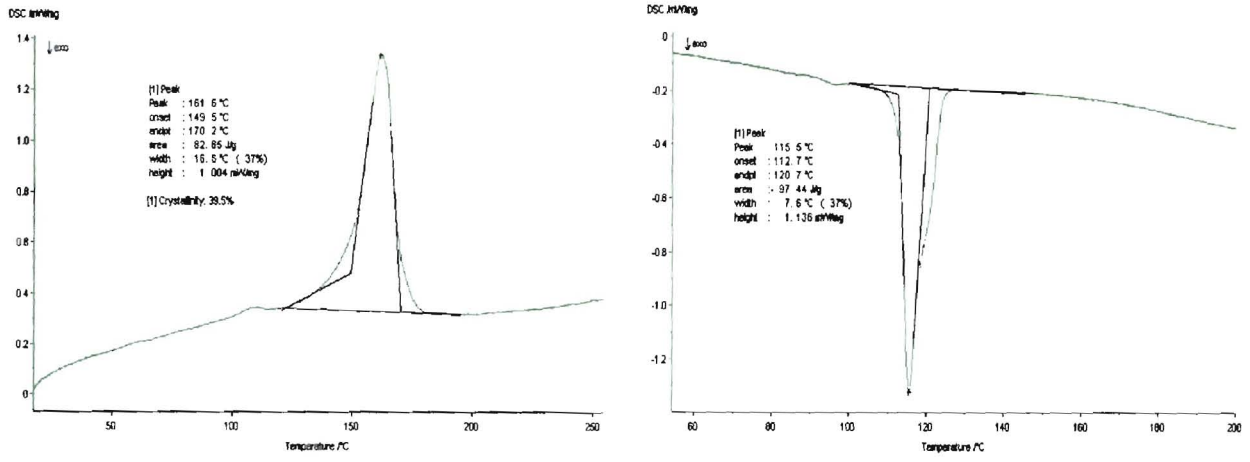

sample #16

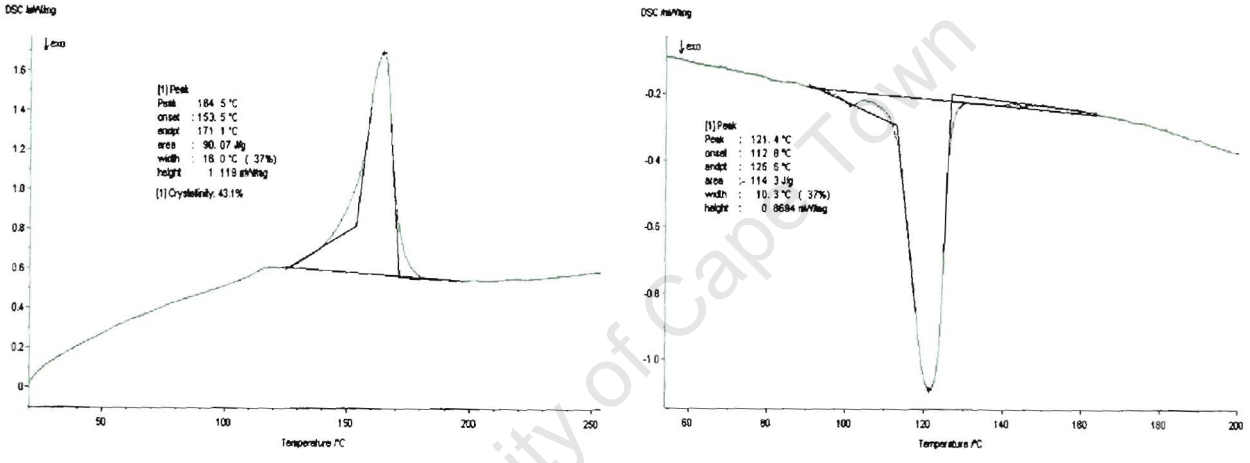

sample #17

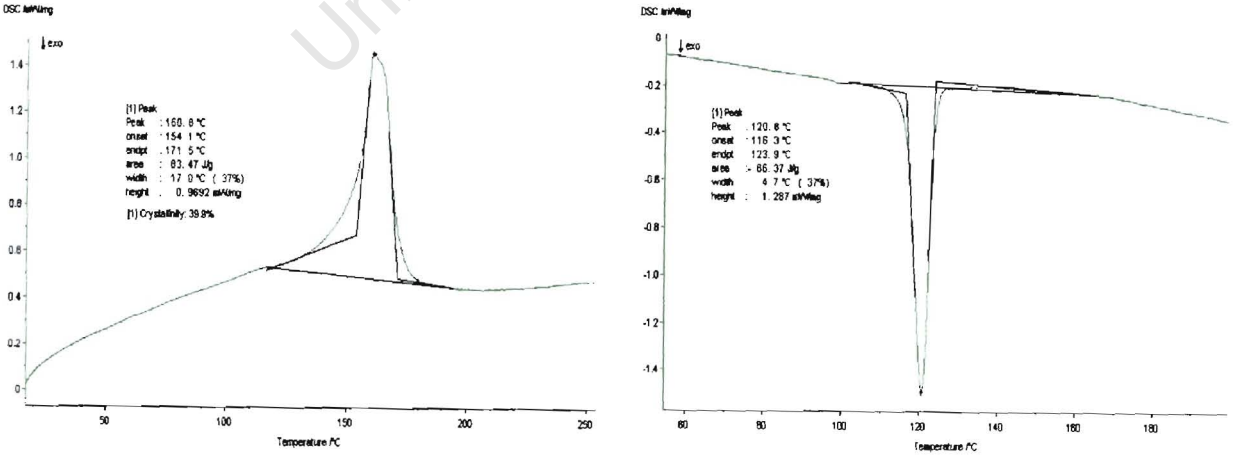

sample #18

University of Cape Town

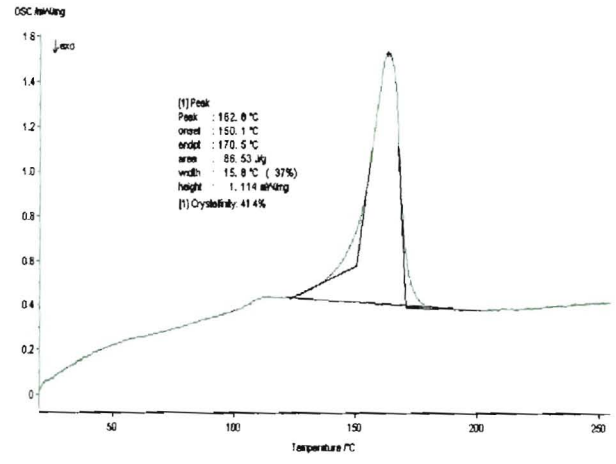

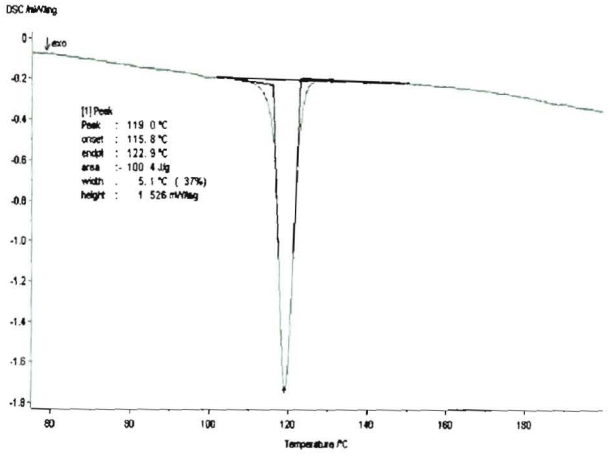

sample #19

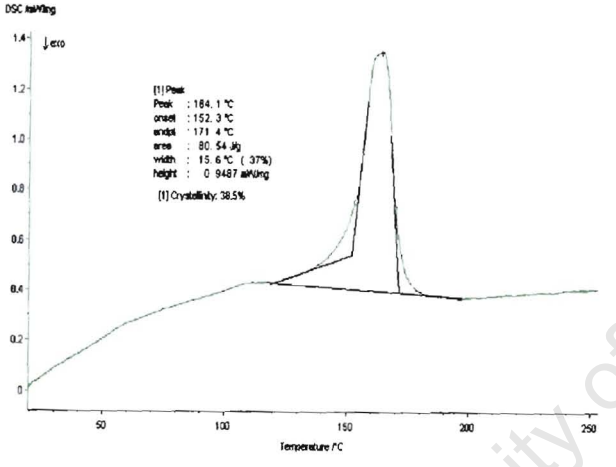

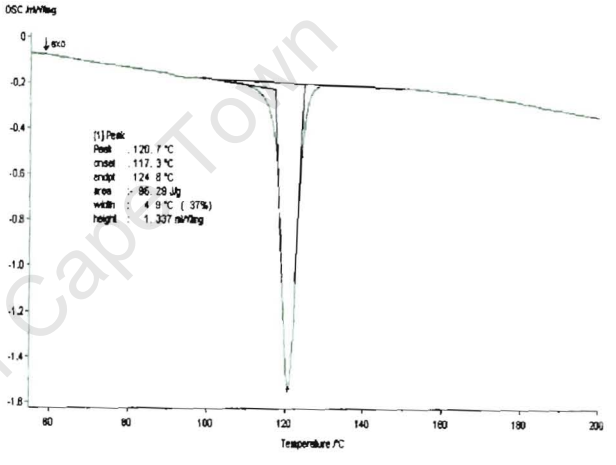

sample #20

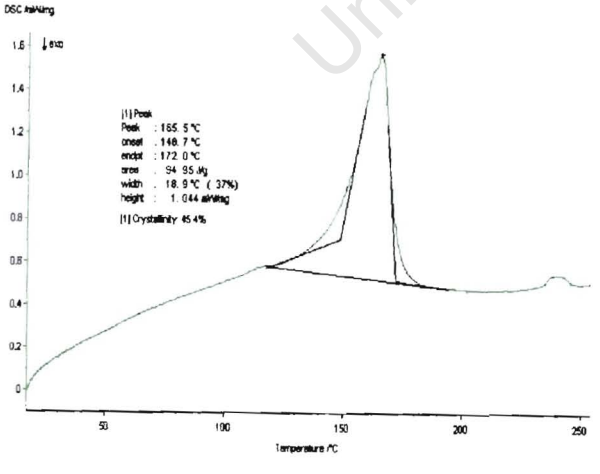

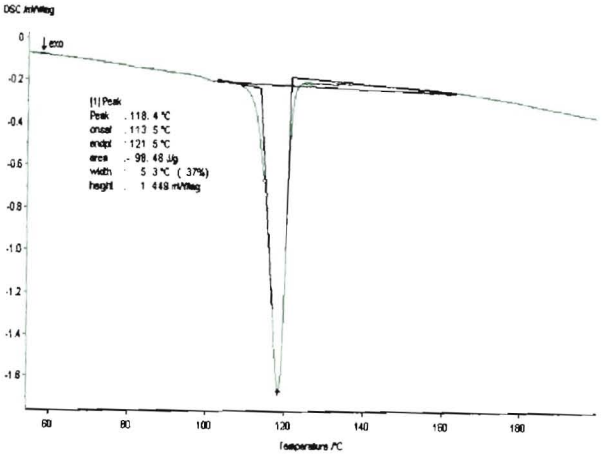

sample #21

University of Cape Town

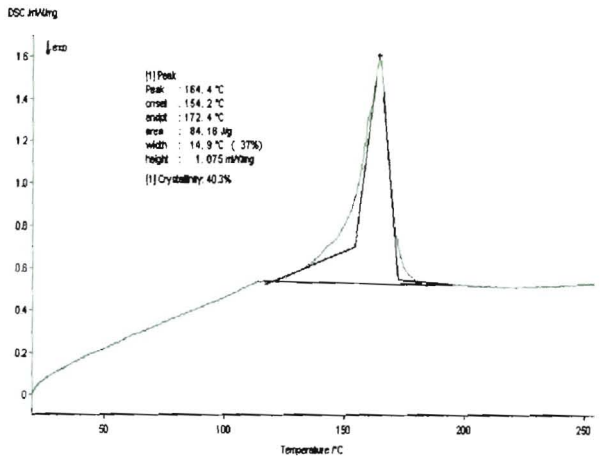

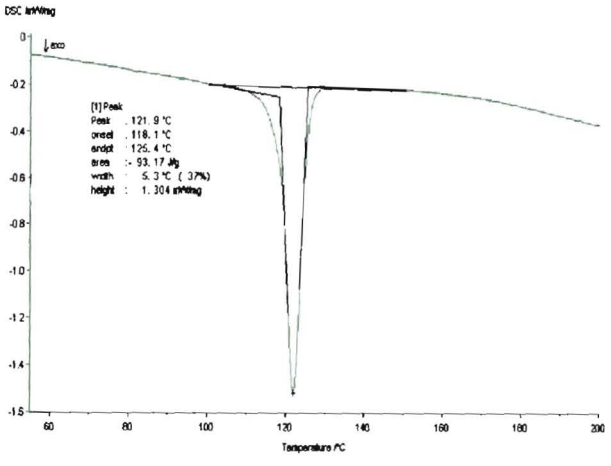

sample #22

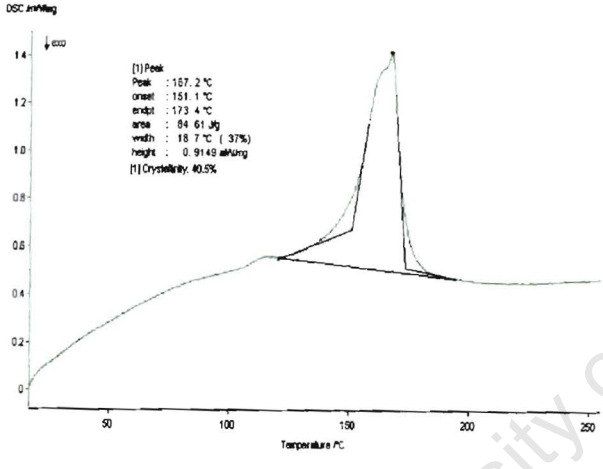

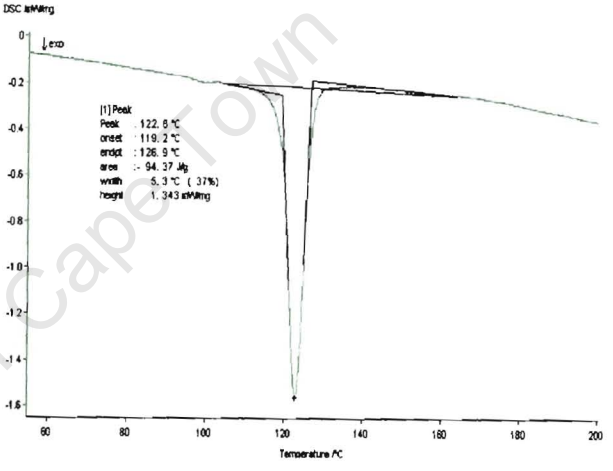

sample #23

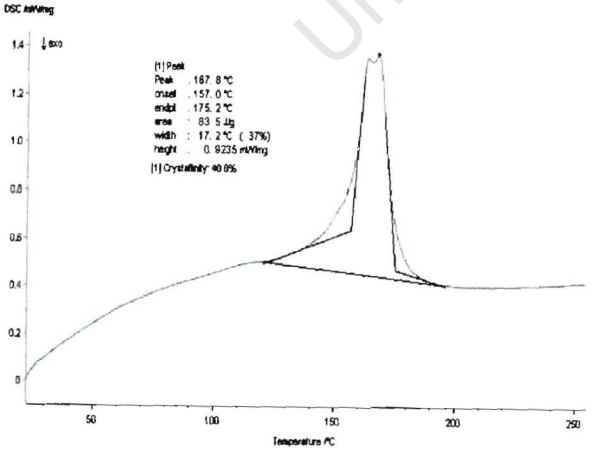

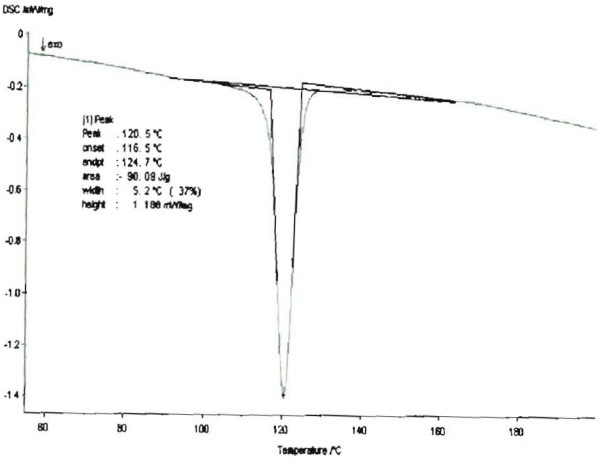

sample #24

University of Cape Town

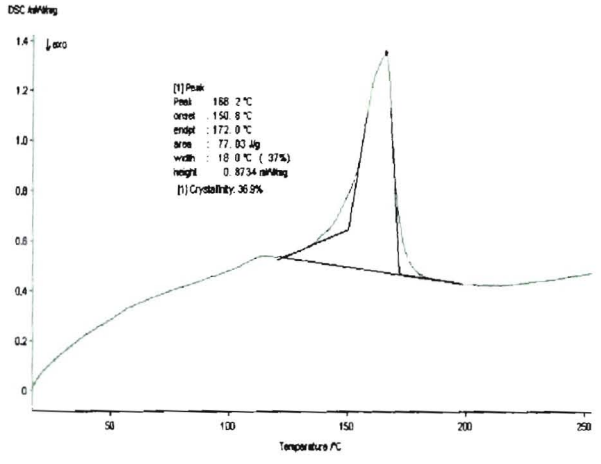

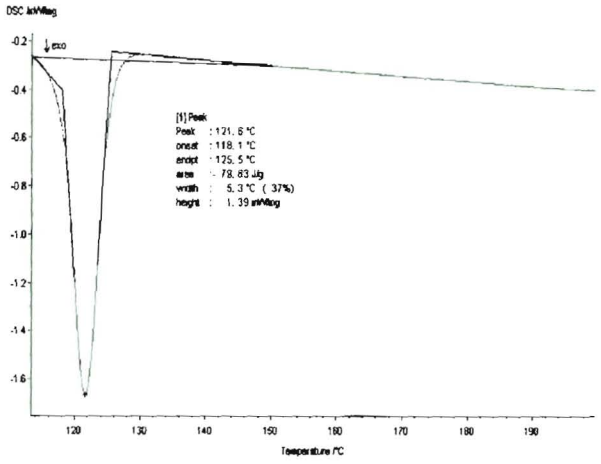

sample #25

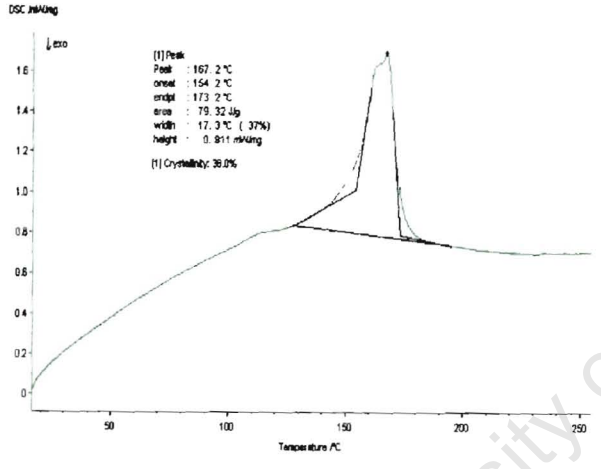

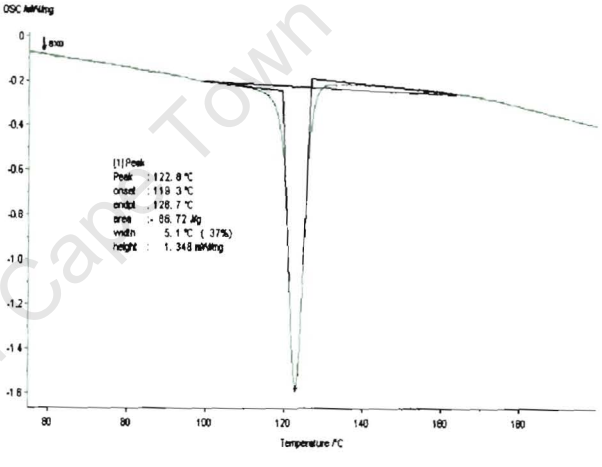

sample #26

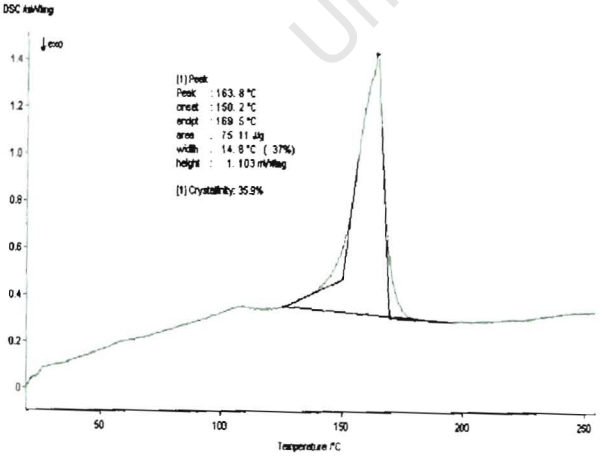

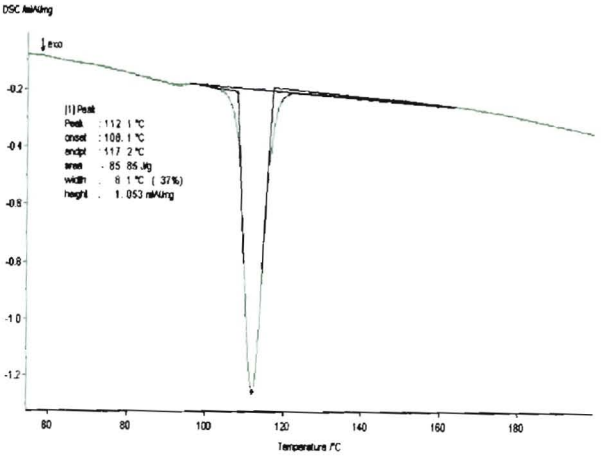

sample #27

University of Cape Town

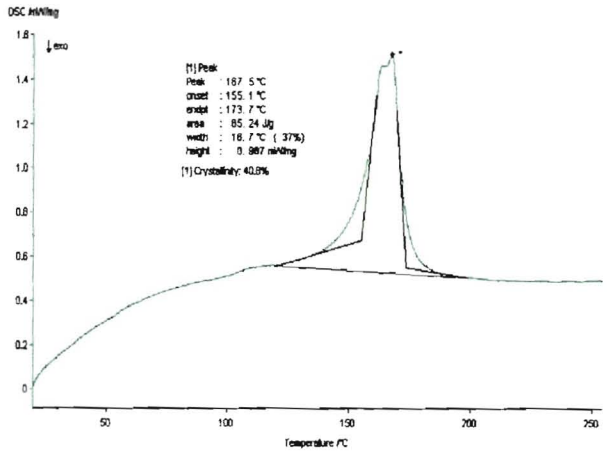

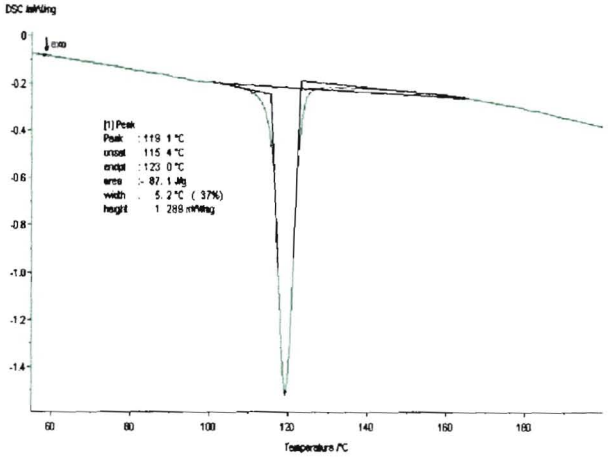

sample #28

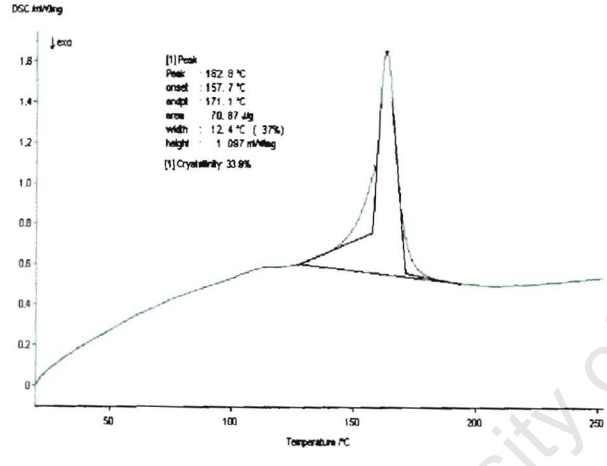

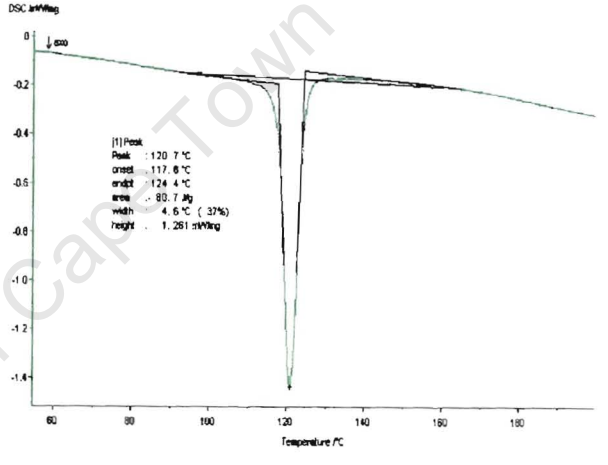

sample #29

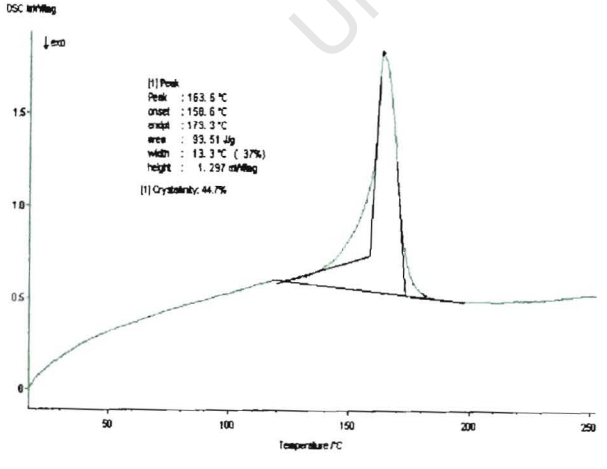

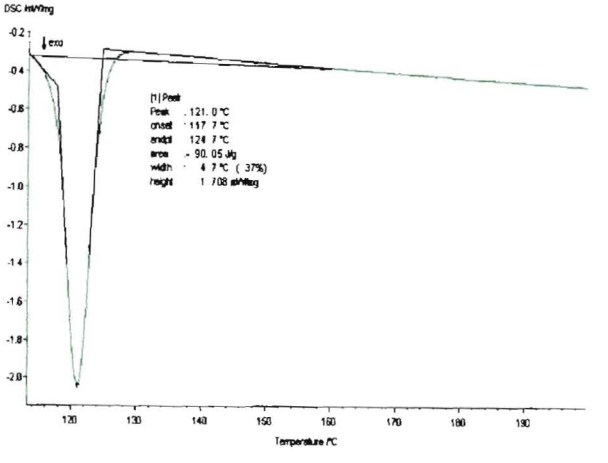

sample #30

University of Cape Town

APPENDIX C: DMA CURVES

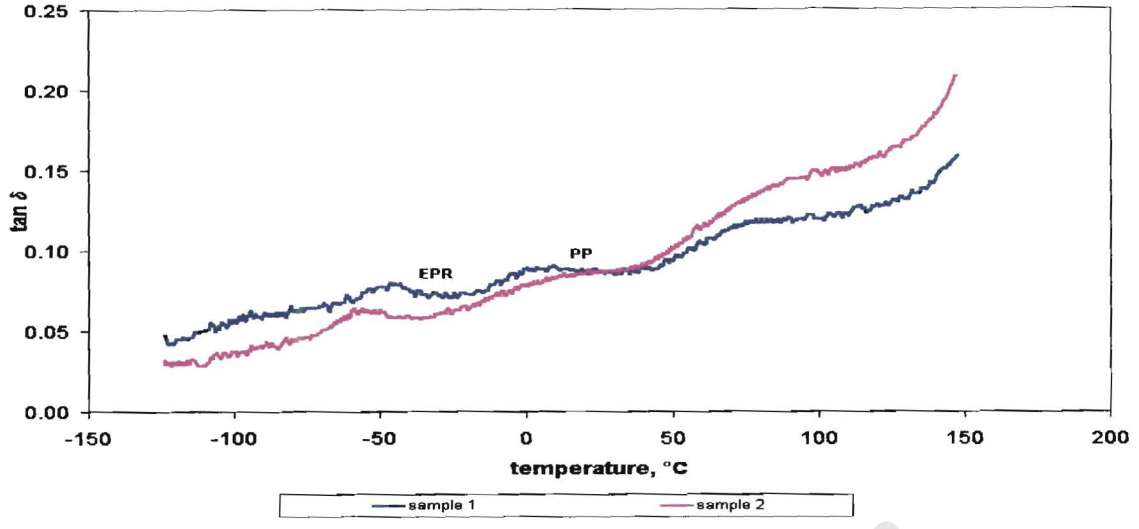

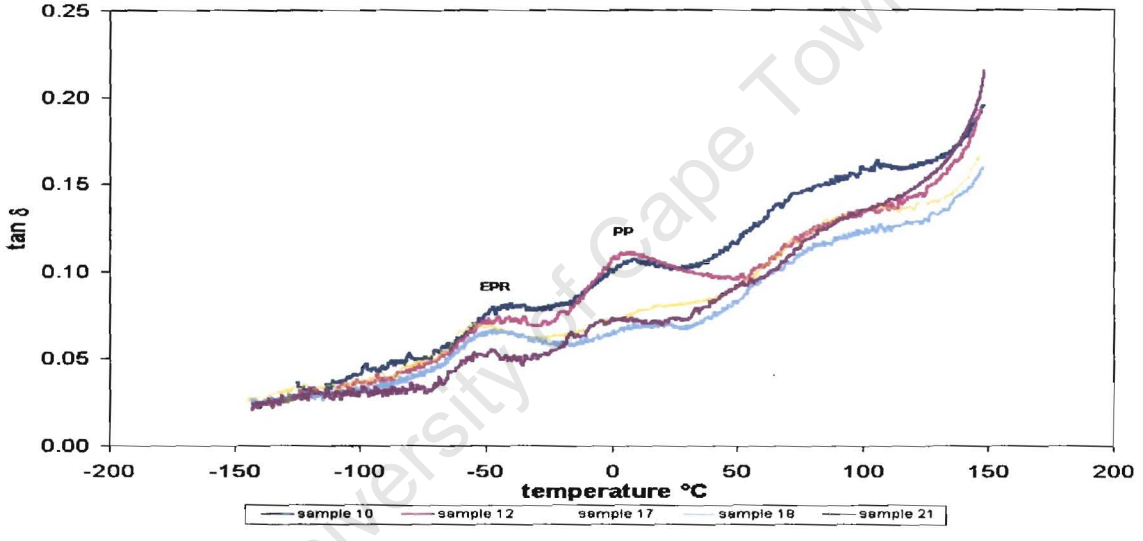

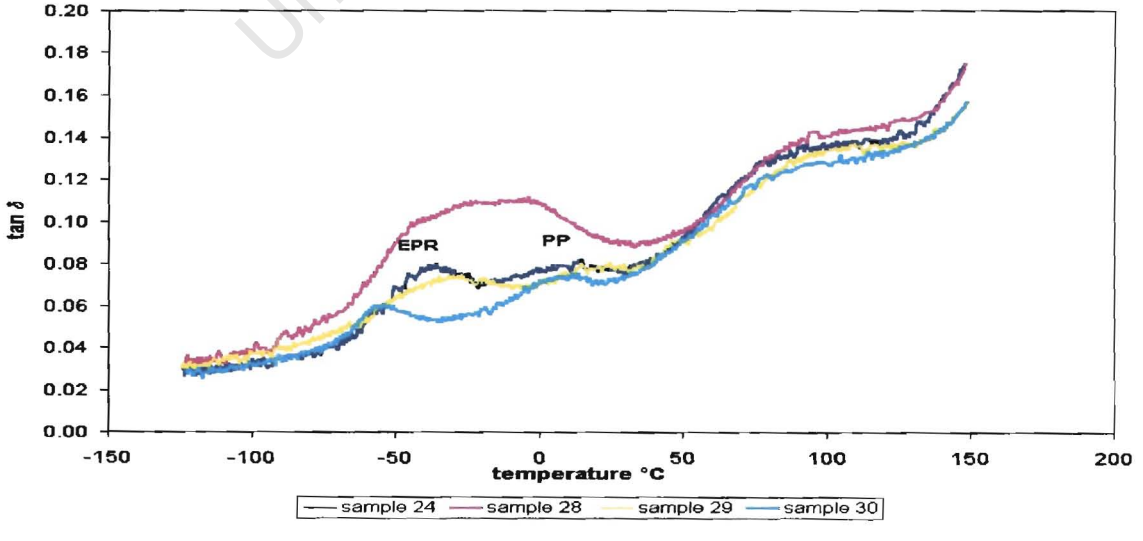

University of Cape Town

APPENDIX D: WAXS CURVES

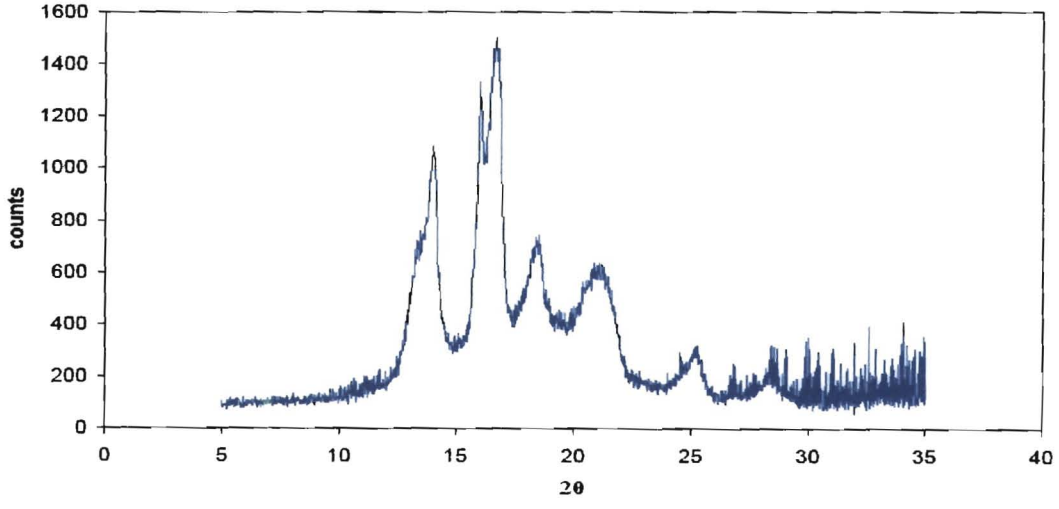

sample #1

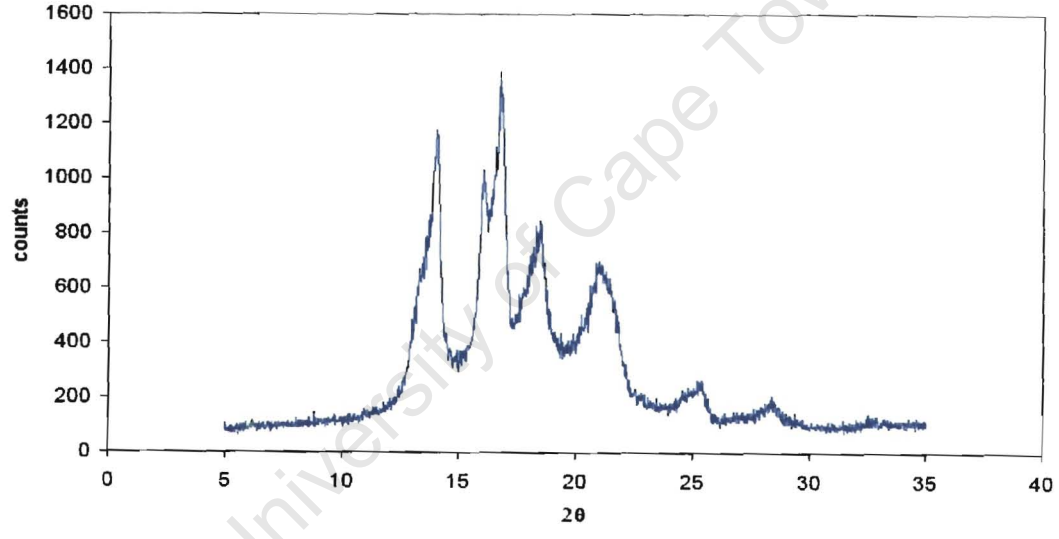

sample #2

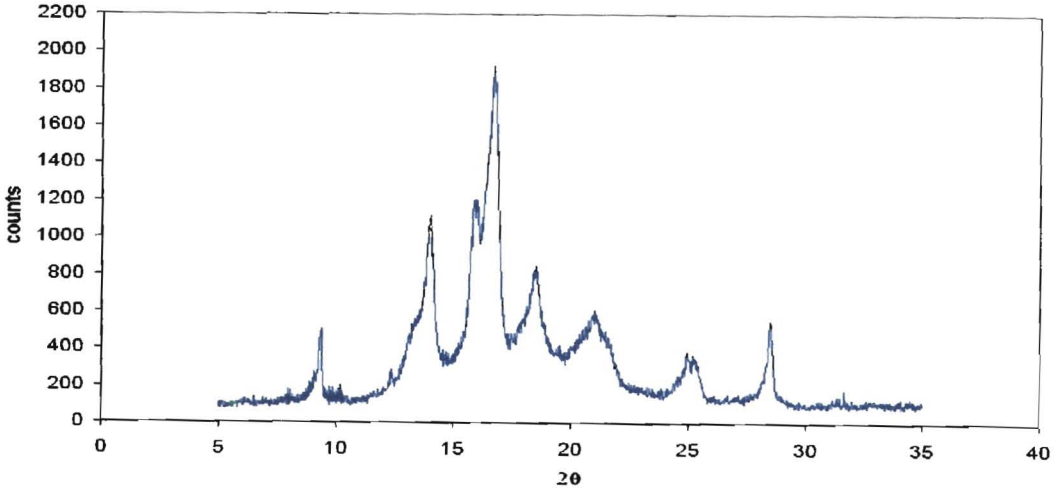

sample #3

University of Cape Town

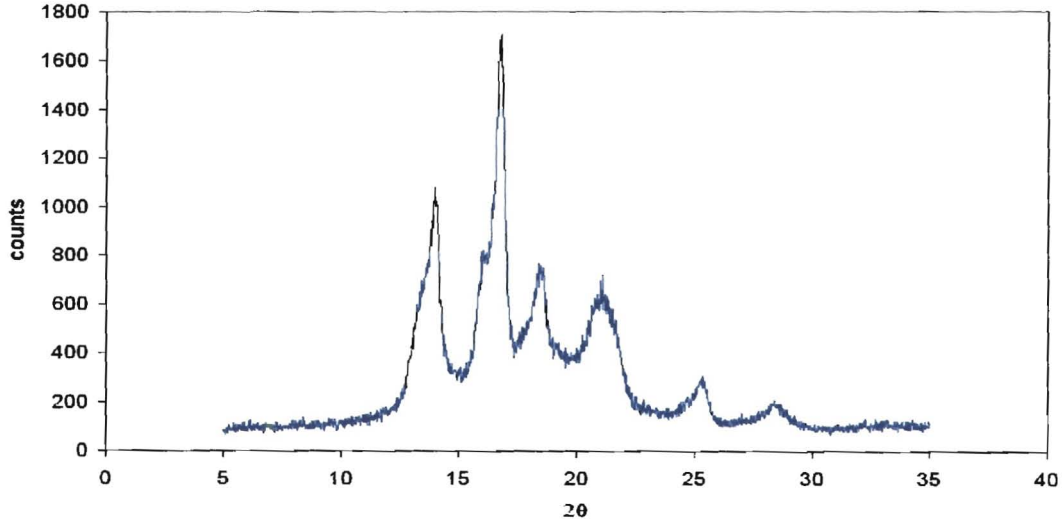

sample #4

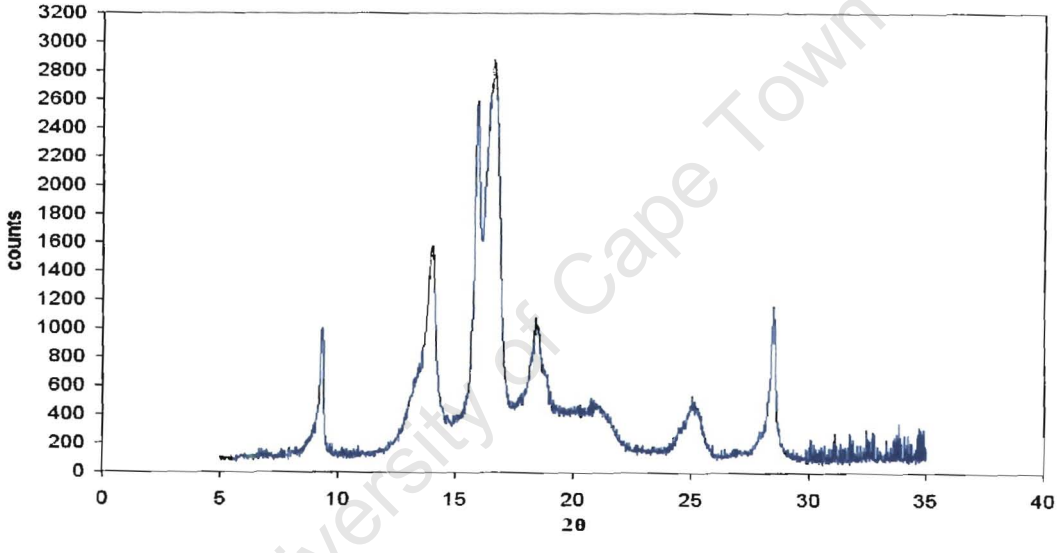

sample #5

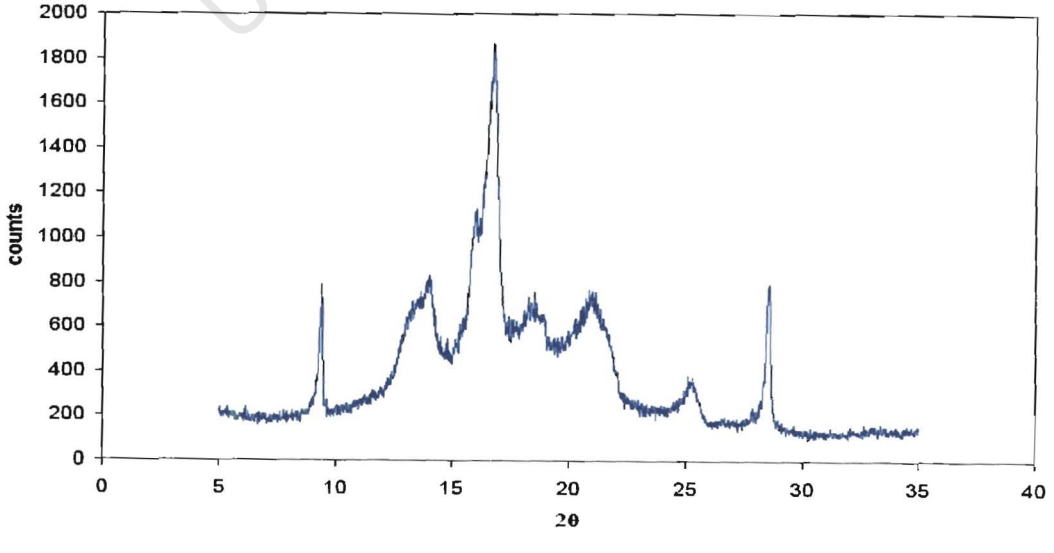

sample #6

University of Cape Town

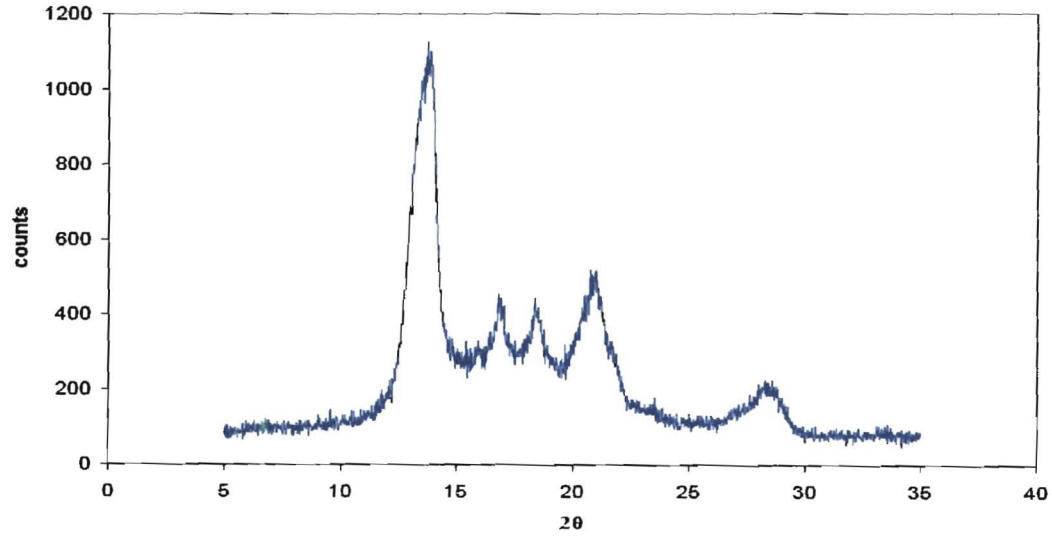

sample #8

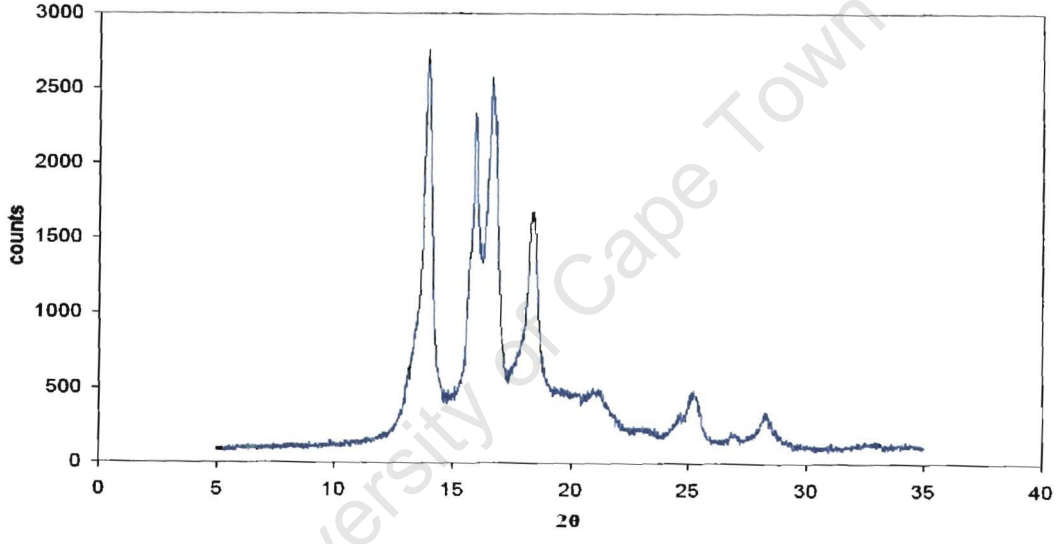

sample #9

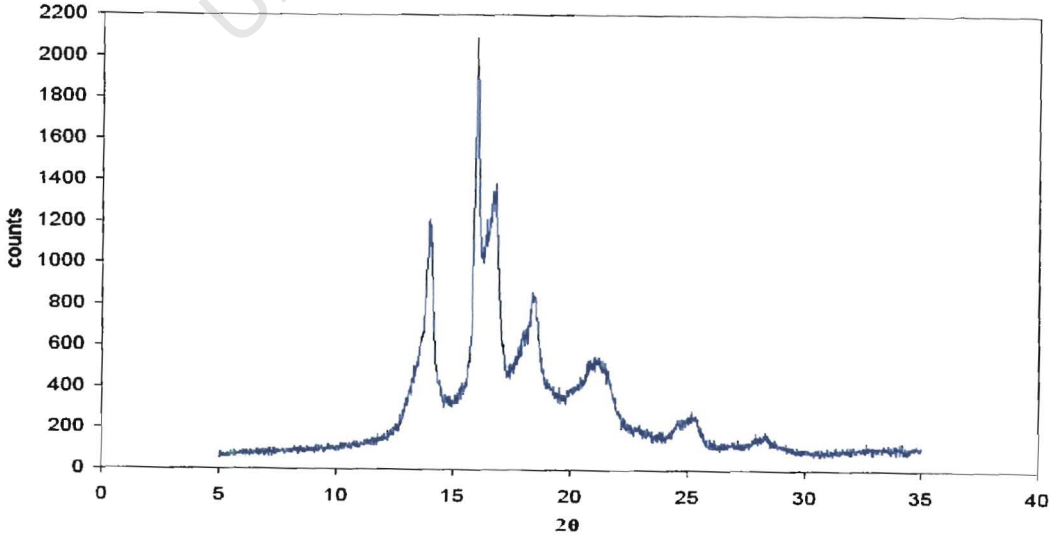

sample #10

University of Cape Town

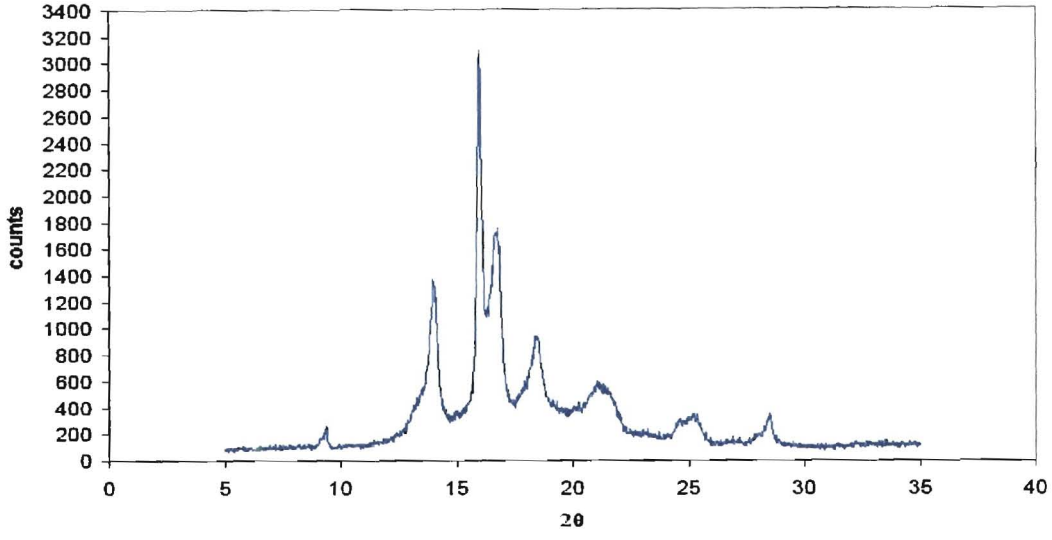

sample #11

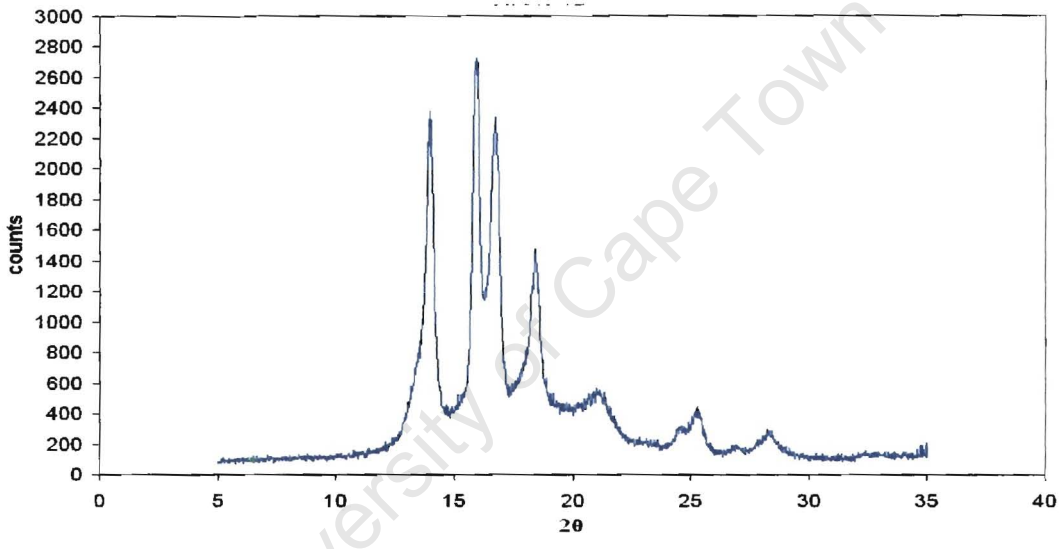

sample #12

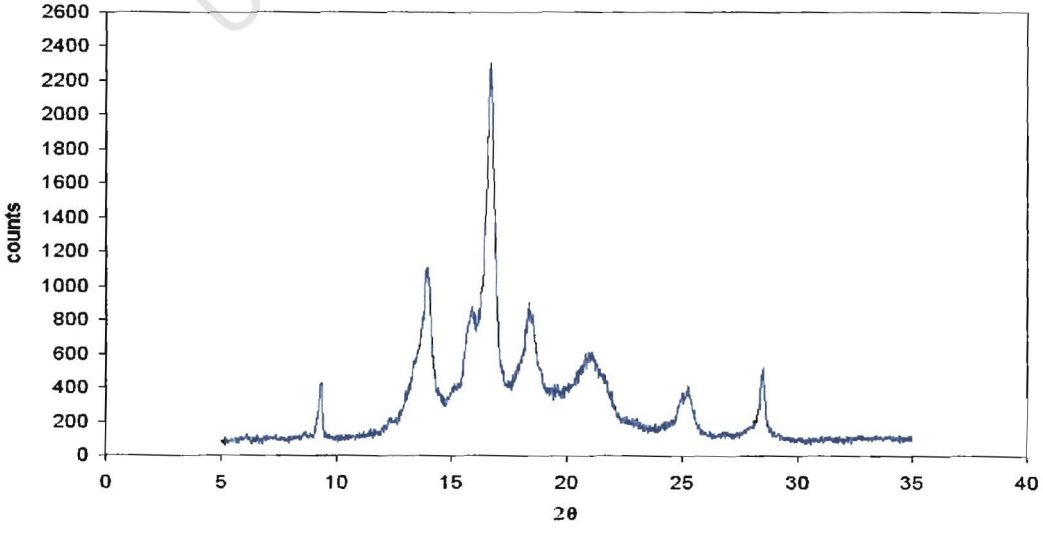

sample #14

University of Cape Town

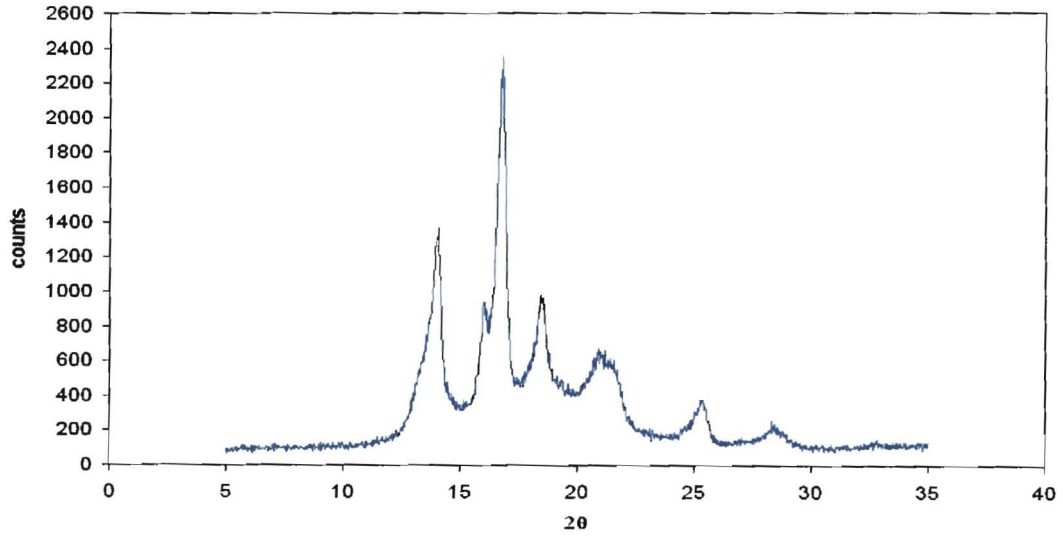

sample #15

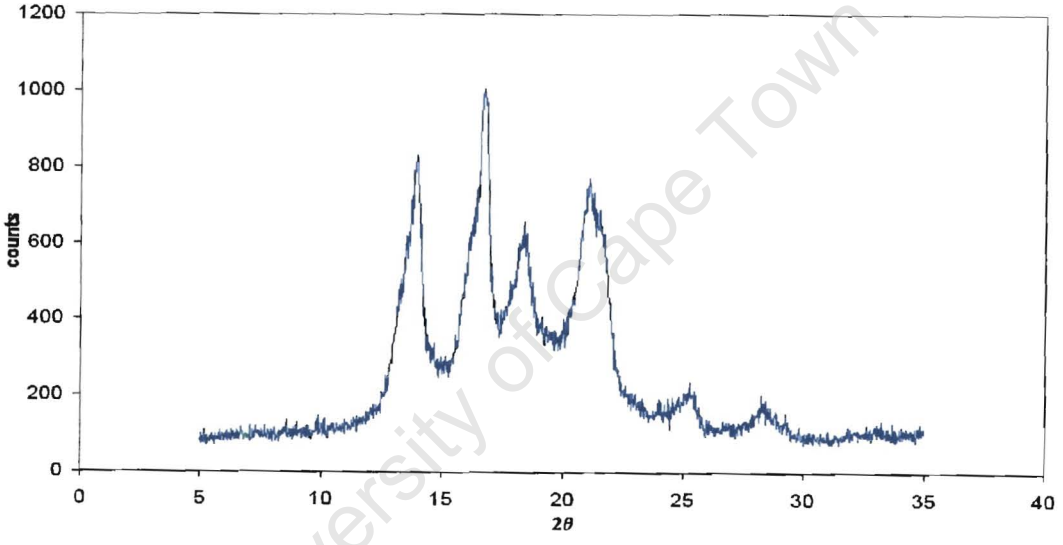

sample #16

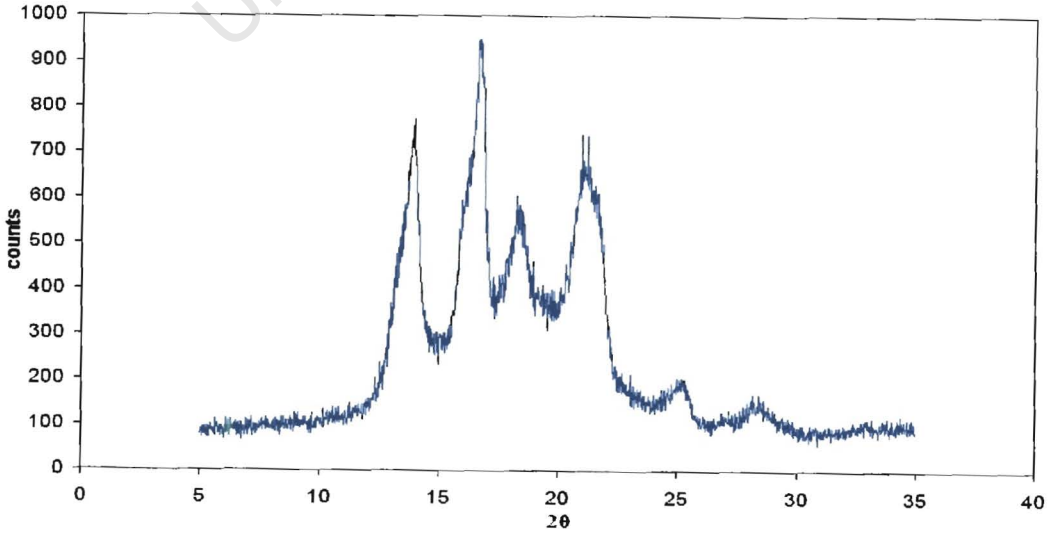

sample #17

University of Cape Town

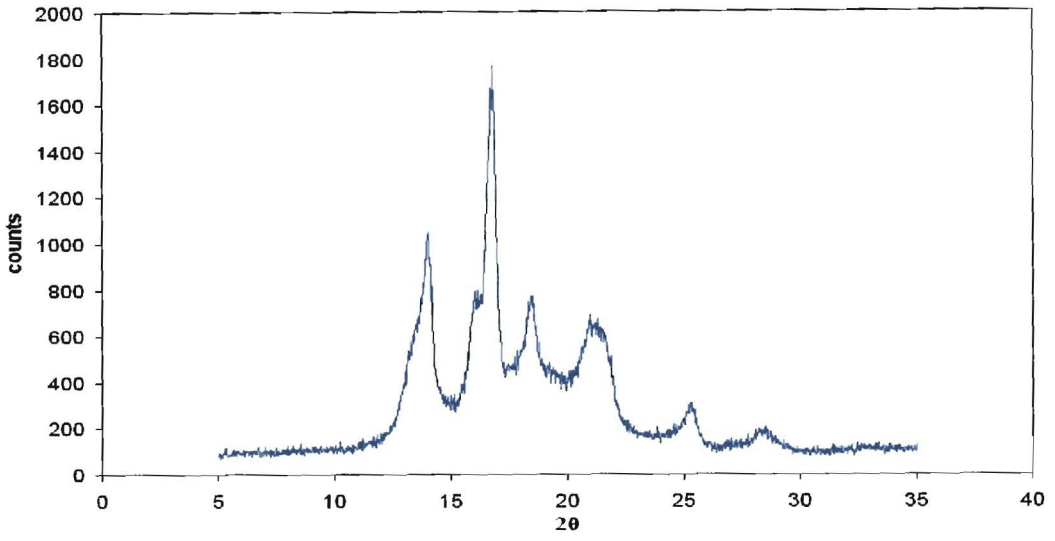

sample #18

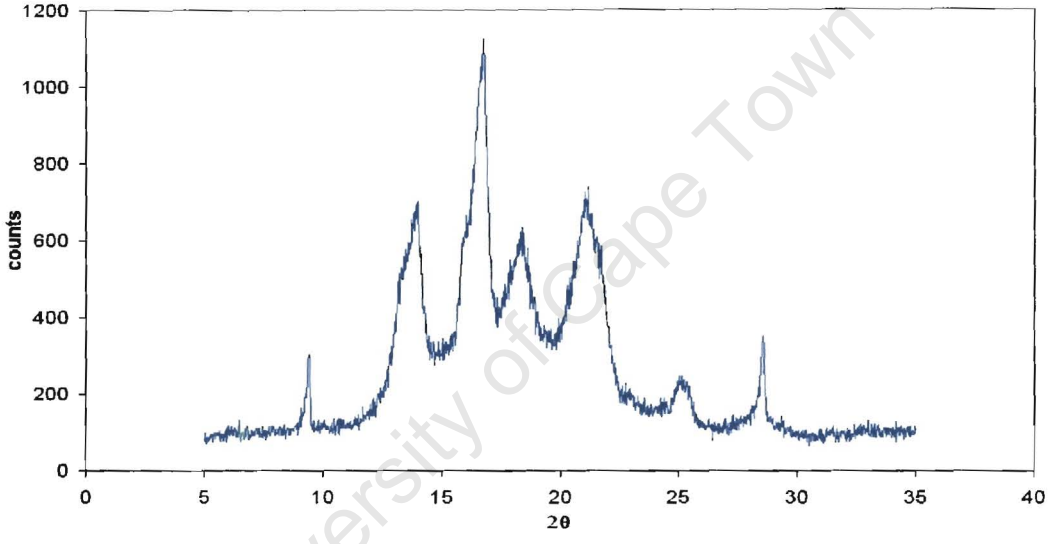

sample #19

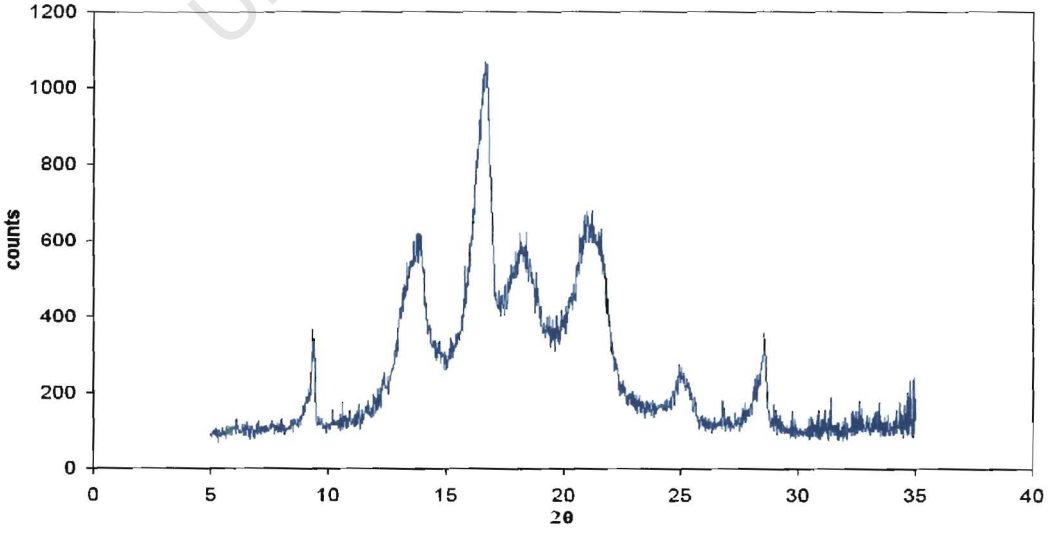

sample #20

University of Cape Town

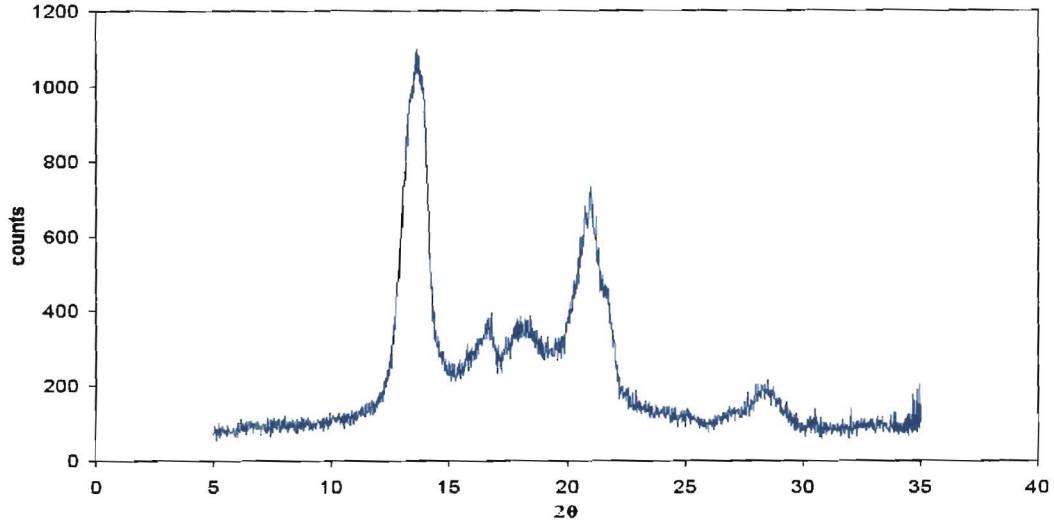

sample #21

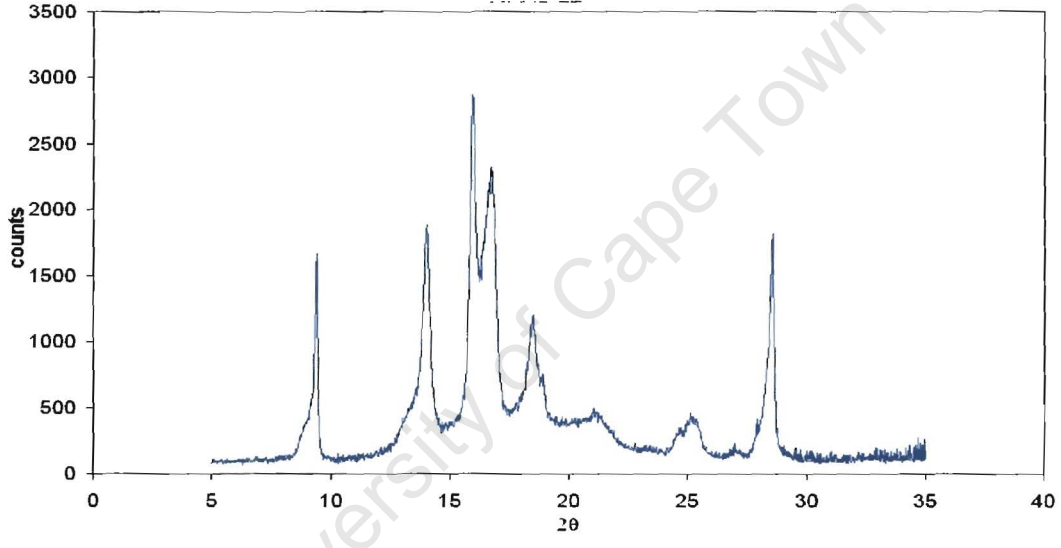

sample #22

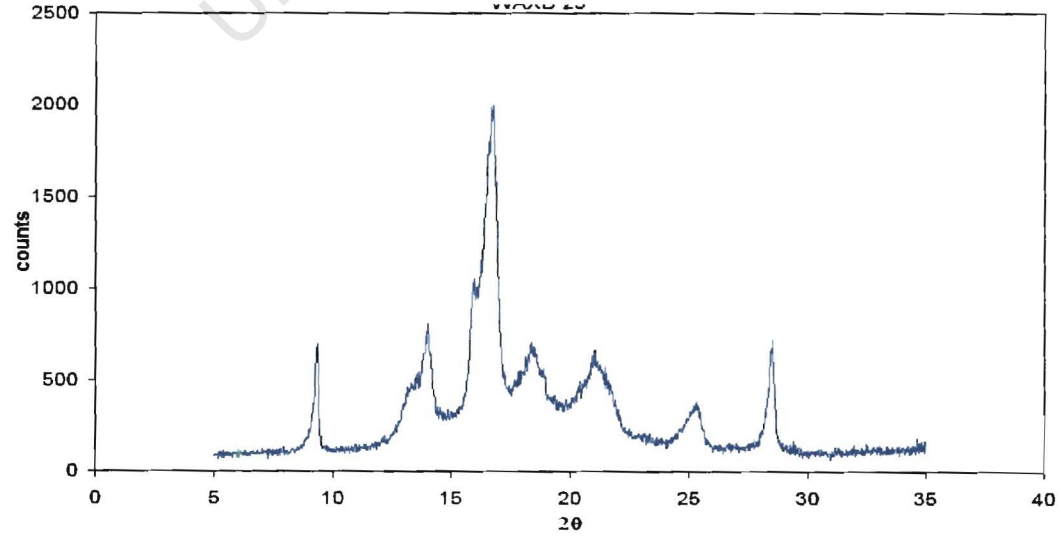

sample #23

University of Cape Town

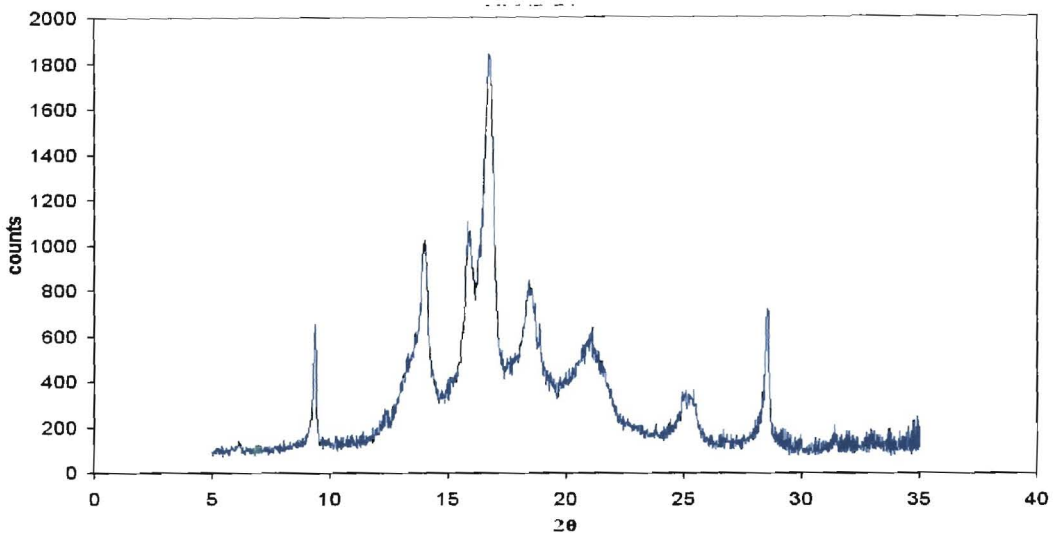

sample #24

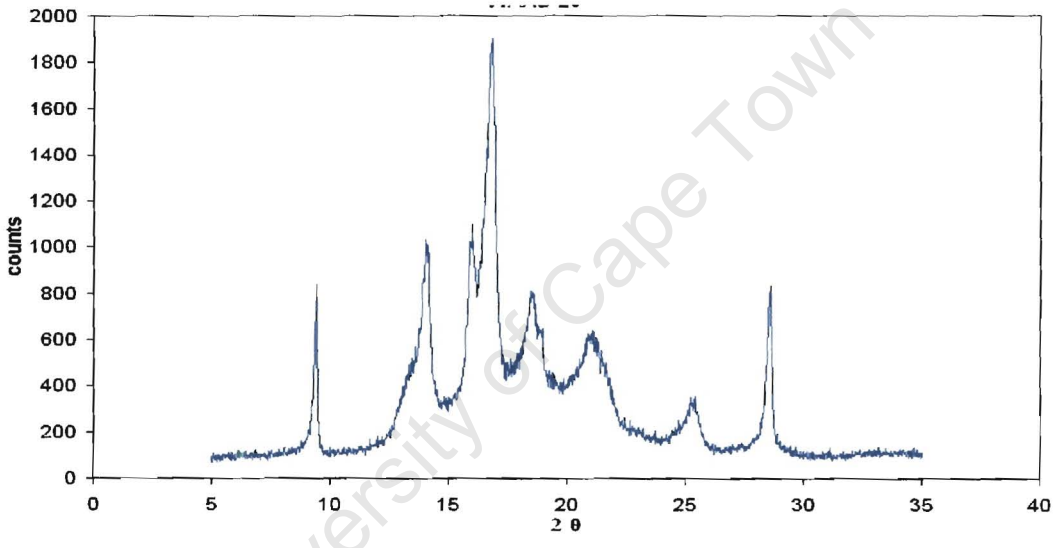

sample #25

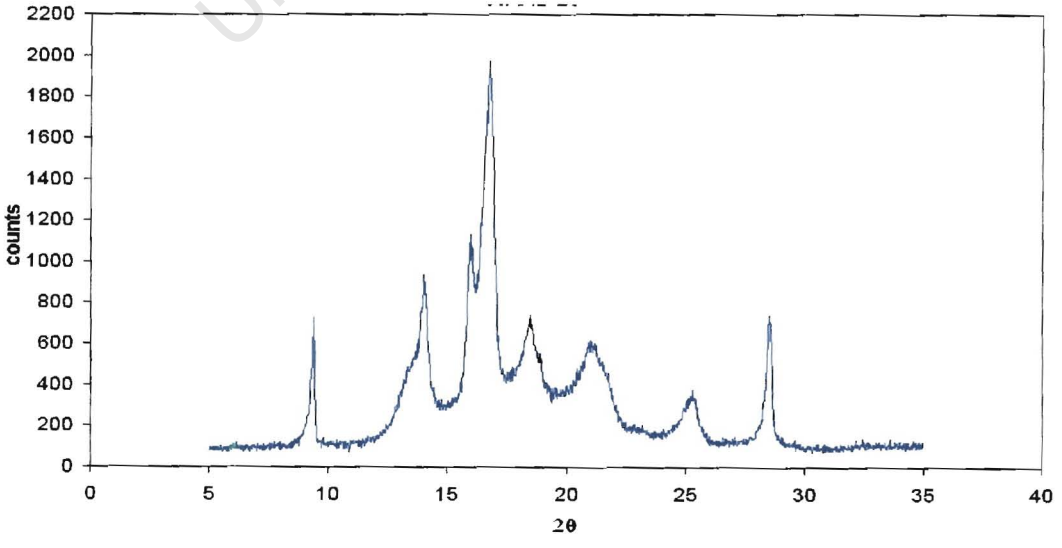

sample #26

University of Cape Town

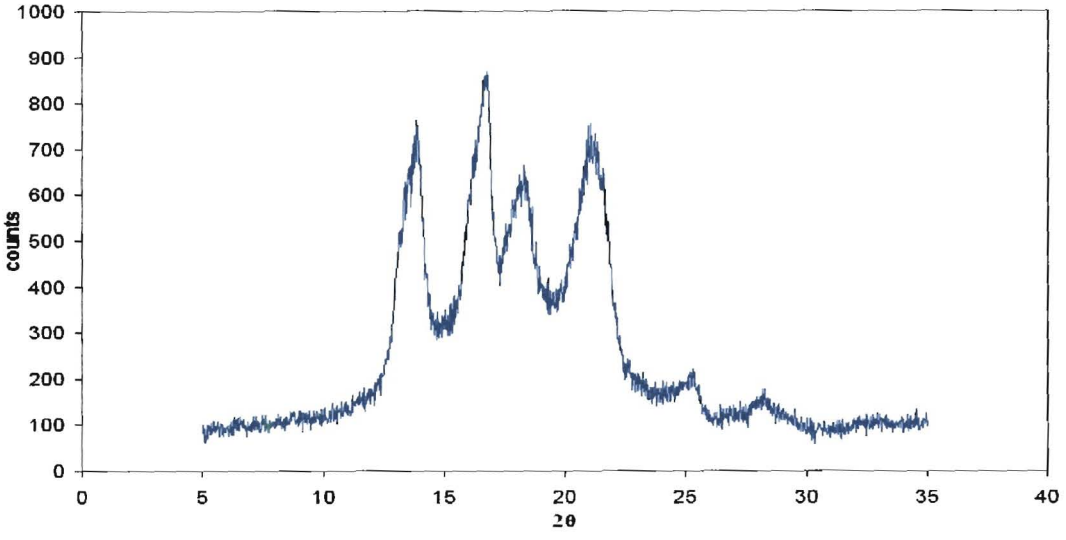

sample #27

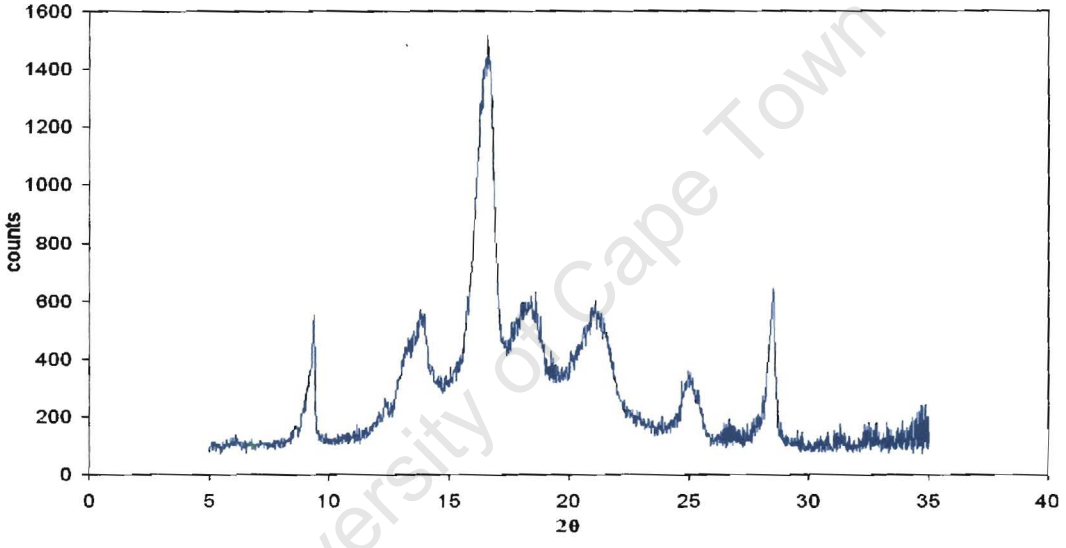

sample #28

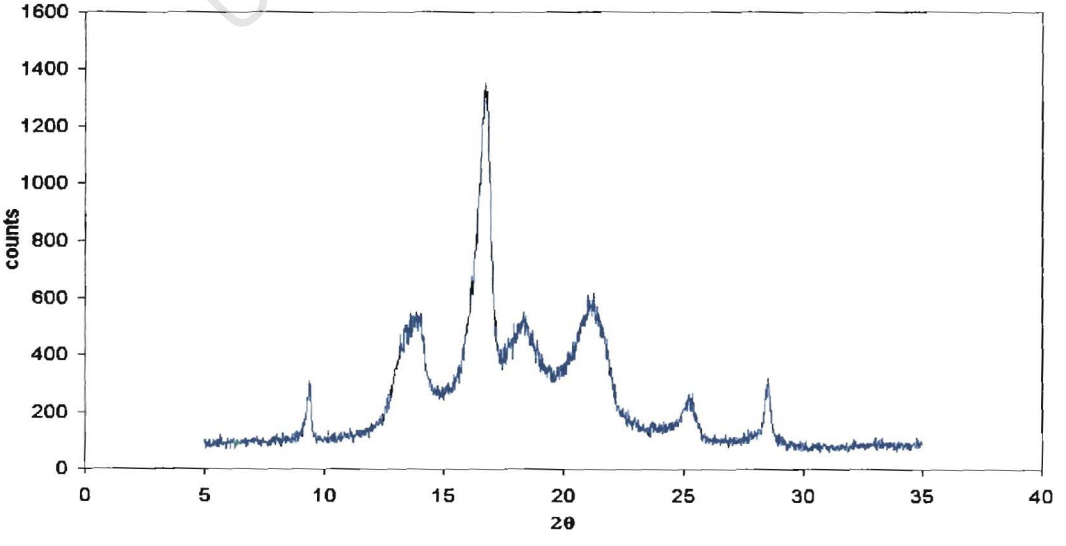

sample #29

University of Cape Town

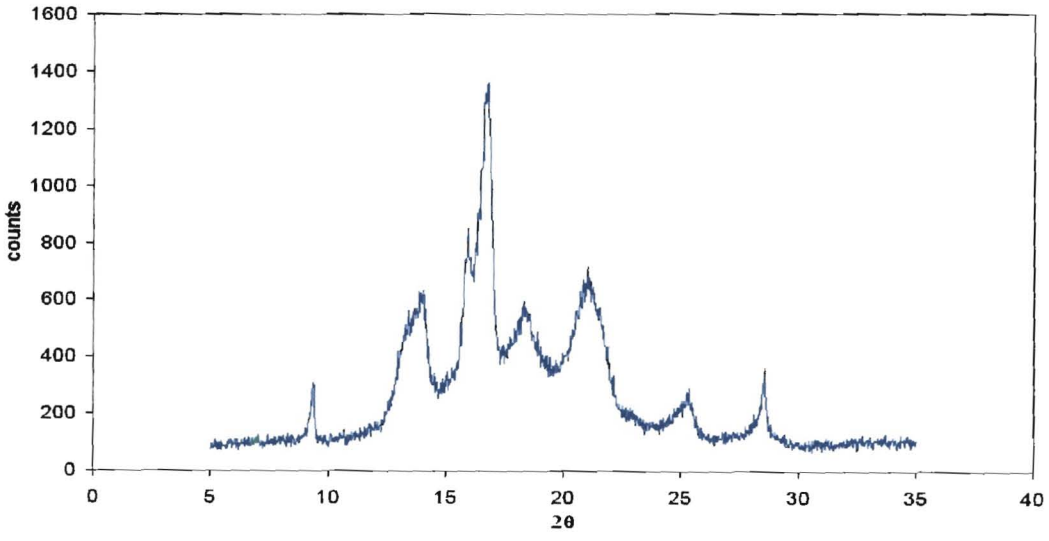

sample #30

University of Cape Town